University of Stavanger

Faculty of Science and Technology

MASTER'S THESIS

Study program/Specialization: Offshore Technology/ Subsea and Marine Technology.	Spring semester, 2017 Restricted access
Writer: Akinsanya Akinyemi Olugbenga	…… (Writer's signature)

Faculty supervisor:
Prof. Ljiljana Djapic Oosterkamp (University of Stavanger, Statoil AS, Stavanger Norway)

External supervisor(s):
Per Richard Nystrøm (Technical Director/Chief engineer, IKM Ocean Design Stavanger, Norway)

Thesis title:
Experimental and Numerical Analysis of Pipeline Rotation with Residual Curvature during Installation
(CONFIDENTIAL)

Credits (ECTS): 30

Key words: Pipelaying, S-lay installation, Subsea Pipelines, Pipeline Rotation, Residual curvature, Nominal curvature, Analytical Pipe rotation, Pipeline Installation experimentation. Free Span, Uneven Seabed,	Pages: 117 + Appendix /enclosure: 33/ 1 CD Stavanger, June /2017

ACKNOWLEDGEMENT

The thesis research is performed and submitted in partial fulfillment of the requirement for the award of Master of Science Degree studies in offshore technology (subsea and marine technology specialization) at the University of Stavanger and it is prepared from January 2017 to June 2017. This thesis work was performed in collaboration IKM Ocean Design AS, Stavanger, Norway.

First and foremost, I expressed my immerse gratitude and appreciation to my Faculty Thesis Supervisor Professor Ljiljana Djapic Oosterkamp, who initiated this thesis research effort at the university of Stavanger and offered invaluable support, encouragements and useful suggestions throughout the duration of this research work, despite her busy schedules. Also my special thanks also goes to my external supervisor Per Richard Nystrøm of IKM Ocean Design, Stavanger, for his intellectual suggestions, criticism, advise and for sharing from his wealth of experience on various technical subjects relating to the scopes of this thesis and for given me the opportunity to be part of the IKM family. My profound gratitude also goes to the laboratory manager John Grønli, who made available the fund for the experimental test and for his unwavering support throughout the duration of the experiments.

My heartfelt gratitude and unconditional love go to my ever-loving wife Okumodi Atinuke Akinsanya for her unparallel supports in all ramifications, care, motivation and extreme understanding with which my postgraduate studies in Norway was made possible. And to my daughter Moriyanuoluwa Shiloh Akinsanya thank you for your endurance and patient while I was away in Norway. Special thanks go to my mother (-in law) Alhaja Okumodi for her unwavering prayers and motivations for me and my household, I appreciate your efforts and the confidence you had in me. My acknowledgement will not be complete without appreciating the efforts and prayers of my siblings and in-laws, who when I think of, remind me of a greater responsibility to shun play and embrace hard-work and seriousness and to all my friends, who contributed to the success of my study in one way or the other.

Above all, my deepest appreciation goes to the Almighty God, the author of wisdom and knowledge, for His steadfast love, mercy, grace and protection and for fulfillment of His promises, that sustained me throughout the duration of this postgraduate studies.

Akinyemi Olugbenga Akinsanya
Stavanger, June 2017

ABSTRACT

In the oil and gas industry, subsea pipeline plays a very important role in the transportation of the crude oil between subsea production system (SPS) components and from seabed to the offshore platform/facility, or from an offshore field to an onshore facility for processing, thus serving as in-field line and trunk line (export and import transportation line) respectively. Hence its design, fabrication and installation are very vital to the successful operation of any subsea infrastructure. In the past, detail assessment of pipeline installation methods and design has been performed and documented in several literatures. However, following the decline in the price of oil and gas and the inclination of the exploitation of oil and gas production towards deep and deeper water, it becomes imperative to re-evaluate all aspects that made up of subsea field development in terms of design, construction and operation, in order to reduce the overall project cost, while meeting all the technical challenges associated with subsea field development in deep water.

In lieu of this, for pipeline, being a critical aspect of subsea development project, additional engineering effort is required to minimize the cost of pipeline installation, since its material and installation together can make up to 85% of the total pipeline budget (*Bai et al. 1999*). To achieve this, focus is given to the utilization of pipeline rotation during installation via optimization of the use of pipeline residual curvature, in meeting the technical challenges associated with pipeline free span and in minimizing the cost that comes with mitigations via material dumping and other span supports as well as understanding pipeline rotation phenomenon in the case of inline structure installation such as Tees, Wyes, Connectors, thus saving operation time and reducing the cost of pipeline intervention on the seabed.

This Thesis work, concentrate on the validation of the numerical analysis of estimating pipeline rotation during S-lay, using an experimental test on pipeline rotation, based on this, parametric studies are carried out. Also an experimental test is performed to determine the value of residual strain and curvature length required to induce a pipeline rotation of above 90degree. Additional experimental test is performed to establish the operational principle of conforming pipeline to uneven seabed using residual curvature, this is considered relevant as residual curvature can be adopted in solving the technical challenges that come with installation of pipeline by S-lay method on uneven seabed, since such pipeline are subjected to bending moments, vortex induced vibration (VIV) and so on, as a result of free span.

To meet the objective of this study, both experimental and numerical approaches were adopted. First, experimental tests were performed using an already existing model test set-up components of a real-life scenario is adopted, this set-up components comprises of all the important installation vessel parameters that are used in real life S-lay installation operation of pipeline. These components include the model stinger and associated rollers, the top tension system, bottom horizontal tension system and model pipe of 10mm for simulating the S-shape and nominal curvature. In addition to the existing component, wooden stands, with seabed features, are constructed and used to simulate the uneven seabed. The experimental test is performed by introducing several pre-bends of different residual strains and curvature length on the model pipeline for the cases of rotation test and free-span test. The pipe paying out operation was simulated by pulling the model pipeline at the bottom while measuring the angle of rotation and the horizontal force for the rotation test and change in span between the contact point and the depth from seabed to mid span for the case of free-span. Also, the free span test includes simulation of additional measures such as introduction of local weights and their effect in the suppressing pipeline free span. Afterward numerical analyses were performed to quantify the pipeline rotation, using commercial finite

element software, ORCAFLEX. In the numerical analysis, a beam model of the pipeline is built in the software using the same properties of the model test rig (listed subsequently in the thesis work), the pipe properties, inline structure and boundary conditions (BC). Then parametric studies are performed by varying several parameters, such as pre-define residual curvatures length and plastic strain, which affect the value of the rotation, with major focus on the rotation phenomenon at the touch down point (TDP).

LIST OF FIGURES

LIST OF TABLES

ABBREVIATIONS

BC	Boundary Condition
Dn	Deflection Number
DPS	Dynamic Positioning System
ID	Internal Diameter
OD	Outer Diameter
RCL	Residual Curvature Length
RSL	Residula Strain Level
RS	Residula Strain
TDP	Touch Down Point
WD	Water Depth
UiS	University of Stavanger
WASP	West Africa Swell Project
VIV	Vortex Induced Vibration

ALPHABETIC SYMBOLS

Symbols	Description	Units
a	Constant equal to H per w_s	1/m
A	Cross section Area	m^2
b	Constant	-
c	Constant	-
d	Constant	-
D	pipe outer diameter	m
D_w	Water Depth	m
e	Extension	mm
E	elastic modulus	MPa
f_D	design factor	-
F	Applied Force	N
G	Shear modulus	MPa
h	Non dimensional tension contribution	-
H	Horizontal Force at vessel tensioner	N
H_0	Horizontal Force at TDP	N
I	Second moment of Area	m^4
I_T	Polar Moment of Inertia	m^4
K	Spring constant	N/mm
k(s)	Nominal Pipe Curvature	1/m
k_r	Residual Curvature	1/m
k_{res}	Residual curvature	1/m
$k_{nom(max)}$	maximum nominal curvature	1/m
k_{tot}	total curvature	1/m
L	Length of suspended pipe	m
L_{curve}	Residual curvature length	m
M	bending moment	Nm
M_0	bending moment components due to initial curvature	Nm
M_B	Moment due to Bending	Nm
M_R	Moment due to rotation	Nm
P	Applied Load	N
r	Outer radius of the pipeline	m
R	Bending radius of pipeline	m
R_{cv}	radius of curvature of the pipeline	m
R_{res}	residual radius	m
R_{st}	radius from pipe centerline to stinger centerline	m
s	Length of pipeline free span	m
T	Axial tension	N
T_t	Torque	Nm
V	Vertical Component of axial tension in Newton	N
x	horizontal distance from TDP to the lay barge	m
y	Distance along pipeline centreline	m
z	height above seafloor in meter	m
W_d	pipeline dry weight	N

w_s	Pipe submerged weight per unit length	N/m
W_B	Work due to Bending	
W_R	Work due to rotation	
W_{tot}	Total Work done	

GREEK SYMBOLS

Symbols	Description	Units
θ	Lift angle in degrees	deg.
$\boldsymbol{\sigma}$	applied stress	MPa
$\boldsymbol{\sigma}_y$	yield stress of the pipeline	MPa
$\boldsymbol{\sigma}_A$	axial bending stress	MPa
ε	Applied Strain	-
ε_0	Accepted strain	-
ε_{res}	Residual strain	-
$\varepsilon_{nom(max)}$	Maximum nominal strain	-
ε_{st}	Distribution of strain	-
ε_{plt}	Residual Plastic strain	
ε_y	yield strain	
α_s	Non-dimensional quantity which measures the effect of the bending stiffness compared to the non-dimensional tension contribution h	-
K	Cross-sectional average of the curvature in the pipeline	1/m
λ	Load factor relating the bending stiffness with the horizontal tension	m
γ	Load factor relating the bending stiffness with the axial tension	m
β	Angle of attack of the current	rad
ΔL	Change in Length	m
ν	Poisson's ratio	-
$\emptyset(x)$	Roll or Rotation angle	rad
$\emptyset_0$	Maximum torsional/roll angle at the seabed	rad

1. INTRODUCTION

Pipeline has proven to be the most economical means of transporting hydrocarbon from the sea. It use encompasses transportation within a subsea field, transportation to nearby platform and /or to an onshore facility for processing. It can as well be the most economical option for large scale overland transit of hydrocarbon. As shown in Figure 1-1, pipeline can be classified, depending on its function and location, as infield flowlines, export and import pipelines (trunk lines), water, chemical and gas injection flowline and oil and gas production flowlines.

Pipeline development project is one phase out of the several sub-project phases in any subsea field development project and offshore pipe laying is a crucial and capital intensive operation in the pipeline development project. A sound understanding of the phenomenon of pipelaying and the behavior of the pipeline during installation is therefore very important in order to ensure successful installation as well as to achieve this in the most effective, efficient and economical way. For safety and effective performance of the pipeline during operation, it is very necessary that some control equipment such as Valves, Tees etc., are installed along the pipeline, thus the verticality of these equipment on the seabed are of utmost important so as to avoid additional cost due to subsea interventions and any incident that follows inaccurate installation of these equipment. To ensure this, pipeline rotations and residual curvature which the primary cause of the rotation become phenomena to be well understood and how the residual curvature can be further optimized to meet the challenges associated with free spanning due to uneven seabed is given serious consideration.

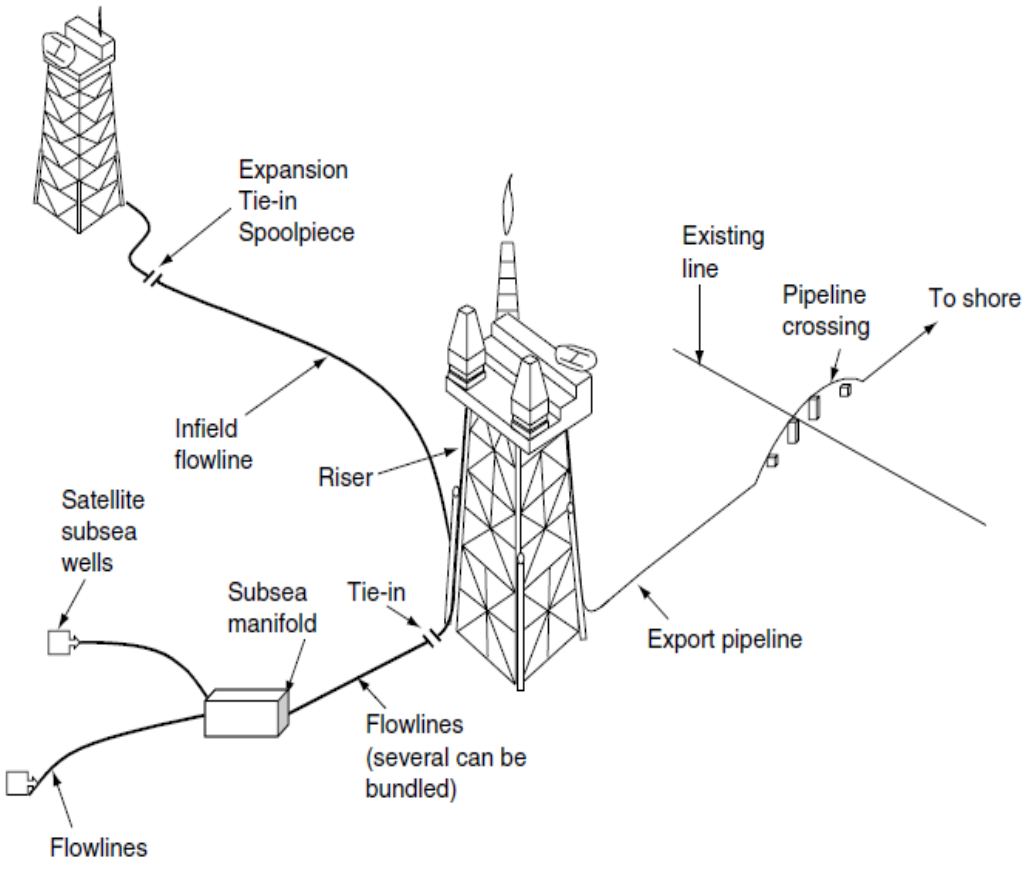

Figure 1-1; Use of Offshore Pipeline (Boyun et al., 2005)

1.1 BACKGROUND STUDY AND MOTIVATION

Much of the present interest in pipeline rotation comes from the active exploitation for oil and gas in deep water, which in turn calls for deep water field developments, since pipeline plays a pivotal role in

ensuring safe transportation of the hydrocarbons from the seabed to the processing facility. Although the technology of shallow water has already been known and developed, however increasing water depth ranging from deep to ultra-deep, uneven seabed with large span lengths and heights, high pressure and temperature and harsh environmental conditions, pose a great deal of several technical challenges, in terms of engineering design, installation and operation, and high cost of field development, which consequently hinders the development of several fields in deep water, as there are needs for subsea intervention operations, mitigation measures put in place for free span and buckling. Thus, the need for improved and cost efficient technology to meet all the technical challenges that comes with development in deep and ultra-deep water and further to this, recent decline in oil and gas price has put pressure on the need to for cost-effective technical solution.

In furtherance to this, pipeline installation, becomes technically challenging to install in deep and ultra-deep water as there are limitations in the available installation vessels such as the capacity of vessel/barge tensioner as well as to the length of stinger in the case of S-lay installation. In response to this need, understanding the phenomenon of pipeline rotation is important in predicting and quantifying the rotation angle, which is of great consideration while inline structures are to be installed along with the pipes. In recent times, the mechanism of pipeline rotation as well as residual curvature has been tailored towards solving many technical problems, such as buckling and free spans, that plague in-place subsea pipeline during operation and installation.

Not until recently, pipeline rotation due to residual curvature has been considered problematic during pipeline installation. This is primarily as a result of the difficulty in achieving verticality of inline structures installed along with the pipeline, although different mitigation measures as been proposed by several experts such as *Gilchrist (2008) and Endal and Verley (1995).* The situation was worst as there is little technical knowledge about the behavior of subsea pipelines subjected to residual curvature during laying. The recent inclination of the oil industry towards deep water technology has called for improved methods of meeting most of the technical challenges relating to pipeline installation, this challenge has propelled several research efforts to better understand the phenomenon and mechanism of pipeline rotation during laying. This thesis research however focuses on the rotation during S-lay method of pipeline installation as well as the optimization of residual curvature in pipeline free span. For pipeline problems related to free span, static bending moments, VIV, that occur when pipeline is laid across a scar due to uneven seabed topography, pipeline residual curvature can be optimized to reduce the effects of such problematic. This can be achieved by creating local residual curvature during installation along the pipeline, in order to make the pipeline conform to the seabed topography, thus reducing the need for mitigating measures to ensure pipeline integrity on uneven seabed *(Endal et al. 2015).*

During S-lay installation of subsea pipeline, the pipeline exceeds the elastic curvature upon passing over the stinger, thus the pipe is exposed to plastic bending strain, and consequently residual curvature. As the pipeline is been paid-out, it has the tendency to rotate as its move through the suspended section and experience reverse bent at the sag bend (under bend) due to itself weight. As pipeline rotation follows the principle of potential energy minimization, the pipe may experience torsional rotation which is refer to as pipe roll, from the installation vessel or lay barge to the seafloor at the TDP *(Yousun, 2005)*. Hence pipeline rotation can be quantify using this principle, and the type of potential energy minimization to be adopted for a problem depend solely on the most suitable solution for the problem at hand. This type can either be the gravity or strain energy minimization *(Vaughan & Nystrom, 2016).* It is worthy of note that pipeline rotation during laying is dependent on several number of factors which are not limited to the water depth of the field, the applied top tension, the stinger configuration, the mechanical and geometrical

properties of the pipe and the environmental condition at the installation site.

In S-lay installation method, the local residual curvature can be created at different sections along the pipeline, by using the active roller on the stinger or by adjusting the radius of the stinger to generate a curvature beyond the elastic limit. The same can be achieved in reel-lay method of pipeline installation, by using the reel-ship's straightner system during laying *(Endal et al. 2015).* Although residual curvature can easily be generated using the Reel-lay method, and thus frequently used where residual curvature are to be created most especially for laying small diameter pipes. However the application of this method is limited by the size of the pipe diameter and the type of coating applied on the pipe, as Reel-lay is not suitable for laying concrete coated pipes.

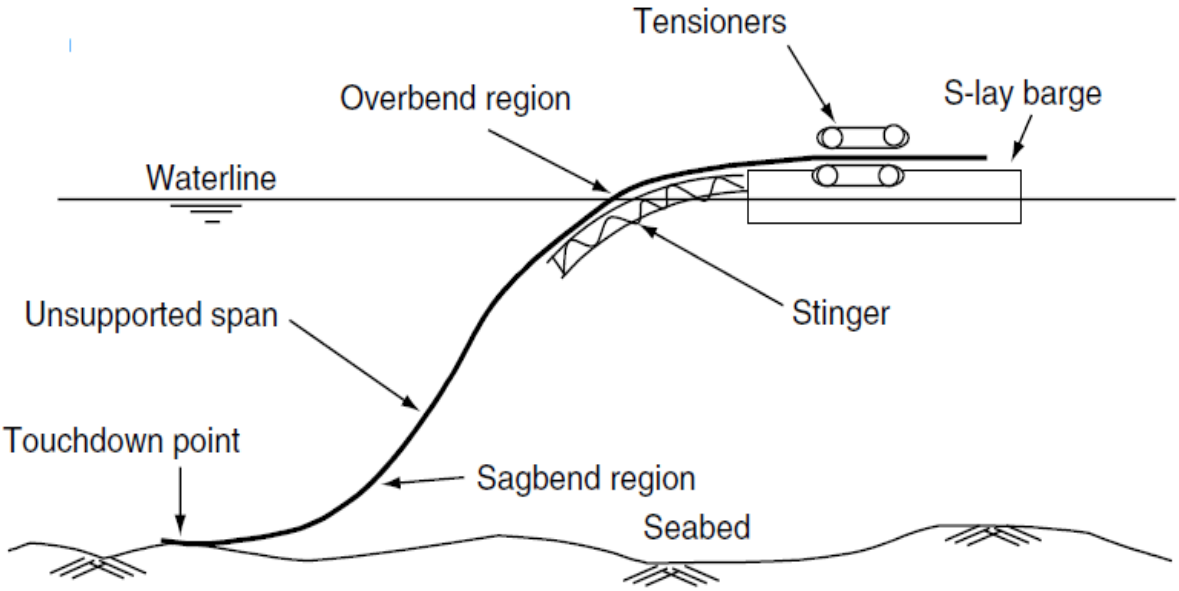

Figure 1-2; Offshore Pipeline Installation on an Uneven Seabed (Boyun et al., 2005)

The sea bed condition of virtually all subsea fields are very irregular, although route selection study is performed to avoid most of the obstacles on the seabed, however because of the high level of the irregularity of the seabed pipelines, it is very difficult to find a obstruction free route, thus pipelines are installed on the uneven sea bed, see Figure 1-2. In past year, free spanning has been a daunting challenges militating against the structural integrity of unburied subsea pipeline laid on the sea bed. To mitigate the effect of free spanning, such as unacceptable fatigue damage, vortex induced vibrations (VIV), excessive bending and deflections, that the free span posses on structural safety and performance of subsea pipelines, measure such as rock dumping, structural support installation etc., are commonly installed in practice. These measures can be very costly and requires additional project time.

Endal et al. (2015) indicated several ways of adapting pipeline to seabed topography and further identify that the importance of residual curvature encompasses pipeline stability during installation, with regards to rolling. This may be as a result of lower Center of Gravity of the curvature, concave upward and downward configuration, depending on which option is adopted. For the reason, this project aim to investigate and improve the understanding, through experimental test, of the use of residual curvature in meeting the free span challenges of pipeline laid on even seabed, with the primary objective of promoting residual curvature as a cost effective way of meeting free span problems.

1.2 STUDY OBJECTIVES

This study effort focuses primarily on the experimental parametric study of pipeline rotation due to residual curvature during S-lay installation with the purpose of achieving a pipeline rotation above 90deg. and in addition, establish the fundamental principle of conforming subsea pipeline to uneven seabed topography, thus revealing the effect of span length and height which will have consequence relief effect on static bending moments via the measuring of strains at the span shoulders and mid span. The effect varying residual curvature along the pipe is also being considered.

In addition to the primary goal stated above, the numerical analysis of estimating pipeline rotation is performed and validated by comparison with results of experimental test, thus given a high reliability on numerical solution of pipe rotation estimation. The numerical analysis is also parametric based, this gives a clearer insight into how different parameters such as plastic strains and residual curvature length, boundary condition affect the pipeline rotation and the most critical parameters are established.

1.3 STUDY SCOPE

In order to meet the objective of this thesis the following scope were covered in this thesis work;

Experimental Phase;

- Normal pipe lay configuration was established and validated by analytical method.
- The pipe was pre-bend for different residual strain levels (0.30%, 0.35% and 0.40%) and curvature lengths (2meters and 3meters)
- Rotation test was performed for;
  - ✓ No rotational restraints at the pipeline bottom end
  - ✓ 1 set of rotational springs
  - ✓ 2 sets of rotational springs
  - ✓ Inline structure
- The pipe is pre-bent downward (sagging) and Free span test was performed with;
  - ✓ Normal pipe lay configuration
  - ✓ Local residual curvature at mid-span
  - ✓ Residual curvature at the uneven seabed shoulder
  - ✓ Weight at mid-span
- Parametric numerical studies of pipeline rotation due to residual curvature
- Comparison of the experimental test and the numerical analysis

Numerical Analysis Phase;

Using the lay parameters as of the experiments numerical analysis is performed for all the experimental load cases.

1.4 OUTLINE OF THESIS

The content of this thesis is based on the following outline:

Chapter 2: Overview of Offshore Pipeline Installation

This chapter gives a general overview of pipeline and offshore pipeline installation technology, in terms of the history, the installation methods, installation challenges, load and configuration of pipeline during

installation and introduction to pipeline installed on uneven seabed topography

Chapter 3: Introduction to Pipeline Residual Curvature and Rotation

Detailed insight into the pipeline rotation during installation is given in this chapter. The causes and methods/theories of estimation of pipeline rotation, the residual curvature as a major cause of rotation during installation and its importance when pipeline is laid on uneven seabed were elaborated.

Chapter 4: Methodology

This chapter discusses the approaches used in achieving the objectives of this thesis. Detailed discussion on both the experimental set up and the numerical approach, modeling and features of ORCAFLEX were given

Chapter 5: Model Scaling

Should there is need for estimating or comparing the result of the experiment with a real life situation, this chapter presents the laws governing model and prototype by using non-dimensional parameter

Chapter 6: Experimental and Numerical Test Results

This chapter presents the results of the experimental test for all the scenarios considered to meet the objectives of this thesis.

Chapter 7: Discussion of Experimental and Numerical Result

The results of both the experimental test and numerical analysis are presented in graph for easy interpretation and the plots are discussed in detailed. The results are also compared in this chapter and the discrepancies identified

Chapter 8: Sources of Errors and Uncertainties

For every experimental work has uncertainties and limitations that affects the accuracy of the test results, these uncertainties, limitations and challenges of the experimental test and the numerical analyses are presented in this chapter

Chapter 9: Conclusion and Recommendation

The summary of the results of this study as well as recommendations for future or further studies are given in this chapter

2. OVERVIEW OF OFFSHORE PIPELINE INSTALLATION

A very important part of the marine operation during any subsea field development project is the installation of pipeline for the safe transportation of hydrocarbons. Pipeline installation is an offshore operation that involves accurate placement or positioning of a pipeline on the seabed by paying out sections of line pipes from a surface vessel. It has been established based on past project experience that pipe laying operation is one of the most delicate and challenging marine operations, thus a successful implementation of such operation requires a high level of technical know-how as much as extensive engineering effort. The cost of such operation can be considered to be very high as well depending of the size of the pipe to be installed, the installation method etc which in turn plays a pivotal role in the selection of a suitable installation vessel.

It is worthy of note that pipeline development project encompasses four different phases which are; the design phase, fabrication phase, installation phase and commissioning and operation phase, as shown in Figure 2-1.

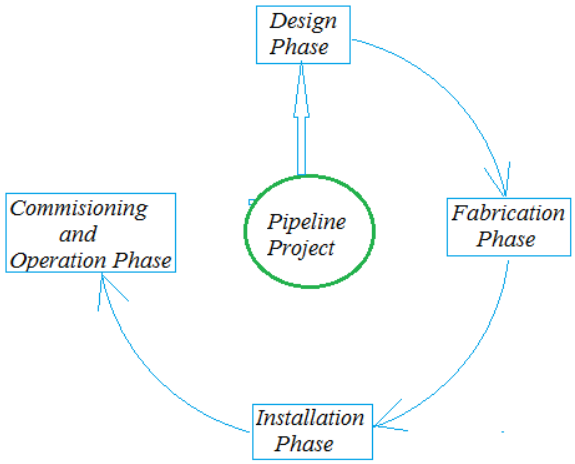

Figure 2-1: Phases of Pipeline Development Project

The design phase of the pipeline development project involves the determination of a suitable pipeline path through documented in the form of detailed layout drawings, alignment sheets and bathymetry maps. Also the pipe properties such as the pipe diameter, wall thickness, material grade, thermal insulation and coating if required, are determined in the design phase through both static and dynamic analyses. Pipeline is as well checked to ensure it meets all operating and installation requirements. To determine all parameters required for safe installation and ensure stresses and strains in the pipeline during laying are within limit, both static and dynamic installation analyses are performed.

The procurement and fabricating phase of any pipeline developments projects involves the acquisition of material based on material take off and construction of the line pipes. This phase encompasses the application of thermal insulation and coating on the line pipes as well as preparation of all pipe joints. Following the fabrication phase is the most challenging phase which is the positioning of the pipeline in the pre-determined path or route on the seabed. This operation posse a great deal of challenge and costly depending on the installation method considered most suitable for the installation, which in turn influences the design parameters as well as the type of installation vessel to be used. Upon successful laying of the pipeline on the seabed, the pipeline is checked and ensure all parameters for safe and continuous operation have been installed and they all meet their corresponding requirements. This chapter serves to provide the basic knowledge required for a sound understanding of the objectives, challenges, methods and background for offshore pipelaying.

2.1 HISTORY OF PIPELAYING

The complexity and challenges involve in pipeline projects has enabled it grow into a stand-alone discipline and over the years the offshore pipeline technology has been developed. Due to market demand and the urge for energy, the oil and gas industry ventured into a search for oil and gas resource in deeper and harsh environment, which generate a need for a technology that meets the challenges associated to this environment. Another key factor that drive the development of the offshore pipeline technology is the fluctuation of the oil and gas price, this plays a pivotal role in propelling the oil and gas industry, through engineering skills and past experience, to crave for cost effective solutions to most of the challenges that plague the development of new oil field as the trend moves toward deeper and hostile environment.

The technology involve in offshore pipeline is dated back to the 1920s and 1930s where the ocean was a barrier to O&G development, however in 1936, Brown & Root successfully constructed a short pipeline in Galveston Bay (*Acergy Academy 2008)*. 1940s witness the beginning of modern offshore pipelaying, where 17 subsea pipelines are installed across English Channel and in 1947 the first offshore pipeline laid in Gulf of Mexico (GoM) by Brown & Root. This period also witness the first attempt at reel lay, the development of laybarge system and the shallow water GoM development (*Acergy Academy 2008)*. The execution of Operation Pluto is a secret World War II project between the oil industry and the armed forces *Searle (2004).*

The first generation of laybarges in the GoM is witness in the 1950s and 1960s as oil companies activities was geared from onshore towards offshore; this period marked the beginning of modern pipeline technology in the GoM. It was a pioneering time for pipelay through S-lay method and welding of 12m pipe length and the J-lay method was used to install pipeline by Bechtel semi hull design in the 1960s (Austin et al., 2004). During a period of recession in for the oil industry due to fall in oil price, the North Sea harsh environment witness its first pipelines laid by the 1970s between 1968 and 1975 after several discoveries such as the Ekofisk field. The installation was made with 2nd generation laybarge Chocktaw. By 1980s the period of recession was followed by Boom and bust, and the period experienced intensive research and development in many areas of pipeline such as new welding techniques (*Acergy Academy 2008)*. The 1990s there was an upswing in the market and a refocus on the GoM. The J-lay method was further developed for use in deeper water. Deep water development accelerates in Coast of Brazil, West Africa and GOM, with 12inch and 18inch pipeline being laid in water depth of 1600m and 1800m respectively in the GoM (Knight and Palathingal, 2007). By 2000s there is huge world-wide demand for fuel as China and India develop, Barrel of oil continues to rise, exceeding $60 GoM continues into deeper reaches, Steel catenary risers are popular West Africa regularly exceeds 1000m, GoM pipelay reaches 2750 by mid 2000s. Langeled – Worlds longest subsea pipeline was installed during this period.

Today as barrel of oil falls below $60, the oil industry is under pressure to develop more economical solutions for both new pipeline technology and existing as well as to meet New Deep water fronteir – 3000 m

2.2 PIPELINE INSTALLATION METHODS

Different methods has been adopted for the installation on pipeline, regardless of the installation method adopted, the primary goal of all the methods remains the same and the goal is ensure the pipeline remain under tension and the bending and axial stresses within an allowable range is maintained. The type of installation method to be used is project specific and the selection is been governed by several factors not limited to the pipe properties such as diameter, the type of coating selected if required, water depth,

weather conditions, the length of pipe to be laid, installation vessel available and so on. The most common methods of pipeline lay installation methods are the S-lay, J-lay and Reel lay methods, other method that is still in use till date is the Tow method. Figure 2-2 shows the offshore pipe laying methods.

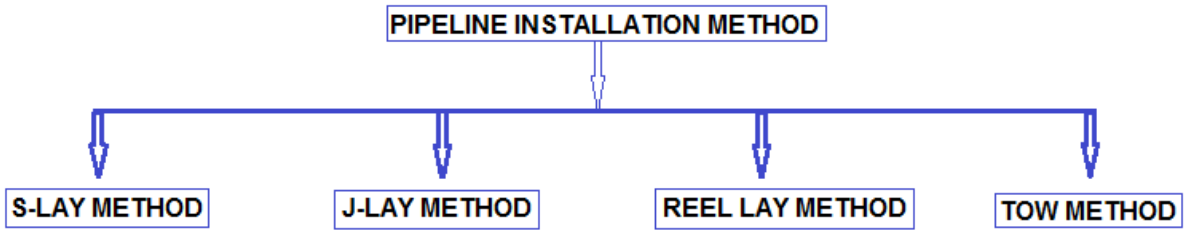

Figure 2-2: Phases of Pipeline Development Project

The S-lay method is the most common type of pipeline installation and it is suitable for laying pipe in shallow to deep water depth, while the J-lay and Reel lay are only applicable in intermediate to deep water depth. It is worthy of note that two methods can be used for installing pipelines from shallow water depths to deepwater depths depending on the design requirements.

Depending on the method, a marine pipeline is exposed to different loads during installation from a lay-vessel. These loads are hydrostatic pressure, tension and bending. An installation analysis is conducted to estimate the minimum lay-tension for the pipeline for a given radius of curvature to ensure that the load effects on the pipeline is within the strength design criteria *(Bai Y., 2001)*. The main international companies that perform pipelaying are: *Acergy, The Allseas Group, Saipem, Technip, Heerema, J. Ray McDermott, Global and Subsea7.*

The installation methods are described in details in the following sections. Detailed description of the various pipe laying methods are documented in several literatures such as *Kyriakides and Corona (2007).*

2.2.1 S-Lay Method

S-lay is the first commonly used method and it still stands as the most common use world-wide. It is widely used in shallow waters, where the installation vessel is either anchored or use dynamically positioned and also suitable for deep water where the vessel can only be dynamically positioned. Its deep water capability can be further enhanced with the use of 'steep s-lay' criteria.

The main components that make up the S-lay installations are;

- Installation Vessel
- Stinger
- Roller
- Line Pipes,
- Tensioner
- Abandoments and Recovery Winch
- Pipe Handling Crane
- Firing Line

Detailed descriptions of the components are documented in *Gullik Anthon (2010) and Kyriakides and Corona (2007)* and the classification of the S–lay vessels into generations can be found in *Guo et al., (2005).*

Principle of S-lay Method

The S–lay installation method involve welding of the line pipes, non-destructive testing of the welds and coating of both the pipes and weld onboard the laying vessel on to the end of the pipeline in a horizontal production facility called the firing line. While these processes are on-going the pipeline being constructed is

held in place to facilitate continued construction by the tensioners. Has the construction pipe continues, the pipe is been pay-out at a pay-out speed controlled by the tensioner while still maintaining the tension on the pipe as the vessel moves forward *(Gullik Anthon 2010)*.

As the pipeline been constructed moves towards the end f the vessel, it is been supported by the rollers which are in turn supported by the stinger, which is long open curve structure that controls the curvature of the pipeline at the overbend (see a typical 130m length stinger in Figure 2-4 for by Allseas group). The pipeline then leaves the stinger at a departure angle; thus it is suspended as the pipeline is been paid-out. The stinger shape and curvature can be controlled by setting these segments at chosen angles. The pay-out process continues, the pipeline is suspended in the water all the way to the seabed, thus forming the sag-bend (see Figure 2-3), the curvature at the sagbend is controlled by the top tension applied to the pipe onboard the vessel. In other to ensure the pipe does not exceed the elastic limit, the top tension needs to be optimised. The over-bend and sag-bend form the shape of an ‘‘S’’. The main segments of the pipeline during S-lay installation are shown in Figure 2-3. The pipeline experiences a significant level of stress at the overbend and the sagbend.

Implication of S-lay Method

A major advantage of the S-lay method is quicker production rate due to the long firing line with parallel workstation, running from the vessel bow to the stern, thus supporting up to four pipe joints at the same time. This method also compete reasonably well when water depth and pipe diameter are governing criteria.

However, S-lay in deepwater, it is necessary the pipe is supported at a high vertical depature angle, thus requiring a large stinger to avoid damaging the pipe, high tensioner capacity which is directly transferred to high fuel expenses, induces a higher strain than for J-lay and can be as high as 0.45% in the overbend. (*Palmer, 1994 and Boyun et al., 2005)*. There is high tendency for the pipe to rotate due to the residual curvature that results from the plastic strain generated in the overbend by the stinger, more discussion on residual curvature and rotation are given in section 3.

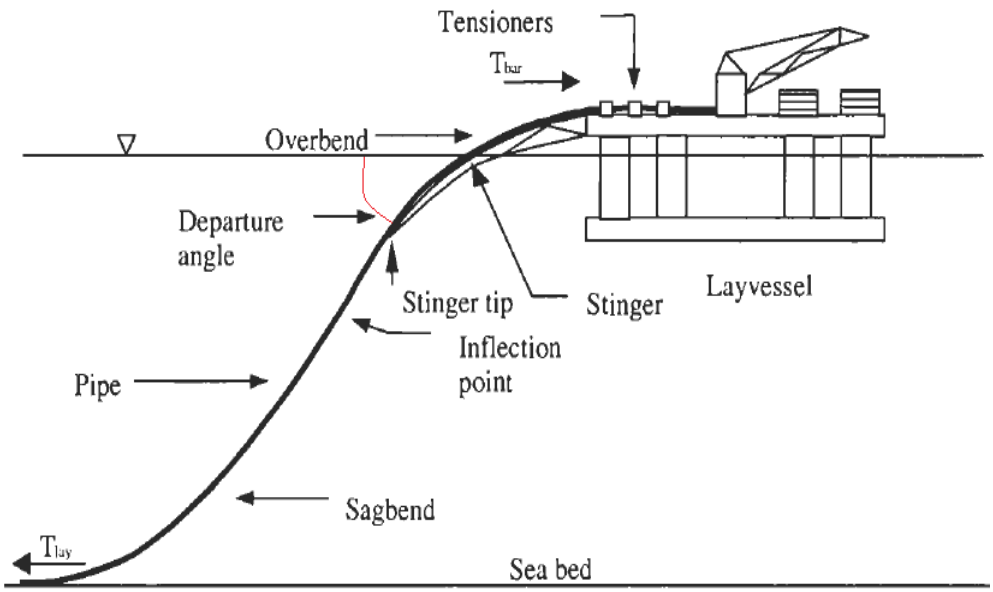

Figure 2-3: S-lay Configuration (Bai Y., 2001)

Figure 2-4: S-lay installation Vessel (Courtesy of Allseas Group)

2.2.2 J-Lay Method

The J-lay installation method is a relatively new type of installation method and it is specifically designed to meet the challenges that plague deepwater and ultra-deepwate pipeline installation projects. J-lay method is only suitable for intermediate to deepwater application and the installation vessel used for the operation can only be dynamically positioned. This is primarily beacuse water depths are normally too high for moored lay vessels to operate, because the required tensions and pipe bending stresses are too large (*Boyun et al., 2005)*. The first dedicated J–lay installation facility was installed on the DP derrick barge DB 50. Since 1998 several vessels have been fitted with J–lay capabilities. Two of the largest are the vessel Saipem 7000 (S–7000) that was fitted with a J–lay tower in 1999 (Faldini, 1999).

The main components needed for a successful installation of pipeline using the J-lay method are as follows;

- Installation Vessel
- Vertical Ramp/ J-lay Tower
- J-lay Collars/Tensioner

Detailed descriptions of these components are documented in *Kyriakides and Corona (2007)*

Principle of J-lay Method

The J-Lay principle is to lay the pipe in a quasi vertical position by using a J-Lay tower while the full pipe catenary is maintained at the tower bushing. In the J-lay method the length of line pipes are welded in a near vertical or vertical position, the joint tested by NDT and the joint Field joint coating (FJC) applied in the J-lay tower which can accommodate at least two work stations and also fitted with tensioner. The pipe then leaves the pipelay vessel in a nearly vertical position to the sea bed, thus eliminating the overbend region from S–lay completely, consequently avoiding significant pipe rotation. The pipeline is paid out of the installation vessel at a high departure angle (see Figure 2-5) such that the total length of the suspended pipe is shortened and less applied tension is required for sagbend control. At the seabed the configuration of the suspended pipe resembles the letter J from the TDP to the Ramp, Figure 2-5 shows the configuration of the pipeline during J-lay installation operation. The pipe length is restricted by the height of the tower and the pipe pay out between

welds equals the length of joint entered into the lay system and the angle of the J–lay tower may typically vary between 0◦ and 15◦ from the vertical. J–lay has many advantages (Palmer and King, 2008).

Implication of J-lay Method

In configuration, the pipeline from the surface to the seabed is one large radius bend resulting in lower stresses than an S-lay system in the same water depth. The stresses and strain close to the top are minimized, as well as the horizontal tension component at the top and the horizontal tension at the mudline, thus reducing seabed spans. Another major advantage of the J-lay method is the elimination of the complexity involved with a stinger, thus no overbend and reducing the pipe rotation that can result from residual curvature for line without inline structure. Good for in-line fittings and end fittings slower production times than S-lay

One main drawback of the J-lay method is the limited number of work stations that can be accommodated by the tower, which consequently makes the J–lay method inherently slower than the S–lay method. However, since the large J-lay towers are capable of handling prefabricated quad joints (160 feet long), the speed of pipelaying is increased.

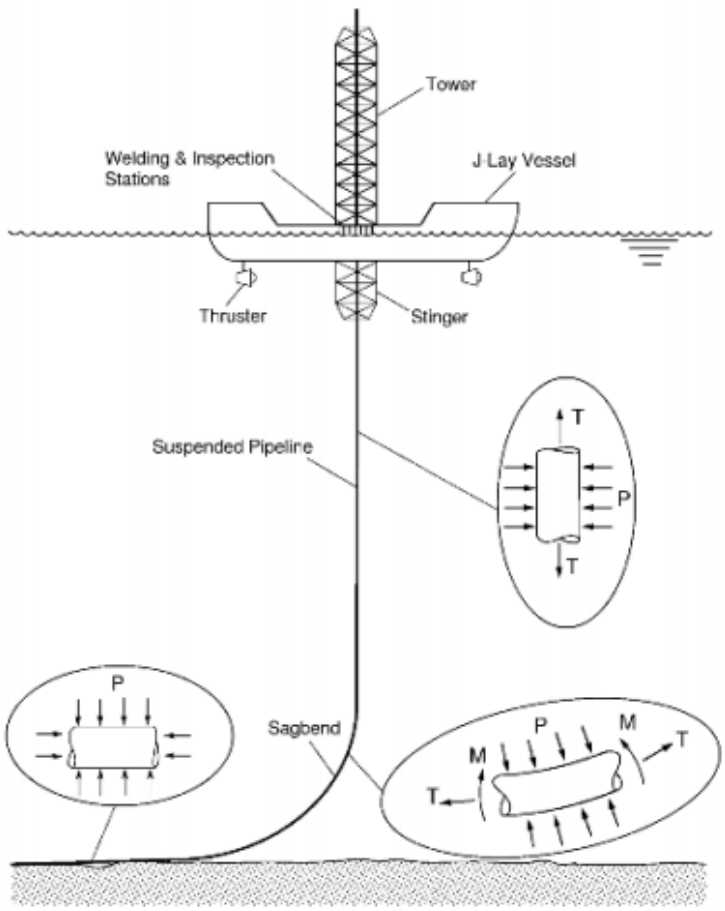

Figure 2-5: J-lay Configuration and Loading (Kyriakides and Corona, 2007)

Figure 2-6: J-lay installation Vessel (Courtesy of Subsea7)

2.2.3 Reel Lay Method

The Reel lay method is a very efficient installation methods and it is generally suited for laying small diameter cables, umbilicals and flexible pipes and for small–diameter rigid pipes (up to 18 inches) without concrete coating. The first application of the reeled pipeline was on D-Day when the allies were supplied with fuel across the English Channel using a small diameter pipeline unreeled from a vessel. Commercial application of reeled pipeline technology was not available until the early 1970s when Santa Fe Corporation built the first reel vessel (*Boyun et al., 2005).*

The main components needed for a successful installation of pipeline using the J-lay method are as follows;

- Reeling Vessel
- Tensioner
- Straightner
- Abandoments and Recovery Winch
- Reel
- Line Pipes
- Spooling Base

Detailed descriptions of these components are documented in *Kyriakides and Corona (2007)*

Principle of Reel Lay Method

In the Reel lay method, the pipe is constructed under a controlled environment in an onshore spooling base facility and reeled onto a large diameter reel fitted on the reeling vessel at the spooling–base. The loaded vessel then travels to the installation site where the pipe is unreeled, straightened (because of the large strain, in the range of 2%, it experience when spooled onto the reel drum), de-ovalized, and connected to the wire rope from the seabed pre-installed hold back anchor while the reeling vessel moves. As the vessel moves the pipe is unspooled from the reel, the pipe is straighned and paid into the sea via stinger (see Figures 2-7 and 2-8). When the entire pipe in the reel drum has been unreeled, the end of the pipeline is then lowered to the seabed via pullhead of the A&R wire rope. The reel vessel returns to the spool base to load more welded pipeline on the reel drum. On returning, it pulls the end of the pipeline using the A&R cable, removes the pullhead, and welds it to the pipeline on the drum. It then begins the unreeling process

again. (*Boyun et al., 2005).* It is worthy of note that reeling vessel can be either barge shaped or ship shaped, this govern the orientation of the reel (horizontal and vertical respectively) and the presence of a stinger and J-lay tower respectively.

Implication of Reel Lay Method

The flexibility reel lay makes it a very efficient method of pipelaying as it combine the strength of both S-lay and J-lay in the form of horizontal and vertical reel configurations. The use of these reel configuration is project specific, with the horizontal reel configuration been adopted in the case of shallow to intermediate water depth and the vertical reel used in the case of deep water depth. Since the assembly of the pipeline is done in an onshore facility the reel lay technology also provides a safer and more stable work environment, thus speeding pipeline installation up to 10 times faster than conventional pipelay (*Boyun et al., 2005).*

However the use of reel lay technology is limited by concrete coated pipeline, pipe-in-pipe pipelined designed specifically for the operation, presence of buckling in the pipeline, thinning of pipe and coating wall, loss of yield strength of the pipe material in some localized area

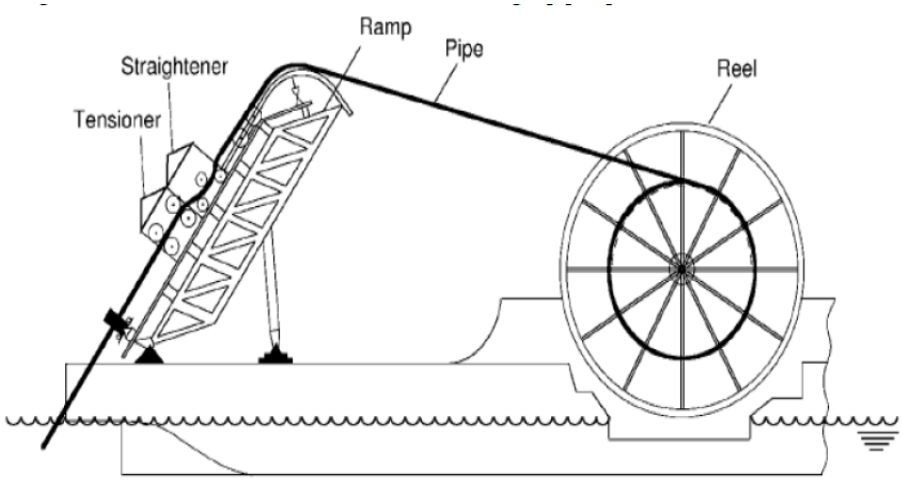

Figure 2-7: Reeling installation Configuration (Kyriakides & Corona, 2007)

Figure 2-8: Reel Lay installation Vessel (Denniel, 2009)

2.2.4 Tow Method

The tow method of pipelay has not enjoyed wide application due to its limitation of pipe size but it is an efficient method of installing pipeline across wide rivers and inland lakes as well as offshore. It is advantageous in the sense that the line pipes can be welded in an onshore facility with an onshore pipeline spread and once welding is completed, the pipeline is hydrotested, dewatered and attached to the tow vessel/barge through an anchor handling vessel, after which it is towed/moved to the offshore site where the pipeline is to be installed, see Figure 2-10. At the offshore site the whole length of pipeline and its end structures are aligned one straight line, then towing of the pipeline by the tow barge commenced along the pre-determined tow route. A major advantage of the tow method is it capability to install several small pipelines which can be laid in bundle inside a larger pipe.

Depending of the location of the towed pipeline, there are different types of tow method (see Figure 2-9), and the type to be considered is project specific and a case-by-case analysis will be required to evaluate the risk involved.

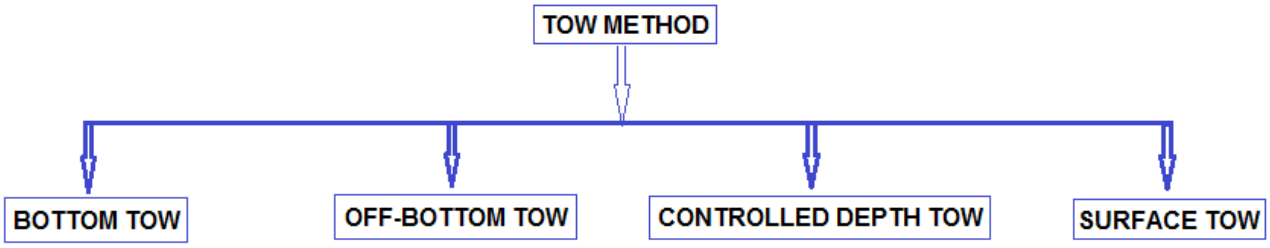

Figure 2-9: Types of Tow Method of Pipe lay

Detailed description of these different tow methods are documented in *Boyun et al., 2005.*

Figure 2-10: Tow installation - Pipeline ready to be towed (Courtesy of Subsea7)

2.3 PIPELINE LOADS DURING INSTALLATION

There are several loads the pipeline is subjected to during laying regardless of the method of installation. According to *Small (1970)* these loads can be static and/or dynamic depending on the source of the load, these sources can be either or combination of the following;

- Gravitation
- Operation
- Environmental
- Construction

However this section will focus on the most important load that affect the static configuration of the pipeline during installation. These loads are the pipelay tension and the installation load.

2.3.1 Pipelay Tension

The pipelay tension applied to the pipeline at the tensioner is a very important load that controls the configuration of the pipeline, thus it is a major parameter that must be optimized to for the pipelay operation to be successful. The primary function of the lay-tension is to sustain the submerged weight of the pipeline behind the lay vessel as vessel moves forward and more length pipe is been paid out. The value of the lay tension is largely dependent on the water depth, the pipe properties such as diameter and weight.

Pipe laying operation requires that a pipeline installation analysis be performed prior to the laying operation, the installation analysis to be performed can be only static analysis, however dynamic analysis maybe required depending on if the pipeline, equipment and/or vessel capacity is been exceeded based the outcome of the static analysis, this occurs most especially for installation in deep waters. Hence pipelay tension can either be a static load or dynamic load and it can be categorized as construction and operation loads. Vessel motion, hydrodynamics loads and support condition at the TDP on the seabed are the additional parameters that influence the value of the pipelay tension.

For S-lay method of installation, consider the free-body geometry of the pipeline during installation with only the lay tension and components of the pipeline axial force indicated as shown in Figure 2-11.

Assuming no external force is acting on the pipeline, at static equilibrium, the resolution of forces in the horizontal direction is given as;

$$H + H_0 = 0 \tag{2.1}$$

H and $\mathbf{H_0}$ are the horizontal forces acting at the vessel tensioner and at the TDP respectively.

Force resolution in the vertical direction gives;

$$V = w_S L \tag{2.2}$$

Where **V** is the vertical component of the axial tension, $\mathbf{w_s}$ is the submerged weight per unit length of the pipeline and **L** is the length of the suspended pipe.

In terms of the axial tension T and the lift angle **ɵ,** the vertical and horizontal components are;

$$H = T\sin\theta \tag{2.3}$$

$$V = T\sin\theta \tag{2.4}$$

Thus the axial tension is given as;

$$T = \sqrt{H^2 + V^2} \tag{2.5}$$

In order to keep the free spans low, to have a reduced residual tension in the pipeline and shorter radii of

the curve segment, it is a recommended practice to maintain a low horizontal tension at the touchdown point. This also has the advantage of reducing the fuel consumption of the lay vessel during the lay operation, as well as reduces the need for seabed preparation. However high tension results in low span, low bending stress, high tension stress and low equivalent stress.

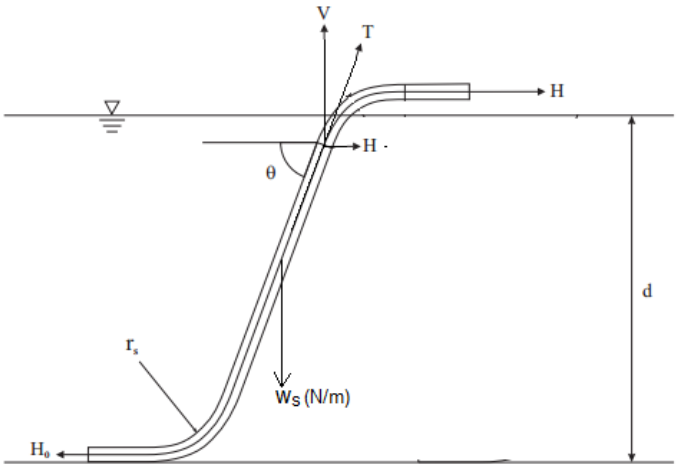

Figure 2-11: Pipeline S-lay Equilibrium Configuration

2.3.2 Pipeline Installation Loads

We regard every other load acting on the pipeline during the laying operation asides the lay-tension as pipeline installation loads and these include but not limited to the following load

- The dry weight of the pipeline
- The buoyancy force due to submergence in water
- The hydrodynamic load which include waves and currents
- Frictional resistant due to pipe-soil interaction
- Vessel motion due to environmental loads including waves and wind

Detailed description of these loads are given in several literatures such as *Gullik Anthon J., 2010*

2.4 PIPELINE CONFIGURATION AND BENDING STRESS

Pipeline assume a static configuration regardless of the installation method considered, this configuration is as a result of combination of load, such as tension, bending, pressure and contact forces at the stinger and at the seabed, the pipeline is subjected to during laying. However, the configuration the pipeline assumes is largely dependent on the pipe-laying method.

The focus of this thesis work is on S-lay method of pipeline installation, thus for the parameters that govern the static configuration of a pipeline installed by S-lay method as identified by *Bai and Bai, (2005)* is thus shown in Figure 2-12.

- Tension at the pipelay vessel
- Radius of curvature for the stinger
- Roller positions
- Departure angle form stinger
- Pipe weight
- Pipe bending stiffness

- Water depth.

As shown in Figure 2-12, the most important section of the pipeline in S- configuration are the over-bend, and the sag bend. This is because these segments are subjected to not only axial tension T and external pressure P, but also bending moments M, as a result of curvature and contact force from the stinger.

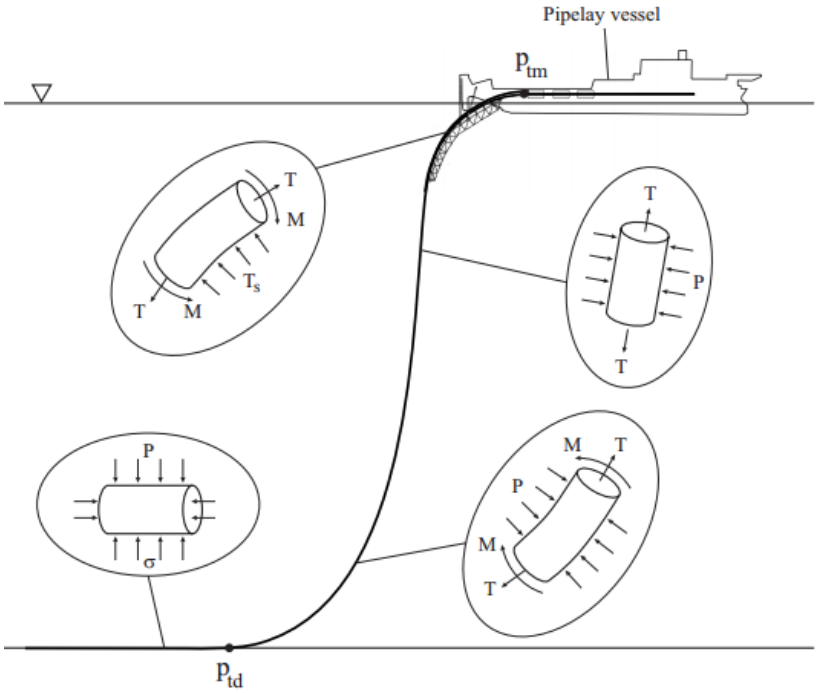

Figure 2-12; Loads on the equilibrium configuration for S–Lay pipe (Gullik Anthon J., 2010)

2.4.1 Curvature in Over-bend

The Over-bend in S-configuration is the segment of the pipeline that is fully supported by the stinger through the roller, as such the geometry and curvature of this pipeline segment is fully controlled by the stinger (see Figure 2-13). The stinger is usually curve in geometry and it provides support to the rollers which are spaced depending on the curvature of the stinger. Thus stinger provides a curve support to the pipeline with an overall radius of curvature, hence this result in bending moments and strains in the pipeline. This strain needs to be checked to ensure it does not exceed the allowable strain level stipulated in some international codes. A typical allowable strain level according to DNV OS-F101 is provided in Table 2-1. One major consequence of the over-bend strains exceeding the allowable range is a potential rotation of the pipeline during the installation and eventual twisting on the seabed due to the resistance against rotation provided by soil friction on the seabed. Also, the bending moment is not constant along the pipeline stinger as the rollers do not provide a continuous support to the pipeline and the stinger does not as well provide a support with constant curvature *(Bai Y., 2001),* hence the distribution of moments in the pipeline over the stinger is as shown in Figure 2-13.

It should be noted that the roller contacts are mono lateral and *Callegari et al., (2000)* identifies that from the third roller counted from the tip and up, the configuration and curvature of the pipe section is displacement-controlled. This therefore means that the properties of stinger and roller governs the pipeline displacement

One primary goal of an installation analysis will be to determine the stinger configuration that best suit the pipeline installation at hand, thus it is very imperative to represent the stinger geometry as accurate as

possible in the finite element model.

The bending stress in the over-bend region is given as follows

$$\sigma_A = \frac{ED}{2R_{CV}} \tag{2.6}$$

Thus the minimum radius of curvature of the pipeline that keeps the pipe in elastic state is estimated to be;

$$R_{CV.} = \frac{ED}{2\sigma_y f_D} \tag{2.7}$$

Where E is the elastic modulus, D is the pipe outer diameter, R_{cv} is the radius of curvature of the pipeline, $\boldsymbol{\sigma}_y$ is the yield stress of the pipeline, $\boldsymbol{\sigma}_A$ is the axial bending stress and f_D is the design factor usually given as 0.85

Table 2-1; Overbend Simplified Criteria (DNV OS-F101, 2000)

Criterion	X70	X65	X60	X52
I	0.270%	0.250%	0.230%	0.205%
II	0.325%	0.305%	0.290%	0.260%

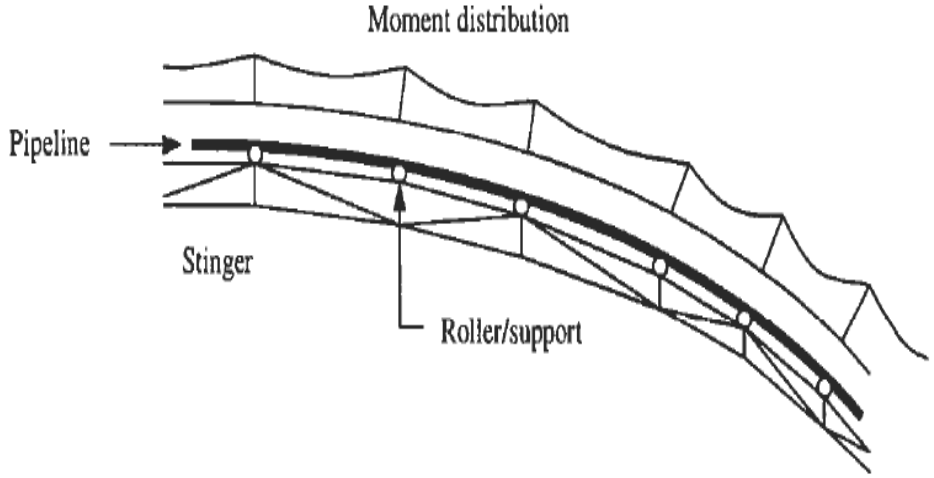

Figure 2-13: Pipeline and Moment Distribution over Stinger (Bai Y., 2001)

2.4.2 Curvature in Sag Bend

The pipeline assumes sag-bend curvature as the pipe is been paid out from the vessel, thus the free span region from the inflection point after the end of the stinger to the touchdown point is the sag-bend. The sag-bend curvature is formed as a result of the axial tension, the submerged weight of the pipe, the properties of the pipe such as bending stiffness and the externa pressure due to sea water, these factors govern the static load effect experienced by the pipeline in the sag-bend. Unlike the over-bend, the equilibrium configuration of the pipeline in the sag bend is load-controlled since there is absence of physical boundaries such as roller/support in the case of the over-bend. Thus the configuration of the pipeline in the sag-bend is considered essentially the same. Figure 2-14 shows the configuration of the pipeline in the sag-bend as well as the loads, such as the submerged weight w_s and axial tension T, acting on it. As seen in Figure 2-14, there are two components of the axial tension, the vertical component T_v

and the horizontal component T_h. The vertical component varies along the length of the pipeline because of the pipeline submerged weight and reaching maximum at the stinger and it is that the vertical component should be approximately zero at the TDP on the seabed. While the horizontal component is constant although the length of the pipeline. The pipelines shall be controlled against the load controlled condition criteria in the sagbend, according to DNV (2007).

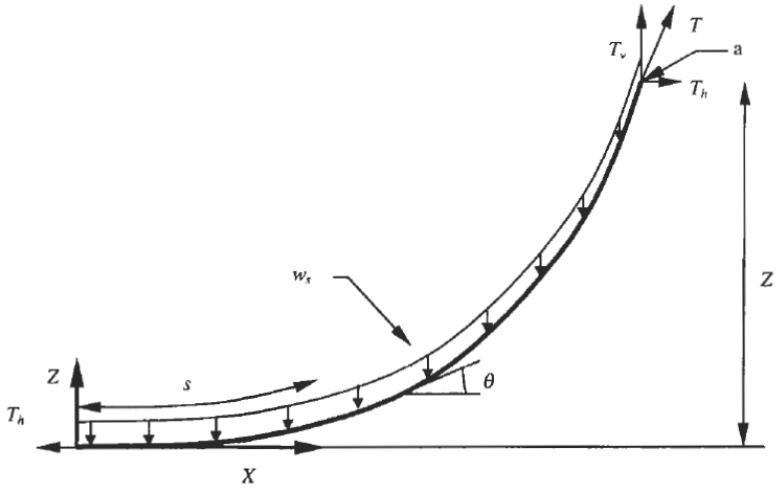

Figure 2-14: Pipeline and Moment Distribution over Stinger (Bai Y., 2001)

2.4.3 Bending Stress in Pipeline

As identified in section 2.4, the overbend and the sagbend regions are considered as critical region in S-laying, while the region that extend from the tensioner to the lift-off pointm where the stinger no longer give support to the pipeline is the overbend, the sagbend is the extends from the inflection point to the TDP. These two regions posses a major concern during installation because beside the tension and external pressure acting on the pipeline during laying theses regions are susceptible to bending stresses/strains as shown in Figure 2-12. Thus during installation of the pipeline, it is very imperative to check that these bending stresses and strains are within the allowable range provided by the international standards and codes such as API RP 1111, and DNV OS F101 2000.

It is worthy of note that the Reel lay method could also be prone to bending stresses/strain at one or the two regions depending on the type of Reel lay adopted and it goes further to set the pipeline into a cycle of plastic deformation and straightening during spooling and unreeling while in J-lay bending is only experienced in sagbend region (see description of J-lay in section 2-2).

In order to fully understand the principle of bending stress/strain during installation and also on which most of the computer application used for pipeline installation analyses, such as OFFPIPE, ANSYS, FLECOM 3D ORCAFLEX etc., are built-on, it is very necessary to examine the basic differential equations that describe the shape or catenary of the pipeline during laying especially in the sagbend region.

There are several methods of approximating the pipeline shape during installation; these methods are classified as either analytical or numerical. The major difference between these method of approximation is in the assumptions made and the boundary conditions. Figure 2-15 shows the classification of the different methods

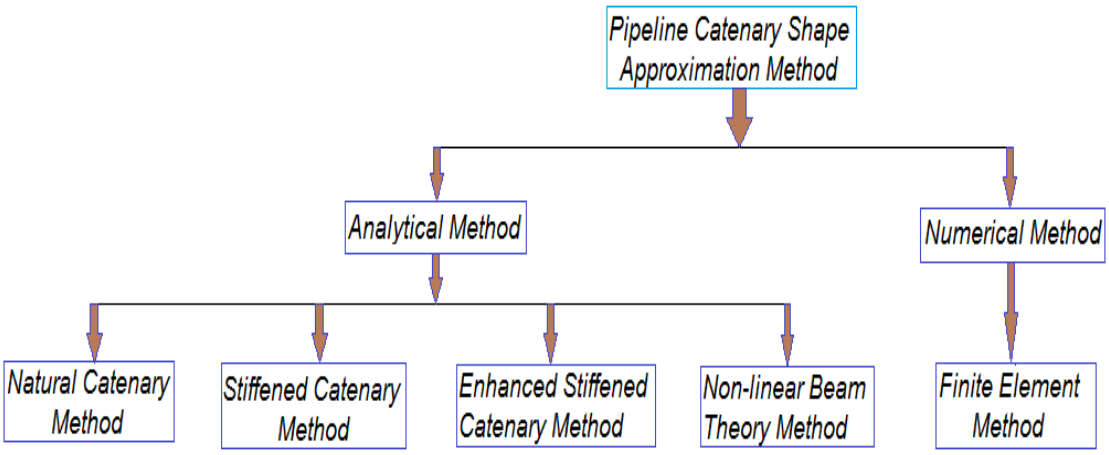

Figure 2-15: Methods of Pipeline Shape Approximation

Details of descriptions of all these methods are documented in several expert literatures, journals, publications such as *Plunkett R., (1967),* however a cursory descriptions are given in this section

Natural Catenary Method

The natural catenary is the simplest method of approximating the pipe shape in lay configuration, the curvature is developed ignoring the pipe bending stiffness and the dynamic stresses in the pipe. This was achieved by assuming the same top boundary condition of a natural catenary see Figure 2-16. By resolving the forces in Figure 2-16, we obtained the classical equation of natural catenary *(NOU, 1974);*

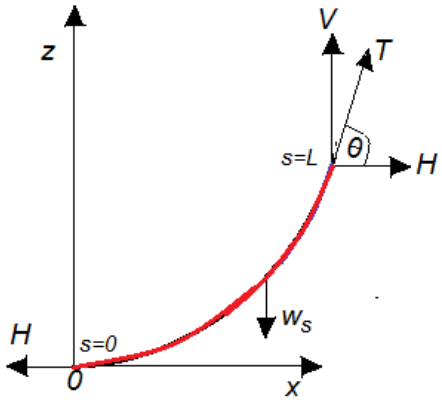

Figure 2-16: Pipeline Geometry during Installation

$$z = \frac{H}{W_S}\left[cosh\left(\frac{x.W_S}{H}\right) - 1\right] \quad (2.8)$$

$$\theta = \left[tan^{-1}\left(\frac{s.W_S}{H}\right) - 1\right] \quad (2.9)$$

Where the length of the free span s, is given as (NOU, 1974);

$$s = z.\sqrt{\left[1 + 2\left(\frac{H}{z.W_S}\right)\right]} \quad (2.10)$$

$$\frac{d\theta}{ds} = k = \frac{1}{R} = \left(\frac{a}{a^2 + s^2}\right) \quad (2.11)$$

Equation for the minimum tension to avoid plastic deformation of the pipe is given as;

$$T = W_S\left[\left(D_w + \frac{r}{\varepsilon_0}\right) + W_d x\right] \quad (2.12)$$

Where z = height above seafloor in meter
x=horizontal distance from TDP to the lay barge
W_s=submerged weight of the pipeline N/m
H=horizontal component of the axial tension
V=vertical component of the axial tension
D_w=Water Depth
W_d= pipeline dry weight

Stiffened Catenary Method

A more realistic method of estimating the pipe catenary is the Stiffened catenary method, although it ignores the dynamic stresses in the pipe however it incorporates the pipe bending stiffness. This method is most suitable for describing the catenary of the pipeline in shallow water. *Dixon et al., (1968)* pointed out that for the analysis of stiff and short pipes, the pipe bending stiffness is of significant importance. This method of approximation does not adopt the boundary condition of a natural catenary, but the boundary conditions used to derive the curvature are very complex compare to the ones used in natural catenary. It is also considered to be a good method as it approximates nearly all the length of the catenary due to its incorporation of the pipe bending stiffness.

In order to incorporate the effect of the bending stiffness and axial tension on the pipeline curvature, non-dimensional terms α_s and h respectively were introduced. These quantities are defined as *Plunkett R., (1967);*

$$\propto_s{}^2 = \left(\frac{EI}{W_S L^3}\right) \; and \quad h = \left(\frac{H}{W_S L}\right)$$

The ratio of the two non-dimensional quantities indicates the impact of the bending stiffness and the tension on the pipeline catenary shape and it varies between 0 and 1.

$$0 \leq \frac{\propto_S{}^3}{h^2} \leq 1$$

The water depth as a function of the two non-dimensional quantities and length of the pipeline can be estimated as;

$$D_w = L\left[\sqrt{h^2+1} - \sqrt{h^2 + \frac{\propto_S{}^2}{h}} + \propto_S{}^2 \left(\frac{1}{\sqrt{h}(h^2 + \frac{\propto_S{}^2}{h})^{\frac{3}{4}}} - \frac{h^2}{(h^2+1)^2}\right)\right] \quad (2.13)$$

The minimum axial tension and the top angle is as given as

$$T = W_S L\sqrt{h^2+1} \quad (2.14)$$

$$\theta = \left[\frac{\pi}{2} - tan^{-1}(h) - \frac{\propto_s h}{(h^2+1)^{\frac{1}{4}}}\right] \quad (2.15)$$

Applying boundary conditions to equation 2.13 and 2.15 by setting them to zero, the stiffened catenary equation is given as;

$$\frac{d\theta}{ds} = k = \frac{1}{R} = \left[\frac{a}{a^2+s^2}\right] - \left[\frac{a}{(a+D_w)^2}\right] e^{(\frac{s}{\gamma} - \frac{L}{\gamma})} \quad (2.16)$$

$$T = \sqrt{\frac{EI}{H}} \quad (2.17)$$

Enhanced Stiffened Catenary Method

An improved method of the Stiffened Catenary method is the Enhanced Stiffened Catenary method, this method introduced an additional load factor that add the effect of the horizontal tension in order to improve the accuracy of the boundary condition at the seabed. The enhanced stiffened catenary equation according to *Endal et al., (2014)* is given as;

$$\frac{d\theta}{ds} = k = \frac{1}{R} = \left[\frac{a}{a^2+s^2}\right] - \left[\frac{a}{(a+D_w)^2}\right] e^{(\frac{s}{\gamma} - \frac{L}{\gamma})} - \left[\frac{a}{(a+s)^2}\right] \frac{e^{(\frac{L}{\lambda} - \frac{s}{\lambda})}}{e^{(\frac{L}{\lambda})}} \quad (2.18)$$

Where the additional load factor **λ** that incorporate the effect of the horizontal tension is given as

$$T = \sqrt{\frac{EI}{H}} \quad (2.19)$$

Non-Linear Beam Theory

This method is best suited for estimating the pipeline internal shear force, bending moments and normal force. The differential equation can be derived by considering a finite element of the pipeline in the sagbend region as shown in Figure 2-17. The Figure shows the forces acting on a small element of length ds, the unit submerged weight w_s , the bending moment M and differential moment dM, the axial tension force T and its differential dT, and the angle of deviation of the element ɵ. following the derivation by *Gullik Anthon J., 2010;*

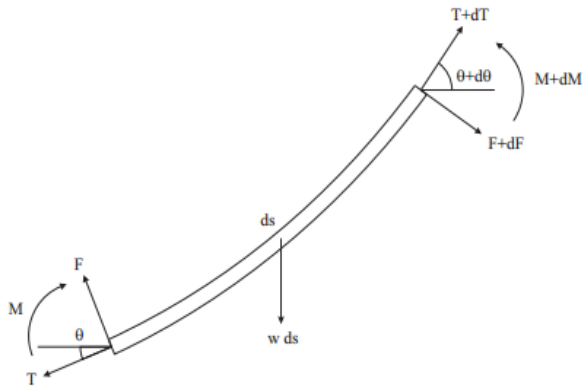

Figure 2-17: Equilibrium Forces on the Cater (Gullik Anthon J., 2010)

At equilibrium, resolving the forces in the both horizontal and vertical directions gives;

$$\sum F_X = 0$$

$$(T + \delta T)\cos(\theta + \delta\theta) - T\cos(\theta) + (F + \delta F)\sin(\theta + \delta\theta) - F\sin(\theta) = 0 \quad (2.20)$$

$$\sum F_Z = 0$$

$$(T + \delta T)\sin(\theta + \delta\theta) - T\sin(\theta) + (F + \delta F)\cos(\theta + \delta\theta) - F\cos(\theta) - ws\,\delta s = 0 \quad (2.21)$$

$$T\frac{d\theta}{ds} - \frac{dF}{ds} - w_s\cos(\theta) = 0 \quad (2.22)$$

$$k = \frac{1}{R} = \frac{M}{EI} = \frac{d\theta}{ds} \quad (2.23)$$

Where k is the curvature of the pipeline

$$F = \frac{dM}{ds} = EI\frac{d^2\theta}{ds^2} \quad (2.24)$$

Thus equation 2.22 becomes;

$$T\frac{d\theta}{ds} - EI\frac{d^3\theta}{ds^3} - w_s\cos(\theta) = 0 \quad (2.25)$$

Also resolving the forces in the pipeline axial direction at equilibrium we have;

$$\sum F_A = 0$$

$$(T + \delta T)\cos(\delta\theta) - T - Ws\,\delta s.\sin(\theta + \delta\theta) - F\sin(\theta) = 0 \quad (2.26)$$

$$\frac{dT}{ds} = w_s\cos(\theta) \quad (2.27)$$

When equation 2.25 is decomposed, the horizontal component of the axial tension becomes;

$$H_0 = T\cos(\theta) + F\sin(\theta) \quad (2.28)$$

Where H_0 is the effective lower pipe tension EI is the pipe bending stiffness

$$EI\frac{d}{ds}\left(\sec(\theta)\frac{d^2\theta}{ds^2}\right) - H_0\sec^2(\theta)\frac{d\theta}{ds} - w_s = 0 \quad (2.29)$$

The differential equation 2.15 is a 2nd order non-linear degree bending equation, which can be solve by numerical methods or by simplications through assumptions and it is applicable most especially to the sagbend region and suitable for both deep and shallow water application for all method of pipe-lay and it is also valid for both small and large deflection *(Seyed and Patel, 1992).* In a situation where the effect of an existing force V, such as current/waves, the non-linear differential equations becomes *(Zeng et al., 2014);*

$$EI\frac{d^2\theta}{ds^2} + EI\frac{d}{ds}\left(sec(\theta)\frac{d^2\theta}{ds^2}\right) - H_0sec^2(\theta)\frac{d\theta}{ds} - W_s + V\tan(\theta) = 0 \quad (2.30)$$

Equations 2.27 and/or 2.28 can be solved by the application of boundary conditions at the end points of the pipeline length s, at the TDP on the seabed where s=0 and at the first connecting between the pipeline and the lay barge point, where s=L. by determining the pipeline rotations, the slope, the bending moments and the shear/normal forces at these two locations. It should be observed that in the case where the bending stiffness is ignored, that is EI, the equations yield the solution of a natural catenary.

Finite Element Method

The Finite element method is a numerical method of approximating the catenary shape. There are several commercial computer applications that can be used, this software are not limited to ANSYS, ABAQUS etc. this method gives a high level of accuracy as compared with the other methods

2.5 PIPELINE INSTALLATION CHALLENGES

There are quite a number of difficulties encountered during the installation of pipeline using S-lay method, as the pipe is subjected to several loads, passes through several stages and phases of the installation operation from welding the line pipes at the firing line, to passing through the tensioner and then over the stinger to the touch down point. Upon passing over the stinger structure in S-laying, the pipe section and the whole length of the pipeline from the tensioner to the touch down point on the seabed, experience the following conditions;

- Strain concentration and Residual strain
- rotation
- twisting
- Ovality

These parameters influence the behavior of the pipeline, from the surface to the TDP. There are scenarios that require a good understanding of the behavior of the pipeline such as where inline structures are to be installed along with the pipeline; hence it is imperative to evaluate the causes, implications and estimations of these factors, which are discussed in details in section 3 of this thesis.

2.6 PIPELINE ON UNEVEN SEABED

The different methods of pipeline have been discuss in previous section, it should be noted that pipelines are laid either as buried pipeline, where it is embedded in a trench or laid as unburied pipeline. In practice, due to rapid and economic performance, most offshore pipelines are laid as unburied pipelines and these unburied pipelines are usually laid on uneven seabed as virtually all subsea fields have very irregular seabed conditions. Example of field with irregular seabed is the Ormen Lange field offshore West Norway in the Norwegian Sea (Finn et al., 2002). The uneven seabed therefore results in various length of free spanning of the pipeline on the seabed (see Figures 1-2 and 2-18), which not only threaten the safety of subsea pipeline but is also very costly to installed mitigation measures.
A cursory insight into challenges of pipeline on uneven sea bed will be discussed in section 3.

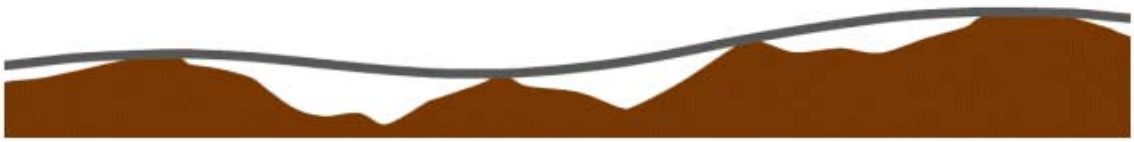

Figure 2-18: Free Spanning on Uneven Seabed

3. INTRODUCTION TO PIPELINE RESIDUAL CURVATURE AND ROTATION

In oil and gas industry steel materials is used in the manufacturing of the pipeline used in transportation of hydrocarbon. Although there are several types of steel materials (such as carbon steel, stainless steel etc) used in the industry, however type to be used is project specific and its selection might be based on several factors which are not limited to the type and properties of fluid to be transported, the life span of the oil field, client specifications and requirements, the type of environment in which the pipeline is to be installed. Details of the different steel types and their applications can be found in several expert textbooks, rule books and company manuals. Of great importance in pipeline technology is the properties of the steels which are primarily governed by the chemical compositions, the types of treatments and manufacturing processes *(Staff Awwa, 2004)*. The steel properties that are considered to be of utmost importance in pipeline design and installation for you in the oil and gas industry are;

- The Yield Strength; which represent the ability of the steel to deflect under the influence of load,
- The Ductility; which represents the ability to bend without breaking
- The Toughness; which represent the ability of the steel to resist or absorb shock load

Other properties are the weldability and the durability. Detailed description of these properties can be found in textbooks such as *Bhadeshia and Honeycombe, (2006)*.

When steel are materials are subjected to load per unit area called stress, thus the material stretches as a result of the stress, the change in length, area and/or volume of the material is termed strain which could be a linear, plane and volumetric strains respectively. The relationship between the stress and the strains is described by the stress-strain curve. For steel material this curve is shown in Figure 3-1.

Upon application of stress **σ** on steels, it experiences deformation and change in shape per unit length and the cross-section decreases in area up to the maximum or ultimate tensile strength of the steel, where it begins to experience necking, where local reduction of steel area begins.(F in Figure 3-1). Figure 3-1 shows the various parts of the stress-strain curve for steel. The straight or nearly straight portion (**A to B**) of the curve indicates the elastic region, where the stress range does not exceed the elastic limit of the steel material, a loaded steel within this range regains its initial status when unloaded. This straight region has a slope equivalent to the elastic modulus **E** of the steel material. The modulus of elasticity for steel is approximately 762TPa *(Staff Awwa, 2004)*. The expression for the modulus of elasticity is given as;

$$E = \frac{\text{Stress}}{\text{Strain}} = \frac{\sigma}{\varepsilon} \tag{3.1}$$

Where

$$\sigma = \frac{\text{Applied Load}}{\text{Cross} - \text{sectional Area}} = \frac{P}{A} \tag{3.2}$$

$$\varepsilon = \frac{\text{Change in Length}}{\text{Original Length}} = \frac{\Delta L}{L} \tag{3.3}$$

Continuous loading of the steel will cause the material to reach and exceed its proportional limit, where the deviation from the straight portion begins (point B). Between point B and C, occurs the offset strains and a further loading beyond the yield strength of the steel results plastic deformation of the steel material, where permanent deformation occur even after unloading the steel material. As shown in the Figure 3-1, at point C there is a total or nominal strain which equals the sum of the plastic and the elastic strains. The plastic strain

leaves the steel material with a residual strain, which is the strain remaining in the steel material after unloading or removing the applied stress.

The residual strain is obtained by drawing a parallel line to the elastic region of the curve, from the intersection point of the line drawn from the normal stress axis corresponding to the normal stress causing the residual strain and the stress-strain curve, to the normal strain axis. The corresponding strain is the residual strain, see Figure 3-1.

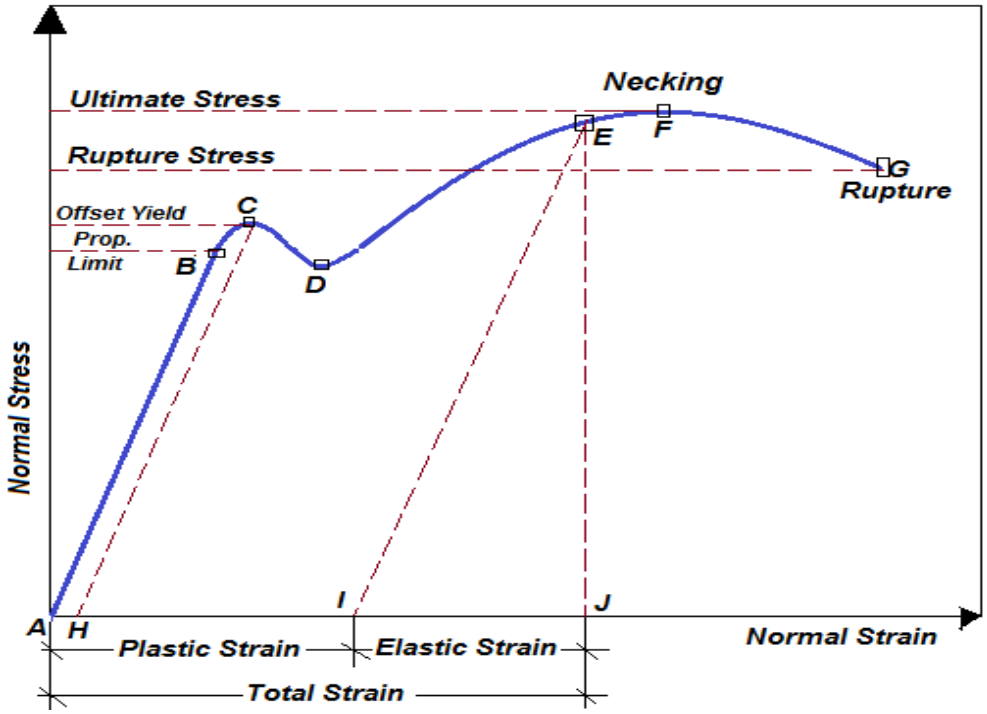

Figure 3-1: Stress-Stain Curve for Steel Material

3.1 RESIDUAL CURVATURE DURING INSTALLATION OF PIPELINE

During pipe lay operations, pipeline is subjected to plastic strains as they travels or passes over the stinger in the case of S-lay method of laying. The pipeline undergoes bending beyond its elastic limit into the yield point, thus having a permanent or residual curvature as its leaves the stinger. There are several causes of residual curvature in pipeline this causes are not limited to

- Uneven Seabed,
- Higher Strains in Sagbend
- Higher Strains in Overbend Region on the Stinger.

Upon passing the inflection point in the suspended section, the pipeline experience reversed bending at the under bend region (sag bend); this is as a result of partial bending and twisting of the pipeline due to sag by its self weight. The pipeline will have residual curvature which results from corresponding residual strain when it is installed at the seabed because it has been exposed to plastic strains *(Endal et al., 1995)*. In Reel lay method of laying the plastic strains by when spooling, unspooling of the pipeline on the reel and when passing it over the ramp/aligner.

Residual curvature section is now widely applicable today, as it presence along the pipeline has been optimized to meet some of the challenges faced in pipeline technology as well as a means to reduce the cost

of installation. As such residual curvatures are now intentional created along the pipeline to in order to meet some of these challenges. The local residual curvature sections generated is achieved in S-lay method by the use of the active roller or stinger adjustments and in the Reel-lay method by the active use of the hydraulic adjustment of the straightener system, this method was patented by Statoil in 2002 in Norway, Denmark, UK and USA *(Endal and Nystrøm, 2015*). Its importance is highlighted in the next section.

3.1.1 Estimation of Residual Curvature

The plastic bending deformation experienced by the pipeline when it passed over the stinger during S-laying can be estimated based on the stinger configuration, it surface condition and the roller spacing. According to *Yousun Li (2005),* for smooth stinger surface condition, the strain distribution, at any point y along the pipe centerline, in the pipe cross-section A, is the sum of the elastic strain caused by barge tension TB and the elastic-plastic strain around the stinger. It is thus written as;

$$\varepsilon_{st} = \frac{T_B}{EA} + \frac{y}{R_{st}} \tag{3.4}$$

Where R_{st} = radius from pipe centerline to stinger centerline.

The pipe stress is relieved and the moment redistributed immediate it leaves the stinger and a residual radius R_{res} is therefore formed. For equilibrium, the moment will be zero

$$M = E\int_A^- \left(\frac{y}{R_{res}} - \varepsilon_{plt}(y)\right) y dA = 0 \tag{3.5}$$

Where residual plastic deformation is given for ideal material as;

$$\varepsilon_{plt}(y) = 0 \qquad if\ \varepsilon_{st}(y) \leq \varepsilon_y \text{ and}$$

$$\varepsilon_{plt}(y) = \varepsilon_{st}(y) - \varepsilon_y \qquad if\ \varepsilon_{st}(y) > \varepsilon_y$$

and ε_y is the yield strain. Thus for practical situation equations 3.5 and 3.6 can be adopted for computing the residual curvature.

3.1.2 Benefits of Residual Curvature in Pipeline Technology

Residual curvature sections have been found very useful in meeting some offshore pipeline installation challenges in both reel-lay and S-lay methods, detailed emphasis on the benefits of local residual curvature in pipeline laying are documented in *Endal and Nystrøm, (2015).* Although residual curvature causes pipeline rotation, however it has quite a lot of advantages *(Endal et al., 1995),* the benefits of creating local residual curvature of different configurations (that is residual strains and lengths) along the length of the pipeline, most especially in deep water, are not limited to the following.

- Large residual curvature due to stinger curvature will permit reduced tension in the pipe end and, on an uneven seabed, hence less rectification or intervention of free spans *(Endal et al., 1995).*
- For large diameter pipes in deep water the total suspended submerged weight can be so large that the pipe cannot be installed due to the limited tension capacity of the laybarge. In such cases the weight must be reduced and the pipe stabilized by trenching. Larger stinger curvature, however, may allow installation of heavy large diameter pipes *(Endal et al., 1995)*.
- Larger curvature of the stinger will result in further cost-reductions being expected since the

frequency of the laybarge modifications when installing a new pipe will be reduced *(Endal et al., 1995)*.

- The residual curvature method was used successfully to control global buckling and expansion on the 14" - 16" dual diameter Skuld pipeline in the Norwegian Sea in 2012, *Endal and Egeli (2014)*.Thus residual curvatures are used to control global buckling
- Residual curvature near the end of the pipeline can be utilized for direct tie-in of pipelines to subsea structures. This is done by solving the existing direct tie-in challenges with large forces on the connection and large pipeline stresses close to the connection point *(Nystrøm, et al., 2015)*.

Thus, it is recommended that for deep water and large diameter pipeline installation of large diameter pipeline, large plastic strain should be permitted to allow for cost saving.

3.2 PIPELINE ROTATIONS DURING S-LAY INSTALLATION

As mentioned in section 3.1, the pipeline experienced plastic strain due to bending beyond the elastic range when it passes through the stinger, which in turn generates a corresponding residual curvature in the pipe. Although the pipe is retrained by the tensioner on the installation vessel and by the soil friction at the sea bed, however the residual curvature may thus cause an axial rotation or torsional rotation of the pipe under its self weigh along its suspended length and thus transferred into the sagbend through the torsional stiffness of the pipeline. The rotation follows the principle of potential energy minimization and there are primarily two main driving mechanism of the rotation which and these are *(Vaughan and Nystrøm, 2016)*

- The strain energy minimization
- The gravitational energy minimization

The pipeline curvature exceeds the elastic limit and plastically hog at the overbend on the stinger and due to its self weight it sags at the sag bend region below the inflection point, *Bynum and Havik, (1981)* identifies that in some situations the pipeline requires more energy to reverse-bend the pipe into the sagbend than to distort the pipe torsionally, thus the pipeline tends to rotate during installation.

Additional factors that contribute to the rotation of pipeline during installation are not limited to the ones listed below. Details of the influence of some of these factors on rotation was investigated and documented in *Endal, et al., 1995*

- possible tensioner misalignments,
- Pipeline curves or vessel offsets.
- water depth,
- pipeline characteristics (bending stiffness, submerged weight, etc) and
- stinger configuration
- laying in curves
- current and waves
- dynamics during pull
- etc

Understanding the mechanism and prediction of pipeline rotation is of utmost importance in subsea pipeline technology, especially when installing in-line components such as tees, pig launcher, control value and so on. Since it is imperative these in-line components maintain a vertical position, with a tolerance orientation angle of +/- 15deg. allowed (*Damsleth, et al., 1999)*, on the seabed, uncontrolled and excessive pipeline rotation therefore becomes problematic, thus is very important to be able to estimate or predict the rotation of pipeline at the touch down point(TDP).

3.3 METHODS OF ESTIMATING OFFSHORE PIPELINE ROTATION

There are several methods through which the pipe rotation can predicted at the TDP, these methods are as shown in Figure 3-2. This section elaborate the methods

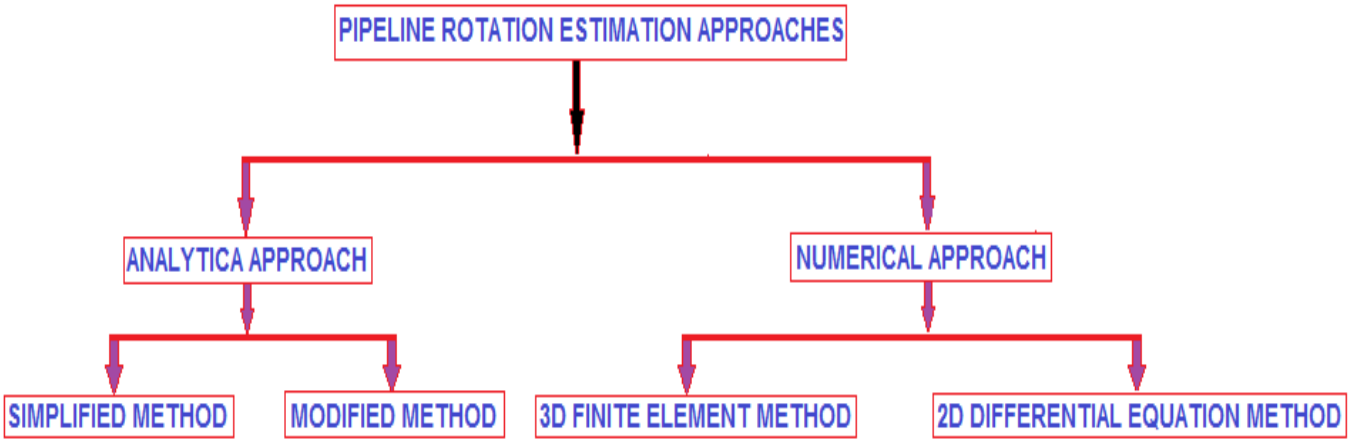

Figure 3-2: Methods of Estimating Pipeline Rotation

3.3.1 Analytical Method

This method can be classified into simplified and modified methods. It is based on the principle of potential energy minimization by employing the internal and the external virtual work balance approach. There are two types of potential minimization energy, these are;

- The strain energy minimization; this is used when plastic strain are present in the pipe
- The gravitational energy minimization; this results due to top heavy structures which are unstable and eccentric loadings such as valves, tees and so on, acting downwards causing torsion and load to increase rotation

Simplified Analytical Method

This method of pipeline rotation approximation considers only the bending and torsional effect on the pipeline without considering the rotational effect of the gravitational effect due to minimization of gravity potential energy, thus the simplified analytical approach focuses on the strain energy minimization. *Endal, et al., 1995* stated the assumptions adopted to simplify the strain energy minimization; these assumptions are as follows;

- The pipeline rolls between the inflection and TDP.
- The pipeline residual curvature is assumed to be formed on the stinger over bend region due to exceeding nominal strain ε_r. the residual curvature $\boldsymbol{K_r}$ can be found:

$$K_r = \frac{\varepsilon_r}{r} \tag{3.6}$$

- The total under bend curvature of the pipeline is the sum of nominal curvature and residual curvature K_r and it can be expressed by equation 3.7
-

$$K_{tot}(x) = K_0(x) + K_r cos\theta(x) \tag{3.7}$$

Where (x) = total curvature of the pipe and (x) = roll angle.

The expression for the pipeline nominal curvature from the inflection point to TDP as shown in Figure 3-2, can be described 2nd degree polynomial as given in equation 3.8

$$K_0(x) = \alpha x^2 + \beta x + \gamma \quad (3.8)$$

Where (x) = nominal curvature from the inflection point to the TDP.

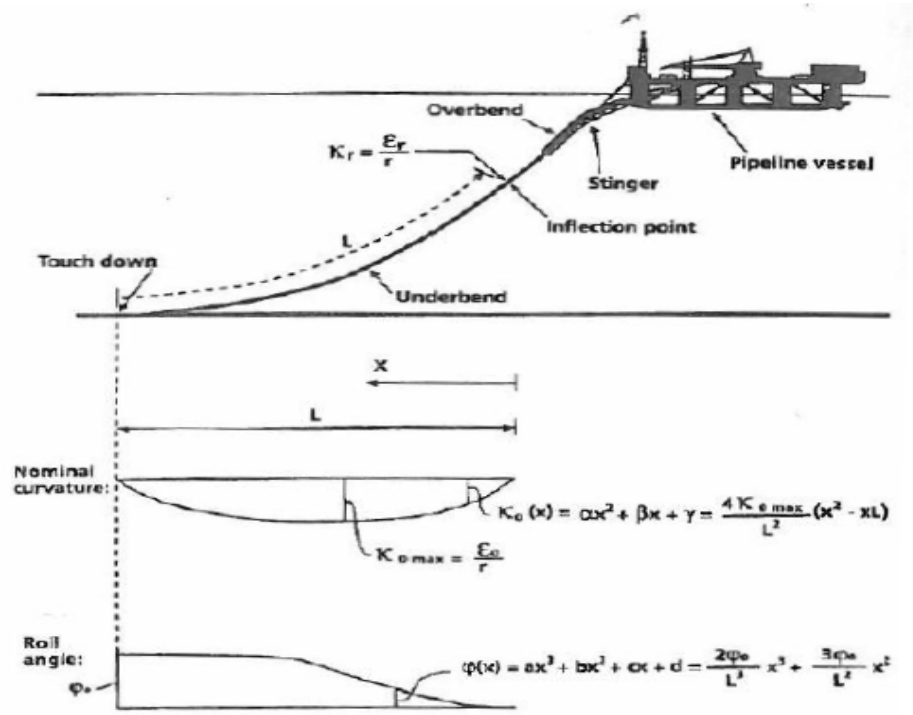

Figure 3-3: Simplified Energy Approach for S-lay installation, from (Endal, et al., 1995)

equation 3.8 can be solve using the boundary condition, $K_0(0) = K_0(L) = 0$, thus

$$K_0(x) = \frac{4K_{0(max)}}{L^2}(x^2 - Lx) \quad (3.9)$$

L =length of pipe from the inflection point to TDP.

$K_0(x)$ = the nominal pipeline curvature, the maximum nominal curvature can be derive from 3.9

$$K_{0(\max)} = \frac{\varepsilon_{0(max)}}{r} \quad (3.10)$$

Where $K_{0(max)}$ = maximum nominal curvature of the pipe,

$\varepsilon_{0(max)}$ = maximum nominal strain of the pipe,

The **Roll angle (**shown in Figure 3-3) can be expressed by a 3rd order polynomial as given in equation 3.11 *(Endal, et al., 1995).*

$$\emptyset(x) = ax^3 + bx^2 + cx + d \quad (3.11)$$

Equation 3.11 can be solved by using the boundary condition Ø (0) = Ø' (0) = Ø'' (0) = 0 and Ø (L) = $Ø_0$

$$\emptyset(x) = \frac{2\emptyset_0}{L^3}x^3 + \frac{3\emptyset_0}{L^2}x^2 \quad (3.12)$$

Thus the total work due to bending and pipe rotation is expressed as the sum of the work done due to

bending and work done due to rolling.

$$W_{tot}(\emptyset_0) = W_B(\emptyset_0) + W_R(\emptyset_0) \tag{3.13}$$

$$W_B(\emptyset_0) = \int_0^L M_B(x).K_{tot}(x)\,dx \tag{3.14}$$

$$M_B(x) = EI.K_{tot}(x) \tag{3.15}$$

$$W_R(\emptyset_0) = \int_0^L M_R(x).\emptyset(x)\,dx \tag{3.16}$$

$$M_R(x) = GI_T.\frac{d\emptyset}{dx} \tag{3.17}$$

Therefore the total work done is given as;

$$W_{tot}(\emptyset_0) = GI_T.\frac{6}{5}\emptyset_0^2 + EI\int_0^L \left[\frac{4K_{0(max)}}{L^2}(x^2 - Lx) + K_r\cos\left(\frac{2\emptyset_0}{L^3}x^3 + \frac{3\emptyset_0}{L^2}x^2\right)\right]^2 dx \tag{3.18}$$

As seen from equation 3.18, the total work done is dependent on the residual curvature K_r from the overbend, the length L of the pipeline from the inflection point to the TDP and the maximum nominal curvature $K_{0(max)}$. Equation 3.18 can be solved by making initial assumption of the roll angles, hence the solution of equation 3.18 is t the minimum value of the total work W_{tot} obtained from the several values of the roll angle and the roll angle that produces this minimum total work is the roll angle at the TDP.

Modified Analytical Method

This method is another method of calculating the minimum total work of the lay configuration, in this method the pipeline rotation is assumed to be between the top vessels to the touch down point. Only the region of pipe from the sea surface to touch down point is to be considered and is represented by length L. there are several methods of approximating the curvature of the pipeline during laying as described in section 2.4.3, however the stiffened catenary method of approximation for pipeline laying configuration is adopted for here for the estimation of the total work (see section 2.4.3 for detailed description) and the under lying assumption in this method is given as follows;

- The pipe is free to rotate at TDP while fixed at laying vessel, *Endal, et al., (2014)* shows that the modified method gives higher rolls angle at TDP this is because of the boundary conditions assumed in this method in reality, and pipeline is not free to rotate at the bottom and has some seabed friction.
- It is also assumed that rotation of the pipeline occurs between the top vessels to the touch down point, the only the section of the pipeline from the sea surface to TDP is to be considered and this length as shown in Figure 3-4 is represented as L
- Based on the complete assumption of the catenary theory, the curvature will be maximum at the TDP however, since the pipelines bending stiffness plays a pivotal role as compared with catenary system, the assumption of maximum curvature at the TDP is untrue for pipeline.
- It is assumed that the length of the pipeline from the TDP to the sea surface is simply supported at both ends, hence curvature is taken zero at the sea surface (laying vessel) and seabed. This implies that at the TDP s = 0 and at the sea surface s = L *(Endal, et al., 2014)*.

The residual curvature of the pipeline due to under-straightening region is defined as K_{res},

$$K_{res} = \frac{\varepsilon_{res}}{r} \quad (3.19)$$

Where ε_{res} = residual strain and r = outer pipeline radius.

Thus the total curvature of the pipeline is expressed by;

$$K_{tot}(s, \emptyset_0) = K_{nom}(s) + K_{res} cos\theta(s, \emptyset_0) \qquad if \quad s \leq L_{curv} \quad (3.20)$$

$$K_{tot}(s, \emptyset_0) = K_{nom}(s) \qquad otherwise \quad (3.21)$$

Where $(s, \emptyset_0)$ = total curvature of the pipe and $\theta(s, \emptyset_0)$ = roll angle.

K_{non}(s) = maximum nominal curvature of the pipe,

ε_{res} = residual strain of the pipe,

L_{curv} = length of residual curvature section, see Figure 3-4

s = distance along the pipeline, where s = 0 is located at the seabed, and s = L is located at the sea surface

$$K_{nom}(s) = \frac{a}{a^2 + s^2} - \frac{A}{(a+d)^2} e^{\left[\frac{s}{\gamma} - \frac{L}{\gamma}\right]} - \frac{a}{(a+s)^2} \frac{e^{\left[\frac{L}{\gamma} - \frac{s}{\gamma}\right]}}{e^{\left[\frac{L}{\gamma}\right]}} \quad (3.22)$$

Where d = water depth,

a is the ratio of the lay tension H, and the pipe submerged weight w_s

γ is the ratio of the bending or flexural stiffness EI and the twice the top tension T

While the **Roll angle**, as shown in Figure 3-4, can be expressed by a 2nd order polynomial as given in equation 3.23*(Endal, et al., 2014)*.

$$\emptyset(x) = bs^2 + cs + d \quad (3.23)$$

The solution of equation 3.23 was arrived at using the following boundary condition;

$$\emptyset(\mathrm{L}) = \emptyset'(0) = 0 \;\&\; \emptyset(0) = \emptyset_0$$

$$\emptyset(x) = \frac{-\emptyset_0}{L^2} s^2 + \emptyset_0 \quad (3.24)$$

$Ø_0$= Maximum torsional/roll angle at the seabed

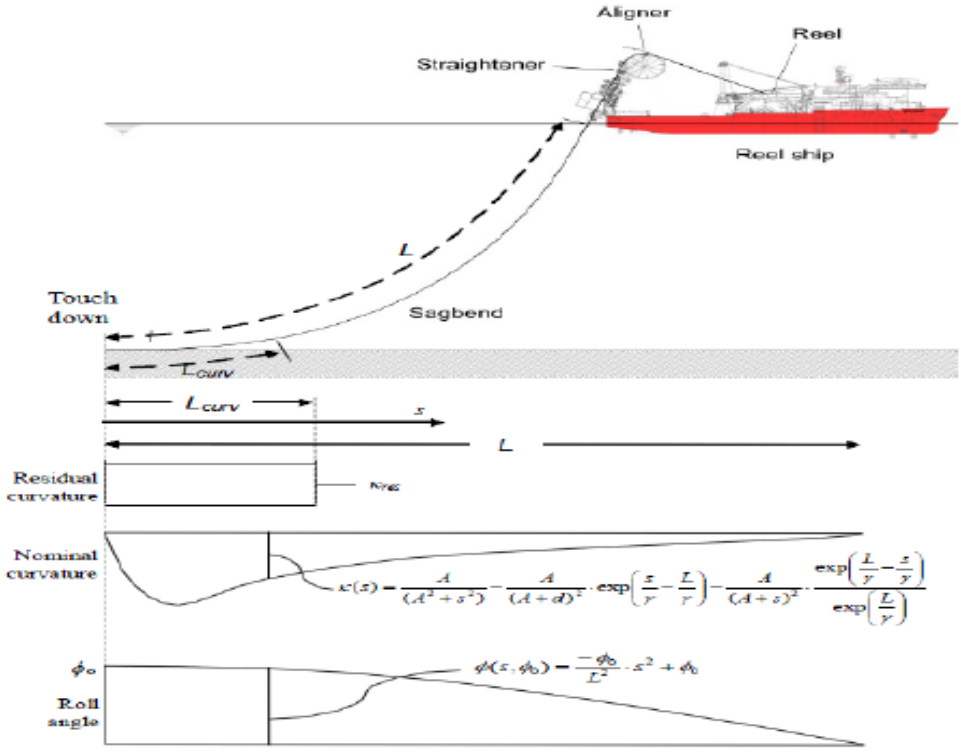

Figure 3-4: Modified analytical approach for pipeline roll prediction, from (Endal, et al., 2014)

Thus the total work due to bending and pipe rotation is expressed as the sum of the work done due to bending and work done due to rolling

$$W_{tot}(\emptyset_0) = W_B(\emptyset_0) + W_R(\emptyset_0) \tag{3.24}$$

While the bending strain energy is given as

$$W_B(\emptyset_0) = \int_0^{L_{curv}} EI[K_{nom}(s) + K_{res}\cos(\emptyset(s,\emptyset_0))]^2 dx + \int_0^{L_{curv}} EI.K_{nom}(s)ds \quad if\ L_{curv} < L \tag{3.25}$$

$$W_B(\emptyset_0) = \int_0^{L_{curv}} EI[K_{nom}(s) + K_{res}\cos(\emptyset(s,\emptyset_0))]^2 dx \quad otherwise \tag{3.26}$$

While the torsional strain energy is given as

$$W_R(\emptyset_0) = \int_0^{L} M_R(s,\emptyset_0).\frac{d}{dx}(\emptyset(s,\emptyset_0)).ds = \int_0^{L} GI_T.\left[\frac{d}{dx}(\emptyset(s,\emptyset_0))\right]^2.ds \tag{3.27}$$

$$\text{where } M_R(x) = GI_T.\frac{d\emptyset}{ds} \tag{3.28}$$

Therefore the total work done is given as;

$$W_{tot}(\emptyset_0) = \int_0^{L_{curv}} EI[K(s) + K_{res}\cos(\emptyset(s,\emptyset_0))]^2 ds + \int_0^{L_{curv}} EI.K_{nom}(s)ds + \int_0^{L} GI_T.\left[\frac{d}{ds}(\emptyset(s,\emptyset_0))\right]^2.ds \quad (3.29)$$

As seen from equation 3.18, the total work done is dependent on the residual curvature K_{res} from the overbend, the material properties and geometric configuration of the pipeline, the torsional rotational angle and the maximum nominal curvature $K_{nom(max)}$. Equation 3.18 can be solved by making initial assumption of the roll angle and iteratively solving for the total energy, hence the solution of equation 3.29 is the minimum value of the total work W_{tot} obtained from the several values of the roll angle and the roll angle that produces this minimum total work is the roll angle at the TDP.

3.3.2 Numerical Method

It has been established that rotation or twist of pipeline during installation are very difficult to predict, this is as a result of the dynamic behavior of the pipeline which is largely dependent on the pipeline characteristics, the environmental loading, vessel motions, the installation configuration and so on. Hence the effect of residual strains, residual curvature and pipe tension on pipeline rotation can as be assessed or investigated using the numerical method of approximation of the pipeline roll during laying and the roll can be predicted either by adopting a non-linear 3D finite element approach (FE) or a 2D approach using the differential equations (see Figure 3-1). It is worthy to note that there are different numerical analyses that can be adopted for estimating the pipe roll during laying *(Li Y., 2005)* regardless of the approach adopted

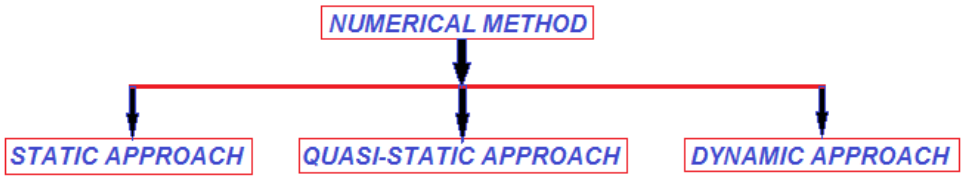

Figure 3-5: Numerical Approaches of Estimating Pipeline Rotation

3D Finite Element Method

The 3D FE numerical method is achieved through the use of commercial finite element computer program such as ANSYS and ABAQUS. These programs model the pipeline using a 6 degree of freedom (DOF) elasto-plastic beam and/or as friction contact elements and the programs are capable of investigating the existence of the potential energy minimization through a check for the presence of torsion or pipeline rotation. *Bai Y., (2001)* pointed out that *'The model will be able to compute static load effects on a pipeline during installation, based on the lay-ramp geometry, pipeline design data and water depth for the pipeline to be installed. The established model should be a tool for analyzing the static configuration of a pipeline during installation. The static configuration of the pipeline is the shape of the pipeline from the lay-vessel to the seabed when it is in static equilibrium. The model should also be capable of analyzing the load effects on the pipeline when a section like a valve is installed. The model should also be capable of letting the pipeline slide over the stinger. A pipeline cross section will then move from the lay-vessel, over the stinger and through the sagbend to the seabed.*'

The inputs for the program are as shown in Figure 3-6 *(Endal, et al., 1995);*

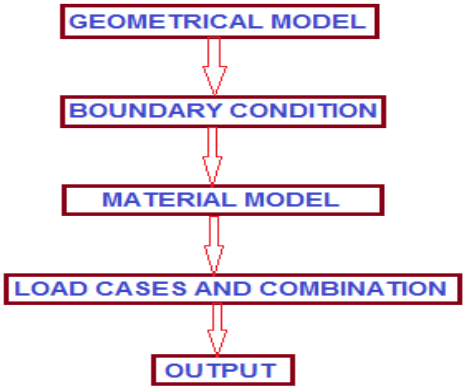

Figure 3-6: 3D Finite Element Analysis Input

1. Geometrical/Numerical Model

   To initiate a numerical analysis using the non-linear 3D FE, the first step is to define the geometric properties of the key parameters that are involve in the installation process, these parameters are;

   - The pipeline; the pipeline is modeled as a 6DOF beam element
   - The lay-barge/stinger; this is modeled as a smooth cylindrical surface, defined with coulomb friction in contact with the pipeline
   - The seabed; this is modeled as horizontal rigid plane

2. Initial/Boundary Conditions

   There are six degree of freedom, 3 translation directions and 3 rotational directions see Figure 3-7, the boundary conditions can thus be are specified in any of these directions when there is a resistance to movement in that direction. In pipe laying the boundary conditions are applied at the TDP on the seabed and at the tensioner and/or on top of the stinger. The BCs are applied to simulate real life support conditions of the pipeline and are carefully chosen to avoid pipeline instability.

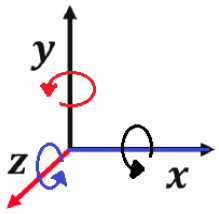

Figure 3-7: 3D Finite Element 6 Degree of Freedom

3. Material Model

   The material properties of the pipes such as the pipe diameter and thickness, coating thickness, dry and submerged pipe weight, material grade (such as API X65, X70 etc), the density, mesh density and pipeline-seabed interaction properties

4. Load cases and Load Combination

   The pipeline is subjected to several loads such as axial tension, bending moments, gravity loads etc as mentioned in section 2.3. These loads can be applied in any of the 6DOF directions depending on the directions of the load is present or acting

2D Differential Equation Method

This method is similar to the 3D FE, however it considers only 4DOF see Figure 3-8 (a), 2 translation directions and two rotational directions, with the out-of-place displacements ignored *(Endal, et al., 1995)*. Thus the pipe is modeled as 2D beam element configuration. The 2D analysis can be performed using commercial program such as ORCAFLEX and PIPELAY. This approach estimates the pipeline rotations by generating and solving a set of non-linear differential equations from the equilibrium equations of the pipe in 2D as-laid configuration. Figure 3-8 (b) shows the free-body diagram of a pipe element, the Figure indicates only the torque and the bending moments acting on a pipe element.

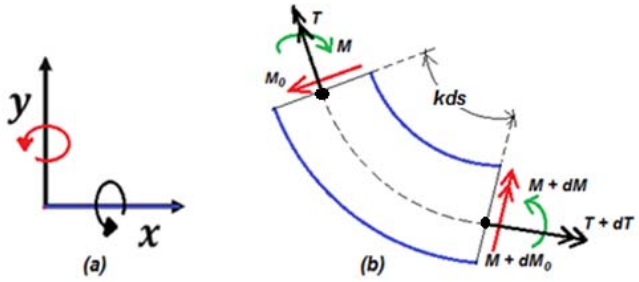

Figure 3-8: 2D Pipe Element with Moment Load Effects (Endal, et al., 1995)

Summation of moments along the axial axis of the element, which is the s-axis

$$\sum M = 0; \qquad M_0 k = \frac{\partial T_t}{\partial s} \tag{3.30}$$

Where M_0 = bending moment components due to initial curvature

T_t = Torque and *k(s)* = vertical pipe curvature

The expression for the torque T, the In-plane bending moment M and the bending moment component M_0 are obtained based on the linear elastic material behavior in unloading provided the pipe has attained it maximum plastic curvature k_0 *(Endal, et al., 1995).*

$$\text{where } T_t = GI_T.\frac{\partial \theta}{\partial s} \quad and \quad M_0 = EI.k_0.\sin\theta \tag{3.31}$$

Where k_0 = initial curvature of the pipe, which is largest plastic curvature at the overbend

θ = roll angle and

EI = Bending Stiffness and GI_T = Torsional Stiffness

Inserting equations 3.31 into equation 3.30 generates the non-linear differential equation as given in equation 3.32.

$$\frac{\partial^2 \theta}{\partial s^2} + (1+v).|k_0|\, k\sin\theta = 0 \tag{3.32}$$

$$\text{where the in} - \text{plane bending moments}$$

$$\text{M} = EI(k - k_0\cos\theta) \;\; and \quad (1+v) = \frac{EI}{GI_T} \tag{3.33}$$

According to *Endal, et al., (1995)* equation 3.32 can be solved by adopting the Galerkin procedure and the final system equation generated using this procedure is solved by iterating the nodal roll angles using the Newton-Raphson techniques.

In formulating the differential equations used for the 2D analysis of the pipeline during laying operation, the following steps are followed according to *Endal, et al., (1995)*

- The pipeline is divided into series of 2-noded 2D finite beam elements (see Figure 3-8(b)), with the vertical displacement and the rotation being the key DOF and the geometric stiffness (EA) of the pipeline is incorporated

- The lay barge stinger is modeled as a rigid circular shape body and support via roller to pipeline by the stinger is provided at certain locations along the length of the stinger

- The steel material is modeled by adopting the non-linear hardening stress-strain curve for the bending moment vs the curvature, this is to avoid the outer pressure, the steel axial & shear forces, the ovalization and torque been ignored, the *Bauschinger* effect and the elastic unloading are also incorporated

3.4 PIPELINE ON UNEVEN SEABED TOPOGRAPHY

3.4.1 Pipeline Free Span

The terrain of all ocean floors in reality are uneven, thus pipeline free span, which is the unsupported length of the pipeline due to contact loss, is inevitable in locations where there are depressions on the seabed. The causes of free span encompass *(Karunakaran, 2015);*

- Seabed irregularities (rough seabed)
- Subsequent scouring movement (mobile seabed)
- Sand Waves
- Rock Berm
- Rocks and Boulders

The unsupported length of the pipeline lying on the seabed are prone to both static and dynamic loads due to current, waves, self-weight of the pipeline, drop objects, high residual tension, pipe content, coating weight and so on (see Figure 3-9), hence it poses a great deal of problems, (such as fatigue damage and pipeline overstress) to the section of pipeline on the seabed, and the severity of problem or challenges are largely dependent on the span height and length.

A major problem that plaque the free span is the vortex induced vibration (VIV) which is a consequence of motion of the ocean current passing across the pipeline and can result in fatigue damages when pipeline natural frequency is very close the vortex shedding frequency and in the case where pipeline is coated, damages are noticed on the pipeline. The natural frequency of the free span length is in turn depends on the span length, the pipe weight per unit length, the pipe flexural and axial stiffness , the support conditions at the shoulders, this implies that the longer the span length the higher the chance of VIV and consequently fatigue damage.
Another major problem of free span is pipeline overstress due to unacceptable bending caused by weight of the pipeline, coating, drag & lift forces and pipe content. This can result in local permanent deformation and buckling (see Figure 3-9). It is worth noting that free spanning of the pipeline made it susceptible to hooking by fishing gear.

As a result of the challenges associated with pipeline free span, it becomes imperative to mitigate these problems in order to ensure the safety and integrity of the subsea pipeline. There are several mitigation

measures that can be installed such as installation of VIV suppression devices like strakes and shroud, rock dumping, mechanical support installation, trenching, anchor and so on, (see Figure 3-10). The installation of these measures therefore calls for subsea intervention, which in most cases due to unstable seabed and soft clayey seabed condition requires sea floor preparation to stabilize the seabed, thereby making subsea intervention operations costly and more costly as water depth increase, with experience statistics showing that typical subsea intervention of in the range of 15-20% of the total pipeline cost(*Endal, et al., 2015)* and it is also time consuming thus increase the duration for the marine operations *(McKinnon, 1999).*

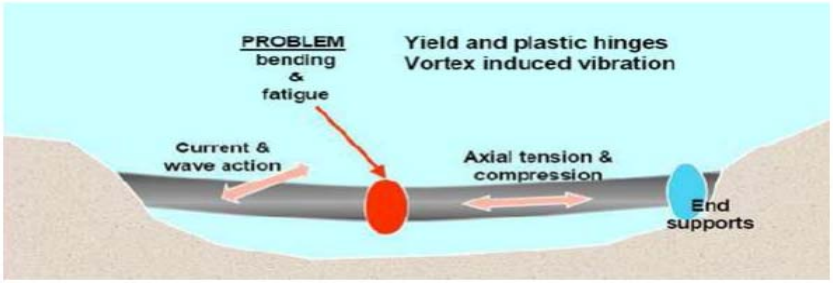

Figure 3-9: Loads on Free Span Pipeline (Karunakaran, 2015)

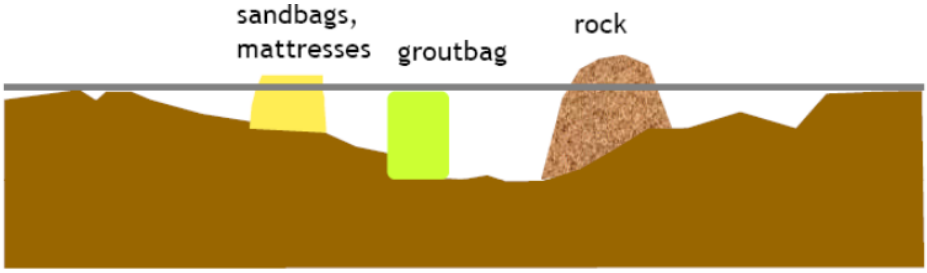

Figure 3-10: Pipeline Free Span Mitigation Measures (Karunakaran, 2015)

3.4.2 Conforming Pipeline to Seabed Topography

The results of the numerical investigation performed by *Endal, et al., (2015)* show that conformation of the pipeline to the terrain of the seabed is a cost effective and safer way of resolving some challenges listed in section 3.4.1. The pipeline can be made to assume the shape of the terrain by creating local residual curvature sections along the length of the pipeline. The creation of these local residual curvatures can be achieved in S-lay installation method by the use of the active roller and/or stinger curvature adjustments *(Endal and Nystrøm, 2015)* while in Reel-lay, the straightener can be hydraulically adjusted to achieve the same goal *(Statoil, 2002).* This procedure is considered as a cost effective method because is used reduce or eliminate the need for any other measures to ensure pipeline integrity on the uneven seabed (*Endal, et al., 2015)*

Endal, et al., (2015) identifies that there are several methods of adapting the pipeline to the sea bed terrain which are most suitable for Reel-lay method. These methods are

- **The under-straightening method**; in this method convex or concave downward residual curvatures are created along the pipeline and these pipe curvature rest on the span shoulders as shown in Figure 3-11(A), it is applicable for both S-lay and Reel lay method
- **The Over-straightening method;** here a concave upward residual curvature is created along the length of the pipeline and the curvature is positioned in the mid span section, as shown in Figure 3-11(B), this is also applicable for Reel lay method and for S-lay method a roll angle of approximately 180 deg. is achievable at the TDP.

- **The Combined method;** this method combined both under- and over straightening methods and it is only applicable for the Reel lay method. See Figure 3-11(C)

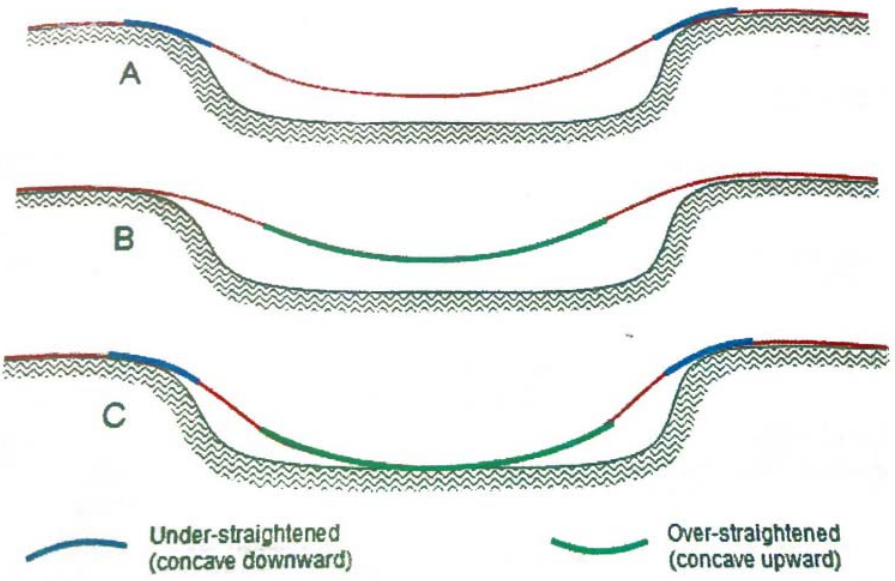

Figure 3-11: Methods of Suppressing Pipeline free span by Residual Curvature (Endal, et al., 2015)

The methods described above are achieved by creating local residual curvatures sections along the pipeline, there are other methods curvature in the already laid pipeline on the seabed as identified by *Endal, et al., (2015),* these methods can be used alone or in combination with the method listed above

- **Wire and Buoyancy Method**; in this method adopt a system of wire and buoyancy as shown in Figure 3-12(1), to create curvature at the free span section of the pipeline.
- **Local Weight Method**; as shown in Figure 3-12(2) weight can be placed at the mid span of pipeline in order to create curvature.

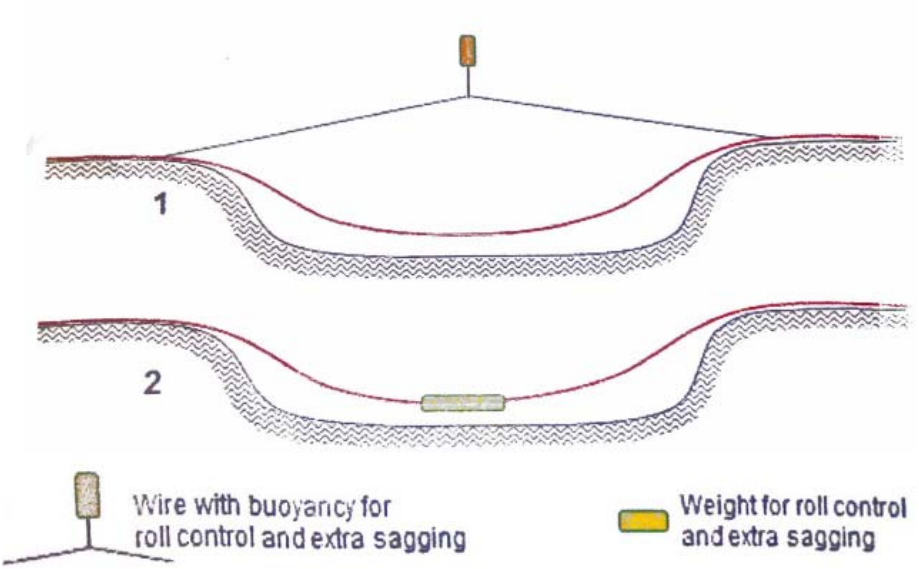

Figure 3-12: Methods of Suppressing Pipeline free span by adding Curvature (Endal, et al., 2015)

This thesis research also assess, through experimental test, the significance of various strain level of local residual curvature on the integrity of the pipeline at the free span by adapting the model pipeline using the

under-straightening, over-straightening methods and the local weight method, hereby validating the numerical test

3.4.3 Benefit of Conforming Pipeline to Seabed Topography

The benefits of conforming the pipeline to the uneven sea bed terrain as investigated by *Endal, et al., (2015)* are not limited to the following;

- Free span suppression
- Acceptable bending moment's utilization
- Reduction of subsea intervention cost

Endal, et al., (2015) validate, through numerical test the, robustness and the cost reduction potential of local residual curvatures sections along pipeline when installed on uneven seabed topography using the S-lay and Reel lay methods by identifying that up to 10% reduction in the cost of the subsea pipeline project can be achieved depending on the strain level while ensuring the structural integrity of the pipeline at the free span sections.

4. METHODOLOGY

4.1 EXPERIMENTAL SET-UP

The primary purpose of the experiment is to investigate the parameters that would induce pipe rotation above 90degree at the TDP as well as to establish the basic principle of conforming pipeline to uneven seabed topography using residual curvatures and weight during S-lay installation. Thus the parameters that are of primary focus in the experiment are the residual strain, the residual curvature length, In-line structure and the pipeline end boundary condition (fixed condition or torsional restraint condition). The experiment also establishes the influence of different residual strain and curvature length on the horizontal force. It is worthy to note that other parameters such as variation in the water depth; the applied tension etc could not be investigated due to unavailability of the space where the stinger was positioned

The experiment was performed in a 12m x 3m x 3m swimming pool located at the University of Stavanger. As a result of space constrain, the model was scaled down to suit the size of the swimming pool in terms of the size of model pipe, the water depth adopted, the stinger size and radius, the position of the residual curvature section along the model pipeline and so on.

In order to perform this pipe rotation and free span experiment to reasonable level of accuracy and minimized errors, several components and equipment were used, tested, constructed, soldered and prepared. The key parameters used in the experiment are list below and this section gives cursory details of some of these parameters

- Pipe Properties
- Pool
- Model stinger
- Model Rollers on stinger
- Load cell
- Applied Tension System
- Pipe Pre-bending
- Inline structure
- Torque measuring Device
- Uneven Seabed

Table 4-1; General Experimental Test Parameter

Water Depth (m)	Applied Tension (N)	Stinger Radius (m)	Load Cell Capacity (kg)	Weight of Inline structure (N)	Pool Size (m)
4.88	40	4	200	10.2	12 x 4 x 3

Table 4-2; General Experimental Residual Strain

Experiment	Residual Starin Level (%)			Residual Curvature length (m)	
Pipeline Rotation	0.30	0.35	0.40	2	3
Uneven Seabed	0.15	0.26	0.30	1	2

The following experimental test were performed in this thesis work

Residual Strain	Length of Residual Curvature	Bottom Boundary Condition	Measured Parameter (Output)

- **Pipe Rotation Experiments**

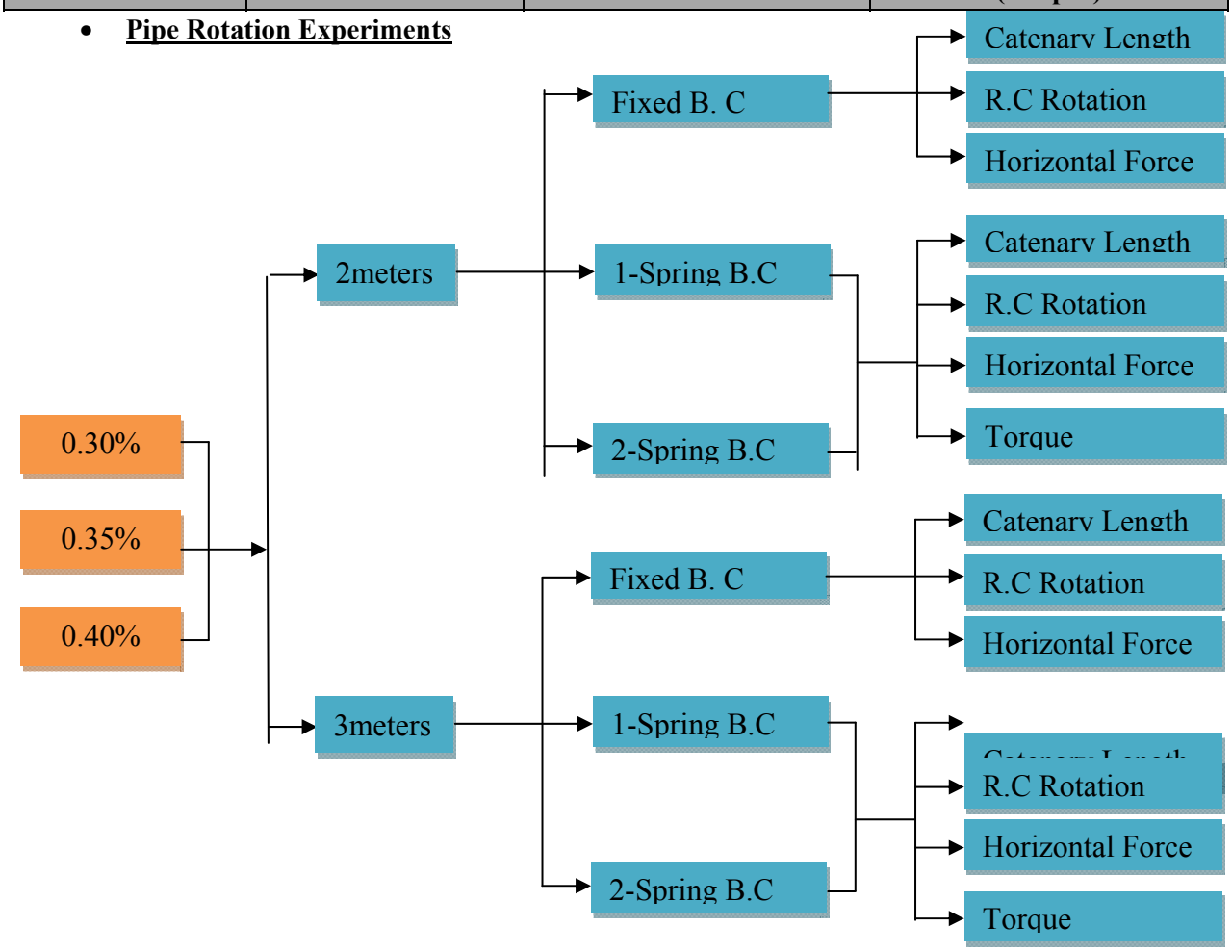

Figure 4-0: Pipeline Rotation Test

- **Uneven seabed Experiment**

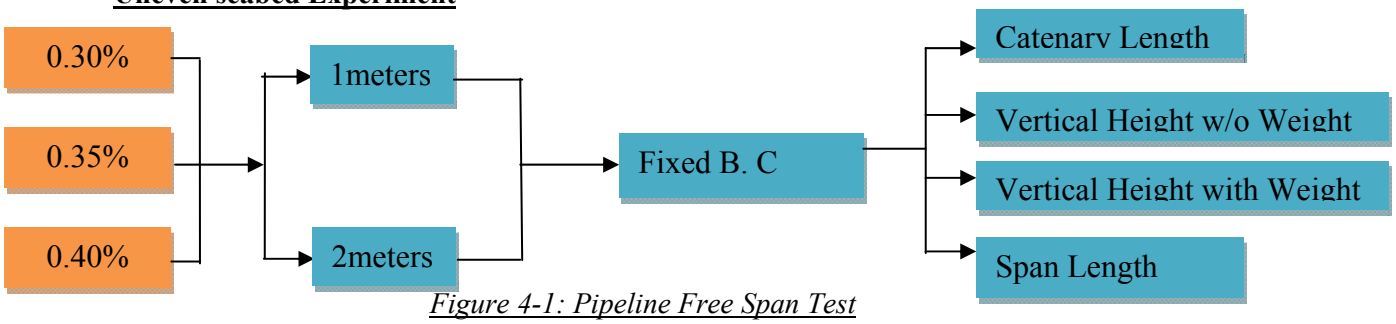

Figure 4-1: Pipeline Free Span Test

- **Inline structure Experiment**

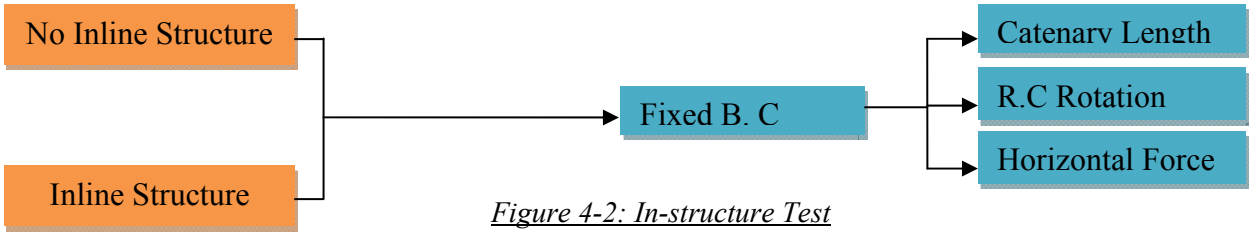

Figure 4-2: In-structure Test

4.1.1 Pipe Material and Geometric Properties

Several factors were considered in selecting a suitable model pipe material for the experiments and these factors are not limited to the pipe material type, size of pool, the availability of pipe, the stiffness of pipe, the available length of pipe and so on.

Based on all these factors 3meter long of 10mm outer diameter copper pipes were considered most suitable, the choice of copper material as against steel material, which is what is required for the actual pipeline material in the real life, is largely based on the high material stiffness of steel material which requires a larger size of pool. The copper pipes used are manufactured according to European standard of EN1057.

The properties of the 10mm copper pipes are obtained from the manufacturer specifications, the uniaxial tensile test and the EN1057 (R290) Standard and these properties are as specified in Table 4-3, 4-4 and 4-5 respectively.

Table 4-3; Measured Pipe Properties

Pipe Outer Diameter (mm)	Pipe Wall Thickness (mm)	Pipe Mass per unit Length (kg/m)	Pipe Piece Length (mm)
10	0.80	0.19	3

Table 4-4; Pipe Properties Obtained from Uniaxial Test

Modulus of Elasticity (GPa)	Material Yield Strength (GPa)	Tensile Force (N)
120	304.9	0.19

Table 4-5; Pipe Properties obtained from EN1057 (R290) Standard

Pipe Density (Kg/m^2)	Poisson Ratio
120	304.9

Pipe Material Uniaxial Tensile Test

The primary purpose of performing the uniaxial test on the pipe material is to determine the material modulus of elasticity and yield strength, these serve a input for the numerical analysis and consequently a comparison between the numerical and experimental result.

The uniaxial tensile test was performed using the Instron testing machine in machine laboratory at the University of Stavanger. And the test was performed based on the guidelines outlined for the mechanical testing of metal in Annexes C and E of *ISO 2009 standard.* The pipe test piece dimensions are given in Table 4-1 and the length is 300mm. The stress-strain curved as well as the tensile force-extension curve (see Appendix II for detailed results) were obtained for 3 test pipe pieces and values for the properties (modulus, yield etc.) for the test pieces were average to obtain the overall values of the modulus of elasticity and yield strength of the model pipe reported in Table 4-4. Figures 4-3 and 4-4 show the length of old and new model pipe piece cut for testing and Instron testing machine with test piece in place during testing respectively.

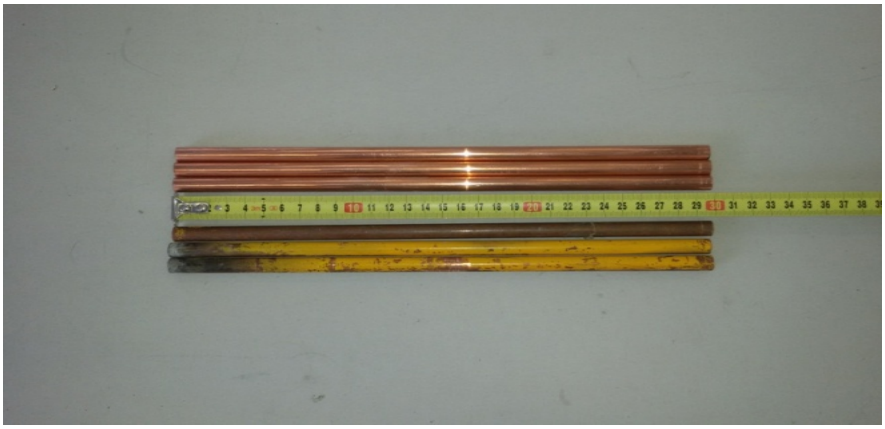

Figure 4-3: 300mm length of the old and New Pipe Pieces

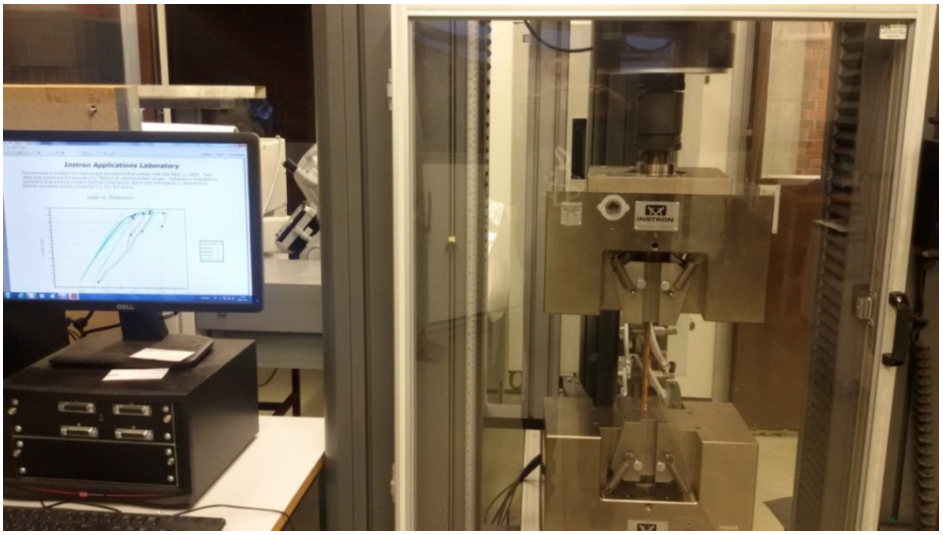

Figure 4-4: Uniaxial Tensile Testing of the Pipe Pieces

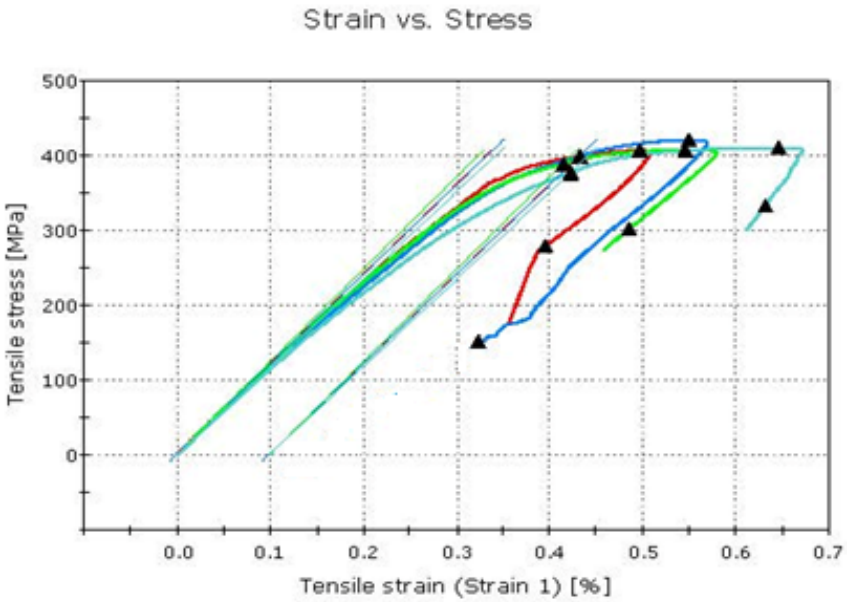

Figure 4-5: Stress-Strain curve of the model Pipe as obtained from the Uniaxial Tensile Testing

Model Pipe Connection

The model pipeline was created by soldering together several lengths of the 3 meters pipe. The choice of soldering was opted for due to the low melting point of copper material and to ensure a rigid and stiff joint at the point of soldering, small pieces 8mm copper pipe of 40mm length were inserted at every connecting joint before soldering and soldered together with the lengths of pipe. Propane gas burner with filler metal was used for the soldering operation. Figure 4-6, shows the pipe lengths been soldered together. In order to add or remove the pipe length with residual curvatures during the experiment, the mode pipeline was also disconnected by using the gas burner to heat up the joint

Figure 4-6: Pipe Connection with 8mm Diameter Pipe Inserted

4.1.2 Pool

The experiment was carried out in the material laboratory pool at the University of Stavanger. As state previously, the pool posed a great deal of limitation to the scope of the experiment in terms of the size and its availability; however the full size (see Table 4-1) of the pool was utilized for the experiment.

The experiment was performed when the pool was empty (dry experiment test) and In order to validate the nominal curvature of the catenary shape of the model pipeline under the applied load specified in Table 4-1, the pool wall was painted for visibility and then gridded in size 15cm by 15cm (see Figure 4-7)

Figure 4-7: Gridded Pool Wall

4.1.3 Model Stinger

The model stinger is a wooden structure with straight and curve sections (see Figure 4-8) was constructed in 2016 and it radius was estimated based on the tensile test of the model pipe and the final radius of the stinger selected (see Table 4-6) is such that the pipe does not experience any plastic strains has it passes through the stinger (*Kashif, 2016).* The model stinger was positioned at a height specified in Table 4-1 from the pool floor. It should be noted that the stinger height, consequently the water depth, could not be varied as a result of time constraint and availability of the space where the stinger was positioned.

Table 4-6; Model Stinger Geometrical Dimension and Height above Pool Floor

Height above Pool Floor(m)	Overall Length (m)	Radius (m)
4.5	9	4

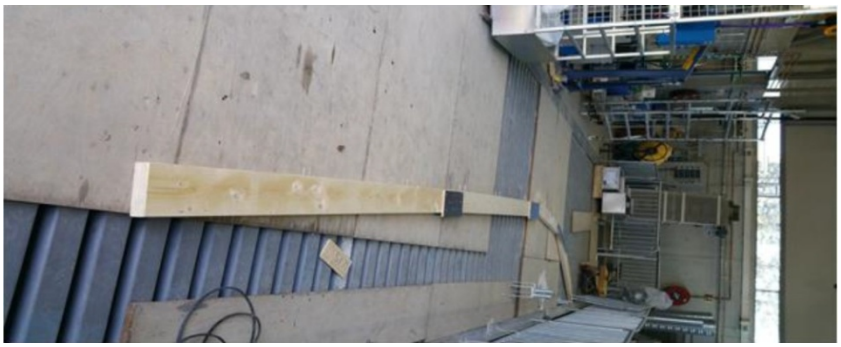

Figure 4-8: Model Stinger lying on the floor of the laboratory (Kashif, 2016)

4.1.4 Model Stinger Roller

To simulate the payout process through the stinger, rollers of 20mm length and 10mm diameter are positioned at interval on the model stinger, the pipeline are therefore being supported by these rollers. The rollers are needed to reduce the friction due to the wooden stinger just as in real life situations where adjustable rollers are placed at interval on the stinger. See Figure 4-9 shows the interval placement of the rollers on the whole length of the stinger

Figure 4-9: Rollers Placed on Stinger at Interval

4.1.5 Tensioning System

Due to the laboratory space constraints, a top tensioning system was developed using a pulley system as shown in Figure 4-10. The pulley system consists of four rollers firmly secured to the wooden stinger and a string attached to the pipeline end at one end and to the applied load (see Table 4-1) on the other end.

This system was also very useful in placing the soldered length of the pipeline from the pool floor to the stinger. Figure 4-11 shows the pulley system as while as the load

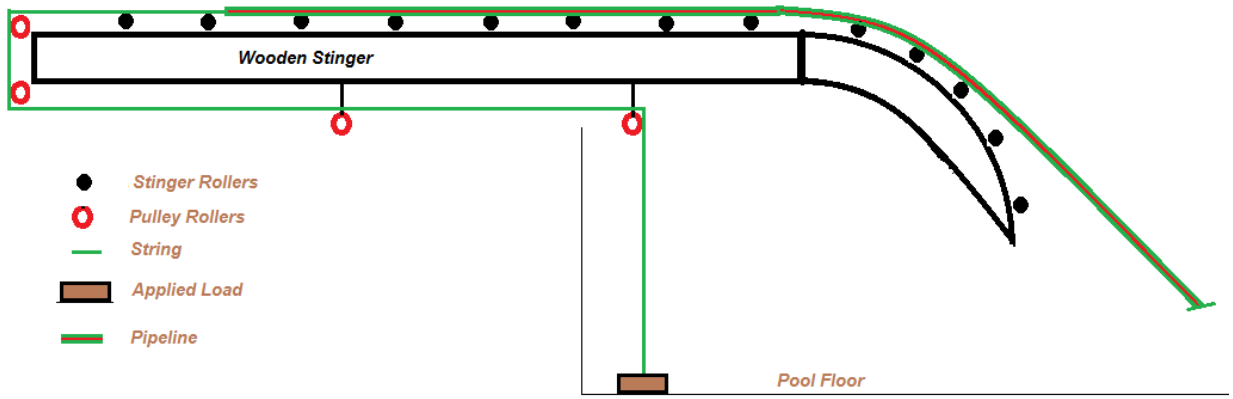

Figure 4-10: Schematics of the Applied Tensioned System

Figure 4-11: Applied Tension Pulley System on Stinger

4.1.6 Pipe Pre-bend

Has established in previous section that the main cause of pipeline roll is the presence of residual curvature section and inline structures along the length of the pipeline during S-lay and Reel-lay installation and the primary purpose of this experimental test is to establish the parameter that cause rotation above 90degree. Since the model stinger curvature cannot induce residual curvature in the model straight pipe as can be achieved in S-lay using the stinger/roller system, the model pipes were pre-bent at different residual strains levels and residual curvature length before soldering to the mainline. The strain is expressed in Equation 4.1

$$\varepsilon = \frac{r}{R} \qquad (4.1)$$

Where r = pipe outer radius in meter

R = pipe bending radius in meter

ε = pipe strain (nominal or residual) in %

Due to lack of pipe bending machine, manual bending methods were adopted for bending the pipes. There are two different methods of achieving the pipe bend/curvature the methods are as follows;

Using the stress-strain curved (Figure 4-5) obtained from the tensile test and the discussion of section 3.0, the nominal residual strain levels and using Equation 4.1, the bending radius R is determined. This means that if the pipe is bent to this nominal bending radius, and afterward released from the stress, it will be left with a residual strain corresponding to that used to obtain the nominal strain.
The second method is to obtain the residual bending radius by using the residual strains directly in Equation 4.1 and then the straight pipes are bent to assume the curvature corresponding to the residual curvature depending on the curvature length in consideration. Figure 4-12 shows the bending of the straight pipe to conform to the residual curve

For the purpose of this test and for easiness the second approach was adopted, Table 4-7 shows the values of the radius as obtained from Equation 4.1. Figure 4-13 shows the residual curvatures for various the residual strains as given in Table 4-7.

Table 4-7; Model Stinger Geometrical Dimension and Height above Pool Floor

Residual Stain, ε (%)	0.15	0.26	0.3	0.35	0.40
Residual Curvature Radius, R (m)	6.67	3.85	3.33	2.86	2.50

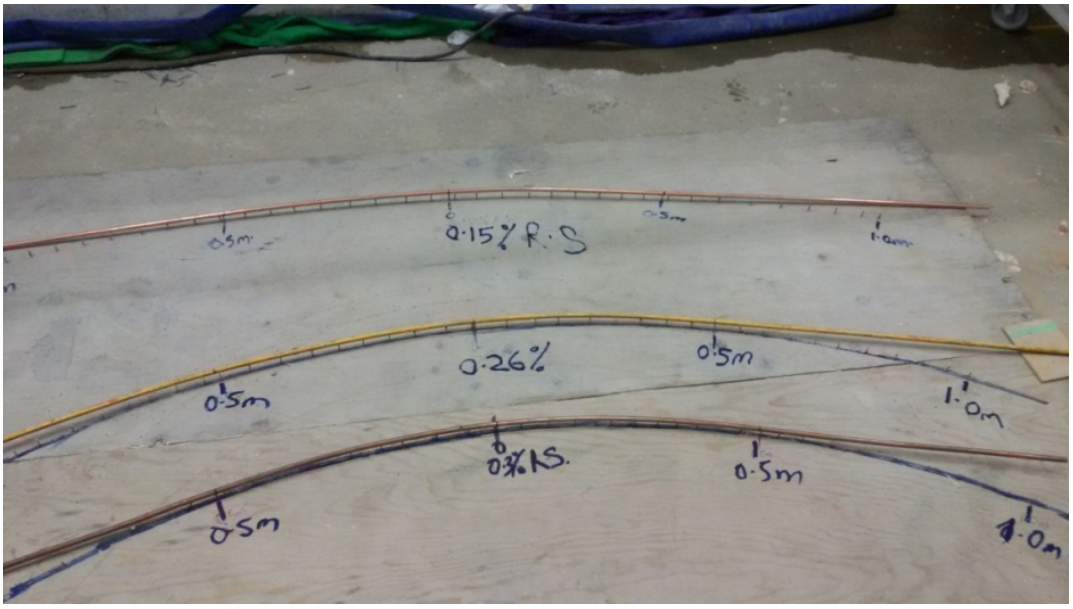

Figure 4-12: Bending of Straight Pipe to Conform to Residual Curve

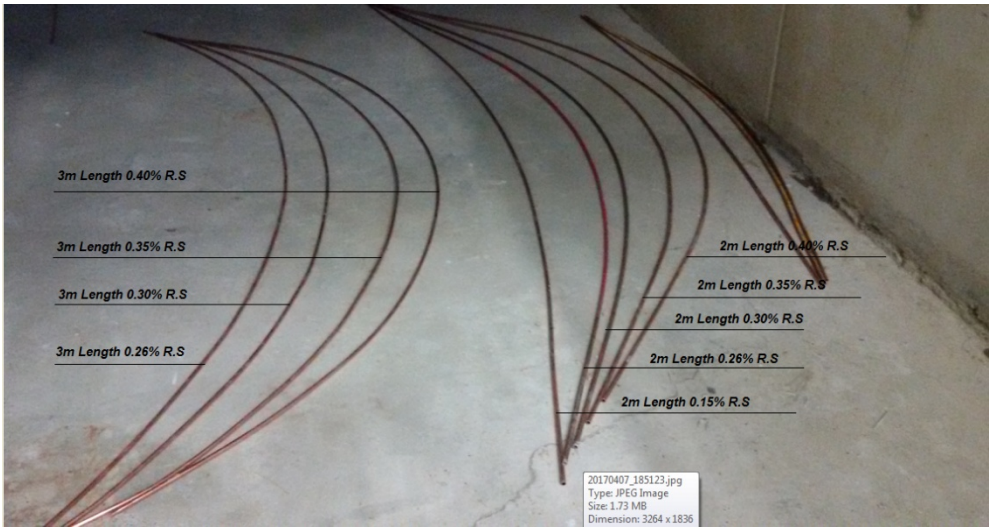

Figure 4-13: Pre-bend pipes with Residual Curvatures

4.1.7 Inline Structure

Additional test is also performed to establish the influence of inline structure on pipeline rotation. In real life the inline structure could be control valves, inline tees, pig launcher and so on.

The inline structure for the purpose of this experiment is an angle wooden frame with a small length of pipe firmly secure through, the dimension of the wooden frame is shown in Figure 4-14. The weight of the wooden frame is 10.2N. The inline structure is soldered to the pipeline through the small length of pipe. See Figure 4-15

Additional test will be to check the influence of CoG position on the pipeline rotation; however because of time constraint this test was not performed.

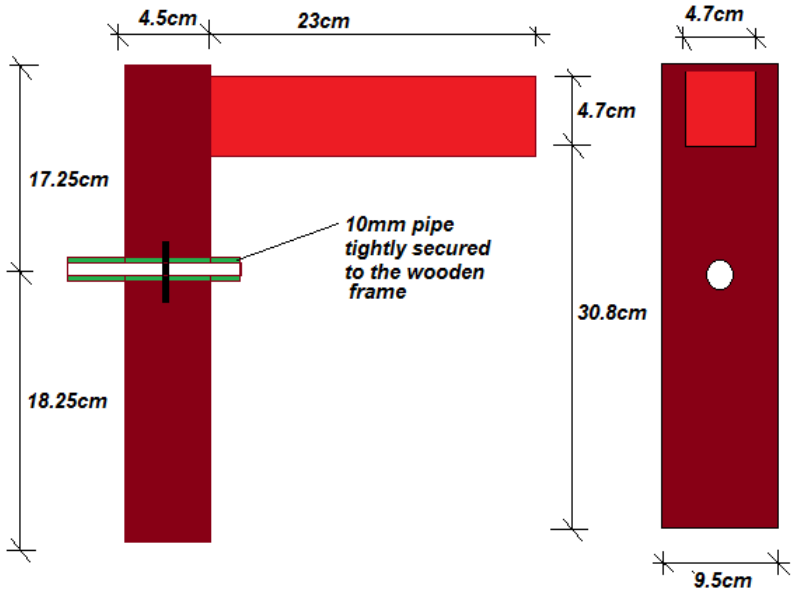

Figure 4-14: dimension of the wooden inline frame

Figure 4-15: Inline Structure Connected to the Pipeline

4.1.8 Pipeline End Support Conditions

In order to obtain a reasonable results, it is imperative to simulate the actual end conditions of the pipeline to be as close as possible to what is obtainable in reality, however this posses a great deal of challenge. The end conditions of the model pipeline are termed; stinger end which is the top end of the model pipeline on the stinger and the seabed end which is the end of the pipeline on the seabed, the descriptions of these end conditions are given below.

Stinger End

This end of the pipeline is similar to the end help or supported by the tensioner in reality, this end is attached to the applied load (tension) via the pulley system (see Figure 4-8) as describe in section 4.2.5. However, unlike the real tensioner, the boundary condition only provides control to axial movement of the pipe, thus the pipeline at this end is free in all the other degrees of freedom. Figure 4-16, shows the direct connection of the pipeline end to the pulley string.

Figure 4-16: Pipeline End on Stinger Connected to Pulley System via String

Seabed End

For the purpose of this experimental test two different boundary conditions are considered for the seabed end of the model pipeline and the results obtained are compared. These boundary conditions are;

- **Fixed end**; this condition provides full restraint to movements in all the 6 DoF. The end of the pipeline is nailed to a wooden plate (see Figure 4-17) to prevent rotational movement while the wooden plate has wheels underneath to allow axial movement with reduced friction. It is worthy to note that the final rotation at the TDP is largely dependent on the proximity to the fixed end, that is the closer the residual curvature length or inline structure to the end condition the lower the angle of rotation and vice versa.

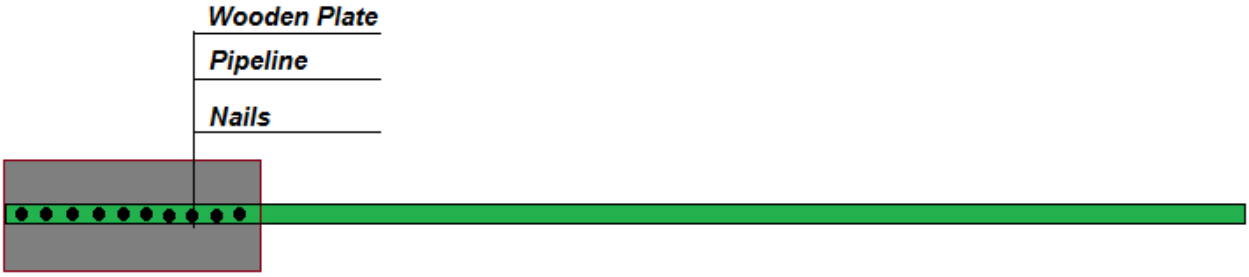

Figure 4-17: Pipeline End Nailed to Wooden Plate

- **Partially Free End**; the boundary condition provided to simulate the torsional resistant of the pipe to rotation as well as to measure the torque acting on the pipeline, as it is very difficult to measure. To achieve this, a torsional resistant device was constructed (see Figure 4-18(a)). The device was built of wooden frame and tension springs and it allows axial movement under reduced friction by the installation of rollers (wheels) underneath. In order to control the torsional stiffness of the pipe, the device is built in such a way that the number of spring can be increased. The higher the number of springs, the greater the torsional stiffness introduced. For the purpose of this experimental test, one and two spring's system were considered, see Figure 4-18 (a) and (b) respectively
  It should be noted that the torsional test was not performed on the pipe material due time constraint

  Torque Device Built; the device works on the basic principle of mechanical potential energy of spring. The device is build with tension spring's system as shown in Figure 4-16, the tension springs are rigidly fixed to a wooden plate termed spring wooden plate which has a 10.1mm diameter hole at the center and it is free to rotate but restrained against lateral movement, the pipeline end is inserted into the hole of the plate and firmly fastened to it. The wooden plate is then attached to another wooden plate, termed support wooden plate, which is firmly secured to the device supporting structure. The device supporting structure is made of wooden frame and has 4 wheels to allow for axial movement of the pipeline, see Figure 18.
  The stiffness of the spring is determined using the Hooke formula

$$\boldsymbol{K = \frac{F}{e}} \qquad (\mathbf{4.2})$$

  Where K = Spring Stiffness Constant in Newton per meter
  F = Applied Force in Newton
  e = Extension or elongation in meter

  A spring displacement test was performed to determine the spring stiffness constant of the tension spring. Two samples of the tension spring were collected and forces were applied on them through the load cell to elongate them (see Figure 4-19), the magnitudes of the force causing corresponding displacement, measured at every 10mm displacement, were recorded through the load cell and by

using Equation 2 the stiffness were calculated.
The force-extension curves for the two samples and their average were plotted as shown in Figure 4-20. The average of all the average stiffness is taken to be the stiffness constant K of the tension spring, this value is reported in Table 4-8. Detailed calculations of the average stiffness as well as the stiffness constant K of the tension spring is documented in Appendix I. It should be noted that the load cell measures forces in mV/V which can be converted to Newton using the factor in Table 4-1

Torque Device Working Principle; Thus as the pipe rotate or twist it causes the spring wooden plate to rotate since the pipe is fixed to it, consequently resulting in the spring displacement. The displacements are measure at different distance during the test until the residual curvature reaches the TDP.
The force causing the rotation can be determined by using Equation 4.2 after making force F the subject of the formula and the perpendicular distance d from the center of rotation to the point of spring connection (Moment arm) is measured, see Table 4-8, then the Torque T was calculated based on the assumption that magnitude of the torque generated by the pipe rotation is equal the torque resistant of the tension spring, hence the torque resistance of the tension spring is determined by using Equation 4.3

$$\boldsymbol{T = F\ x\ d} \qquad (\mathbf{4}.3)$$

Where T = Torque in Newton/meter
F = Applied Force in Newton
d = Moment arm in meter

Table 4-8; Torque Measuring Device Parameters

Moment Arm (m)		Spring Stiffness Constant (N/m)	Spring Original Length (m)
D1	**D2**		
		144.53	0.04

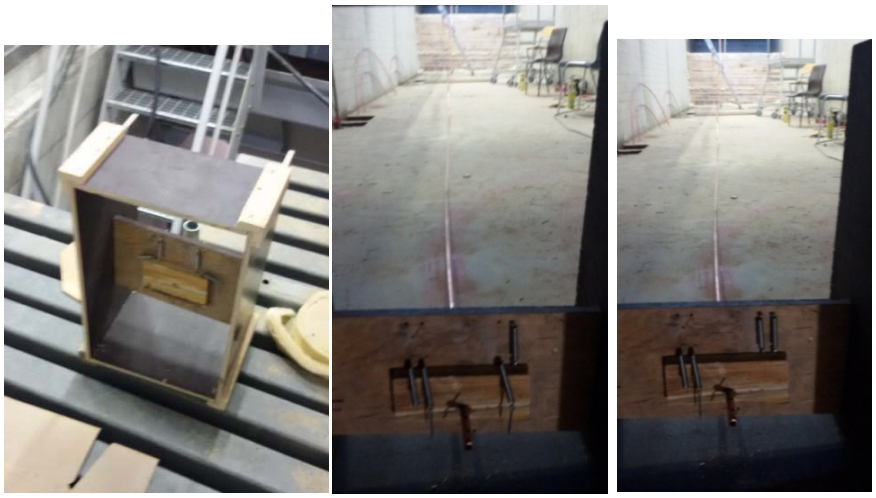

(a) *(b)* *(c)*

Figure 4-18: (a) Torsional Restraint device, (b) 2-springs system and (c) 1-spring System

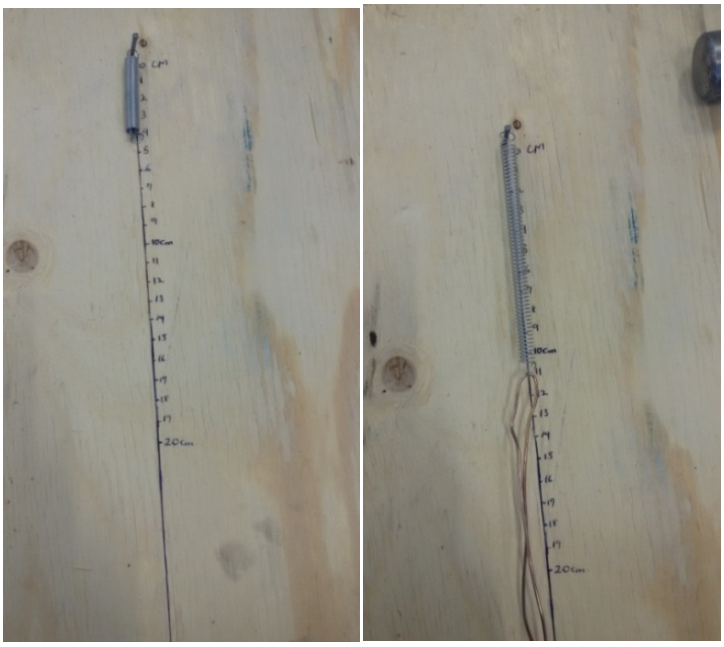

Figure 4-19: Displacement Test of Tension Spring

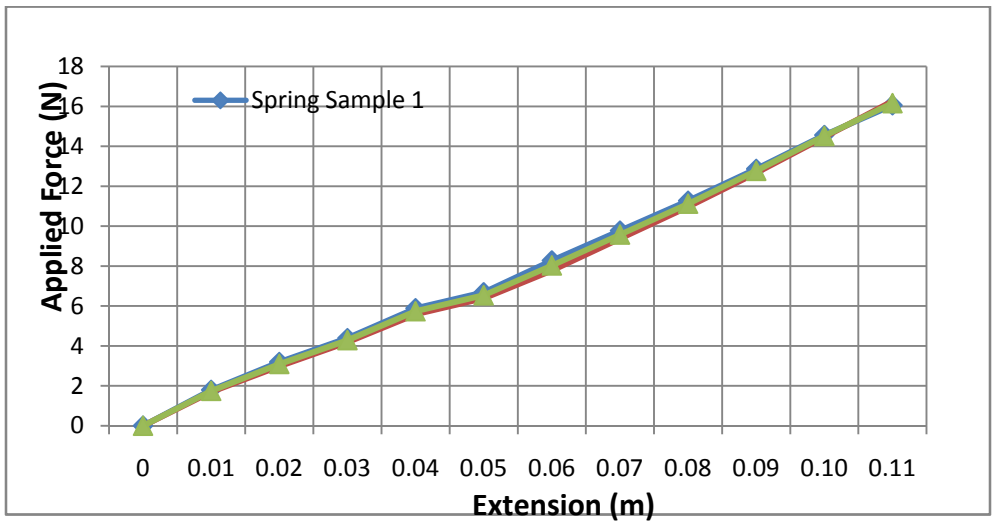

Figure 4-20: Force-Extension Curves of Sample Springs

4.1.9 Uneven Seabed

In order to establish the basic principle of conforming pipeline to uneven seabed, separate experimental tests were perform with the residual curvature pipe in a sagging configuration along the pipeline and then paid out into the seabed depression. To perform this test, a wooden uneven seabed was constructed with the main dimensions as indicated in Table 4-9. Figure 4-21 shows the schematic of the uneven seabed with the dimension parameters and Figure 4-22shows the finished uneven seabed. The value of the span length was selected based on the value that can give visible pipe displacement and the seabed shoulder b was considered as the touch-down point.

Table 4-9; Dimension of the Uneven Seabed

Span Length L (m)	Height H_a (m)	Height H_b (m)	Depression Height H_d (m)
2.280	0.600	0.622	0.515

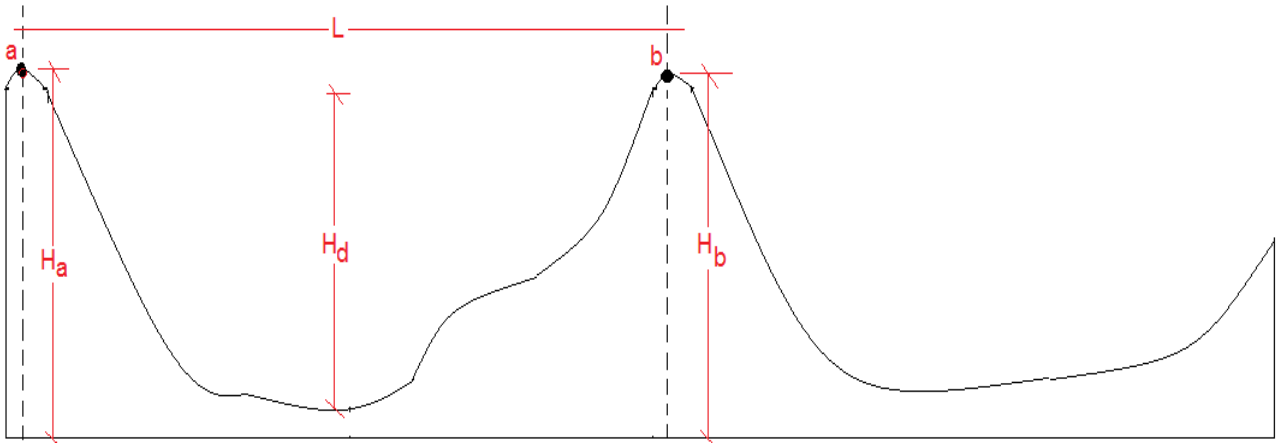

Figure 4-21: Schematics of the Uneven Seabed

Figure 4-22: Uneven Seabed

4.1.10 Force Measuring Device

Horizontal tension force at the end of the pipeline on the seabed was measured by using a load cell. The load cell was connected to the pipeline end on the seabed via a string while it is firmly held in position to avoid movement in any directions, see Figure 4-23. The load cell is connected to a spider 8 device, which receive the signal from the load cell. The spider 8 device is connected to a computer to display the reading

A 200kg capacity HBM U2A-200 Load cell type was considered adequate for this experimental test (see Figure 4-24). This load cell type measure load in mV/V, thus scaling of the load cell is necessary in order to convert this unit to kg. To determine the conversion factor from mV/V to Newton N, a 40N weight was hang off from the load cell and the reading through the spider 8 was taken from the computer recorded, see Table 4-10. Hence from the applied weight and the value of the reading taken, the conversion factor is estimated (Table4-10).

Table 4-10; Load Cell Reading Conversion Factor

Applied Weight (N)	Spider 8 Reading (mV/V)	Conversion Factor to Newton
40	0.00401	997.51

Figure 4-23: Load Cell Firmly Secured

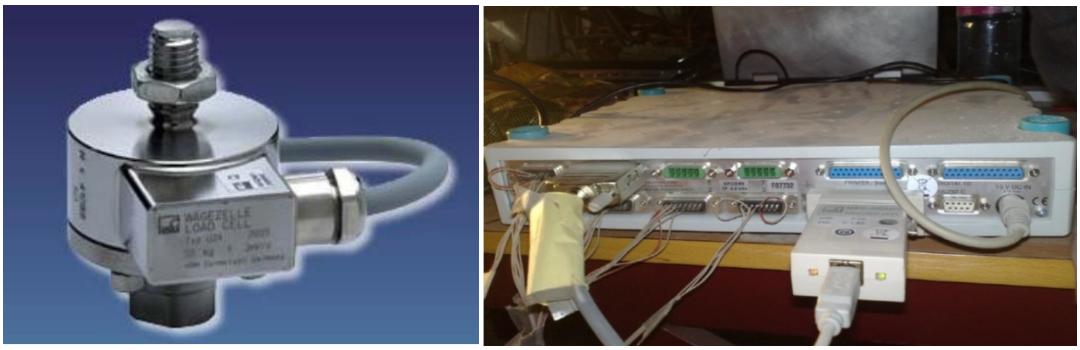

(a) (b)

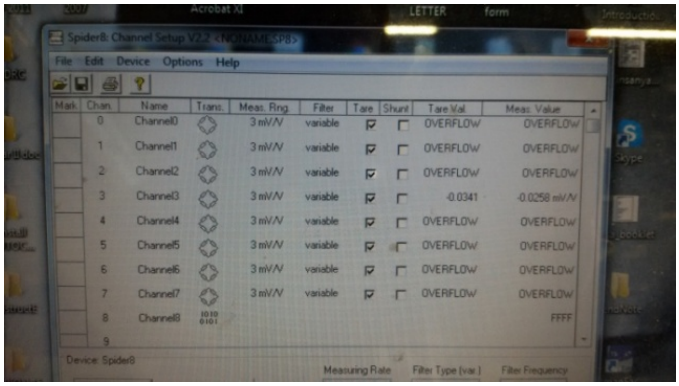

(c)

Figure 4-24: (a) Load Cell, (b) Spider 8 and (c) Reading from Spider 8

4.2 NUMERICAL

There are limited numbers of computer application that can accurately determine the rotation of pipeline with residual curvature length incorporated, however as discussed in section 3.3 numerical analysis of pipeline rotation can be achieved either by a 3D F.E approach or 2D differential equation approach. For the purpose of this thesis work, a 2D differential equation approach will be adopted.

The 2D pipe rotation estimation is therefore performed using the commercial program ORCAFLEX, where the pipe is modeled as 2D beam element configuration. Refer to section 3.3 for details of the principle governing the 2D calculation of pipe rotation.

For the purpose of accurate comparison between the experimental results and the numerical analysis result, the numerical analysis is performed using the same model properties considered in the experimental test, that is, the same properties in terms of the pipe properties, the stinger properties, the tensioner capacity and the environmental conditions.

4.2.1 ORCAFLEX Description

As previously mentioned in section 3.3, Orcaflex can be consider for to 2D pipe rotation calculation during installation either by S-lay or Reel-lay or J-lay method, it is a commercial programme developed solely for marine static and dynamic analysis of offshore systems such as marine risers, umbilical, pipelines and offshore operations such as deployment, installation, mooring, offshore lifting, towing and towed systems. It incorporates the effect of current and waves loads as well as other imposed motions. However the capability of OrcaFlex is not limited to 2D analysis but it can also perform 3D non-linear time or frequency domain finite element analysis which is capable of handling arbitrarily large deflections of the flexible from the initial configuration. Details on the capabilities and features can be found on https://www.orcina.com/SoftwareProducts/OrcaFlex

Since this thesis focus primarily on residual curvature, Orcaflex has the capability to introduce pre-bend sections along the length of the pipeline during installation, it does not have the capability to perform full pipe rotation analysis. Thus for this analysis focus is on the twist of the pipeline when the pre-bends are introduced. It is also worthy to note that a precise comparison of the results from the experimental test and the numerical simulation using Orcaflex is difficult to achieve, this is because several other factors, motions and loads such as wave, current, vessel motions etc. were considered in the numerical analyses which were not put into consideration on the dry experimental test. Hence a great deal of difference is expected as the influence of all these parameter on the final results/output is enormous.

Coordinate Axis

There are primarily two coordinates systems used to define objects or physical models, input data such as model position, in Orcaflex, these are the global coordinate system and the local coordinate systems both are designated by Gxyz and Lxyz respectively, see Figure 4-25.Also the output or results are relative to these coordinate axis.
The coordinate system of the line model that represents the pipeline is shown in Figures 4-28 and 4-29

Directions and Headings

The directions and headings in Orcaflex are given or specified two different angles which are sometimes defined relative to either the global or local axis in Orcaflex. These angles are the Azimuth angle and the Declination angles. The definitions of these angles are based on the axis they are relative to. When relative to the local coordinate axis, the angles are defined as *(Orcina, 2016)*;

- **Azimuth angle;** is the angle from the x axis to the projection of the direction onto the xy plane (Azimuth is 0° for the positive x axis direction and 90° for the positive y axis direction). •
- **Declination angle;** is the angle the direction makes with the z axis. Therefore Declination is 0° for the positive z-direction.
- **Gamma angle;** at line ends, the axial directions as well as the twist orientation about the axial direction of the line were. This is done by first specifying the azimuth and declination of the axial direction and then specifying the twist orientation by giving the gamma angle to be zero.

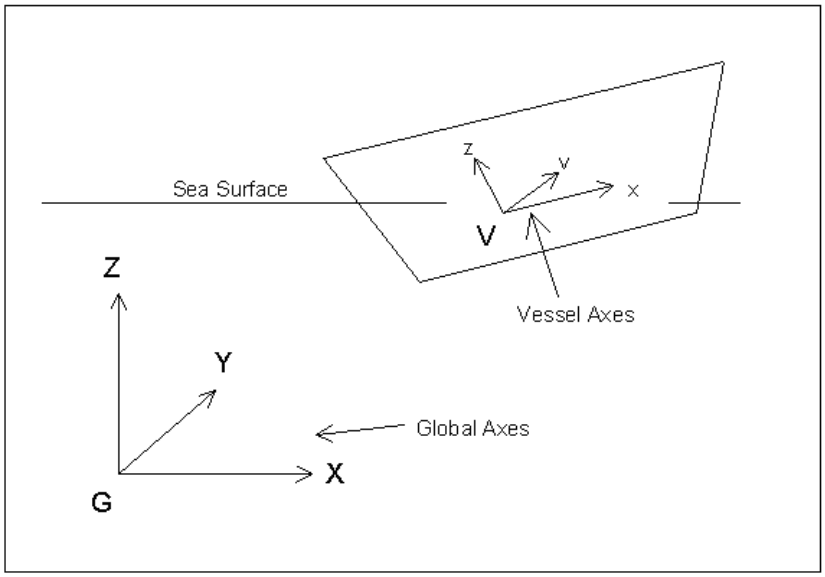

Figure 4-25: Orcaflex Coordinates Systsem (Orcina, 2016)

4.2.2 Modelling

Orcaflex contains several features that aid the modeling of pipeline installation systems, these features can be found in the library of the programme and it includes model of a Vessel, Line, 3 and 6D Buoy, Linked and winch etc.

Modelling of the pipeline with, during S-lay installation, in Orcaflex was done by using the following features;

The Line; this is model features that represent the pipeline from the vessel to the seabed. It has the properties of the model pipe as specified in Tables 4-3 to 4-5, with stiffness of the pipe estimated and inputed as well. The line model has a property called pre-bend which was used to introduce the residual curvature (further details on the pre-bend is given below). The surface end of the line is set as free and connected to the tensioner (see details on tensioner below) while the seabed end of the pipeline is fixed to the anchor which provides restraints in all 6 DoF. Orcaflex represents the TDP in white dots as shown in Figure 2-27.

The Vessel; Orcaflex has a predefine vessel model with several other features in the vessel directory. The default geometric properties of the vessel in Orcaflex was scaled down to a reasonable dimension and used in the numerical analysis as shown in Figure 4-26 and 4-27.

The stinger was model using the support modelling features in the vessel facility, straight and curve (in terms of radius and length) sections of the stinger were defined and the contact position as well as the geometric properties of the contact components (Rollers) are specified, see Figure 4-26 (rollers are shown in pink colours in Figure 4-26).

The Tensioner was model with the used of the winch features in Orcaflex. The tensioner capacity of the winch, as given in Table 4-12, was specified. The two ends of the winch were connected to the vessel and pipe line. In Figures 4-26 and 4-27 the tensioner is shown in blue.

Based on the results of the experimental test, where it was observed that the pipeline residual curvature will rotate beyond 90degree, thus in order to avoid the halting of rotation of the curvature during Orcaflex

simulation, a cylindral elements is incorporated and fixed at the seabed, this was achieved by using the **Block** feature in Orcaflex. See Appendix IV for pictures of the model with the blocks

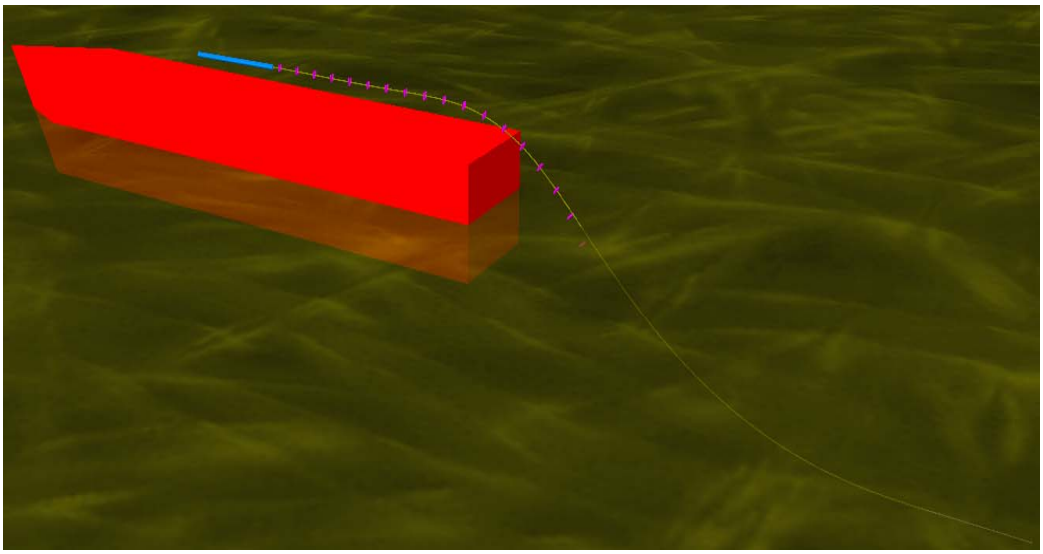

Figure 4-26: 3D S-Lay Pipe Laying Catenary in ORCAFLEX

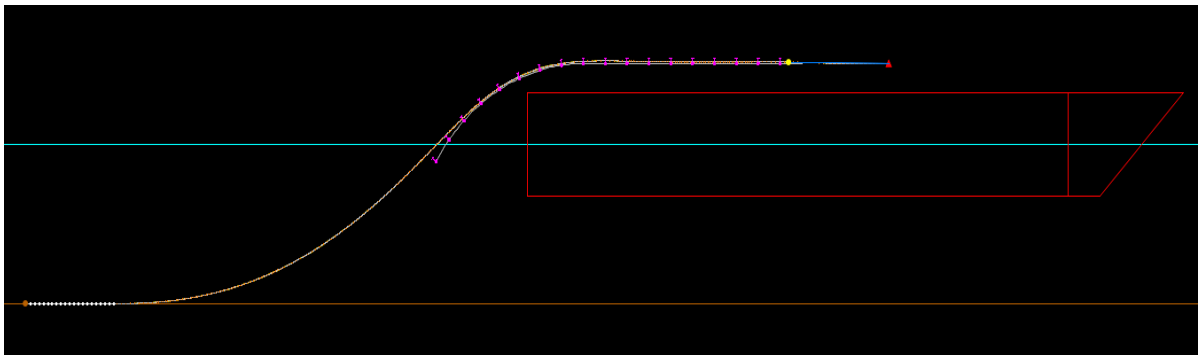

Figure 4-27: S-Lay Pipe Laying Catenary in ORCAFLEX

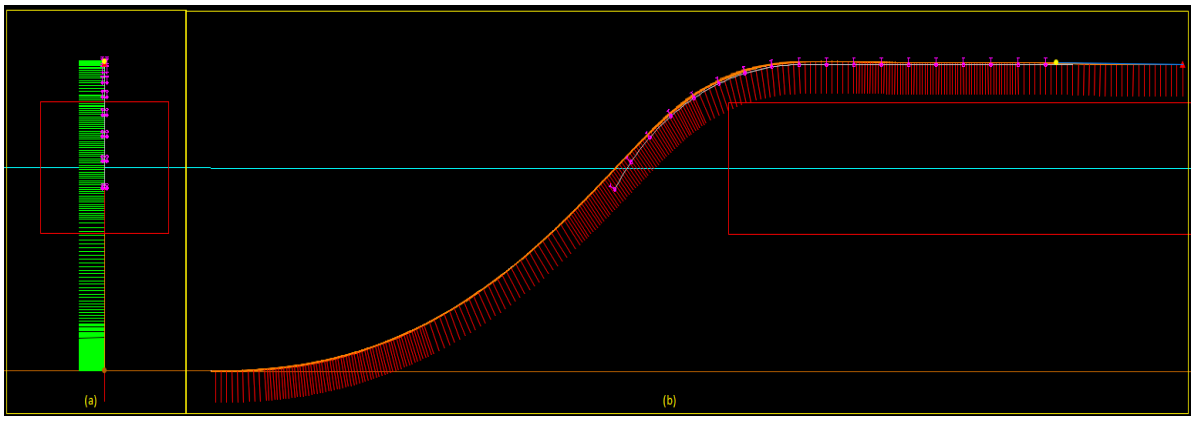

Figure 4-28: Catenary Line in Elevations showing the Local Coordinate axes (a) y-axis in green (b) x-axis in red

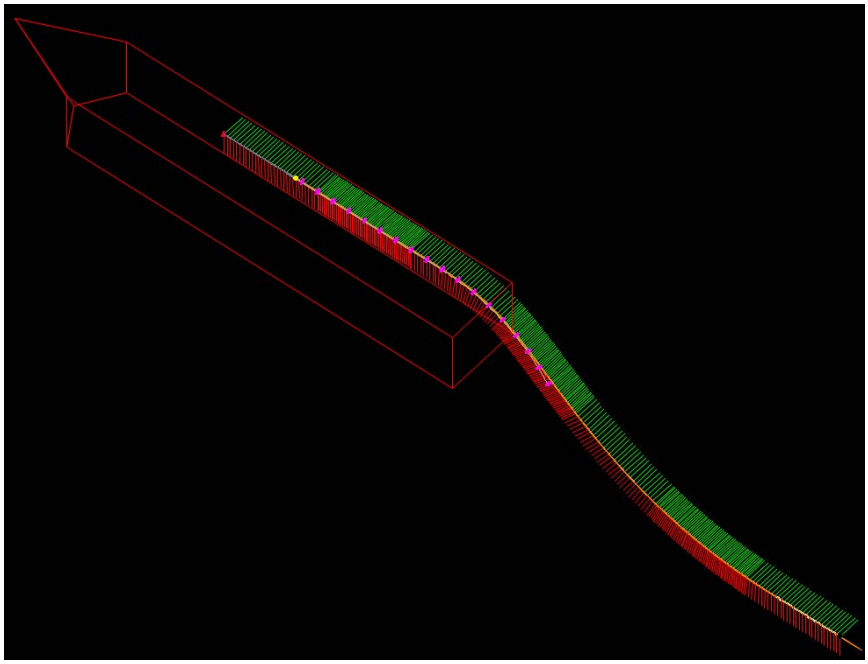

Figure 4-29: Catenary Line in 3D showing the local axes, x-axis in red and y-axis in green

Pre-bend

One primary objective of this thesis is to determine the influence of residual curvature, thus pre-bends of different residual strains are introduced and torsion is enabled in Orcaflex in order to measure the twist of the pipeline due to these pre-bend.

To define pre-bend in Orcaflex, straight line sections with lengths equal to the residual curvature length were specified together with other sections that make up the pipeline catenary, and the pre-bent curvatures of the sections were therefore defined in radians per unit length, with sections without pre-bend, that is, unstressed sections having a pre-bend of zero, which is the default setting. The pre-bend curvature for several residual strains is as shown in Table 4-11 and Figure 4-30 showing a typical S-lay catenary pipeline with pre-bend curvature. The pre-bend curvature values in Table 4-11 are considered in the numerical analysis reported in this thesis.

It should be noted that, the definition of the pre-bend in Orcaflex is in the local axes, directions either in x and/or y direction(s). However, to simplify data preparation and interpretation of results we recommend that you arrange the line's local axes such that the pre-bend is entirely in either the local x or local y direction.

Table 4-11; Corresponding Pre-bend Curvature for different Residual Strains

Residual Stain, ε (%)	0,30 %	0,35 %	0,40 %
Pipe Radius, (m)	0,005	0,005	0,005
Residual Curvature Radius, R (m)	1,67	1,43	1,25
Pre-bend Curvature (1/R), rad/m	0,60	0,70	0,80

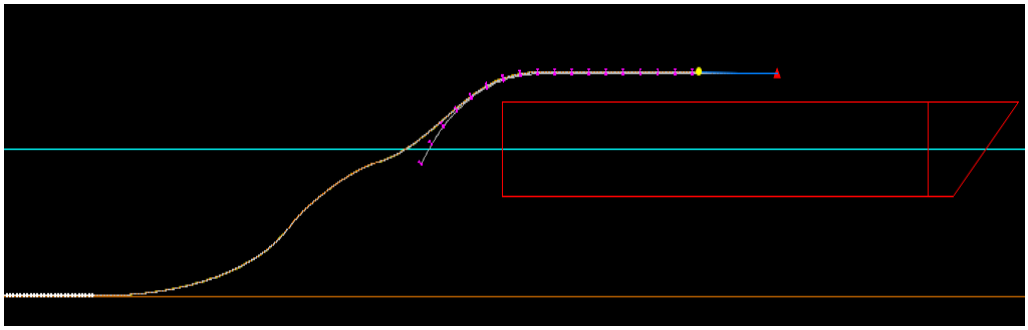

Figure 4-30: pipeline Catenary with Pre-bend section

4.2.3 Design Basis

For the purpose of comparison the following parameters were considered for the numerical analysis. As shown in Table 4-12, the water density is set to the density of air in Orcaflex model while the influence of hydrodynamic loads and motions is ignored by setting the wave height and current speed to zero. Other key model properties used are similar to those used in the experimental test.

Table 4-12; Key Input Parameter in ORCAFLEX

Water Depth (m)	Stinger Radius (m)	Tensioner Capacity (N)	Wave Height (m)	Current Speed (m/s)	Water Density (te/m3)
3	4	40	0	0	0.0013

4.2.4 Boundary Conditions

The boundary conditions at the two ends of the pipeline plays a pivotal role in final twist recorded, thus, the pipeline end boundary conditions considered in the numerical analysis are similar to that used in the experimental test.

The stinger end of the pipeline is free in rotation in all directions, this is achieved by connecting this end to the winch wire and the twisting stiffness of this end connection is extremely small, this means that the stinger end of the pipeline is allowed to rotate freely just as in the experimental test.

For **the seabed end** of the pipeline, three boundary conditions were considered to simulate the scenarios in the experimental test. The first case is fixed boundary condition, that is restraint from rotational and translation movements in all directions, this achieved by anchoring the seabed end of the pipeline and setting the bending and twisting stiffness of the connection to unity, see Table 4-13. The second and the third cases are cases where the end is anchored for stability; however the rotation or twisting stiffness of the end connection (anchor) is set to values estimated based on the rotational stiffness of the torsional devise used in the experimental test. See Appendix III for the calculation of the twisting stiffness of the torsional device depending on the number of spring

Table 4-13; End Connection Stiffness considered in the ORCAFLEX Model

Boundary Conditions	Bending Stiffness (kNm/deg.)	Twisting Stiffness (kNm/deg.)
Fixed	1	$20x10^{-12}$
2-spring	1	$1.29x10^{-6}$
1-spring	1	$8.70x10^{-7}$

4.2.5 Numerical Analysis Description

Orcaflex has the capacity to perform two separate analyses for pipeline installation. These analyses are the **static analysis**, which estimate the catenary and the nominal curvature of the pipeline in the static state, without considering the effect of waves and current. The output of the static analysis serves as one of the input for the second analysis which is the **dynamic analysis. The dyn**amic analysis considered the effect of hydrodynamic loads and motion of vessel on the pipeline catenary.

Since the effect of hydrodynamics is been ignored, the result of the dynamic analysis is the same as that of the static analysis. Hence both static analysis and dynamic analyses were performed and the results reported in this thesis.

5. SCALING

The experimental test is only relevant when scaled up to a real life case, since its application is only meaningful when extended to practical situation or scenario, thus scaling of the model test becomes very imperative. The model experiment in this study effort has been greatly simplified when compared to the physical representation of the offshore installation process and environments, although the absolute laying parameters are preserved in the process of simplification, which enable the model pipeline installation test exhibit some key behavior of the of real life situations of pipeline installation

Scale model is not peculiar to this studies as it application cut across many fields of engineering and non-engineering alike, regardless of the field of study all scale model are based on the same principle and functional requirements. For marine hydrodynamics application the general modeling and scaling laws are applied, these laws are In general governed by the similary theory (similitude) which is built around dimensionless numbers. The dimensionless numbers therefore correlate the test model to the physical model. Figure 5-1 shows some typical dimensionless numbers used for scaling up in offshore technology.
For most engineering applications, in this case offshore engineering (of which thesis study effort falls), the similarity requirements are as follows;

- Geometric Similarity: The model and full scale structures must have the same shape, that is All linear dimensions must have the same scale ratio. This found application in the environment surrounding the model and ship and in the elastic deformations of the model and ship

- Kinematics Similarity: this is also known as the similarity of velocity. It states that the flow and model(s) will have geometrically similar motions in model and full scale

- Dynamic Similarity: this is also known as the similarity of force, and it states that ratios between different forces in full scale must be the same in model scale. Inertia forces, Surface forces, Elastic Forces, Pressure force, Gravitational forces.

All these similarity requirements must be met when scaling up this experimental test to full scale, this is very difficult to achieved in this cases, thus the experimental test in this thesis only satisfies the geometric similarity requirements as satisfying the kinematics (flow velocity) and dynamic (gravitational force, inertial force, viscous force etc) similarities are complex to achieved. However for simplification sake a quick check using only the geometric similarity can be performed using the deflection number and the geometric properties of the model pipe.

Deflection number plays a key role in the geometric scaling of pipeline model to real life line pipes. The deflection number is a dimensionless number used to determine the geometric scale ratios for deflections of pipes under hydrostatic stressess. The expression for the deflection number according to *Clauss & Kuhnlein, 1974 and Clasuu, et al., 1991*, as well as the applications is documented in Appendix III

Symbol	Dimensionless Number	Force Ratio	Definition
R_e	Reynolds Number	Inertia/Viscous	$\frac{UL}{\nu}$
F_n	Froude Number	Inertia/Gravity	$\frac{U}{\sqrt{gL}}$
M_n	Mach's Number	Inertia/Elasticity	$\frac{U}{\sqrt{E_V/\rho}}$
W_n	Weber's Number	Inertia/Surface tension	$\frac{U}{\sqrt{\sigma/\rho L}}$
St	Strouhall number	-	$\frac{f_v D}{U}$
KC	Keulegan-Carpenter Number	Drag/Inertia	$\frac{U_A T}{D}$

Figure 5-1: Scaling Ratios used for Testing Offshore Structures (NTNU, 2016)

6. EXPERIMENTAL AND NUMERICAL TEST RESULTS

6.1 EXPERIMENTAL PROCEDURE/TEST

A total of 25 experimental tests were performed as shown in section 4.1, and this includes simulation with different residual curvature strain levels and lengths, in-line structure, ordinary straight pipes. The experimental tests covered pipeline rotation scenarios due to residual curvatures and inline structures as well free span scenarios with residual curvatures and concentrated load.

The experimental test was performed following procedures listed below;

- **Pipeline Construction:** six 3meter length pipes were soldered on the pool floor to form an 18 meter long model pipeline. For each case of simulations of pipeline lay with residual curvature, the residual curvature length is soldered in between the pipeline, before the simulation begins when the applied tension is on the pool floor, and it is done in such a way that the previous curvature length is disconnected by heating the joints and a new curvature length is soldered in place. Due to space constraint, the residual curvatures were connected to the pipeline at a distance below the inflection point. This is to ensure that the residual curvature length touches the pool floor (seabed) within the limited distance.

- **Lifting pipeline unto Stinger:** due to the flexibility of the model pipeline, the pipeline was lifted unto the stinger with the aid of the tensioner/pulley system. This is achieved by connecting the stinger end of the pipeline to the pulley string and then pulled upward unto the stinger from the pool bottom by the applied tension. This method is considered necessary to avoid plastic deformation of the pipeline during lifting.

- **Experimental Simulation:** the test simulation involved keeping the stinger stationary while the seabed end of the pipeline is being pulled at approximately constant speed and constant applied tension at the stinger end of the pipeline. This is quite unlike the real life scenario where the installation vessel moves instead, however due to the space constraint it is impossible to achieve a moving stinger. The pulling continues until a predetermined point on the pipeline touches TDP and at this point a distance of approximately 4meters would have been covered. For the cases with residual curvatures, the curvature lengths were positioned vertically after the inflection point before the start of the simulations.

6.2 PIPELINE MODEL CATENARY SHAPE

The first experimental test performed is with straight unstressed pipeline without residual curvature or inline structures. The purpose of this test is to validate the catenary shape of the model pipeline with both numerical and analytical solution and also to establish the last point on the pipeline that will touch the pool floor after pulling distance of 4 meters is covered.

In order to validate the pipeline model catenary shape and thus the nominal curvature, pictures of the catenary shape of the first experimental test was taken (see Appendix IV) and digitized by using WebPlotDigitizer (*Rohatgi, A., 2016*). WebPlotDigitizer is a HTML5 developed open source used for obtaining curves or plots from data point. Hence the plot of the experimental catenary curvature was obtained and compared with the nominal curvature obtained using the analytical expression of equation 2-10 of section 2.4. This comparison is as shown in Figure 6-1, detailed data point estimation is documented in Appendix IV.

As shown in Figure 6-2, the experimental nominal curvature as obtained from the Webplot is closely related to the curvature obtained from the analytical expression, thus this shows the experimental test results is reasonably accurate and that the copper pipeline model can give also give a reasonable level of accuracy when compare with steel pipe.

It is worthy of note that the nominal curvature of the catenary shape is largely dependent on several parameters such water depth, applied tension and so on, thus different nominal curvatures should be expected when these parameters are varied.

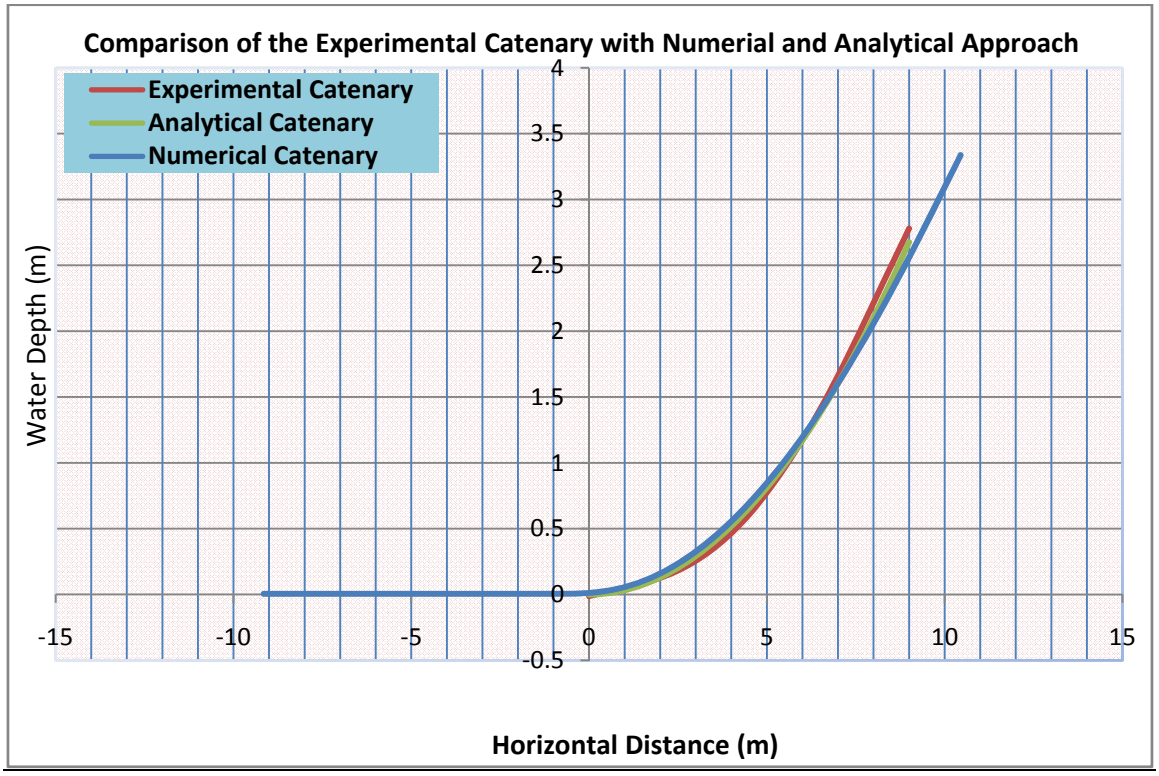

Figure 6-1: Experimental, Numerical and Analytical Nominal Curvature

6.3 PIPE ROTATION EXPERIMENTAL TEST RESULTS

A total 18 experimental simulations of pipeline rotation due to residual curvatures and inline structure were performed. For each of the simulations performed measurements of the outputs such as the catenary length, the angle of rotation and the horizontal force were taken while other parameters such as vertical tension, the resultant tension and the torque were estimated based on Equations 2.2, 2.5, 4.3, respectively. For the pipeline rotation the experimental tests are classified into three based on the pipeline bottom end condition, that is, fixed end condition and partially restrained end (1-spring end and 2-springs end restrained). All the experimental test were carried out under a constant tension of 40N and water depth of 4.53m, thus this thesis does not investigate the influence of top tension and water depth on pipeline rotation.

It is worthy to note that the friction between the pool floor and the pipe significantly affect the accuracy of the rotation angle and well as the horizontal force recorded at the TDP. Thus the results presented ignores the influence of the frictional resistance induced by the contact elements (pool floor and pipe nail guide on the stinger)

6.3.1 Fixed Bottom Conditions

The rotation of the pipeline was determined when the seabed end of the pipeline is fixed as discussed in section 4.1.8. The rotation was determined with variation in the residual strain and curvature length and the catenary length and rotation angles determined.

It should be noted that the value of the rotation angle is largely dependent on the proximity of the fixed end to the residual curvature, that is, the closer the fixed end the smaller the rotation

6.3.1.1 Rotation with 2 meter Residual Curvature Length

Table 6-1 shows the results of the experimental test when three residual strains (R.S) of equal length of 2m are considered while Figures 6-2, 6-3 and 6-4 show (from the left) the picture of the pipeline with the residual curvature before the test begins, the residual curvature at the TDP after the test and the measurement of the pipeline rotation angle at the TDP for 0.30%, 0.35% and 0.40% residual strain respectively. It should be noted that the rotation angle reported in Table 6-1 is the angle of rotation at the middle of the curvature length.

As seen in the Table 6-1, the pipeline rotation angle increases as the residual strain increases, likewise the resultant axial tension in the pipe. However the difference is small, this is as a result of close proximity of the residual curvature to the fixed end of the pipeline.

Table 6-1; Pipeline Rotation and Axial Tension for for 0.30%, 0.35% and 0.40% Residual Strains- Fixed Pipeline Bottom End

Curvature Length, (m)	2		
Applied Load, (N)	40		
Bottom Boundary Condition	Fixed		
Residual Strain Level, (%)	**0.30**	**0.35**	**0.40**
Catenary Length, (m)	9.51	9.78	10.15
Angle of Rotation, (Degree)	12.08	16.7	20.43
Measured Horizontal Force, (N)	49.88	50.27	51.17
Vertical Tension, (N)	17.72	18.22	18.91
Total Tension, (N)	52.93	53.47	54.55

Figure 6-2: 2m Residual Curvature Length of 0.30% R.S with Fixed Bottom Condition

Figure 6-3: 2m Residual Curvature Length of 0.35% R.S with Fixed Bottom Condition

Figure 6-4: 2m Residual Curvature Length of 0.40% R.S with Fixed Bottom Condition

6.3.1.2 Rotation with 3 meters Residual Curvature Length

Table 6-2 shows the results of the experimental test when three residual of equal length of 3m are considered while Figures 6-5, 6-6 and 6-7 show (from the left) the picture of the pipeline with the residual curvature before the test begins, the residual curvature at the TDP after the test and the measurement of the pipeline rotation angle at the TDP for 0.30%, 0.35% and 0.40% residual strain respectively. It should be noted that the rotation angle reported in Table 6-2 is the angle of rotation at the middle of the curvature length.

As seen in the Table 6-2, the pipeline rotation angle increases as the residual strain increases, likewise the resultant axial tension in the pipe. The values of the pipe rotation for the different strain level are significant, hence showing the influence of the curvature length on the rotation of the pipeline.

Table 6-2; Pipeline Rotation and Axial Tension of 3m residual Curvature for 0.30%, 0.35% and 0.40% Residual Strains- Fixed Pipeline Bottom End

Curvature Length (m)	3		
Applied Load (N)	40		
Bottom Boundary Condition	Fixed		
Residual Strain Level (%)	**0.30**	**0.35**	**0.40**
Catenary Length (m)	9.15	9.45	10.6
Angle of Rotation (Degree)	14.04	20.14	38.07
Measured Horizontal Force (N)	53.57	54.46	55.26
Vertical Tension (N)	17.05	17.61	19.75
Total Tension (N)	56.21	57.24	58.68

Figure 6-5: 3m Residual Curvature Length of 0.30% R.S with Fixed Bottom Condition

Figure 6-6: 3m Residual Curvature Length of 0.35% R.S with Fixed Bottom Condition

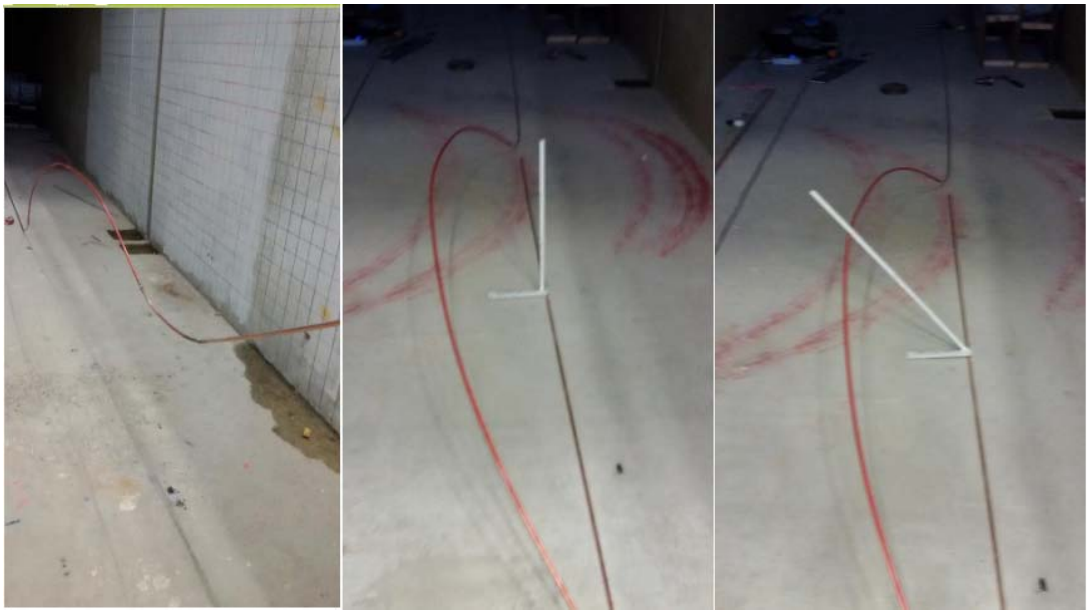

Figure 6-7: 3m Residual Curvature Length of 0.40% R.S with Fixed Bottom Condition

6.3.1.3 Rotation with Inline Structure

Table 6-3 shows the results of the experimental test when three residual strains (R.S) of equal length of 3m are considered while Figure 6-8 shows (from the left) the picture of the pipeline with the inline structure before the test begins and the inline structure at the TDP after the test. It should be noted that the rotation angle reported in Table 6-3 is the angle of rotation at the middle of the inline structure.

As seen in the Table 6-3, the pipeline rotation angle increased as the inline structure was installed along the length of the pipeline, likewise the resultant axial tension in the pipe. However the difference in angle between these two cases is large. It is worthy of note that the larger and higher the weight and CoG of the inline structure the greater the angle of rotation

Table 6-3; Pipeline Rotation and Axial Tension with Inline Structure

Applied Load, (N)	40	
Bottom Boundary Condition	Fixed	
	w/o RC & Weight	**With In-line Weight**
Catenary Length, (m)	10.4	9.92
Angle of Rotation, (Degree)	5.7	73.61
Measured Horizontal Force, (N)	53.57	54.46
Vertical Tension, (N)	19.38	18.48
Total Tension, (N)	56.96	57.51

Figure 6-8: Pipe Rotation with Inline Structure and Fixed Bottom Condition

6.3.2 One Spring Bottom Conditions

This is another case where the rotation of the pipeline was determined when the seabed end of the pipeline is attached to the torque measuring device as discussed in section 4.1.8. In order to simulate a scenario with an model pipe torsional resistance, One-spring system was made active and the rotation was determined with variation in the residual strain and curvature length while the catenary length, rotation angles and the torque at some pre-define distances are taken. It was observed during the experiment, that the residual curvatures rotate beyond 90degree before reaching the TDP; hence in order to measure the actual angle of rotation of the curvature, the pipeline was lifted 600mm above the pool floor.

It should be noted that the value of the rotation angle and consequently the torque recorded are largely dependent on the proximity of the partially restraint end to the residual curvature, that is, the closer the end the higher the rotation.

6.3.2.1 Rotation with 2 meters Residual Curvature Length

Table 6-4 shows the results of the experimental test when two residual strains of equal length of 2meters are considered and the angle of rotation as well as the pipe axial tension were recorded as indicated in Table 6-43. It is observed that with the end partial restraint introduced the angle of rotation increase significantly beyond 90degree, with the maximum angle of 132degree recorded for the 0.40% residual strain for this scenario. An increase of axial tension up to 60N was also observed in the pipeline for 0.40% residual strain Tables 6-5 and 6-6 show the estimation of the torque for 0.35% and 0.40% residual strains respectively from the measure parameters such as the spring extension and so on. It is observed that the torque increases as the distance increases with a maximum of 118Nmm recorded at the TDP (4meter location) for 0.40% residual strain.

Figures 6-9 and 6-10 show (from the left) the picture of the pipeline with the residual curvature before the test begins, the residual curvature at the TDP after the test and the measurement of the pipeline rotation angle at the TDP for 0.35% and 0.40% residual strain respectively. It should be noted that the rotation

angle reported in Table 6-4 is the angle of rotation at the middle of the curvature length. As seen in the Table 6-4, the pipeline rotation angle increases as the residual strain increases, likewise the resultant axial tension in the pipe.

Table 6-4; Pipeline Rotation and Axial Tension of 2m residual Curvature for 0.35% and 0.40% Residual Strains – 1-spring Partially Restraint Pipeline Bottom End

Curvature Length (m)	2	
Applied Load (N)	40	
Bottom Boundary Condition	1-spring	
Residual Strain Level (%)	**0.35**	**0.40**
Catenary Length (m)	9.78	10.15
Angle of Rotation (Degree)	100.68	132.27
Measured Horizontal Force (N)	50.77	51.47
Vertical Tension (N)	18.22	18.91
Total Tension (N)	53.94	54.83

Table 6-5; Pipeline Torque due to 2m residual Curvature for 0.35% Residual Strains

Initial Spring Length		4	cm		
No of Spring		1			
Strain Level		0.35	%		
distance (m)	extension (m)	Stiffness (N/m)	Force (N)	lever arm (cm)	Torgue (Ncm)
d	e1	k	F1	d1	T
1	0.002	144.53	0.28906	5.8	1.676548
2	0.0045		0.65039		3.772233
3	0.0055		0.79492		4.610507
4	0.0119		1.71991		9.9754606

Table 6-6; Pipeline Torque due to 2m residual Curvature for 0.40% Residual Strains

initial Spring Length		4	cm		
No of Spring		1			
Strain Level		0.4	%		
distance (m)	extension (m)	Stiffness (N/m)	Force (N)	lever arm (cm)	torgue (Ncm)
d	e1	k	F1	d1	T
1	0.0022	144.53	0.31797	5.8	1.8442028
2	0.0065		0.93945		5.448781
3	0.0076		1.09843		6.3708824
4	0.0141		2.03787		11.819663

Figure 6-9: Pipe Rotation with a 2m of 0.35% Residual Strain and 1-spring Pipeline Bottom Condition

Figure 6-10: Pipe Rotation with a 2m R.C of 0.40% Residual Strain and 1-spring Pipeline Bottom Condition

6.3.2.2 Rotation with 3 meters Residual Curvature Length

Table 6-7 shows the results of the experimental test when two residual strains of equal length of 3meters are considered and the angle of rotation as well as the pipe axial tension were recorded as indicated in the table. It is observed that with the end partial restraint introduced the angle of rotation increase significantly beyond 90degree, with the maximum angle of 165degree recorded for the 0.40% residual strain for this scenario. An increase of axial tension up to 70N was also observed in the pipeline for 0.40% residual strain Tables 6-8, 6-9 and 6-10 show the estimation of the torque for 0.30%, 0.35% and 0.40% residual strains respectively from the measure parameters such as the spring extension and so on. It is observed that the torque increases as the distance increases with a maximum of 146.7Nmm recorded at the TDP (4meter location) for 0.40% residual strain.

Figures 6-11,6-12 and 6-10 show (from the left) the picture of the pipeline with the residual curvature before the test begins, the residual curvature at the TDP after the test and the measurement of the pipeline rotation angle at the TDP for 0.30%, 0.35% and 0.40% residual strains respectively. It should be noted that the rotation angle reported in Table 6-7 is the angle of rotation at the middle of the curvature length.As seen in the Table 6-7, the pipeline rotation angle increases as the residual strain increases, likewise the resultant axial tension in the pipe.

Table 6-7; Pipeline Rotation and Axial Tension of 3m residual Curvature for 0.30%, 0.35% and 0.40% Residual Strains – 1-spring Partially Restraint Pipeline Bottom End

Curvature Length (m)	3		
Applied Load (N)	40		
Bottom Boundary Condition	1-spring		
Residual Strain Level (%)	**0.30**	**0.35**	**0.40**
Catenary Length (m)	9.15	9.45	10.6
Angle of Rotation (Degree)	128.66	161.57	172.07
Measured Horizontal Force (N)	53.97	54.76	55.66
Vertical Tension (N)	17.05	17.61	19.75
Total Tension (N)	56.59	57.52	59.06

Table 6-8; Pipeline Torque due to 3m residual Curvature for 0.30% Residual Strains

initial Spring Length		4	cm		
No of Spring		1			
Strain Level		0.3	%		
distance (m)	extension (m)	Stiffness (N/m)	Force (N)	lever arm (mm)	torgue (Ncm)
d	e1	k	F1	d1	T
1	0.0028	144.53	0.40468	5.8	2.3471672
2	0.0051		0.7371		4.2751974
3	0.0062		0.89609		5.1972988
4	0.0143		2.06678		11.987318

Table 6-9; Pipeline Torque due to 3m residual Curvature for 0.35% Residual Strains

initial Spring Length		4	cm		
No of Spring		1			
Strain Level		0.35	%		
distance (m)	extension (m)	Stiffness (N/m)	Force (N)	lever arm (cm)	torgue (Ncm)
d	e1	k	F1	d1	T
1	0.003	144.53	0.43359	5.8	2.514822
2	0.0064		0.92499		5.3649536
3	0.0107		1.54647		8.9695318
4	0.016		2.31248		13.412384

Table 6-10; Pipeline Torque due to 3m residual Curvature for 0.40% Residual Strains

initial Spring Length		4	cm		
No of Spring		1			
Strain Level		0.4	%		
distance (m)	extension (m)	Stiffness (N/m)	Force (N)	lever arm (cm)	torgue (Ncm)
d	e1	k	F1	d1	T
1	0.0035	144.53	0.50586	5.8	2.933959
2	0.0094		1.35858		7.8797756
3	0.0137		1.98006		11.484354
4	0.0175		2.52928		14.669795

Figure 6-11: Pipe Rotation with a 3m R.C of 0.30% Residual Strain and 1-spring Pipeline Bottom Condition

Figure 6-12: Pipe Rotation with a 3m R.C of 0.35% Residual Strain and 1-spring Pipeline Bottom Condition

Figure 6-13: Pipe Rotation with a 3m R.C of 0.40% Residual Strain and 1-spring Pipeline Bottom Condition

6.3.3 Two Spring Bottom Conditions

This is the last scenario considered for the pipe rotation experimental test where the rotation of the pipeline was determined when the seabed end of the pipeline is attached to the torque measuring device as discussed in section 4.1.8. In order to simulate a scenario with an model pipe torsional resistance, two-spring system was made active and the rotation was determined with variation in the residual strain and curvature length while the catenary length, rotation angles and the torque are some predefine distances are determined.

It should be noted that the value of the rotation angle and consequently the torque recorded are largely dependent on the proximity of the partially restraint end to the residual curvature, that is, the closer the end the higher the rotation

6.3.3.1 Rotation with 2 meters Residual Curvature Length

Table 6-11 shows the results of the experimental test when two residual strains of equal length of 2meters are considered and the angle of rotation as well as the pipe axial tension were recorded as indicated in the table. It is observed that with the end partial restraint introduced the angle of rotation increase significantly beyond 90degree, with the maximum angle of 103degree recorded for the 0.40% residual strain for this scenario. An increase of axial tension up to 56.8N was also observed in the pipeline for 0.40% residual strain

Tables 6-12 and 6-13 show the estimation of the torque for 0.35% and 0.40% residual strains respectively from the measure parameters such as the spring extension and so on. It is observed that the torque increases as the distance increases with a maximum of 147Nmm recorded at the TDP (4meter location) for 0.40% residual strain.

Figures 6-14 and 6-15 show (from the left) the picture of the pipeline with the residual curvature before the test begins, the residual curvature at the TDP after the test and the measurement of the pipeline rotation angle at the TDP for 0.35% and 0.40% residual strain respectively. It should be noted that the rotation angle reported in Table 6-11 is the angle of rotation at the middle of the curvature length.

As seen in the Table 6-11, the pipeline rotation angle increases as the residual strain increases, likewise the resultant axial tension in the pipe.

Table 6-11; Pipeline Rotation and Axial Tension of 2m residual Curvature for 0.35% and 0.40% Residual Strains – 2-spring Partially Restraint Pipeline Bottom End

Curvature Length (m)	2	
Applied Load (N)	40	
Bottom Boundary Condition	2-spring	
Residual Strain Level (%)	**0.35**	**0.40**
Catenary Length (m)	9.78	10.15
Angle of Rotation (Degree)	64.54	103.71
Measured Horizontal Force (N)	50.57	51.27
Vertical Tension (N)	18.22	18.91
Total Tension (N)	53.76	54.65

Table 6-12; Pipeline Torque due to 2m residual Curvature for 0.35% Residual Strains

2m Residual curvature Length								
Initial Spring Length		4	cm					
No of Spring		2						
Strain Level		0.35	%					
distance (m)	Extension (m)		Stiffness (N/m)	Force (N)		Lever Arm (cm)		Torgue (Ncm)
d	e1	e2	k	F1	F2	d1	d2	T
1	0.0006	0.0003	144.53	0.08672	0.04336	5.8	4.2	0.6850722
2	0.0025	0.0018		0.36133	0.26015			3.1883318
3	0.0027	0.002		0.39023	0.28906			3.4773918
4	0.0056	0.0045		0.80937	0.65039			7.4259514

Table 6-13; Pipeline Torque due to 2m residual Curvature for 0.40% Residual Strains

initial Spring Length		4	cm					
No of Spring		2						
Strain Level		0.4	%					
distance (m)	extension (m)		Stiffness (N/m)	Force (N)		lever arm (cm)		torgue (Ncm)
d	e1	e2	k	F1	F2	d1	d2	T
1	0.0008	0.0005	144.53	0.11562	0.07227	5.8	4.2	0.9741322
2	0.0032	0.0025		0.4625	0.36133			4.2000418
3	0.0038	0.0028		0.54921	0.40468			4.885114
4	0.0107	0.0095		1.54647	1.37304			14.736279

Figure 6-14: Pipe Rotation with a 2m R.C of 0.35% Residual Strain and 2-spring Pipeline Bottom Condition

Figure 6-15: Pipe Rotation with a 2m R.C of 0.40% Residual Strain and 2-spring Pipeline Bottom Condition

6.3.3.2 Rotation with 3 meters Residual Curvature Length

Table 6-14 shows the results of the experimental test when two residual strains of equal length of 3meters are considered and the angle of rotation as well as the pipe axial tension were recorded as indicated in the table. It is observed that with the end partial restraint introduced the angle of rotation increase significantly beyond 90degree, with the maximum angle of 124degree recorded for the 0.40% residual strain for this scenario. An increase of axial tension up to 66N was also observed in the pipeline for 0.40% residual strain
Tables 6-15, 6-16 and 6-17 show the estimation of the torque for 0.30%, 0.35% and 0.40% residual strains respectively from the measure parameters such as the spring extension and so on. It is observed that the torque increases as the distance increases with a maximum of 157.1Nmm recorded at the TDP (4meter location) for 0.40% residual strain.

Figures 6-16,6-17 and 6-18 show (from the left) the picture of the pipeline with the residual curvature

before the test begins, the residual curvature at the TDP after the test and the measurement of the pipeline rotation angle at the TDP for 0.30%, 0.35% and 0.40% residual strains respectively. It should be noted that the rotation angle reported in Table 6-14 is the angle of rotation at the middle of the curvature length.
As seen in the Table 6-14, the pipeline rotation angle increases as the residual strain increases, likewise the resultant axial tension in the pipe.

Table 6-14; Pipeline Rotation and Axial Tension of 3m residual Curvature for 0.30%, 0.35% and 0.40% Residual Strains – 2-spring Partially Restraint Pipeline Bottom End

Curvature Length (m)	3		
Applied Load (N)	40		
Bottom Boundary Condition	2-spring		
Residual Strain Level (%)	**0.30**	**0.35**	**0.40**
Catenary Length (m)	9.15	9.45	10.6
Angle of Rotation (Degree)	105.96	116.57	124.59
Measured Horizontal Force (N)	53.77	54.66	55.56
Vertical Tension (N)	17.05	17.61	19.75
Total Tension (N)	56.40	57.43	58.97

Table 6-15; Pipeline Torque due to 3m residual Curvature for 0.30% Residual Strains

initial Spring Length		4	cm					
No of Spring		2						
Strain Level		0.3	%					
distance (m)	Extension (m)		Stiffness (N/m)	Force (N)		Lever Arm (mm)		torgue (Nmm)
d	e1	e2	k	F1	F2	d1	d2	T
1	0.0006	0.0004	144.53	0.08672	0.05781	5.8	4.2	0.7457748
2	0.0024	0.0019		0.34687	0.27461			3.165207
3	0.0028	0.0024		0.40468	0.34687			3.8040296
4	0.0101	0.0088		1.45975	1.27186			13.808396

Table 6-16; Pipeline Torque due to 3m residual Curvature for 0.35% Residual Strains

initial Spring Length		4	cm					
No of Spring		2						
Strain Level		0.35	%					
distance (m)	Extension (m)		Stiffness (N/m)	Force (N)		Lever Arm (mm)		torgue (Nmm)
d	e1	e2	k	F1	F2	d1	d2	T
1	0.0009	0.0007	144.53	0.13008	0.10117	5.8	4.2	1.1793648
2	0.002	0.0014		0.28906	0.20234			2.5263844
3	0.0029	0.0025		0.41914	0.36133			3.9485596
4	0.0112	0.0099		1.61874	1.43085			15.398226

Table 6-17; Pipeline Torque due to 3m residual Curvature for 0.40% Residual Strains

Initial Spring Length		4	cm					
No of Spring		2						
Strain Level		0.4	%					
Distance (m)	Extension (m)		Stiffness (N/m)	Force (N)		Lever Arm (cm)		Torgue (Ncm)
d	e1	e2	k	F1	F2	d1	d2	T
1	0.0011	0.001	144.53	0.15898	0.14453	5.8	4.2	1.5291274
2	0.0018	0.0013		0.26015	0.18789			2.298027
3	0.0036	0.003		0.52031	0.43359			4.8388644
4	0.0115	0.01		1.6621	1.4453			15.710411

Figure 6-16: Pipe Rotation with a 3m R.C of 0.30% Residual Strain and 2-spring Pipeline Bottom Condition

Figure 6-17: Pipe Rotation with a 3m R.C of 0.35% Residual Strain and 2-spring Pipeline Bottom Condition

Figure 6-18: Pipe Rotation with a 3m R.C of 0.40% Residual Strain and 2-spring Pipeline Bottom Condition

6.4 UNEVEN SEA BED EXPERIMENTAL TEST RESULTS

Previous pipe rotation test have shown that at pipeline rotates or twists beyond 90 degree at a higher residual strains and curvature length the pre-bend pipe is in a sagging configuration before the simulation with a fixed condition of the pipeline bottom end (see Figure 6-19). The test was performed by pulling the bottom end of the pipeline until the residual curvature falls into the seabed depression, at this point the measurements were taken and the first weight (weight 1) was hanged at the mid-span of the pipeline at the depression location then the same set of measurements were taken again and lastly the first weight is replaced by the second weight (weight 2).

The configuration of the uneven seabed is as discussed in section 4.1.9. A total 7 free span experimental test was performed with different residual curvature lengths (2meters and 1meter) and residual strain levels (0.15%, 0.26% and 0.30%). For each of these tests, measurement of the catenary lengths, the height above the seabed floor and the span length were taken.

6.4.1 Free Span with 1 meter Residual Curvature

For 2 meters residual curvature length, the free span test was carried out considering residual strain in the range of 0.0 % to 0.30% as shown in Table 6-18. Measurements of the catenary length, the span length, the initial height/depth (from seabed floor to the pipe centerline) and the final depth when concentrated weights are placed at the span centre, see Table 6-18. This range of residual strain was considered because of the span and depth of the uneven seabed, as shown in Figure 4-19.

It was observed that the span of the pipeline and the initial depth from the seabed floor to the pipeline centerline at the mid-span decrease as the residual curvature increases. Also it was also observed that the depth and span length of the free-span length of the pipeline are largely dependent on the magnitude of concentrated weight at the mid-span, the higher the magnitude the lower the depth and the free-span of the pipeline

Table 6-18; Span Length and Depth of 1m Residual Curvature of Residual Strain 0.0%, 0.15%, 0.26% and 0.30%

Curvature Length (m)		1			
Applied Load (N)		40			
Bottom Boundary Condition		Fixed			
weight 1, (N)		12.0			
weight 2, (N)		18.4			
Residual Strain Level (%)		**0**	0.15	0.26	0.3
Catenary Length (m)		10.44	10.36	10.35	9.62
Initial Height from Seabed (m)		0.52	0.47	0.42	0.38
Final Height with Weight (m)	Weight 1	0.47	0.42	0.36	0.33
	Weight 2	0.44	0.41	0.34	0.31
Distance between support points (m)		2.28	2.26	2.22	2.20

6.4.2 Free Span with 2 meters Residual Curvature

For 2 meters residual curvature length, the free span test was carried out considering residual strain in the range of 0.0% to 0.30% as shown in Table 6-19. Measurements of the catenary length, the span length, the initial height/depth (from seabed floor to the pipe centerline) and the final depth when concentrated weights are placed at the span centre, see Table 6-19.

It was observed that the span of the pipeline and the initial depth from the seabed floor to the pipeline centerline at the mid-span decrease as the residual curvature increases. Also it was also observed that the depth and span length of the free-span length of the pipeline are largely dependent on the magnitude of concentrated weight at the mid-span, the higher the magnitude the lower the depth and the free-span of the pipeline

Table 6-19; Span Length and Depth of 2m Residual Curvature of Residual Strain 0%, 0.15%, 0.26% and 0.30%

Curvature Length (m)		2			
Applied Load (N)		40			
Bottom Boundary Condition		Fixed			
weight 1, (N)		12.0			
weight 2, (N)		18.4			
Residual Strain Level (%)		**0**	**0.15**	**0.26**	**0.3**
Catenary Length (m)		10.44	10.36	10.35	9.62
Initial Height from Seabed (m)		0.52	0.45	0.40	0.37
Final Height with Weight (m)	Weight 1	0.47	0.40	0.35	0.30
	Weight 2	0.44	0.38	0.33	0.28
Distance between support points (m)		2.28	2.21	2.19	2.15

Figure 6-19: Residual Curvature in Sag configuration before Test is performed

6.5 NUMERICAL ANALYSIS RESULTS

Based on the numerical method discussed in section 4, pipeline installation analysis was performed. The purpose of the analysis is to establish the change in the rotation angle or twist of the pipeline due to the residual curvature. Thus the numerical analysis performed encompasses the introduction of several residual strain levels and curvature lengths at the TDP of the pipeline section. For accurate comparison, the numerical analysis considers the same lay parameters, model properties, residual strains and curvature as the experimental test.

Prior to performing the numerical analysis, a case study analysis was performed in other to check the accuracy of the numerical analyses. This case study considered a 3m R.CL of 0.40% residual strain with both ends of the pipeline fully restrained against rotation, the result of the rotation angle (gamma angle in Orcaflex) obtained (see Appendix VII) is compared with the result of the study performed by *Li Y., (2005)* on the distribution of roll angle with zero rotational resistance along the pipe on the both, that considering nearly fixed BC at both ends of the pipeline. The distribution of the rotation angle of this case study agrees well with that obtained from *Li Y., (2005)* study, see Appendix VII. Thus the numerical analyses results presented in this study effort are reasonable and reliable.

The two cases considered are when the curvature length are 2meters and 3 meters, and for each of these cases two BCs are considered, the Fixed and the partially restraints BCs. Figures 6-21 and 6-20, show the plan and elevation view of the catenary. It is observed that the rotation angle is approximately zero as the cordiante axes (in color red and green) remains in the initial position without rotating or twisting

The result of the installation analysis without residual strains and with free and fixed BCs at the top and bottom ends of the pipeline is shown in Figures 6-22, 6-23 and 6.24. The data of the catenary shape is compared with the experimental test initial catenary as shown in Figure 6-1; this comparison shows a reasonable level of agreement. Hence all other analyses preformed with residual strains are based on the Orcaflex model and analysis parameters of this initial configuration except for the change in the residual strain levels and the curvature length and twisting stiffness. The result of the zero residual strain installation analysis performed in Orcaflex, serves as basis of comparison for the cases with residual strain. Figure 6-24

shows that for a catenary without residual strain, the angle of rotation of the pipeline is negligible,

The results of the analyses performed for the cases with residual strains are presented and discussed in chapter 7, and the pictures of the catenary shape and the plot of the twist are documented in Appendix V. The numerical analysis is classified into two different cases and for each of the cases, three scenarios are considered. The scenarios are based on the BCs adopted at the seabed end of the pipeline. For each of the cases, the angle of rotation is measured at the middle of the curvature. The location of this middle is as specified in Table 6-19.;

- Cases 1 – 2m residual curvature length
- Cases 2 – 3m residual curvature length

Table 6-20; Location of the Curvature Mid-span from the Surface End of the Pipeline

Case 1	19m
Case 2	22.5m

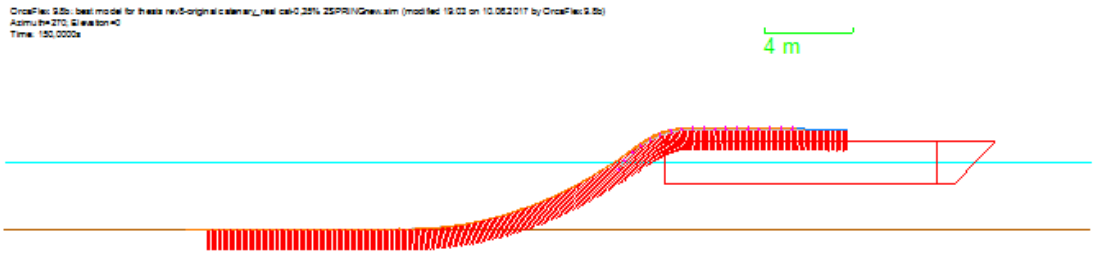

Figure 6-20: Orcaflex Result for the Catenary Shape of Zero-strain Pipeline

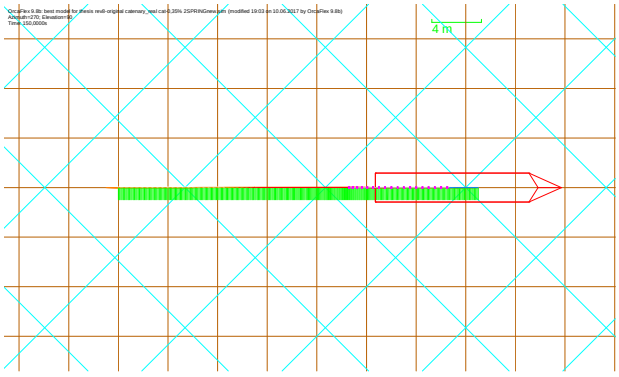

Figure 6-21: Orcaflex Result for the Catenary Shape of Zero-strain Pipeline

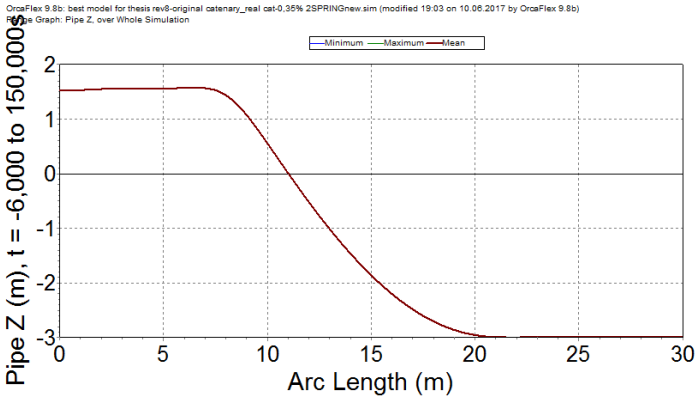

Figure 6-22: Orcaflex Result for the Catenary Shape of Zero-strain Pipeline

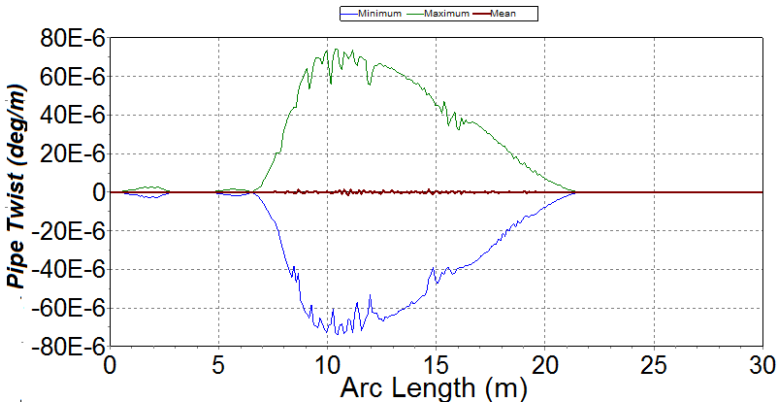

Figure 6-23: Orcaflex Result for the Twist of a Zero-strain Pipeline

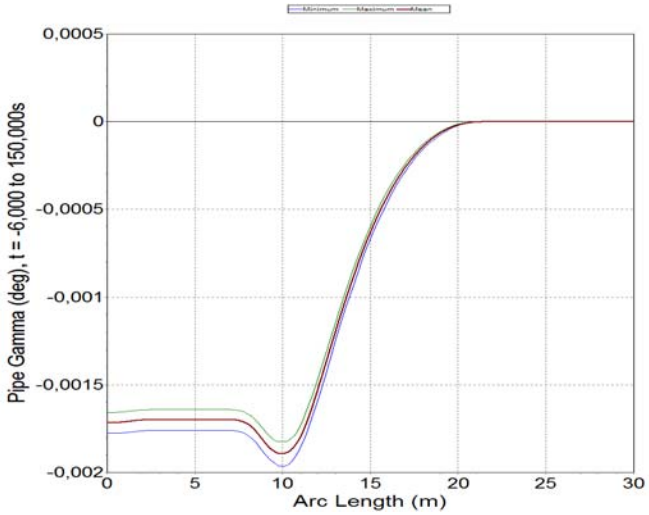

Figure 6-24: Orcaflex Result for the Rotation Angle of a Zero-strain Pipeline

6.5.1 Case 1 – 2m Residual Curvature Length

The result of the numerical analyses performed for each of the cases discussed in **section 6.5** agrees to an extent with the experimental test. For the 2m residual curvature length, Table 6-21 shows the summary of the angle of rotation at the TDP considering different BCs are previously explained. Details of the analysis result can be found in Appendix V, which contains the pictures of the models, the angle of rotation for the whole length of the catenary and the twist in degree/meter for the whole length of the catenary. The pipeline angle of rotation for the 2m R.C.L is shown from Figures 6-26 to 6-33

Fixed Boundary Condition – 0.30% Residual Strains

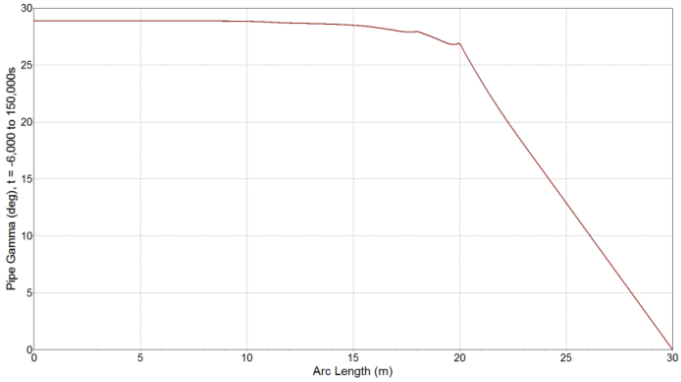

Figure 6-25: Rotation Angle of the Catenary due to 2m R.C.L of 0.30% R.S with Fixed BC

Fixed Boundary Condition – 0.35% Residual Strains

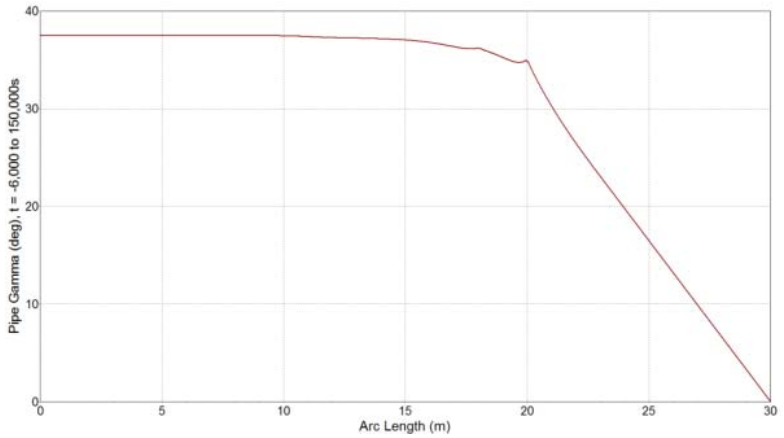

Figure 6-26: Rotation Angle of the Catenary due to 2m R.C.L of 0.35% R.S with Fixed BC

Fixed Boundary Condition – 0.40% Residual Strains

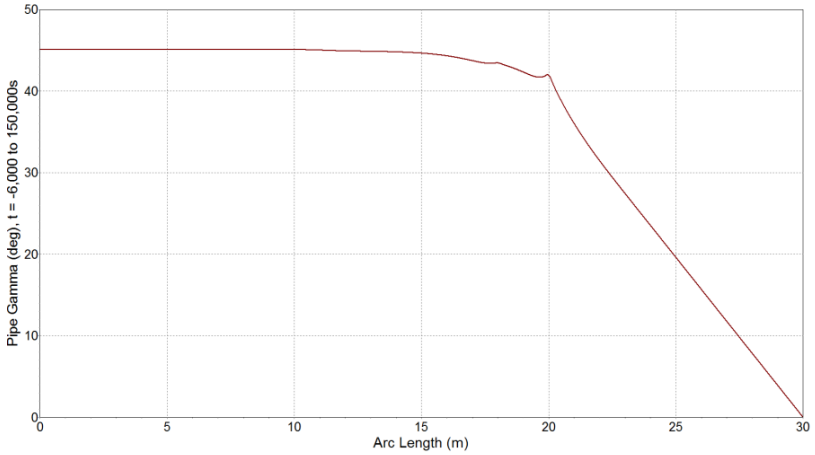

Figure 6-27: Rotation Angle of the Catenary due to 2m R.C.L of 0.40% R.S with Fixed BC

1-spring Boundary Condition – 0.30% Residual Strains

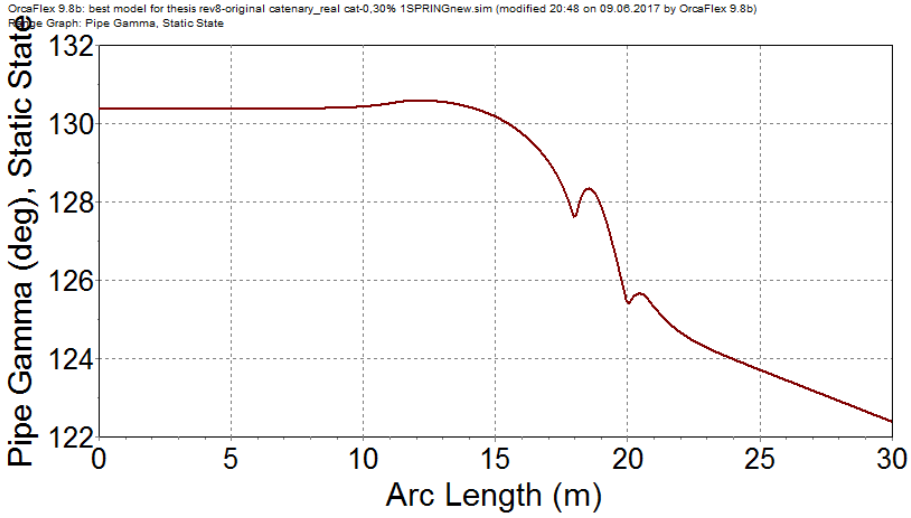

Figure 6-28: Rotation Angle of the Catenary due to 2m R.C.L of 0.30% R.S with 1-spring BC

1-spring Boundary Condition – 0.35% Residual Strains

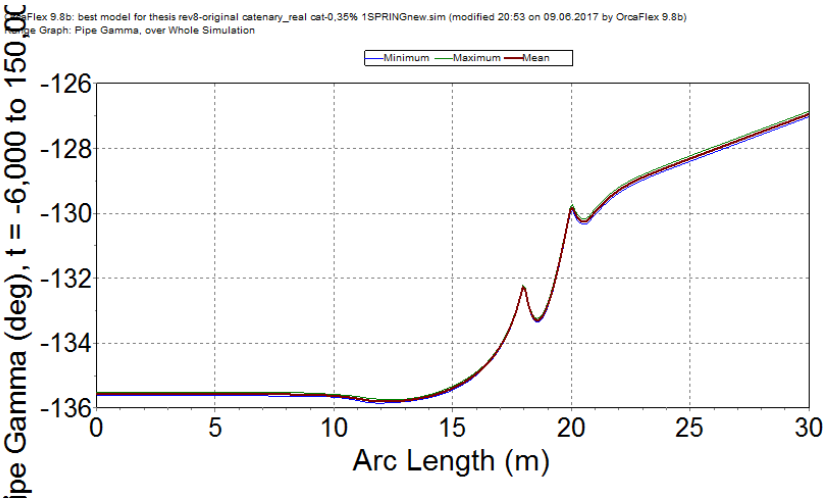

Figure 6-29: Rotation Angle of the Catenary due to 2m R.C.L of 0.35% R.S with 1-spring BC

1-spring Boundary Condition – 0.40% Residual Strains

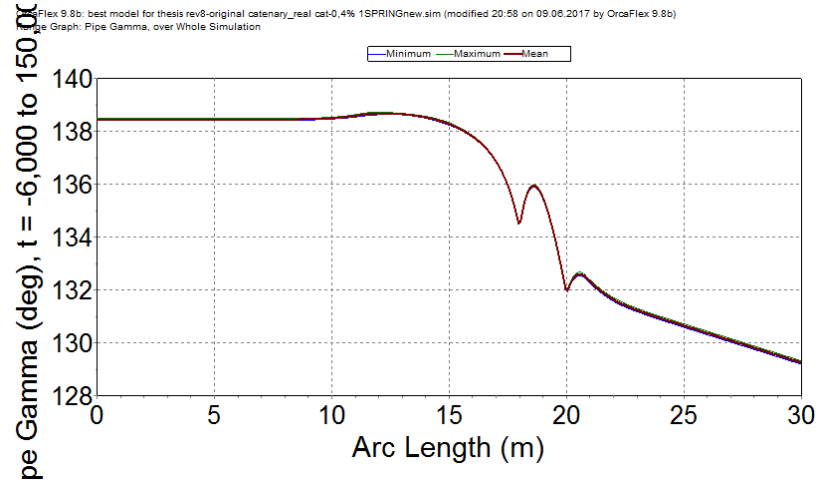

Figure 6-30: Rotation Angle of the Catenary due to 2m R.C.L of 0.40% R.S with 1-spring BC

2-spring Boundary Condition – 0.30% Residual Strains

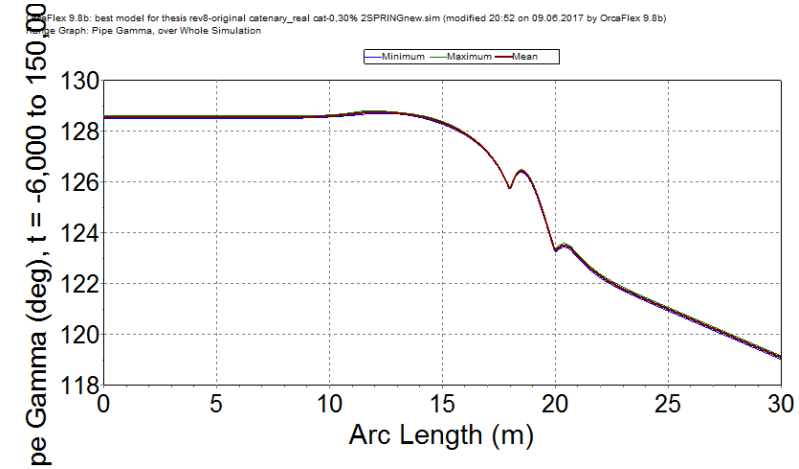

Figure 6-31: Rotation Angle of the Catenary due to 2m R.C.L of 0.30% R.S with 2-spring BC

2-spring Boundary Condition – 0.35% Residual Strains

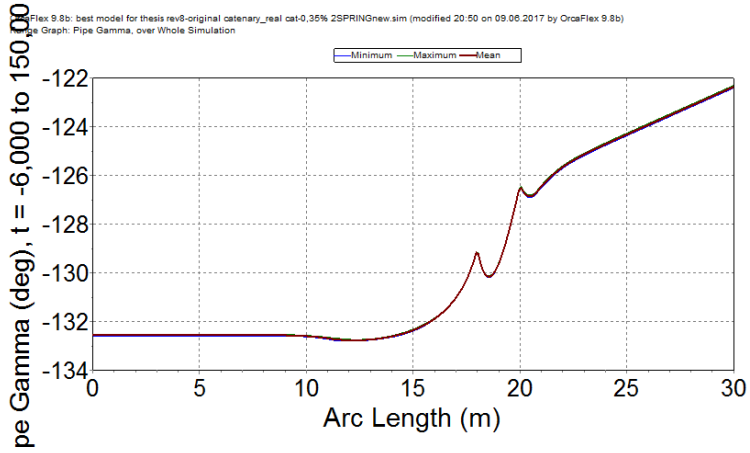

Figure 6-32: Rotation Angle of the Catenary due to 2m R.C.L of 0.35% R.S with 2-spring BC

2-spring Boundary Condition – 0.40% Residual Strains

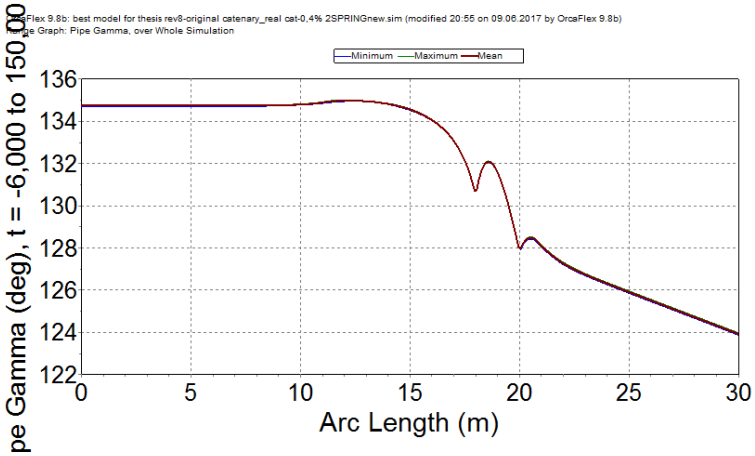

Figure 6-33: Rotation Angle of the Catenary due to 2m R.C.L of 0.40% R.S with 2-spring BC

Table 6-21; Summary of the Numerical Analysis for 2m R.C.L

2m R.C.L			
R.C.L	R.S	BC	ROT
m	%		deg.
2	0.3	FIXED	27.56
		1-SP	128.27
		2-SP	107.01
	0.35	FIXED	35.78
		1-SP	133.56
		2-SP	110.85
	0.4	FIXED	40.35
		1-SP	136.15
		2-SP	132.67

6.5.2 Case 1 – 3m Residual Curvature Length

For the 3m residual curvature length, Table 6-22 shows the summary of the angle of rotation at the TDP considering different BCs. Details of the analysis result can be found in Appendix V. The pipeline angle of rotation for the 2m R.C.L is shown from Figures 6-34 to 6-44

Fixed Boundary Condition – 0.30% Residual Strains

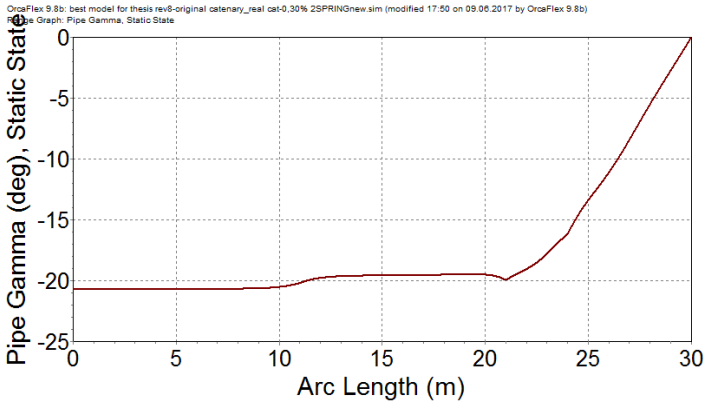

Figure 6-34: Rotation Angle of the Catenary due to 3m R.C.L of 0.30% R.S with Fixed BC

Fixed Boundary Condition – 0.35% Residual Strains

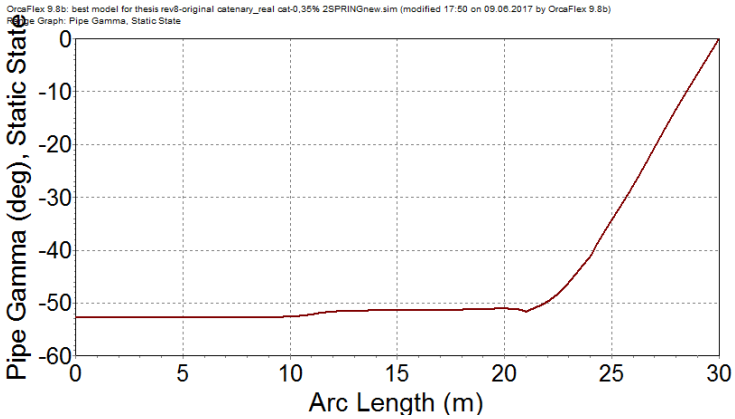

Figure 6-35: Rotation Angle of the Catenary due to 3m R.C.L of 0.35% R.S with Fixed BC

Fixed Boundary Condition – 0.40% Residual Strains

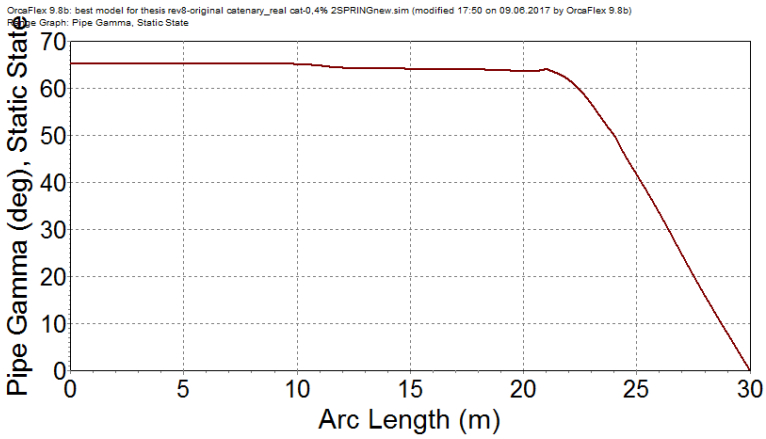

Figure 6-36: Rotation Angle of the Catenary due to 3m R.C.L of 0.40% R.S with Fixed BC

1-spring Boundary Condition – 0.30% Residual Strains

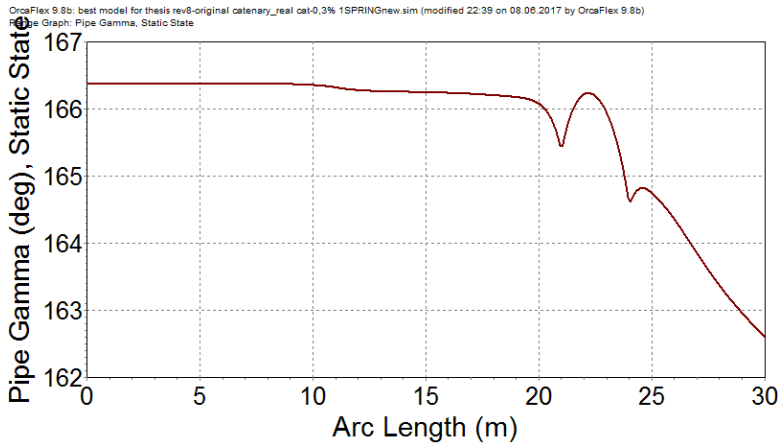

Figure 6-37: Rotation Angle of the Catenary due to 3m R.C.L of 0.30% R.S with 1-Spring BC

1-spring Boundary Condition – 0.35% Residual Strains

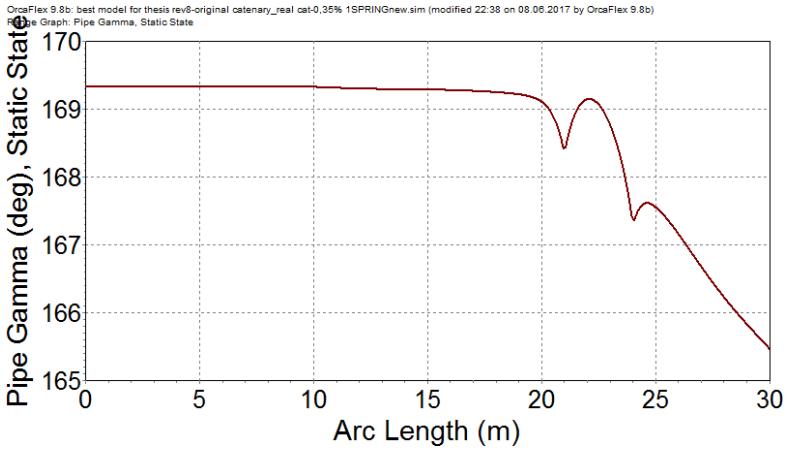

Figure 6-38: Rotation Angle of the Catenary due to 3m R.C.L of 0.35% R.S with 1-Spring BC

1-spring Boundary Condition – 0.40% Residual Strains

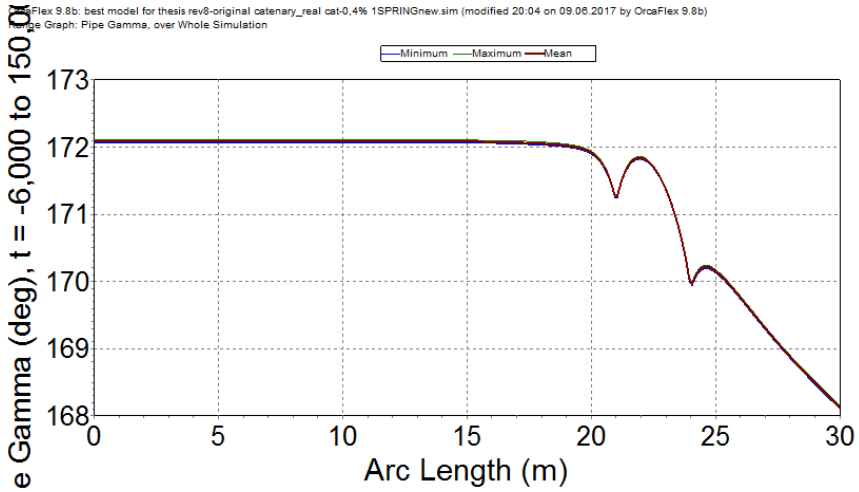

Figure 6-39: Rotation Angle of the Catenary due to 3m R.C.L of 0.40% R.S with 1-Spring BC

2-spring Boundary Condition – 0.30% Residual Strains

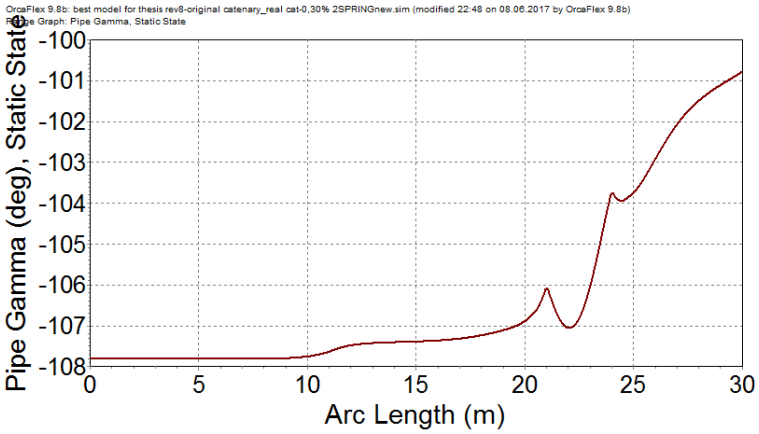

Figure 6-40: Rotation Angle of the Catenary due to 3m R.C.L of 0.30% R.S with 2-Spring BC

2-spring Boundary Condition – 0.35% Residual Strains

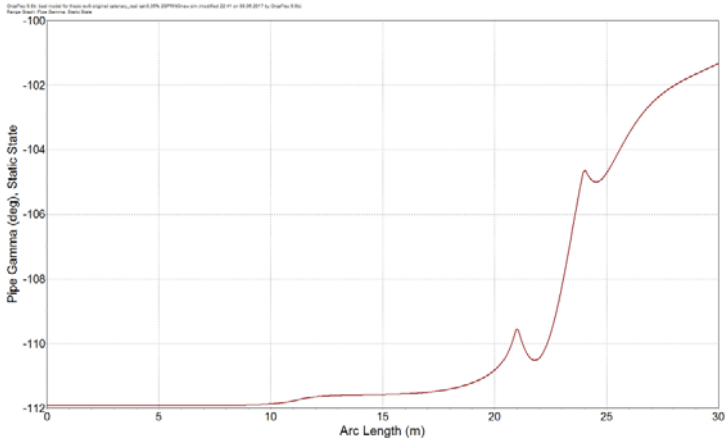

Figure 6-41: Rotation Angle of the Catenary due to 3m R.C.L of 0.35% R.S with 2-Spring BC

Table 6-22; Summary of the Numerical Analysis for 3m R.C.L

3m R.C.L			
R.C.L	R.S	BC	ROT
m	%		deg.
3	0.3	FIXED	45.5
		1-SP	165.5
		2-SP	107.01
	0.35	FIXED	51.55
		1-SP	168.6
		2-SP	130.45
	0.4	FIXED	64.63
		1-SP	171.7
		2-SP	-

7. DISCUSSION AND COMPARISON OF RESULT

The experimental test results presented in section 6.0 and the numerical analysis results are discussed and compared in this section. It should be recalled that parameter of focus for this study in the case of the pipeline rotation (beyond 90degree) during S-lay installation and free-span experimental test are the variation in the boundary condition of the pipeline end at the seabed, the variation in the residual strains, the variation in the length of residual curvature and inline structure.

How these parameter influence rotation or twist beyond 90degreee at the TDP are discussed in this sections by plotting the experimental test results in graphs and compare how the various parameters influences the value of the pipeline rotation.

The numerical analysis results presented here are based on the approach discussed in section 4, the results are also given in terms of the gamma angle (discussed in section 4.2.1), which is a function of degree of rotation or twist of the pipeline about the pipeline axial direction. For the cases that involved partial restraints of the pipeline the twist in degree/meters are also given. The results of the numerical analysis reported here is for the whole length of the pipeline; however it is worthy to note that the point of interest of this thesis is the rotation at the touch down point. The positions of the TDP are as given in section 6.5

7.1 EXPERIMENTAL RESULTS

The experimental test was performed purposely to determine the influence of some key parameters such as residual strains, residual curvature length and boundary conditions on pipeline rotation as well as to establish the basic operational principle of conforming pipeline to uneven seabed topography. The test results given in section 6 were plotted on graphs in order to assess the impact of the variations of these key parameters on the pipeline rotation and the torque induced by these rotations for the cases of partial restraints boundary conditions. Thus the graphs presented in this section as given in terms of the rotation angles against curvature length, the residual strain levels and in-line structure for the rotation experimental test and addition of concentrated weight for the case of free-span.

Further study may include the effect of water depth and top tension on pipeline rotation beyond 90degrees

7.1.1 Boundary Conditions

The pipeline end boundary conditions are pivotal to the value of the rotation angle observed at the TDP. It is expected that a pipeline with residual curvature section and free-to rotate ends will experience approximately 180degree rotation when the frictional resistant with the contacts elements (seabed and rollers) is ignored, this is gain a new stability position, this promotes the need for a boundary condition that includes resistance against rotation at one or the two ends of the pipeline. Thus the magnitude of the rotation angle is largely dependent on the degree of freedom especially rotational restraints.

This experimental test was able to establish the influence of the degree of freedom on the magnitude pipeline rotation angle during S-lay installation. As discussed in previous sections, two end boundary conditions were considered in the experiments, the fully restraints against rotation (Fixed BC) and the partially restraints against rotation. The BC was established for two different scenarios, when the residual strain varies at constant residual curvature length (2m and 3m) and when the residual curvature length varies at constant residual strains (0.35% and 0.40%), see Figures 7-1 to 7-4. It should be noted that the graphs were plotted using the values at the TDP only.

Figures 7-1 and 7-2 show how the BC influences the rotation of a pipeline, with constant residual curvature lengths, during installation while Figures 7-3 and 7-4 shows the influence of BC on rotation angle with constant residual strains.

As shown in both Figures, the rotation angle is largely reduced when a fully restraints against rotation (Fixed BC) at the seabed end of the pipeline is adopted having the minimum rotation angle of approximately 12degrees for the case of 0.30% residual strain and 2m residual curvature length as shown in Figures 7-1 and 7-3 respectively . Of all the boundary conditions considered (Fixed and Partially restraint BC) the maximum rotation angle is observed for the case with minimum torsional restraints, that is the partially restraint BC with 1-spring system, having rotation angle of approximately 172degrees at a residual strain of 0.40% and residual curvature length of 3m as shown in Figures 7-2 and 7-4 respectively.

The behavior of pipeline rotation is much expected since a fixed boundary condition has the capacity to resist rotation because of its high twisting stiffness, hence it is expected that for fixed BC, the rotation will be low but the torque will be high. While 1-spring BC denotes a reduced twisting stiffness and consequently low resistance to pipeline rotation, that lower torque is expected and higher rotation. Addition of another spring to make a 2-spring BC means increasing the twisting capacity of the BC however not as much as what will be provided by a fixed BC.

By comparing the graphs in Figures 7-1 to 7-4, the effect of the residual strains and the curvature length can also be established. For each of the boundary conditions it is observed that higher rotation angle is reported as the residual strain increases with constant curvature length as shown in Figures 7-3 and 7-4 similarly increase is observed in the rotation angle as the curvature length increases at constant residual strains as shown in Figures 7-1 and 7-2.

Thus it can be deduced that provision of torsional restraints at the pipeline ends greatly reduced the rotational angle. Thus, during installation, the pipeline can be conformed to the seabed topography by reducing the twisting capacity of the pipeline end connection this consequently gives an increase in the rotation of the residual curvature and vice versa.

It is worthy of note that, in real life situation, the boundary condition at the tensioner on the laying barge provides restraints against twist, however for the case of deep water, the influence of the resistance to twist provided at the tensioner will be significantly reduced near the seabed, thus the rotation would only be resisted by the pipeline torsional capacity (torsional stiffness) and the frictional resistant due to pipeline-seabed interaction.

Further study or experimental test might is required to establish the behavior of the rotation angles with varying residual strain and curvature length, as Figure 7-2 shows that the relations is not linear. Hence a linear interpolation or interpretation of these plots might be misleading.
It is worthy to note that the value of the angle of rotation documented in the thesis largely dependent on the proximity of the fixed end to the location of the residual curvature section along the pipeline

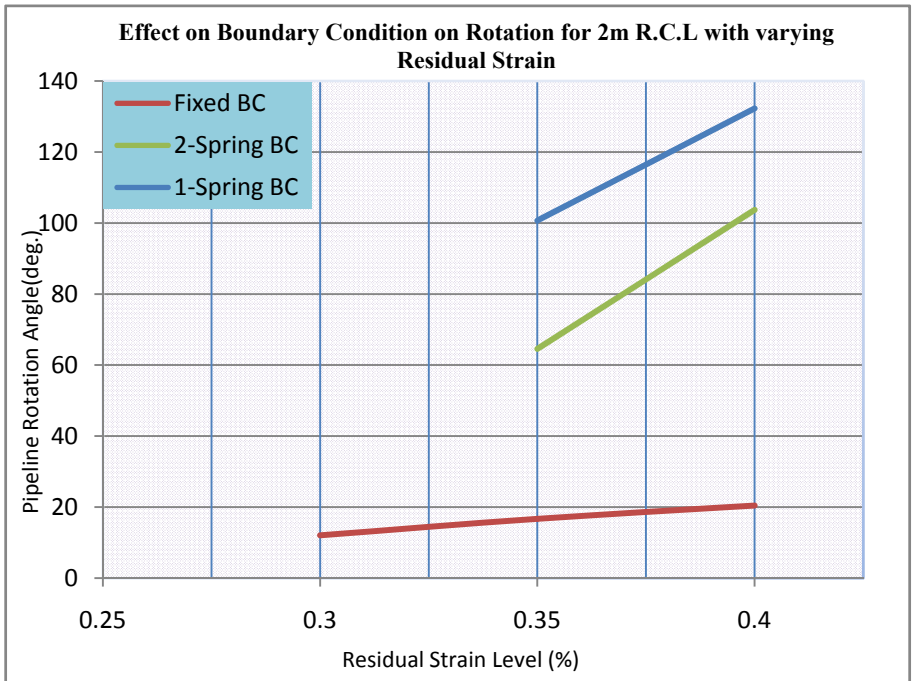

Figure 7-1: Influence of BC on Rotation Angle at TDP of Pipeline with 2m R.C.L

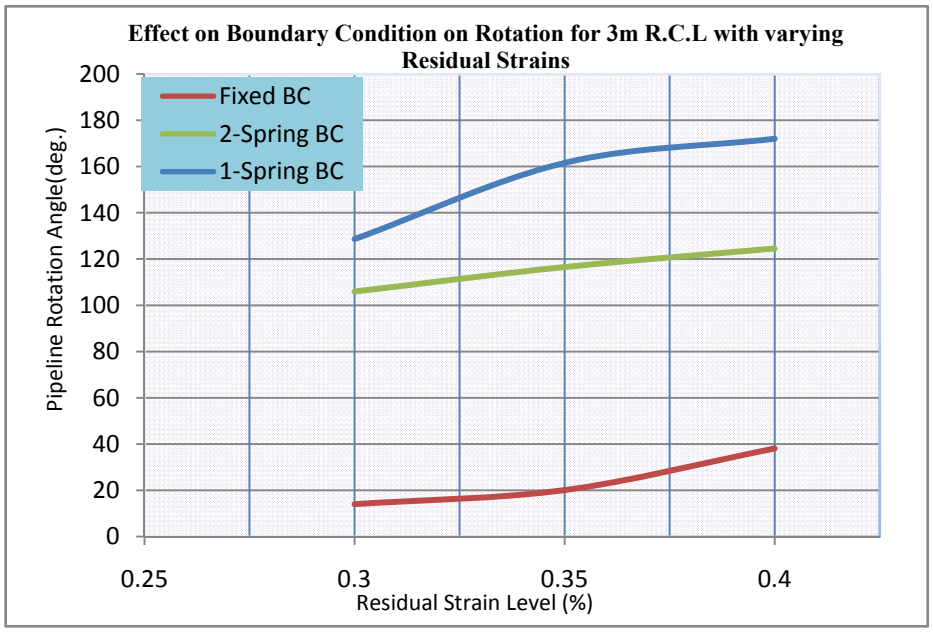

Figure 7-2: Influence of BC on Rotation Angle at TDP of Pipeline with 3m R.C.L

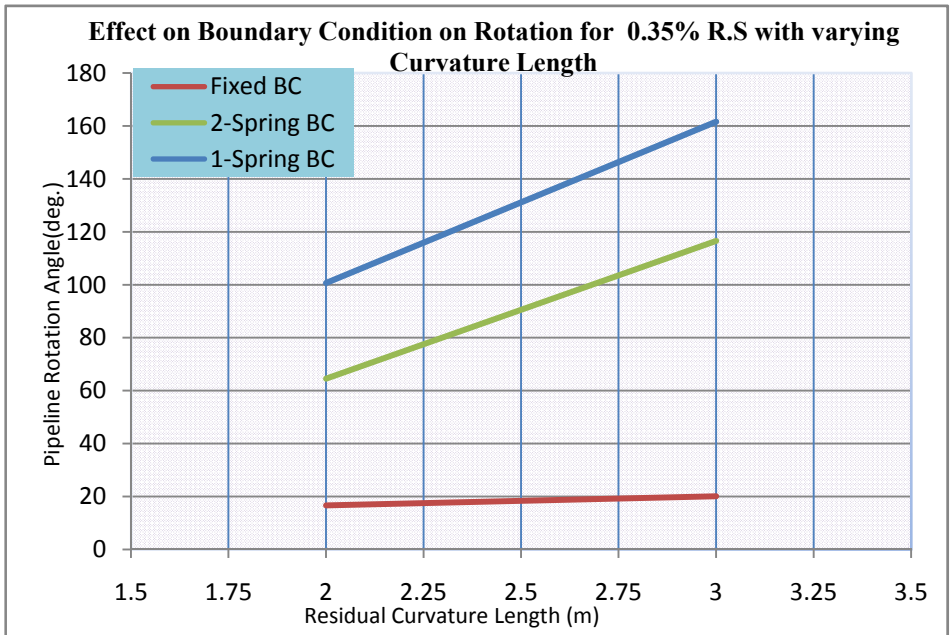

Figure 7-3: Influence of BC on Rotation Angle at TDP of Pipeline with 0.35% R.S

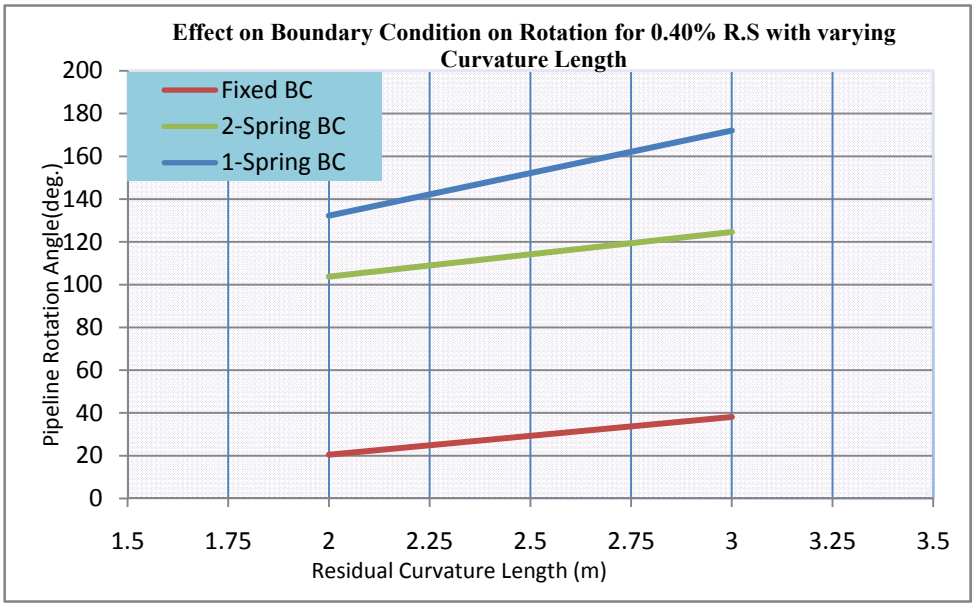

Figure 7-4: Influence of BC on Rotation Angle at TDP of Pipeline with 0.40% R.S

7.1.2 Residual Strain Level

The residual strain is a key parameter that influences the magnitude of rotation during installation. Past experimental and numerical research studies has shown that a pipeline with no residual strain section has an ignorable angle of rotation at the TDP (*Kashif, 2016*). However, in real life situation pipeline are subjects to residual strains as it pass through the stinger in the case of S-lay installation, thus causing pipeline rotation or twist during installation. Hence the magnitude of the rotation angle is largely dependent on the level of residual strains. The experimental test performed in this work covers the establishment of the influence of the different strain levels on the magnitude pipeline rotation angle during S-lay installation for different

pipeline end BC was considered and the plots are as shown in Figures 7-5 to 7-7.

For the fixed BC, Figure 7-5 shows that regardless of the length of curvature, the angle of rotation increases with increase in residual strain level, thus showing maximum rotation of approximately 38degree and 20degree at 3m and 2m respectively for the 0.40% as compare to the corresponding 12degree and 14degree in the case of 0.30%. Attention should be given to the significant divergent of the curves of the residual strains at the upper tail as shown in Figure 7-5, this indicates that the increase in the angle of rotation with residual strain is not directly proportional. While the lower tail of the curves shows convergence. Hence it can be inferred that as the residual strain increase a geometric increase in might be seen, since there is an increase of 90% in rotation angle between 0.40% and 0.35% at the upper tail of the curve, however further experimental investigation might be required to established this fact.

While for the 1-spring BC, Figure 7-6 shows that regardless of the length of curvature, the angle of rotation increases with increase in residual strain level, thus showing maximum rotation of approximately 172degree and 138degree at 3m and 2m respectively for 0.40% as compare to the corresponding 161degree and 100degree in the case of 0.35%. Unlike the Fixed BC the figure shows convergence of the curves of the residual strains at the upper tail and divergence at the lower tail as shown in Figure 7-6. Hence it can be inferred that the residual strain increment does not give a linear increase in the rotation angle, since there is an increase of 7% in rotation angle between 0.40% and 0.35% at the upper tail and about 38% percentage increase at the lower tail.

The curves for the 2-spring BC, Figure 7-7, follow the same pattern as described for the 1-spring BC, Figure 7-7 shows the maximum rotation of approximately 128degree and 100degree at 3m and 2m respectively for the 0.40% as compare to the corresponding 115degree and 68degree in the case of 0.35%. Similarly, to the 1-spring BC the figure shows convergence of the curves of the residual strains at the upper tail and divergence at the lower tail as shown in Figure 7-7. Hence it can be inferred that the residual strain increment does not give a linear increase in the rotation angle, since there is an increase of 11% in rotation angle between 0.40% and 0.35% at the upper tail and about 47% percentage increase at the lower tail.

The behavior shown by the figures are well in agreement with the studies performed by *Damsleth et al., (2000)*…, which shows that the rotation increases as the pipeline strain increases

Thus it can be deduced that increase in the residual strain level regardless of the boundary conditions at the pipeline ends gives an increase in the rotation angle. hence, during installation, in order to achieve the pipeline rotation angle above 90degree, so as to conformed the pipeline to the seabed topography the residual strain level can be safely increase and to prevent significant rotation when verticality of pipeline components installed along the length of the pipeline is of utmost importance, high residual strain level should be avoided Further study or experimental test might be required to establish whether the behavior of the rotation angles with varying curvature length is truly linear, by performing addition test considering more residual curvature length.

This result is in agreement with the study carried by Li Y., (2005), which shows that angle of rotation increases with the residual curvature, with rapid change in rotation for residual strain within the range of 0.30% to 1.0%

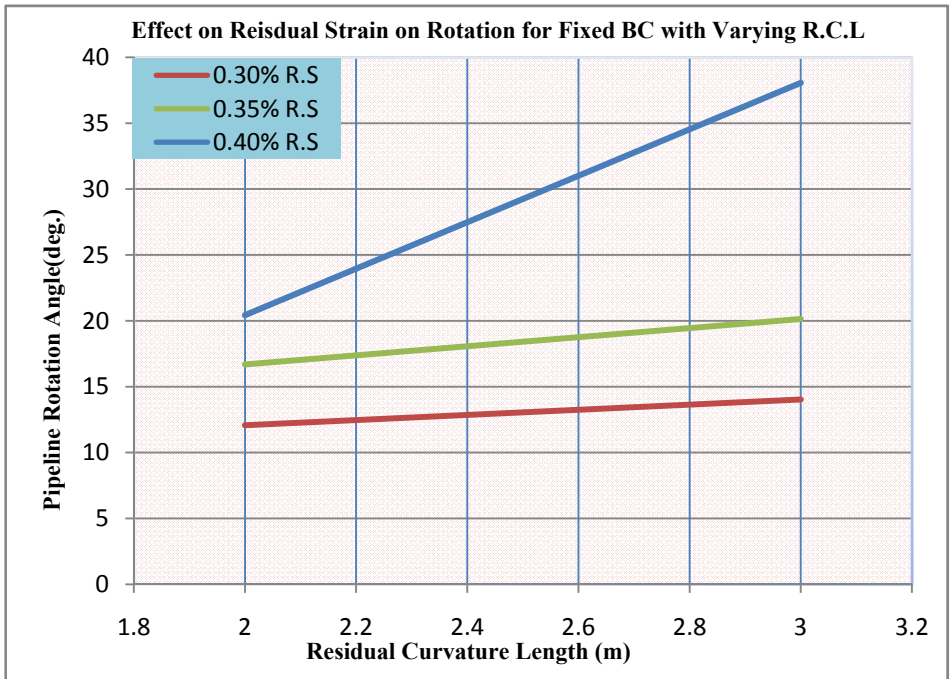

Figure 7-5: Influence of R.S on Rotation Angle at TDP of Pipeline with Fixed BC

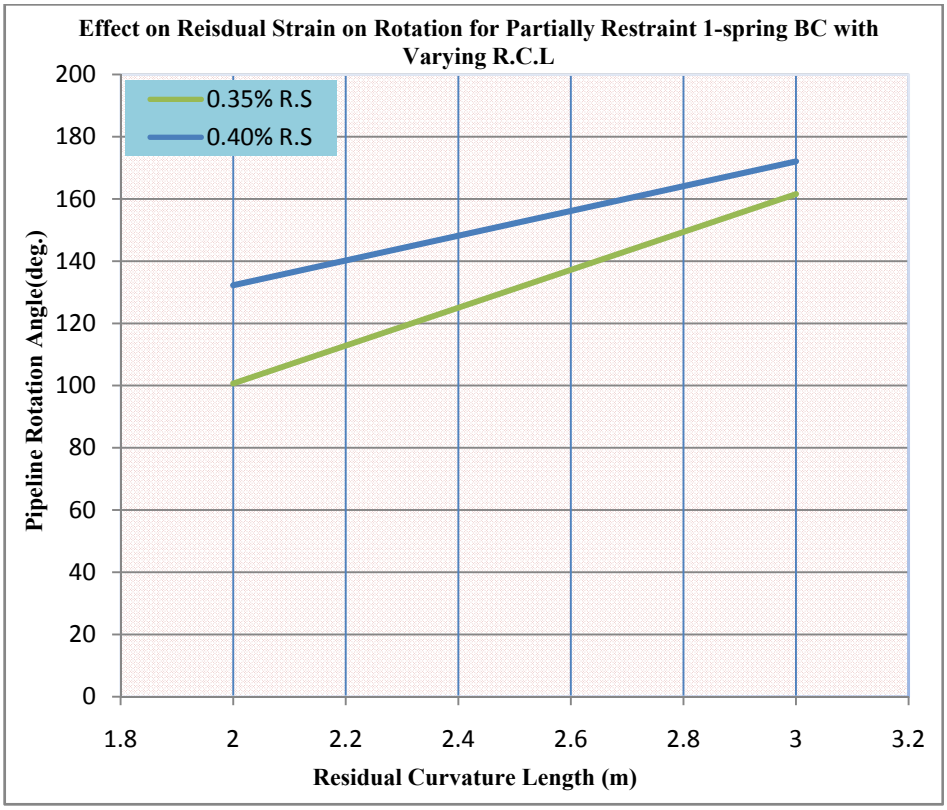

Figure 7-6: Influence of R.S on Rotation Angle at TDP of Pipeline with 1-Spring BC

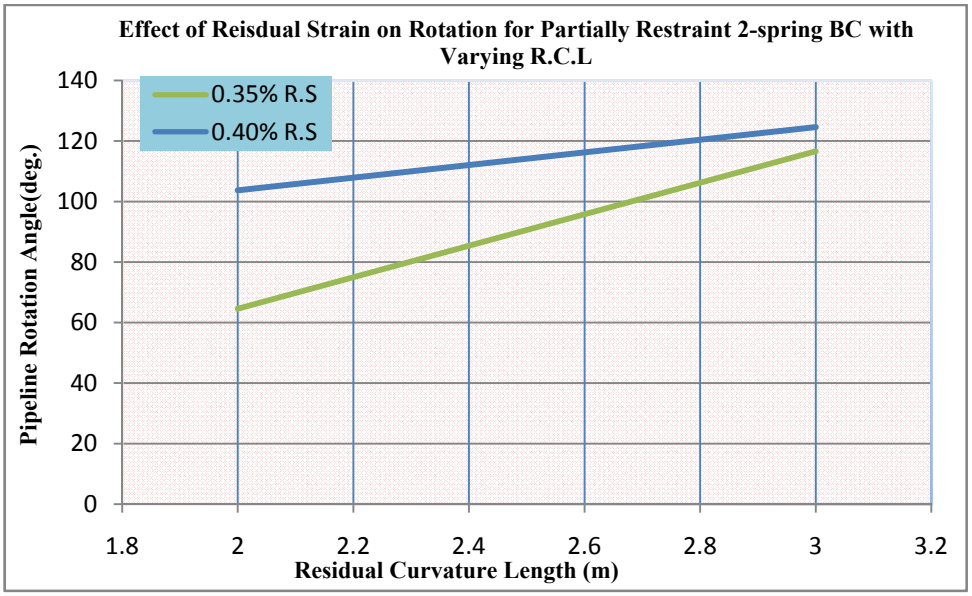

Figure 7-7: Influence of R.S on Rotation Angle at TDP of Pipeline with 2-Spring BC

7.1.3 Residual Curvature Length

Another key parameter that influences the magnitude of rotation during installation is the residual curvature length. Of great deal is the length of residual curvature section along the pipeline, studies have shown that a combination of high residual strain and residual curvature length will induced high rotation angle.
This thesis also investigates the influence of the residual curvature length on the pipeline rotation during installation and results obtained validate the fact that the higher the R.C.L the higher the tendency of rotation of the pipeline during rotation. Figures 7-8 to 7-10 show the plot of the rotation against the R.S for different curvature lengths (2m and 3m)

For the fixed BC, Figure 7-8 shows that regardless of the length of curvature, the angle of rotation increases with increase in R.C.L, thus showing maximum rotation of approximately 38degree and 20degree at 0.40% and 0.30% respectively for the 3m R.C.L as compare to the corresponding 20degree and 12degree in the case of 2m. Attention should be given to the significant divergent of the curves of the residual strains at the upper tail as shown in Figure 7-8, this indicates that the increase in the angle of rotation with R.C.L is not directly proportional. While the lower tail of the curves shows convergence.

While for the 1-spring BC, Figure 7-9 shows that regardless of the R.S, the angle of rotation increases with increase in R.C.L, thus showing maximum rotation of approximately 172degree and 138degree at 0.40% and 0.30% respectively for the 3m R.C.L as compare to the corresponding 161degree and 100degree in the case of 2m. Unlike the Fixed BC the figure shows convergence of the curves of the residual strains at the upper tail and divergence at the lower tail as shown in Figure 7-9

The curves for the 2-spring BC, Figure 7-10, follow the same pattern as described for the 1-spring BC, Figure 7-10 show the maximum rotation of approximately 128degree and 100degree at 0.40% and 0.30% respectively for the 3m R.C.L as compare to the corresponding 115degree and 68degree in the case of 0.35%. Similarly, to the 1-spring BC the figure shows convergence of the curves of the residual strains at the upper tail and divergence at the lower tail as shown in Figure 7-8.

Thus it can therefore be deduced that increase in the residual curvature length regardless of the boundary conditions at the pipeline ends and the R.S results in an increase in the rotation angle. hence, during installation, in order to achieve the pipeline rotation angle above 90degree, so as to conformed the pipeline to the seabed topography the residual curvature length can be safely increase and to prevent significant rotation when verticality of pipeline components installed along the length of the pipeline is of utmost importance, high curvature length should be avoided.

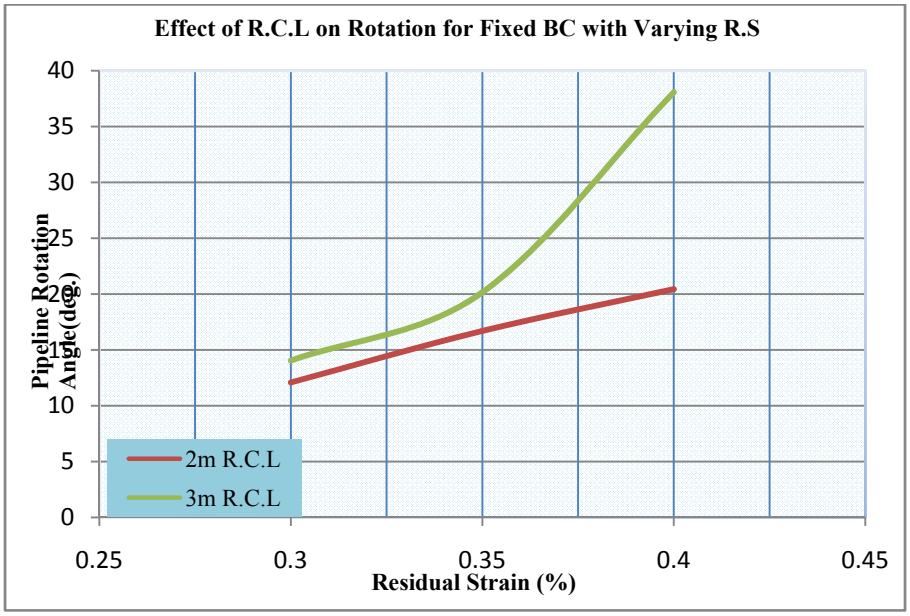

Figure 7-8: Influence of R.C.L on Rotation Angle at TDP of Pipeline with Fixed BC

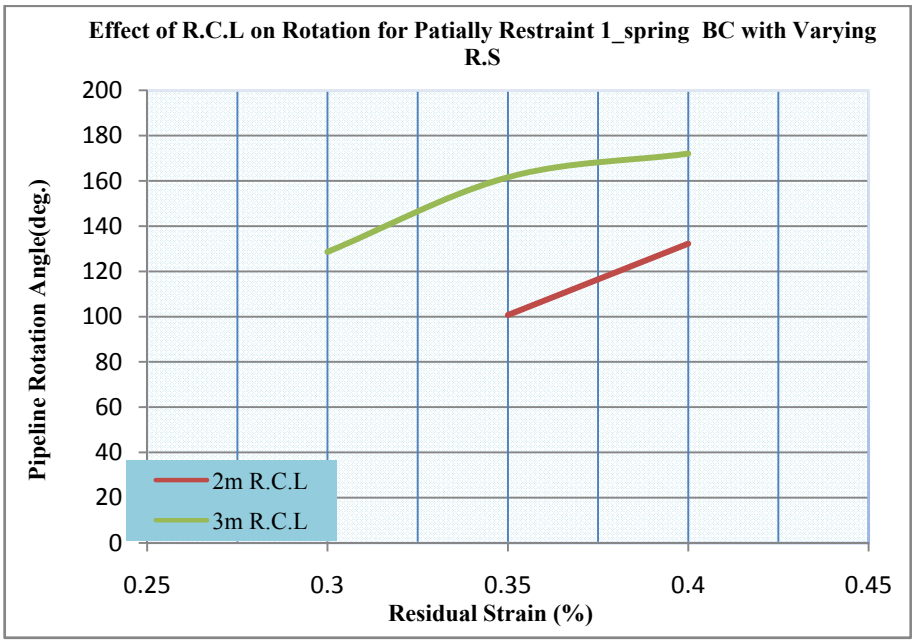

Figure 7-9: Influence of R.C.L on Rotation Angle at TDP of Pipeline with 1-Spring BC

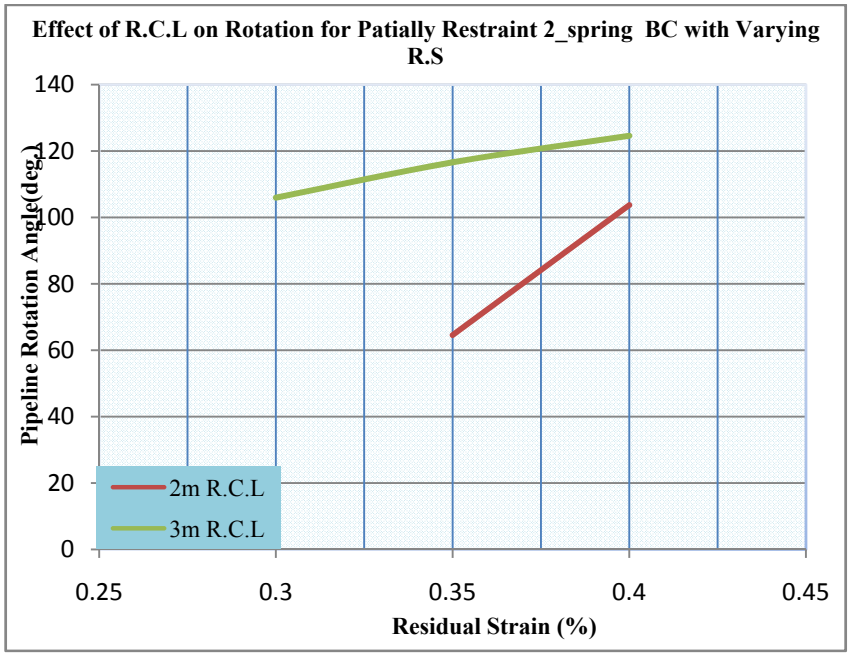

Figure 7-10: Influence of R.C.L on Rotation Angle at TDP of Pipeline with 2-Spring BC

7.1.4 Torque Effect

The pipeline-seabed interaction provides rotation resistant, this interaction when combined with the torsional stiffness of the pipeline provides resistant to pipeline rotation during installation, however the resistant provided by this system might to be adequate to prevent the pipeline from twisting or rotating, as the magnitude of this resistant is largely dependent on the length of the pipeline having contact with the seabed, the geometric and material properties of the pipeline, the depth of water and so on. This study investigate the effect of different torque resistant on rotation and consequently, the influence of the variation in residual strains and residual curvature on torque

Figure 7-11 and 7-12 show the variation of rotation against torque for two difference rotation resistant capacities (1-spring BC and 2-spring BC) and the influence of different restraint capacity on the torque respectively. It is observed that the lower the rotation the higher the torque as shown in Figure 7-11. The figure indicate that the 2-spring BC resist rotation more effectively that the 1-spring BC, that is the reason for the lower rotation of the 2-spring BC. Since the resistance to rotation is high it is expected as shown in Figure 7-11 to have higher torque.

Figure 7-12 shows the influence of the BCs on the torque more clearly with varying residual curvature for the 3m R.C.L. As shown in the figure, the rotation resisting capacity of the 2-spring being approximately 13.8Ncm at a residual strain of 0.3%, is higher than the 1-spring of 11.89Ncm, with a percentage change of 15% at the 0.30% R.S. The graph of Figure 7-12 shows a reduction in this percentage change with increase in residual change, further study is necessary to validate this behavior.

Figures 7-13a and 7-13b show the direct influence of residual curvature length and strain on the torque. Figure 7-13a shows that regardless of the residual strain, the torque increases at higher R.C.L. similarly, regardless of the R.C.L, the torque increases with increase in the residual strain as shown in Figure 13b. Thus, combine effect of both increased curvature length and strain can amount to enormous torque required

to prevent rotation and vice versa.

It can therefore be deduced that higher torque capacity results in reduced pipeline rotation and a lower torque capacity has a reverse effect.

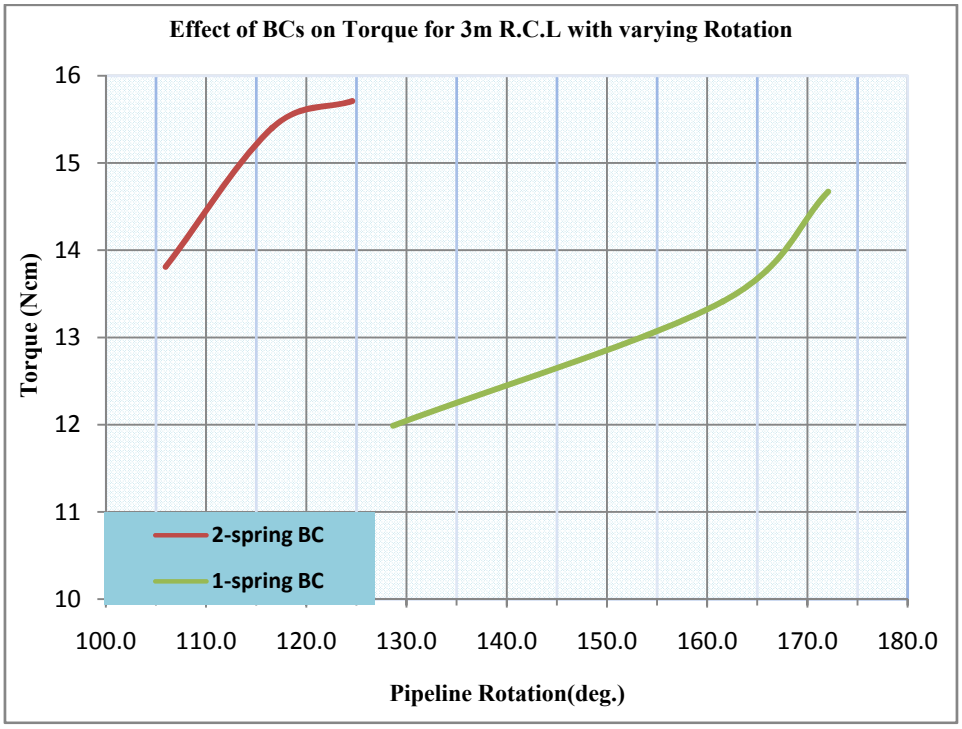

Figure 7-11: Effect of BCs on Torque for the 3m R.C.L with varying Rotation

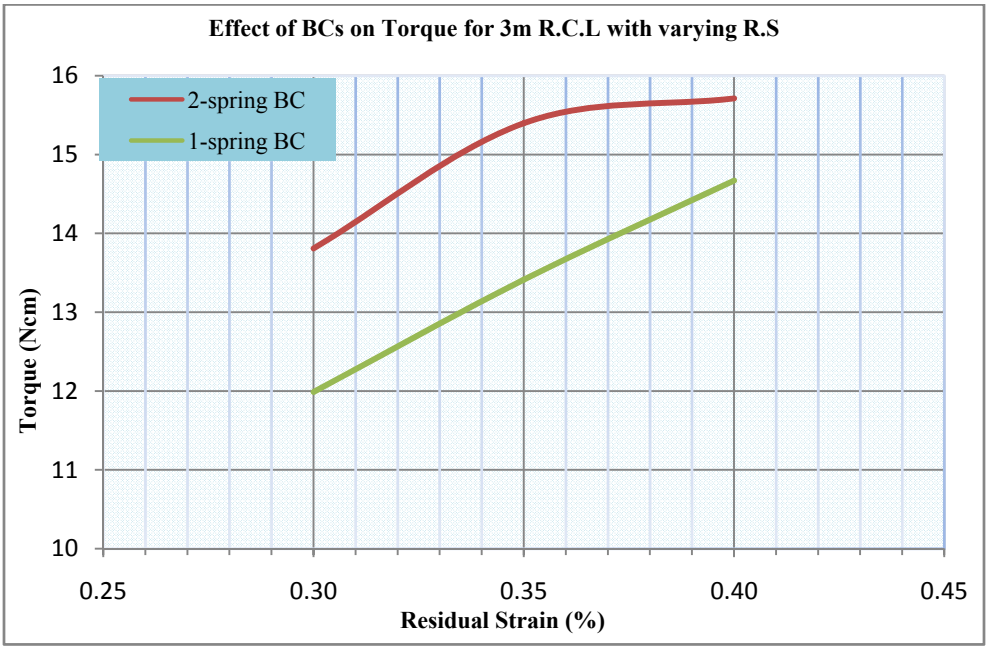

Figure 7-12: Effect of BCs on Torque for the 3m R.C.L with varying Residual Strain

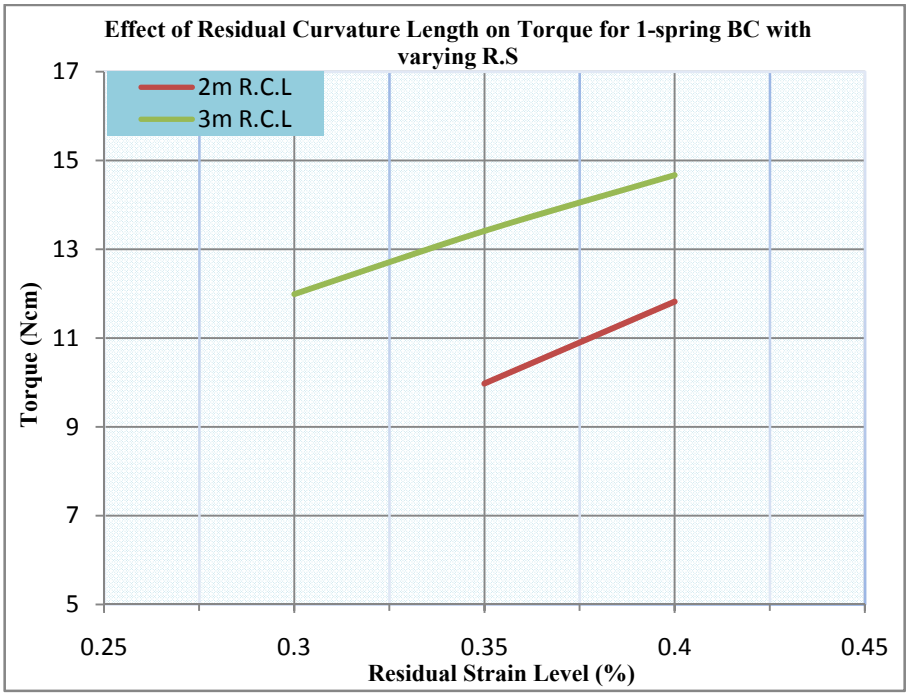

(a)

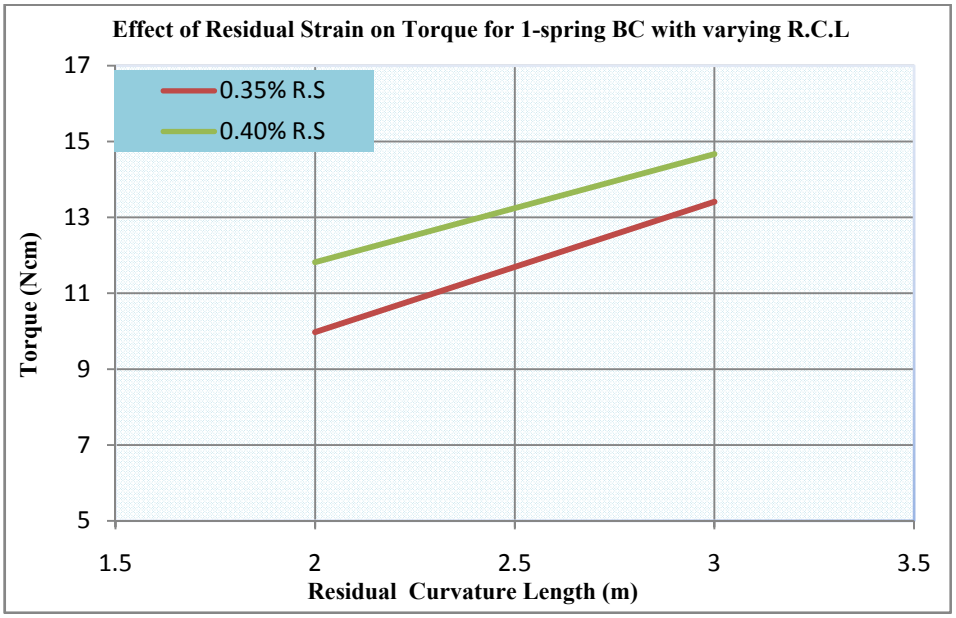

(b)

Figure 7-13: Effect of (a) R.C.L (b) R.S on Torque for the 1-spring BC

7.1.5 Uneven Seabed Topography

It has been established that some of the challenges, such as high bending moment at the shoulders, high cost of subsea intervention and high volume of rocks etc, that plaque free-span on uneven seabed topography can be solved by adopting residual curvature. The results of the experimental tests performed in this study are to establish the basic principle governing this idea. Based on the results, the influence of the residual strain, curvature length and concentrated weight on the depth and pipeline span are investigated.

7.1.5.1 Effect of Depth

The tabulated experimental results from section 6.4 were plotted to reveal the influence of installation

residual strain sections along the length of the pipeline on uneven seabed topography. Figures 7-14 to 7-16 shows impact of residual strains and combine effects of the R.S and concentrated load on the overall depth, from the depression floor to the mid-span of the pipeline.

It is observed from Figure 7-15, that for the scenario with no concentrated load, the relationship between the depression depth and residual strain is inversely proportional, with decrease in depth as the residual strain increases regardless of the length of curvature. This is validated from the Figure 7-14 which indicates a depth of 0.52m for 0% R.S cases and 0.47m for 0.30% which gives approximately 10% decrease. Figure 7-15shows how the depth decreases further with an addition of concentrated load at the mid span of the pipe (see Appendix VI for pictures). The addition gives a further reduction to 0.33m which amount to 37% reduction in depth. Further increase in the concentrated weight results to a further decrease to 0.41m which results to 40.4% reduction when the R.C.L is 1m as shown in Figure 7-16. At 2m residual curvature length a percentage difference of 46.2% is observed in depth when a combination of 0.30% R.S and Weight_2 is considered.

Figures 7-17 and 7-18 show how the depth of the depression for the initial case and the combine case of strain and weight varies with the residual strains. These figures present a clearer view of the influence of the concentrated load when applied to both stressed and unstressed pipe. The result obtained from the graphs agrees reasonably in principle with study performed by *Endal G. et al., (2015)*, which reveals that the depth reduces as the residual strain increases and further support the strain-displacement study performed by *Damsleth et al., (1999),* which pointed out that the displacements increases with increase in strain.

Thus addition of weight at the mid-span of the pipeline laid along depression, further reduce the depth of depression, and decrease in depth is largely dependent on the magnitude of the weight added. It is also observed from the figures that, residual curvature length has an inverse relationship with the depth, which is the higher the R.C.L, the lower the effective depth of the depression.
The percentage difference observed above can be a great deal when scaled up to a real life situation, thus achieving significant save in the cost of a project by reducing the volume of rocks to be dumped in the depression as well reduction in the rock dumping or free-span mitigation activities which consequently reduce project cost.

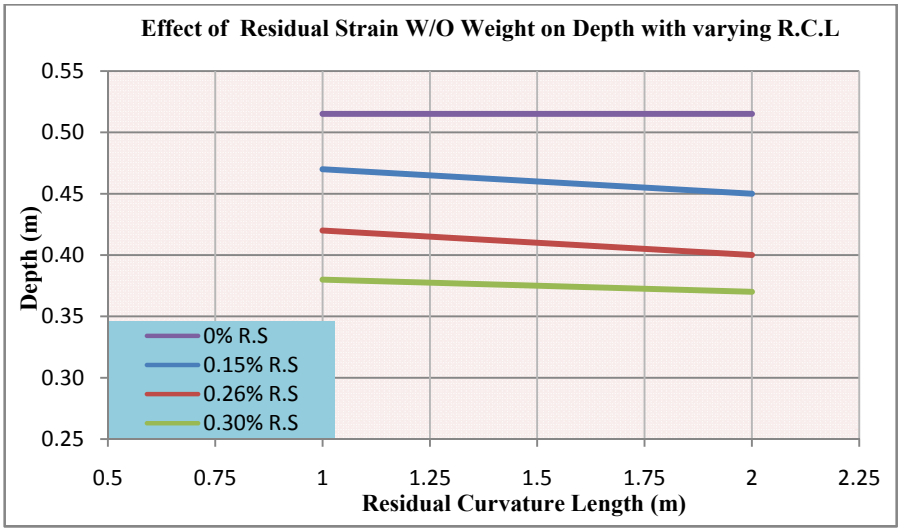

Figure 7-14: Influence of R.S only on Depth

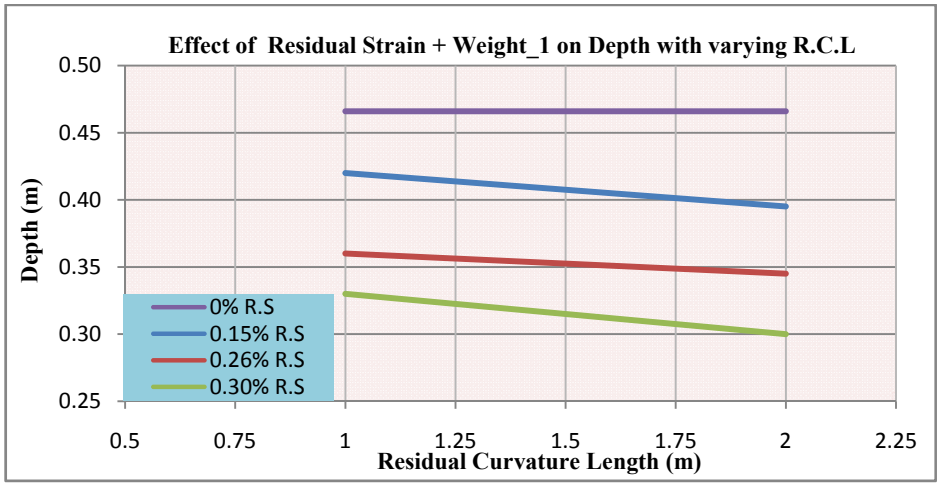

Figure 7-15: Influence of R.S and Weight-1 on Depth

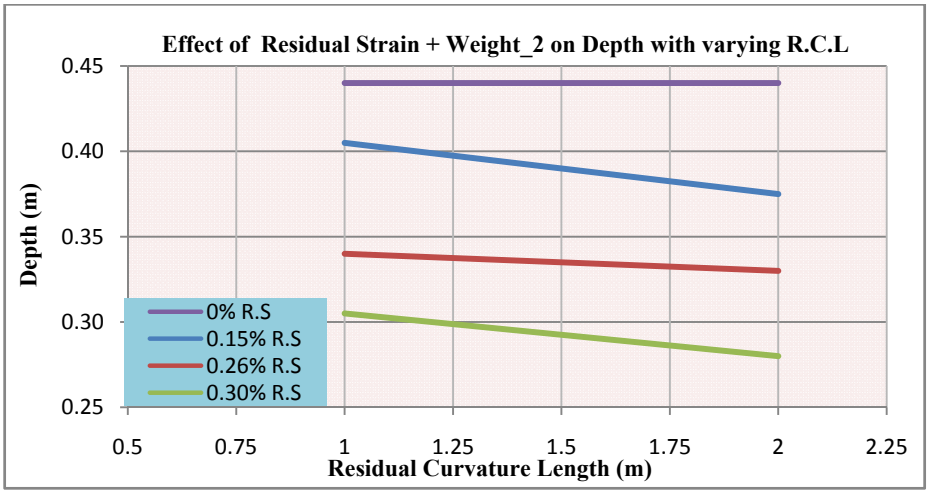

Figure 7-16: Influence of R.S and Weight-2 on Depth

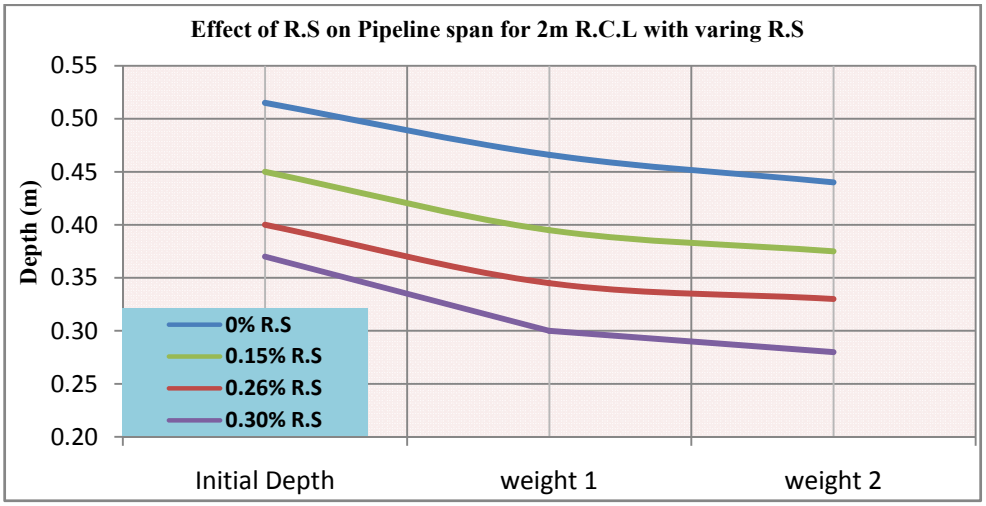

Figure 7-17: Influence of R.S on Depth for 2m R.C.L with varying Stress Conditions

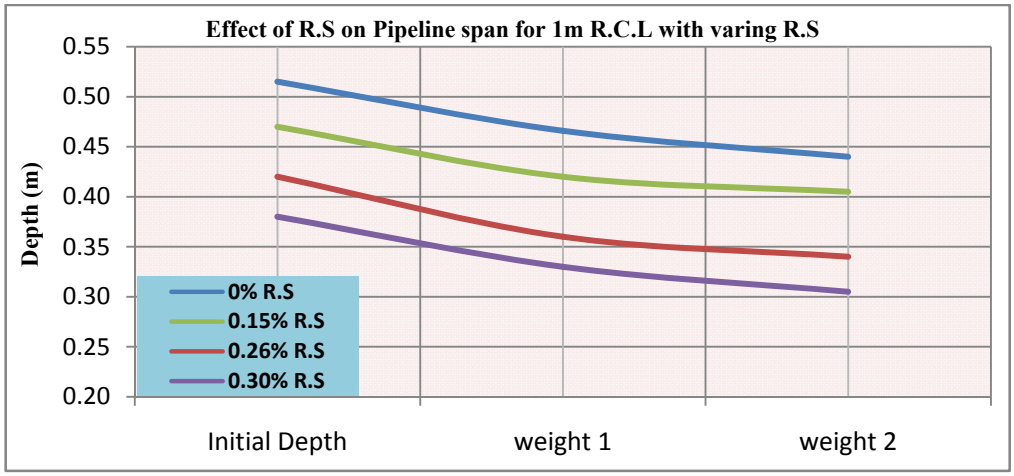

Figure 7-18: Influence of R.S on Depth for 1m R.C.L with varying Stress Conditions

7.1.5.2 Effect on Span Length

The span length is pivotal when mid-span bend moment is a critical criterion in pipeline free span. It is an established fact that the higher the span length the greater the bending moments experience at both the mid-span and at the shoulders. In the experimental test, the change in the span length was measured as the residual strain varies. Figures 7-19 and 7-20 show the variation of the R.S and R.C.L on the free span of the model pipeline respectively.

From Figure 7-19, it is observed that with residual strain, the pipeline free span length will decrease with increase in the residual strain, having an initial span of 2.28m when there is no residual strain and a reduced span length of 2.20m when a 1m length of 0.30% R.S is introduced. That results in a percentage decrease of 3.5%. if the value is compare with the corresponding value for 2m R.C.L, the percentage decrease rises further to approximately 6%.

Thus it can be deduced that regardless of the R.C.L, the pipeline free span decrease with increase in the residual strain and further reduction is experienced when the length of the residual curvature is increased. Hence increase in residual strain and residual curvature length results in lower free span. Figure 7-20 shows the direct effect of R.C.L on the span length

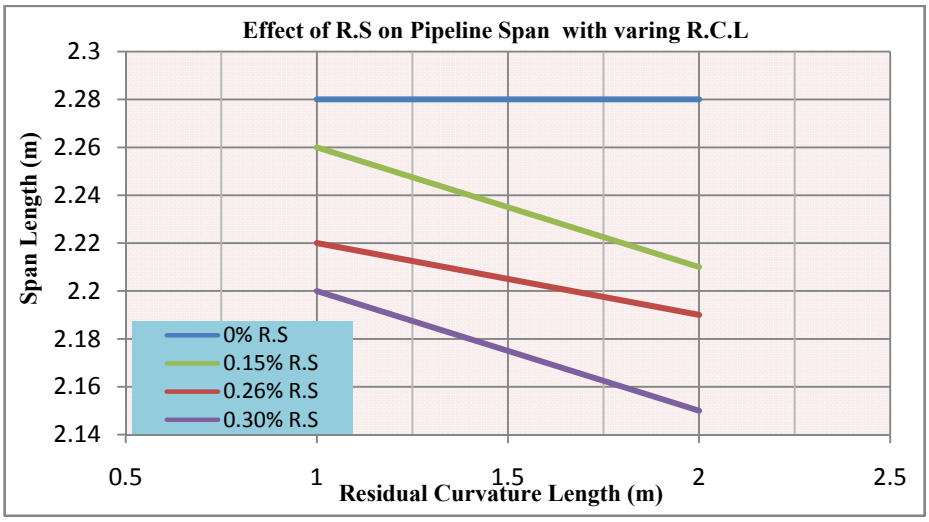

Figure 7-19: Influence of R.S on Span Length with varying R.C.L

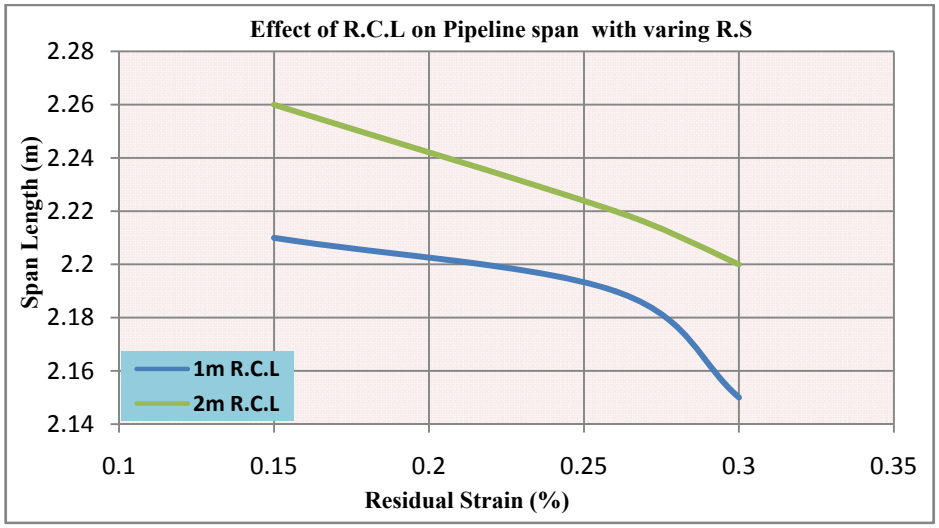

Figure 7-20: Influence of R.C.L on Span Length with varying R.S

7.2 NUMERICAL RESULTS DISCUSSION

The numerical results tabulated in section 6.5 are plotted for clarity and ease of interpretation and comparison with the experimental test results. The numerical analysis performed in this study is limited to the pipeline rotation due to only residual strains. Thus the graphs present the only the influence of the variation in residual strain level, boundary conditions and residual curvature length on pipeline rotation.

7.2.1 Effect of Boundary Conditions

The influence of different boundary condition on pipeline rotation during installation is equally investigated using the same parameters as of the experimental test. Figures 7-21 and 7-22 show how the BCs influence the rotation. Similar to the experimental test results on BCs, the Fixed BC shows the highest resistance to rotation with rotation of 28deg. and 40deg. at 0.30% and 0.40% R.S as compared with the 1-spring BC with 128deg. and 138deg for a 2m R.C.L.

This is an expected difference as a fixed condition has a high capacity to resist twist, since it has a high twisting stiffness contrary to the 1-spring BC with limited twisting stiffness. Thus the higher the torsional capacity of the end components of the pipe the lower the rotation angle or twist and vice versa. The 3m R.C.L follows a similar trend as the 2m R.C.L, having low angle of rotation when fixed BC is considered and highest rotation angle for the 1-spring BC since the twist stiffness at the end is greatly reduced. Thus this behaviour validates the result of the experimental test

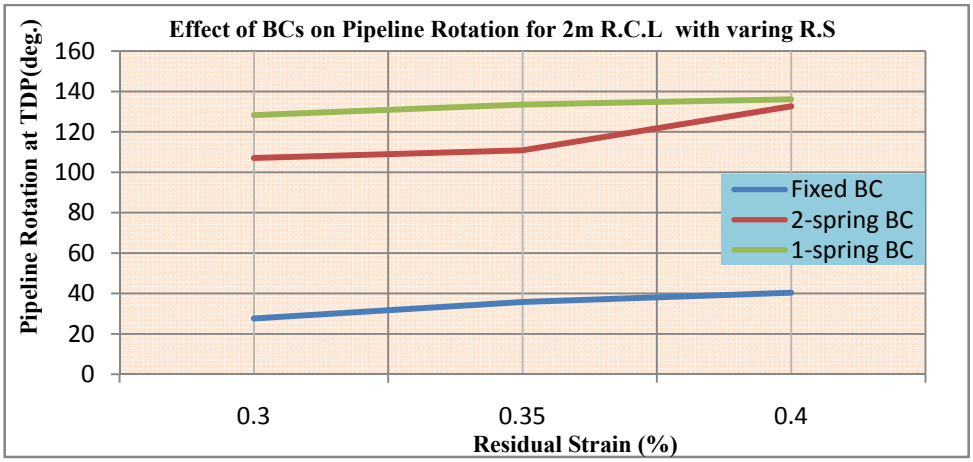

Figure 7-21: Influence of BCs on Pipeline Rotation for 2m R.C.L with varying R.S (Numerical)

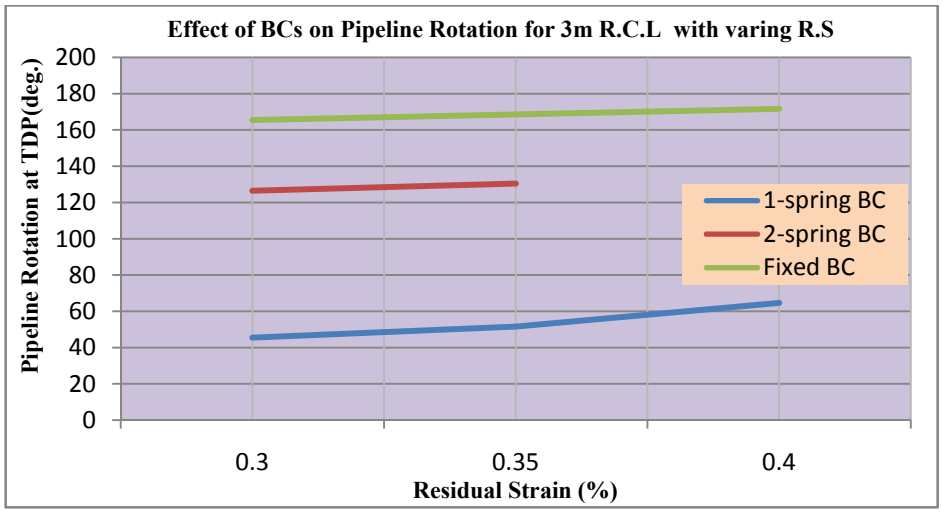

Figure 7-22: Influence of BCs on Pipeline Rotation for 3m R.C.L with varying R.S (Numerical)

7.2.2 Effect of Residual Strain and Curvature length

This numerical test also covers the investigation of the effect of residual strain levels and curvature length on pipeline rotation during installation. Figures 7-23 and 7-24 show how the R.S and the RC.L influence the pipeline rotation for fixed and. 1-spring BC s respectively. The results presented here agree reasonably well in principle with what is obtained in the experimental test, as it shows a higher rotation at higher residual strain and higher residual curvature length.

This result is in agreement with the study carried by Li Y., (2005), which shows that angle of rotation increases with the residual curvature, with rapid change in rotation for residual strain within the range of 0.30% to 1.0%

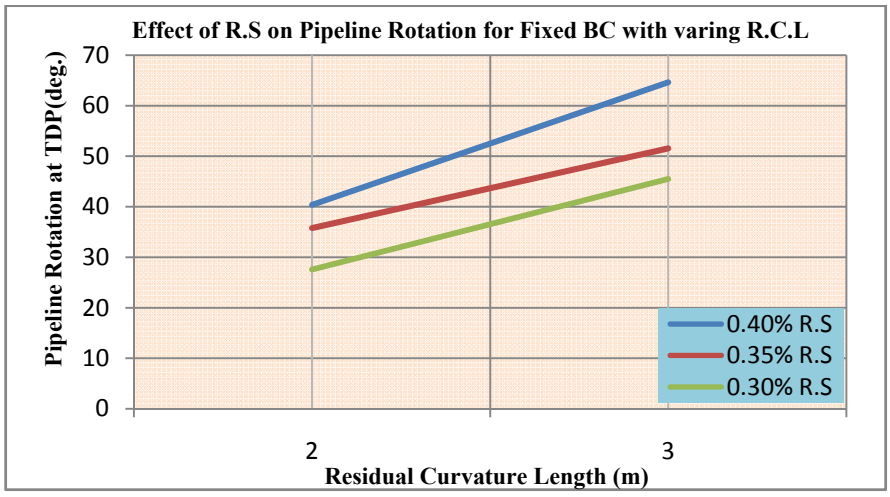

Figure 7-23: Influence of R.S on Pipeline Rotation for Fixed BC with varying R.C.L (Numerical)

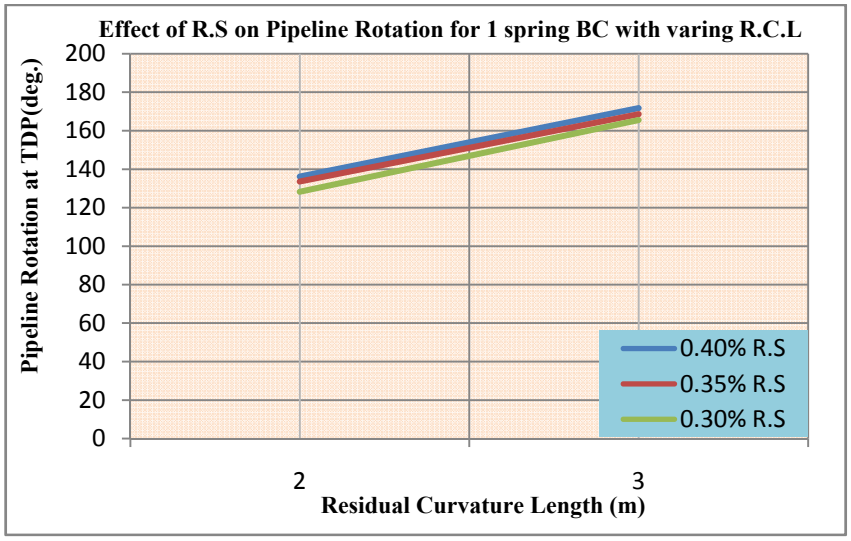

Figure 7-24: Influence of R.S on Pipeline Rotation for 1-spring BC with varying R.C.L (Numerical)

7.3 COMPARISON OF RESULTS

Table 7-1 presents, the value of the rotation for pipeline, for both experimental tests and numerical analyses. The results of the experimental test and the numerical analysis agree to a reasonable extent, with maximum being approximately 20degrees and 38degrees for the 2m and 3m R.C.L respectively in the case of experimental test while the corresponding values in the case of numerical analysis are 40degrees and 68degrees, although this discrepancy is large, as this might be due to several uncertainties in calculation, measurement and measuring tools etc. However, in general, it can be deduced that the angle of rotation when a fixed BC is considered is quite low compared to the other BCs. It is should be noted that there is a high level of agreement in the rotation angle in the case of 1-spring BC for the two approaches, experimental and numerical.

Based on this comparison, it can be concluded that the result of the experiment is reasonably reliable and numerical approached can be used to performed more detailed parametric study of pipeline rotation during installation. Several factors might be the cause of the discrepancies observed between the results of the experimental test and numerical analyses, these factors includes;

The block structures introduced to raise the pipeline at the TDP that the pipeline can rotate beyond 90degrees, these blocks are necessary as previously explained; otherwise contact with the seabed would have prevented further rotation of the pipeline beyond 90degrees. Thus, the introduction of the block might be a source of errors and uncertainties.

Other sources of errors and their associated uncertainties that could have resulted in these discrepancies are discussed in section 8.

Table 7-1; Summary of the Experimental test and Numerical Analysis Results for Pipeline Rotation

RESULTS COMPARISON				
R.C.L	R.S	BC	Experiment. ROT. Angle	Numerical ROT. Angle
m	%		deg.	deg.
2	0.3	FIXED	12.08	27.56
		1-SP	-	128.27
		2-SP	-	126.5
	0.35	FIXED	16.7	35.78
		1-SP	100.68	133.56
		2-SP	64.54	130.45
	0.4	FIXED	20.43	40.35
		1-SP	132.27	136.15
		2-SP	103.71	132.67
3	0.3	FIXED	14.04	19.5
		1-SP	128.66	165.5
		2-SP	105.96	107.01
	0.35	FIXED	20.14	51.55
		1-SP	161.57	168.6
		2-SP	116.57	110.85
	0.4	FIXED	38.07	64.63
		1-SP	172.07	171.7
		2-SP	124.59	-

8. SOURCES OF ERRORS AND UNCERTAINTIES

Due to the nature and complexity of experiments of this magnitude, the experimental test was performed with extreme care and under control measures to minimize the effect errors and uncertain, however the presence of these errors and uncertainty cannot be fully ignored since error reducing measures taken can only minimize the effect on the result obtained. These errors and uncertainties can be classified as human errors, equipment errors and calculation errors.

- **Human Error;** this experiment is single-handedly performed by the author of this study work, thus error or uncertain in measurements and calculation due to fatigue when setting up the experimental test components and when performing the experiment, tiredness and mistakes and/or oversight. However extremely care was taken to ensure such errors are minimized and the author adopt the method of taken a 20mins break after every 2hours to counter fatigue and tiredness and to ascertain minimum errors and uncertainties, some key experiments were performed twice especially in the case of pipeline rotation experiments. Also the experimental test process was carried out under the supervision of my supervisors who approved the process.

- **Equipment Error;** the reading taken from the equipment and tool used in measuring some key parameters during the experimental test are other sources of error and uncertainties. One of such equipment is the load cell, which measures the horizontal tension in meter-volt per volt (mV/V), thus this was calibrated and conversion factor to Newton was obtained. Hence this process of calibration and conversion could introduce some errors from approximation in the result obtained. Also the load cell initial reading is not stead but fluctuates between ranges of value before settling for a particular value, thus this could be perceived as a source of uncertainties. To minimize this errors and uncertainties, the calibration process was performed carefully and repeated so as to obtained accurate calibration factor and the factor obtained was not approximated, that is, it was used in it full 11 decimal places. In addition, the final readings recorded from the load cell were based on the most steady and constant reading after detaching and engaging the load cell from and to end of the pipeline several times for each and every of the experimental test.
  Also the horizontal tension reading taken from the load cell includes, the value of frictional force result from the pipeline-stinger nails contacts, this is considered as another source of errors and poses a great deal of uncertainties in the reading. This is minimized by obtaining the value of this frictional force by setting up the load cell at the stinger end of the pipeline and taken the upper end reading, hence obtaining the difference which is applied to all other readings taken at the seabed end of the pipeline.

  Furthermore, there are errors and uncertainties when manually bending the straight pipes to achieve the various residual strain levels and exact curvature length, since this process was performed manually due to the unavailability of pipe bending machine. However the bending process was performed with extreme precautions; mapping out the configuration of the straight pipe in the bent form with nails and carefully bend the pipes to these configurations, thus minimizing errors and uncertainties due to inaccurate residual strain levels and curvature lengths.

- **Calculation Error;** this error might be due to approximations and oversight, this errors are very minimal in this study effort, as all manual calculations and graphs were double checked and were performed and plotted using Excel and Mathcad whose output have been known to be reliable.
  A major source of error is process of digitizing the experimental test catenary shape for comparison

with other approaches (analytical and numerical), this errors and the associated uncertainties are may result from improper gridding of the pool walls, improper pictures of the catenary shape taken for digitization, inaccurate dot mapping of the pipeline catenary, 4th degree polynomial approximation of the catenary shape using Webplot Digitizers and scaling of plot area in the webplot interface. These errors are minimized by taken necessary precautions ensuring continuous pictures of the pipeline catenary were taken with the camera vertically positioned, and the pool gridline carefully drawn when setting up the experiment and also the dot mapping was done closely and carefully. To avoid error due to polynomial approximations, several order of polynomial (4th, 5th, 6th, and 7th) were used to approximate the catenary, however the difference between these approximation was insignificant, thus for simplicity, the 4th order polynomial was considered accurate with minimum error.

All the errors stated above were significantly minimized using several approaches, thus the results of the experiment test and numerical analyses are precise to a great extent and thus considered accurate and reliable.

9. CONCLUSION AND RECOMMENDATION

9.1 CONCLUSION

Pipeline rotation due to residual strains during S-lay and reel-lay installation has been an intriguing phenomenon in offshore pipeline technology. Relatively little theoretical work has focused on this subject, and there are unresolved challenges that enables a full understand of the pipeline rotational mechanism during pipelay. These challenges are considered to be two-fold, i.e. (1) pipeline rotational theory in itself including effects such as rotational stiffness, boundary conditions on the seabed and on the vessel, effects of tension, out of plane effects etc and (2) practical pipelay effects such as vessel dynamics, material/welding/reeling/ effects, play in the tensioners, lateral current, pipeline route and seabed friction and so and so forth.

This study work is aimed at shedding more light into the physics of pipeline rotation during S-lay and reeling, with the main focus on the rotational effect from introducing a local residual curvature section into the pipeline.

The primary of objectives of the thesis is to investigate the effect of high values of the parameters that causes rotations beyond 90degree during S-lay installation with the sole aim of conforming pipeline to uneven seabed topography, the parameters of interest are the residual strains levels(0.30%, 0.35%, 0.40%), residual curvature lengths (2m and 3m), Inline structure and effect of pipeline end boundary conditions (Fixed and Partially restrained), due to time and availability of space, on this four parameters were considered. In addition to this main objective, the study effort also established the fundamental principle of conforming pipeline to uneven seabed topography by using residual curvatures and concentrated weights, since past studies have established the usefulness of residual curvatures in meeting pipeline free span challenges. To achieve the set objectives of this study effort, experimental test and numerical analysis are performed and the results from both approaches were compared. The experimental test was carried using an existing stinger model with installed rollers similar to what is obtainable in practice, model pipeline, pool, model uneven seabed and all other installation parameter and the boundary conditions considered are the Fixed BC and partially restraint BC (to stimulate the soil seabed-pipeline friction). The numerical analysis was carried out using commercial software, ORCAFLEX, which has the feature to introduce pre-bend along pipeline and measure the rotation of the pipeline in terms of gamma angle. Based on the experimental test and numerical analysis, the results obtained give further insight into the mechanism and causes of rotation of pipeline rotation. The results presented in this study are obtained at the TDP.

Based on comparison, the catenary shape of the experimental test agrees reasonably well with the shape obtained from analytical and numerical methods thus result presented in this report is largely reasonable and reliable. Further to this, the experimental test shows that the pipeline catenary shape as well as the departure angle is a largely dependent on the top tension applied, thus the top tension can be a control parameter for the catenary shape.

Although significant pipeline rotation during installation is discouraged especially when pipeline is installed with inline structure whose verticality at the seabed is of utmost important, the results of both approaches (experimental test and numerical analysis) reveal that pipeline rotates or twist when installed with residual strains or curvature section and the boundary conditions at the ends of the pipeline is pivotal to the magnitude of this rotation.

the results of this study effort has shown that at high residual strains and curvature length, for pipeline with

low frictional capacity from the soil-pipeline interaction, the pipeline rotates beyond 90degree and the magnitude of the rotation experience my the pipeline is directly proportional to the frictional capacity of the soil. In addition, it is established that depending on the weight of inline structure, pipeline experiences rotation when being installed along the line, however, the result of this experimental test does include buoyancy module that counteract the effect of inline structure as it is been done in practice. Hence the eccentric load along the pipeline causes rotation during installation.

The study also reveals that, based on the rotation-causing parameters considered in this thesis, the pipeline end boundary condition in combination with high residual strain level is the most critical in causing high rotation beyond 90degree. This is very important when residual curvature is to be used to conform pipeline to uneven seabed topography. However, other rotation causing parameter such as water depth, pipeline axial tension etc. can also be considered critical as well most especially in deep water. Hence in general the residual curvature length and residual strain levels are considered most critical when studying pipeline rotation, hence a check and balance must be done to achieve desirable rotation when conforming pipeline to uneven seabed topography or to prevent excessive pipeline rotation.

The uneven seabed experimental test result shows that, residual curvature is an effective way of conforming the pipeline to uneven seabed topography and that the higher the residual strain the more cost effective the project. Furthermore, a combination of residual curvature and concentrated weight was found to be better option when reduced depth is of utmost important, however this option must be checked against the structural integrity and deflection criteria of the pipe. The result of this experimental test also shows that the free span length is reduced with increase in residual strain, which is important when estimating the bending stress criteria.

Although quality time was spent building and setting up the experimental test components, the experimental test is not free from errors and uncertainties, such as errors in calculations, hand bending of pipes, uncontrolled release of axial tension in pipe etc. the discrepancies found between the experimental test results and the numerical analysis results are largely as a results of these errors and uncertainties as discussed in details in section 8, thus the results presented in this study effort can be used bearing this in mind.

the results of this study effort has shown that at high residual strains and curvature length, for pipeline with low frictional capacity from the soil-pipeline interaction, the pipeline rotates beyond 90degree and the magnitude of the rotation experience my the pipeline is directly proportional to the frictional capacity of the soil. In addition, it is established that depending on the weight of inline structure, pipeline experiences rotation when being installed along the line, however, the result of this experimental test does include buoyancy module that counteract the effect of inline structure as it is been done in practice. Hence the eccentric load along the pipeline causes rotation during installation.

The study also reveals that, based on the rotation-causing parameters considered in this thesis, the pipeline end boundary condition in combination with high residual strain level is the most critical in causing high rotation beyond 90degree. This is very important when residual curvature is to be used to conform pipeline to uneven seabed topography. However, other rotation causing parameter such as water depth, pipeline axial tension etc. can also be considered critical as well most especially in deep water. Hence in general the residual curvature length and residual strain levels are considered most critical when studying pipeline rotation, hence a check and balance must be done to achieve desirable rotation when conforming pipeline to

uneven seabed topography or to prevent excessive pipeline rotation.

The uneven seabed experimental test result shows that, residual curvature is an effective way of conforming the pipeline to uneven seabed topography and that the higher the residual strain the more cost effective the project. Furthermore, a combination of residual curvature and concentrated weight was found to be better option when reduced depth is of utmost important, however this option must be checked against the structural integrity and deflection criteria of the pipe. The result of this experimental test also shows that the free span length is reduced with increase in residual strain, which is important when estimating the bending stress criteria.

Although quality time was spent building and setting up the experimental test components, the experimental test is not free from errors and uncertainties, such as errors in calculations, hand bending of pipes, uncontrolled release of axial tension in pipe etc. the discrepancies found between the experimental test results and the numerical analysis results are largely as a results of these errors and uncertainties, thus the results presented in this study effort can be used bearing this in mind.

The catenary shape of the experiments test, the numerical and analytical analyses correlates very well, this is simply because the same laying parameters were used in the established the catenary shape and the experimental test was performed with absolute precaution minimizing all errors due to human and equipments as discussed in section 8. However analytical approach was not considered in this study effort. The comparison of the results of the experimental test and the numerical analyses correlate reasonably well with some few exceptions. These exceptions might be as a result of the presence of the errors and uncertainties, these discrepancies can be as a result of the twisting stiffness capacity inputted and the introduction of block objects, that allows for rotation beyond 90degree, in the numerical analyses. The stiffness of this block objects was randomly inputted.

In summary, the results of both experimental test and numerical analyses established that high residual strain level and length of the residual curvature play the most pivotal role in rotating the pipeline beyond 90degree while the influence the boundary conditions has on pipeline rotation during installation is largely dependent on the proximity of the curvature length to BCs, thus the boundary condition is less critical.
Also the results show that of high criticality is the magnitude and eccentric distance of an inline structure to the rotation of pipeline during offshore installation. Another parameter that was observed to be critical to the pipeline rotation during the experiment is the axial tension in the pipeline, it was observed that the higher the axial tension the lower the pipeline rotation.

9.2 RECOMMENDATION

Residual curvatures and pipeline rotation are becoming interesting phenomena to be studied in details. In the past residual curvature has posed a great deal of challenge being the major factor that causes pipeline rotation which is not desirable most especially when installing inline structure along the pipeline. However recent studies have established the importance of pipeline rotation in meeting some of the technical challenges in pipeline technology, thus understanding the physic of pipeline rotation and residual curvature becomes imperative. This thesis has further through more insight into the understanding of the mechanism of pipeline rotation above 90degrees due to residual strains, however further studies are require for improve on the accuracy of the results of this study is necessary as well as explore other intriguing areas that can eventually lead improve installation methodology, design and save cost. These future studies are not limited to the following;

Since the fundamental principle and experimental procedure of pipeline rotation has been establish by this study and other studies, it will be interesting to improve the accuracy of this study by investigate the rotation by simulating actual boundary condition at the tensioner and minimize error due to friction from nails. This is very important so as achieve results close to what is obtainable in practice.

Further experimental study can also be performed to establish the behavior or trend of the rotation curves with various influencing parameters such as the residual strain, water depth, residual curvature length, top tension and so on; this will enable or aid easy prediction of pipeline rotation.

During the course of the experimental test, it was observed that at magnitude of rotation is largely dependent on the amount of axial tension released from the pipeline, further study will include investigation into the relationship between the amount of axial tension released and the magnitude corresponding magnitude of rotation

This study effort has further shown that the numerical analysis can be reliable in estimating pipeline rotation, thus detailed parametric study of pipeline can be performed using commercial FE programme.

REFERENCES

Abbas Yeganeh Bakhtiary, Abbas Ghaheri and Reza Valipour (2007): Analysis of Offshore Pipeline Allowable Free Span Length. Technical Note, International Journal of Civil Engineerng. Vol. 5, No. 1, March 2007

Acergy Academy (2008): Rigid Pipelines Design and Installation Pipeline Installation Overview

API RP 1111 (1999): Design, Construction, Operation, and Maintenance of Offshore Hydrocarbon Pipelines.

Austin, D., Carriker, B., McGuire, T., Pratt, J., Priest, T. and Pulsipher, A. G., (2004): History of the offshore oil and gas industry in Southern Louisiana. Interim report. Volume 1: Papers on the evolving offshore industry. Tech. rep., Mexico.

Bai, Y. and Bai, Q. (2005): Subsea Pipelines and Risers. Elsevier.

Bai Y. (2001): Pipelines And Risers. Ocean Engineering Book Series Volume 3. Elsevier

Bhadeshia, H.K.D.H. and Honeycombe, R.W.K. (2006): Steels: microstructure and properties. 3rd ed. Elsevier, Amsterdam, ISBN0750680849; ISBN9780750680844

Boyun Guo, Shanhong Song, Jacob Chacko, Ali Ghalambor (2005): Offshore Pipelines. Gulf Professional Publishing is an imprint of Elsevier.

Bynum, D. jr. and Havil, K. P. (1981): Marine Pipeline Roll Parameters Study. Oil and Gass Journal, pp 138-146

Callegari, M., Canella, F., Titti, F. M., Bruschi, R., Torselletti, E. and Vitali, L. (2000): Concurrent design of an active automated system for the control of stinger/pipe reaction forces of a marine pipelaying system. In: Proceedings of the Int. Workshop on Harbour, Maritime & Multimodal Logistics Modelling and Simulation, Portofino, Italy.

Clauss, G. F. & Saroukh, A., (1996): Interaction between Vessel, Stinger, And Pipeline During laying operations in high Seas. s.l., s.n.

Clauss, G. & Kuhnlein, W., (1974): Model testing techniques in offshore pipelining. Houston, s.n.

Damsleth, P.A. and Dretvik, S. (1998): The Asgard Flowlines - Phase 1 Design and Installation Challenges. OPT'98.

Damsleth, P.A., Riris C., Viken O. A. and Dretvik S. (2000): Pipeline Rotation Control for Laying of the Midgard Tee. OPT, IBC Conference, Oslo, 28-29 Feb. 2000.

Damsleth, P.A., Nystrøm, P., Bai Y. and Gustafsson C. (1999): Deep Water Installation with Plastic Strain. OMAE'99,PL-99-5046

Denniel, S (2009): Optimising Reeled Pipe Design through Improved Knowledge of Reeling Mechanics. OTC 20043, Offshore Technology Conference, Houston, Texas, USA, May 4–7, 2009.

Det Norske Veritas (2000): Offshore Standard DNV–OS–F101 Submarine Pipeline Systems. DNV.

Dixon D.A. and Rutledge D.R. (1968): Stiffened Catenary Calculations in Pipeline Laying Problem, Journal of Engineering for Industry , 8

Endal G., Ragupathy P., Rao V. and Sriskandarajah T. (2014): Pipeline roll during reel-lay installation due to piggyback DEH cable and local residual curvature, OMAE2014.

Endal, G. and Nystrøm, P. (2015): Benefits of Generating Pipeline Local Residual Curvature during Reel- and S-lay Installation. 2015 OPT Conf., Amsterdam.

Endal, G., Nystrøm, P. and Lyngsaunet O.M (2015): Lay Method to make Pipeline Conform to Uneven Seabed Topography. Proceedings of the Twenty-fifth (2015) International Ocean and Polar Engineering Conference Kona, Big Island, Hawaii, USA, 21-26, by the International Society of Offshore and Polar Engineers (ISOPE)

Faldini, R., (1999): A new horizon. In: Proceedings of the Annual Offshore Technology Conference. OTC 10712.

Finn Gunnar Nielsen, Tore H Søreide, Stig Olav Kvarme, (2002): VIV response of long free spanning pipelines. OMAE PAPER 28075

Gullik Anthon J. (2010): Offshore Pipelaying Dynamics. Thesis for the degree of philosophiae doctor, Norwegian University of Science and Technology

Guo, B., Song, S., Chacko, J. and Ghalambor A. (2005): Offshore Pipelines. Gulf Professional Publishing

Jee Limited (2006): Subsea Pipeline Installation Calculation. Volume 1

Jee Internal (2006): Introduction to pipeline design Volume three, 1st ed. (Jee Limited, 2006):

Jensen G.A. and Fossen T.I. (2009): Mathematical models for model-based control in offshore pipelay operations, OMAE 2009

Karunakaran, D. (2015,a): Pipeline Span and VIV. Lecture notes Pipelines and Risers, University of Stavanger, Stavanger, Norway.

Kyriakides, S. and Corona, E. (2007): Mechanics Of Offshore Pipelines: Buckling and Collapse, Vol. 1. First ed. Oxford: Elsievier BV.

Li Y. (2005): Prediction of Pipeline Roll during S-laying. Proc. Of OMAE2005-67477, 24th Int. Conf. on offshore Mechanics and Artics Engineering. June 12-17, 2005, Halkidiki, Greece

McKinnon, C. (1999): Design Material and Installation Considerations for Ultra Deepwater Pipelines. SPE 56910, Offshore Europe Conference, Aberdeen, Scotland, September 7-9, 1999.

Mousselli A. H. (1981): Offshore Pipeline Design, Analysis and Methods. Pennwell Publishing Company, Tulsa, Oklahoma,

NOU (1974): Rørledninger på dypt vann. Universitetsforlaget

NTNU, (2016): Experimental Methods in Marine Hydrodynamics – lecture in week 34

Nystrøm, P. R., Endal, G. and Lyngsaunet, O. M. (2015): Reel-lay Method to Allow for Direct Tie-in of Pipelines. 2015 TPC-0930.

Orcina, Orcaflex manual 9.5a. Available at http://www.orcina.com/SoftwareProducts/OrcaFlex/Documentation/OrcaFlex.pdf (keep being updated with newer versions)

Palmer, A. C. (1994): Deepwater pipelines: Improving state of the art. In: Proceedings of the Annual Offshore Technology Conference. OTC 7541.

Palmer, A. C., King, R. A. (2008): Subsea Pipeline Engineering, 2nd Edition. PennWell Books.

Plunkett R. (1967): Static Bending stresses in catenaries and drill strings, Journal of Engineering for Industry

Rohatgi, A. (2016). [Online] Available at: http://arohatgi.info/WebPlotDigitizer/

Searle, A. (2004): PLUTO Pipe–Line Under The Ocean, 2nd Edition. Shaklin Chine.

Seyed, F. B. and Patel, M. H. (1992): Mathematics of flexible risers including pressure and interal flow effects. Marine Structures 5 (2–3), 121–150.

Small, S. W. (1970): The submarine pipeline as a structure. In: Proceedings of the Annual Offshore Technology Conference. OTC 1223

Staff, Awwa. (2004): Steel Pipe-A Guide For Design And Installation (M14). 2nd ed. Denver: American Water Works Association. ISBN: 9781583212745; E-ISBN: 9781613000014

Statoil (2002): Method for pipelaying from a coil to the sea bed, controlling thermalexpansion. Norwegian patent 314056, PCT patent EP1358420, US patent US6910830.

Subsea7 website – www. subsea7.com

Vaughan N. J and Nystrøm P. R. (2016): Prediction of Pipeline Rotation during S-lay Installation. International Society of Offshore and Polar Engineers, ISOPE-I-16-466, the 26th International Ocean and Polar Engineering Conference, 26 June-2 July, Rhodes, Greece

Wolbert, G. (1952): American Pipelines 5 (1952).

Zeng X., Duan M. L. and An C. (2014): Mathematical Model of Pipeline Abandonment and Recovery in Deepwater, Journal of AppliedMathematics.

APPENDIX I – Spring Stiffness Calculation

	Load Cell Reading		Force Conversion (N)		Stiffness (N/m)		Average Values	
Extenstion (m)	Spring Sample 1	Sring Sample 2	Force 1 (N)	Force 2 (N)	stiffness 1 (N/m)	stiffness 2 (N/m)	Average Force (N)	Average Stiffness (N/m)
0	0	0	0	0	0	0	0	0
0.01	0.0017	0.002	1.70	1.80	169.58	179.55	1.75	174.56
0.02	0.003	0.003	2.99	3.19	149.63	159.60	3.09	154.61
0.03	0.004	0.004	4.19	4.39	139.65	146.30	4.29	142.98
0.04	0.006	0.006	5.59	5.89	139.65	147.13	5.74	143.39
0.05	0.006	0.007	6.38	6.68	127.68	133.67	6.53	130.67
0.06	0.008	0.008	7.78	8.28	129.68	137.99	8.03	133.83
0.07	0.009	0.010	9.38	9.78	133.95	139.65	9.58	136.80
0.08	0.011	0.011	10.97	11.27	137.16	140.90	11.12	139.03
0.09	0.013	0.013	12.67	12.87	140.76	142.98	12.77	141.87
0.10	0.015	0.015	14.46	14.56	144.64	145.64	14.51	145.14
0.11	0.016	0.016	16.26	16.06	147.81	146.00	16.16	146.91
								144.53

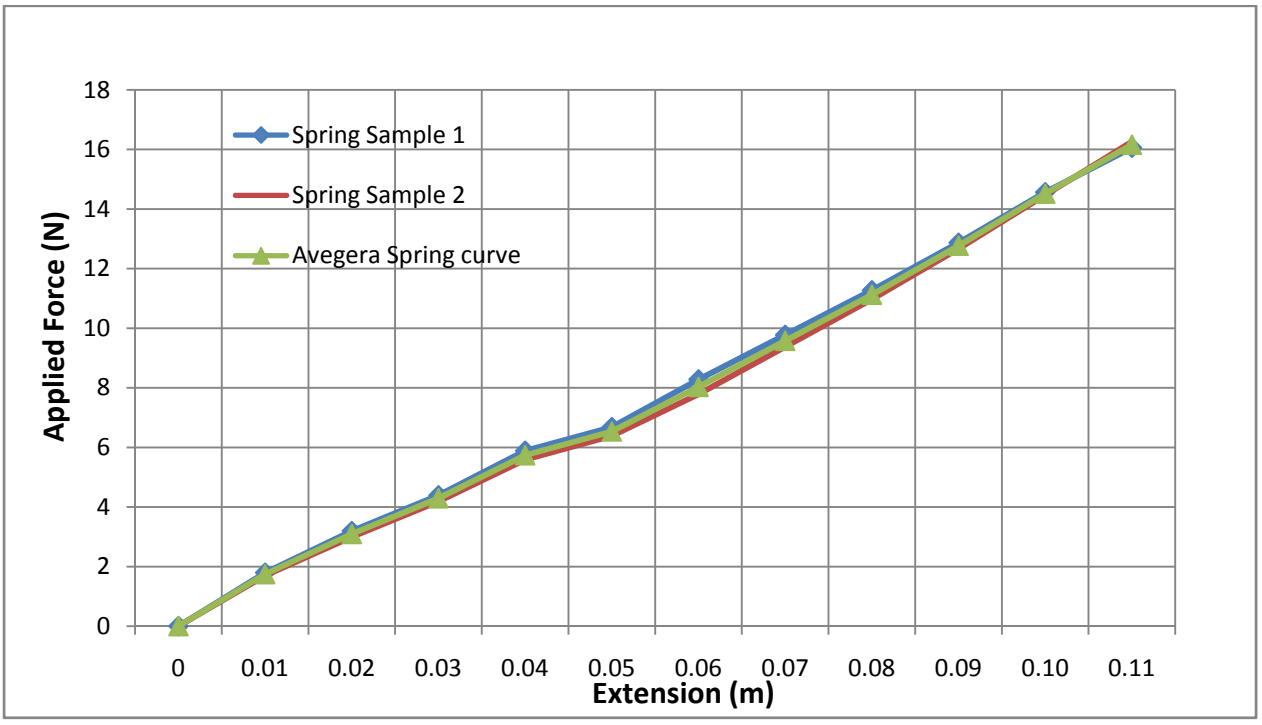

30 March 2017

INSTRON

Instron Applications Laboratory

This template is suitable for creating test procedures that comply with ISO 6892-1: 2009. Test rates and control are set according to "Method A" recommended ranges. Template is intended for specimens that produce a clearly-defined linear elastic region and homogeneous deformation. Default calculated results include Rp 0.2, Fm, Rm and A.

Load vs. Extension

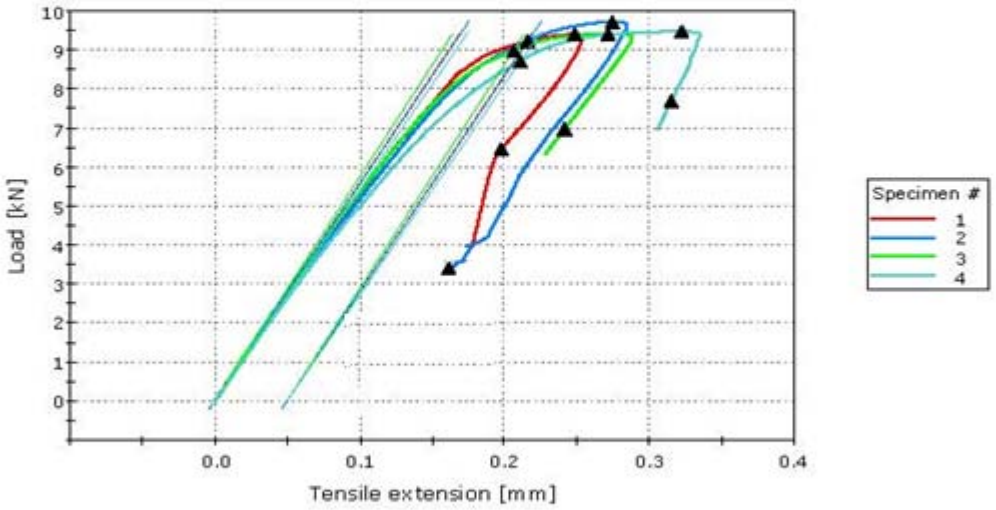

	Modulus (E-Modulus) [GPa]	Tensile stress at Offset yield 0.2% [MPa]	Fm [N]	Tensile stress at Max load [MPa]	Tensile stress at Break (Standard) [MPa]	Strain 1 gauge length [mm]
1	119.9	399.32959	9409.7	406.95453	279.7	49.96555
2	119.6	399.02348	9728.5	420.74579	277.1	49.96463
3	123.4	388.33850	9417.0	407.27209	301.9	49.75263
4	116.7	376.73955	9484.2	410.17780	333.1	49.90115

Page 1 of 2

INSTRON

Graph 2

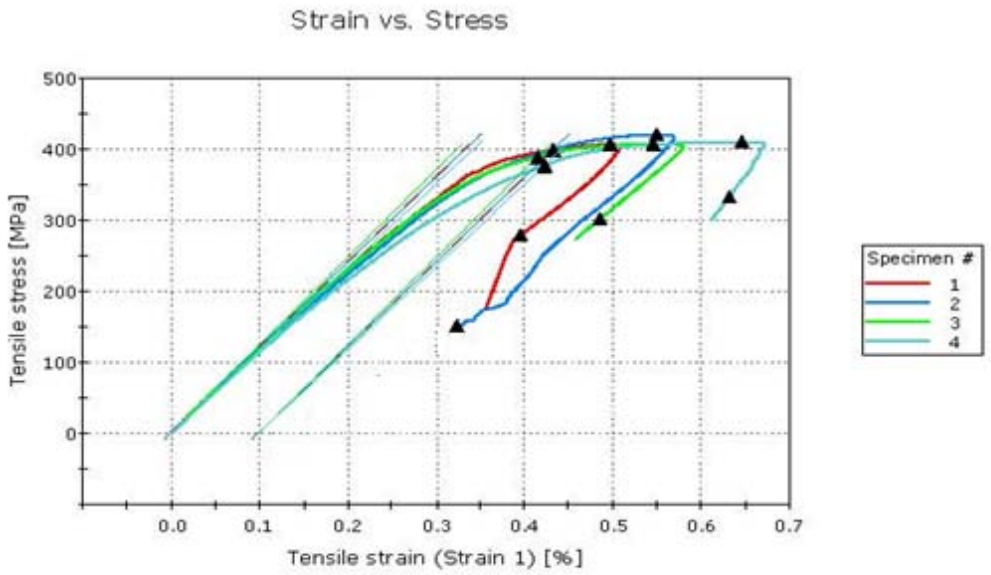

MODEL SCALE APPLICATION

	Model Pipe	20 inch Pipe	30 inch Pipe
pipe outer diametrs	$D := 0.01\,m$	$D_1 := 0.508\,m$	$D_2 := 0.91\,m$
pipe thickness	$t := 0.0008\,m$	$t_1 := 0.017655m$	$t_2 := 0.0312268m$
pipe inner diamter	$d := D - 2\cdot t$	$d_1 := D_1 - 2\cdot t_1$	$d_2 := D_2 - 2\cdot t_2$
pipe elastic modulus	$E := 120.97\cdot 10^9\,\frac{N}{m^2}$	$E_1 := 210\cdot 10^9\cdot\frac{N}{m^2}$	$E_2 := 210\cdot 10^9\cdot\frac{N}{m^2}$
pipe poisson ratio	$v := 0.33$	$v_1 := 0.3$	$v_2 := 0.3$
pipe cross sectional area	$A := \frac{\pi}{4}\left(D^2 - d^2\right)$	$A_1 := \frac{\pi}{4}\left(D_1^2 - d_1^2\right)$	$A_2 := \frac{\pi}{4}\left(D_2^2 - d_2^2\right)$
Pipe density	$\rho := 8940\,\frac{kg}{m^3}$	$\rho_1 := 7850\,\frac{kg}{m^3}$	$\rho_2 := 7850\,\frac{kg}{m^3}$
pipe moment of inertial	$I := \frac{\pi}{64}\left(D^4 - d^4\right)$	$I_1 := \frac{\pi}{64}\left(D_1^4 - d_1^4\right)$	$I_2 := \frac{\pi}{64}\left(D_2^4 - d_2^4\right)$
pipe axial stiffness	$A_s := E\cdot A$	$A_{s.1} := E_1\cdot A_1$	$A_{s.2} := E_2\cdot A_2$
pipe bending stiffness	$A_b := E\cdot I$	$A_{b1} := E_1\cdot I_1$	$A_{b2} := E_2\cdot I_2$
pipe unit weight	$w := 1.863\,\frac{N}{m}$	$w_1 := A_1\cdot\rho_1\cdot g$	$w_2 := A_2\cdot\rho_2\cdot g$
pipe length	$L := 9\,m$	$L_1 := 148.25\,m$	$L_2 := 218.63\,m$
Deflection Factor	$d_f := \frac{w\cdot L^3}{E\cdot t\cdot D^3}$	$d_{f1} := \frac{w_1\cdot L_1^3}{E_1\cdot t_1\cdot D_1^3}$	$d_{f2} := \frac{w_2\cdot L_2^3}{E_2\cdot t_2\cdot D_2^3}$
	$d_f = 14.034$	$d_{f1} = 14.035$	$d_{f2} = 14.035$
Scale Factor		$\frac{L_1}{L} = 16.472$	$\frac{L_2}{L} = 24.292$

CONNECTION TWISTING STIFFNESS CALCULATION

One spring Device

Number of Spring	1		
length of residual curvature	3	m	
Residual Curvature Strain, %	0.3	0.35	0.4
Touque at TDP, Ncm	11.987318	13.412384	14.6698
Rotation Angle at TDP, deg	129	162	172
Twisting Stiffness, Ncm/deg.	0.0929249	0.0827925	0.08529
Average Twisting Stiffness, Ncm/deg	**0.087002316**		

Two spring device

Number of Spring	2		
length of residual curvature	3	m	
Residual Curvature Strain, %	0.3	0.35	0.4
Touque at TDP, Ncm	13.808396	15.398226	15.7104
Rotation Angle at TDP, deg	106	117	125
Twisting Stiffness, Ncm/deg.	0.1302679	0.1316088	0.12568
Average Twisting Stiffness, Ncm/deg	**0.129186649**		

APPENDIX IV – Experimental Test Catenary Calculation

The data points were obtained as discussed in section 4. Four different pictures were taken from the upper section of the experimental catenary to the pool end of the catenary as shown below. The pictures were merged and loaded into the Webplot. Based on the grids, the plot area was scaled and data point created as shown in the pictures. The values of the data points were obtained and plotted. The plot of the data was then fitted to a 4^{th} order polynomial (see equation below) and then constants obtained

$$Z := \left(-0.01377 + 0.075277245s - 0.020969s^2\right) + 0.01024882s^3 - 0.00056s^4$$

$$z := -0.01377 + 0.075277245s - 0.020969s^2 + \left(0.01024882s^3 - 0.00056s^4\right)$$

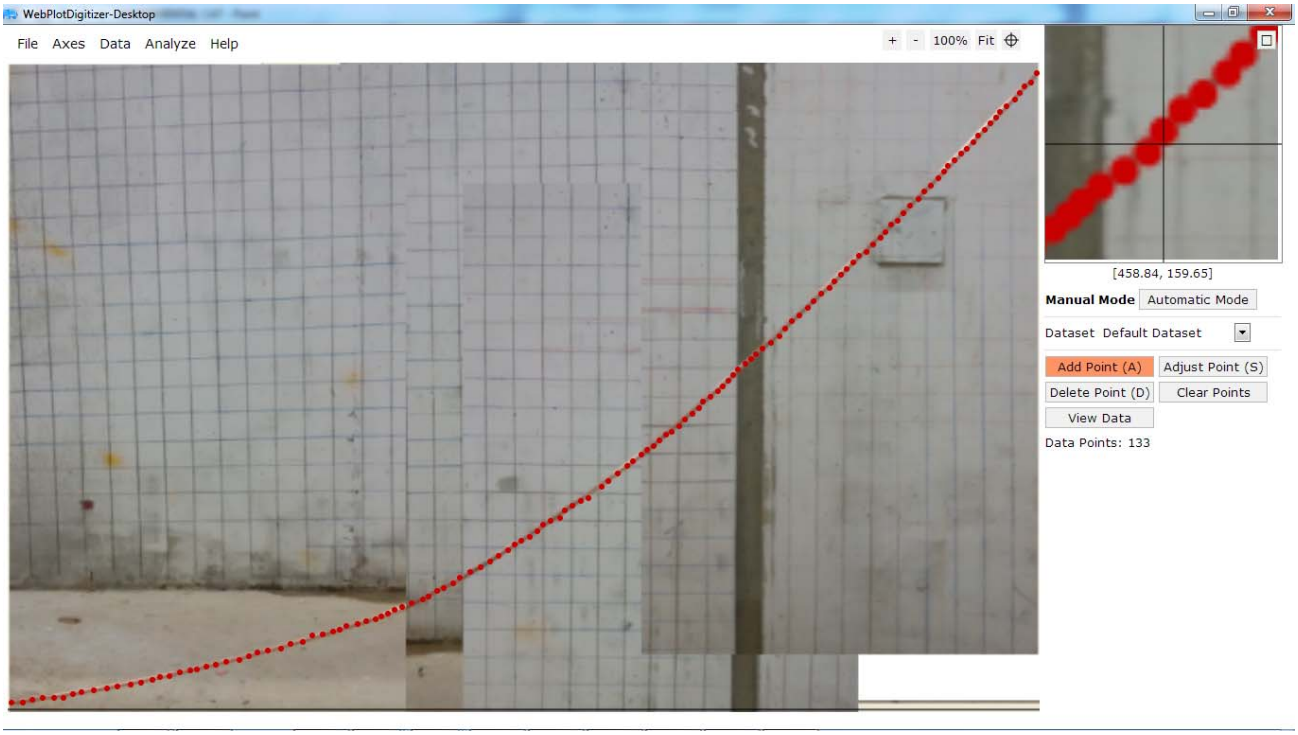
WebPlotDigitizer-Desktop
File Axes Data Analyze Help
+ - 100% Fit
[458.84, 159.65]
Manual Mode
Automatic Mode
Dataset Default Dataset
Add Point (A)
Adjust Point (S)
Delete Point (D)
Clear Points
View Data
Data Points: 133

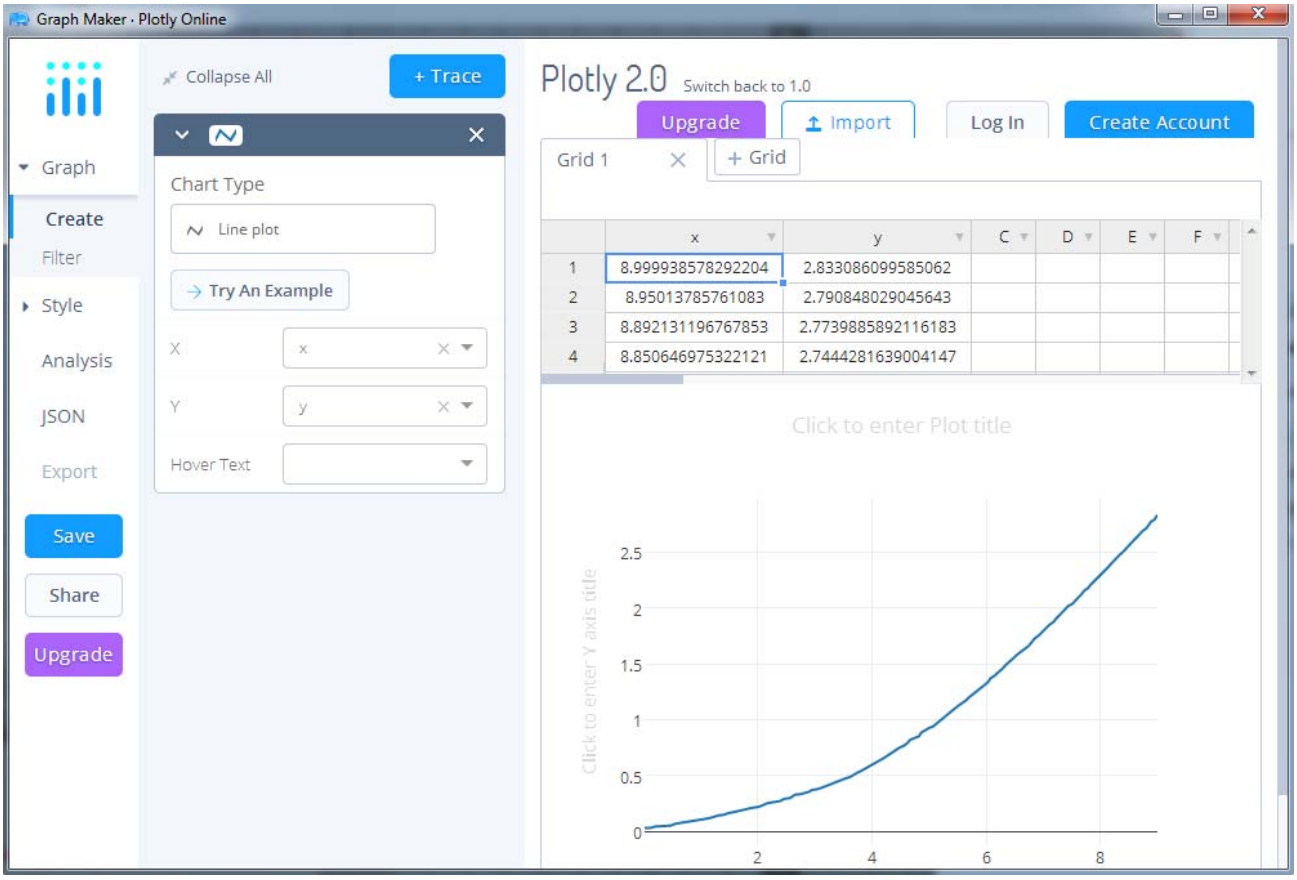
Graph Maker · Plotly Online
Collapse All
+ Trace
Plotly 2.0
Switch back to 1.0
Upgrade
Import
Log In
Create Account
Graph
Create
Filter
Style
Analysis
JSON
Export
Save
Share
Upgrade
Chart Type
Line plot
Try An Example
X
x
Y
y
Hover Text
Grid 1
+ Grid
x
y
C
D
E
F
1 8.999938578292204 2.833086099585062
2 8.95013785761083 2.790848029045643
3 8.892131196767853 2.7739885892116183
4 8.850646975322121 2.7444281639004147
Click to enter Plot title
Click to enter Y axis title
2.5
2
1.5
1
0.5
0
2
4
6
8

Case 1 – 2m Residual Curvature Length

1. Fixed Boundary Condition – 0.30% Residual Strains

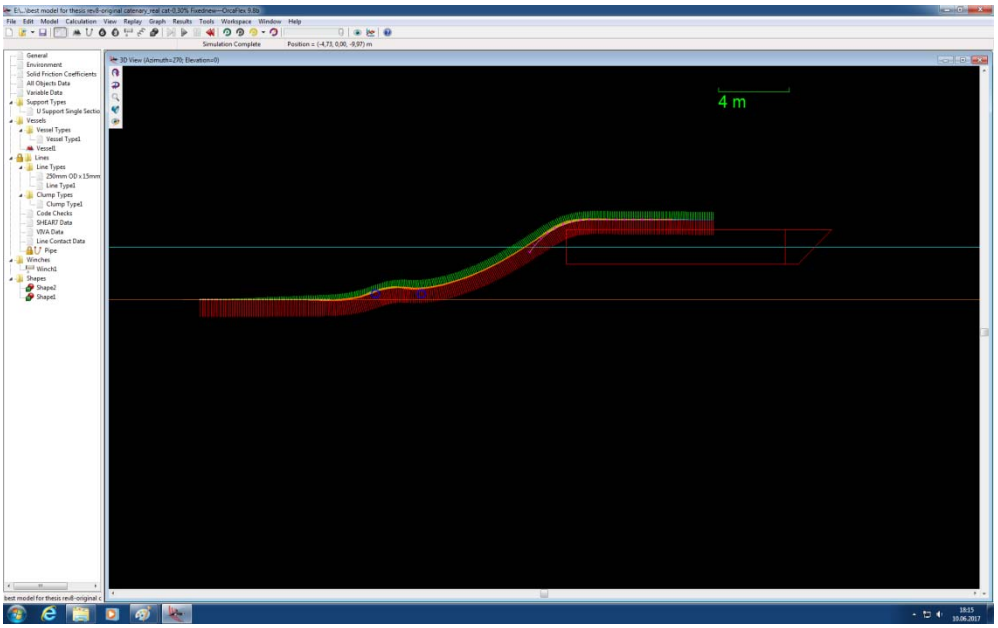

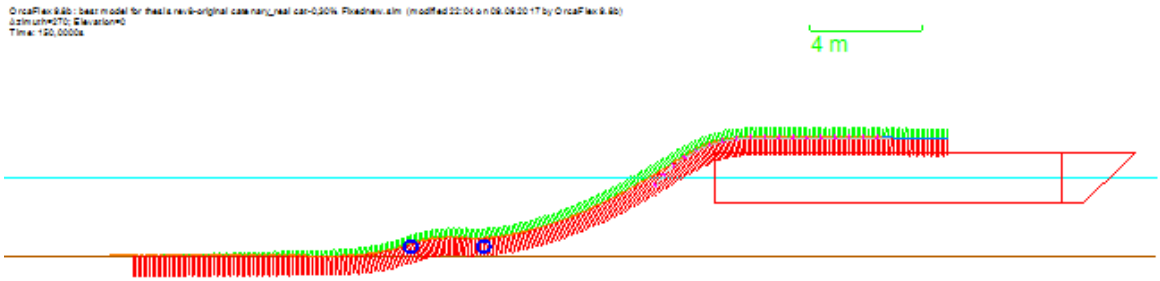

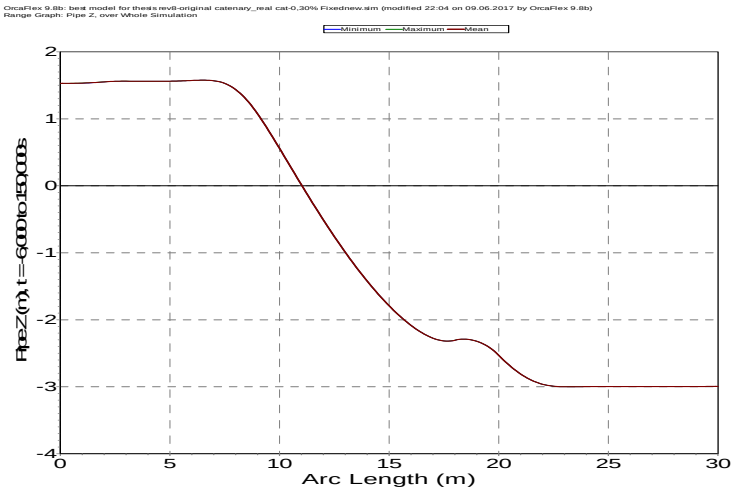

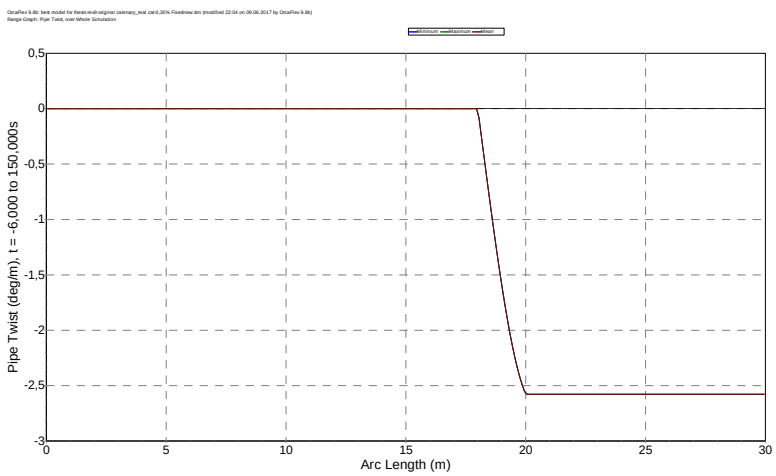

2. Fixed Boundary Condition – 0.35% Residual Strains

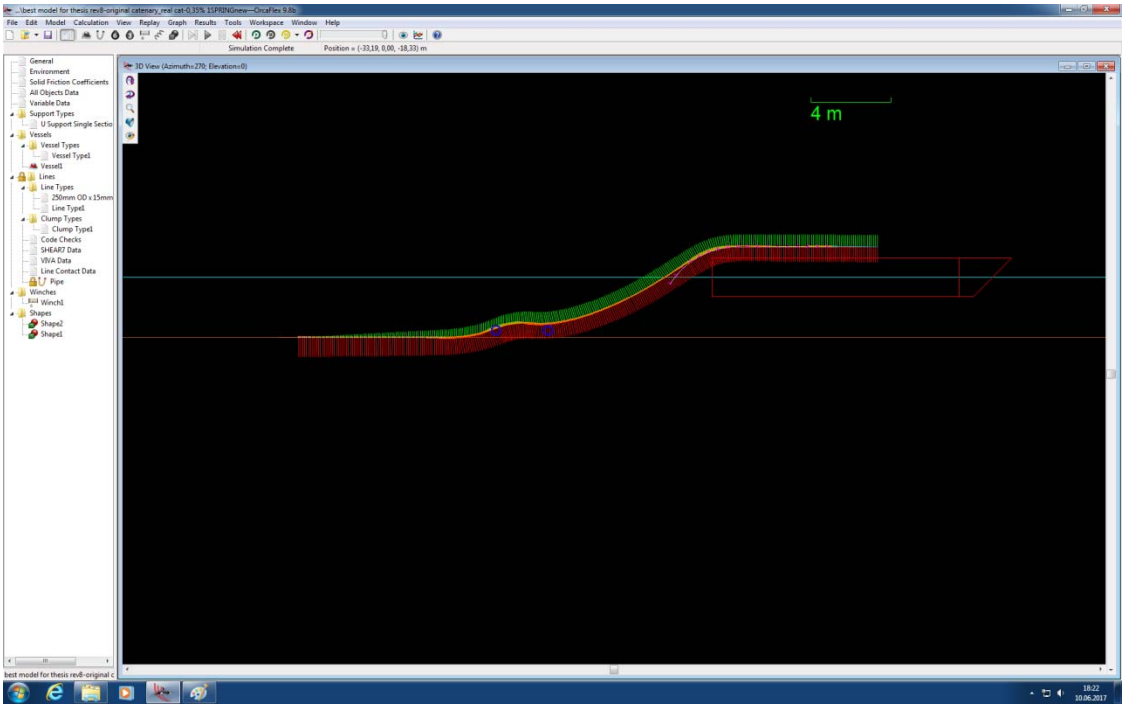

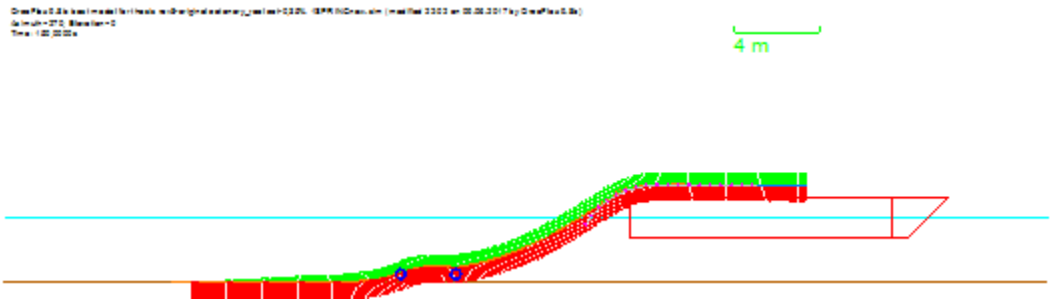

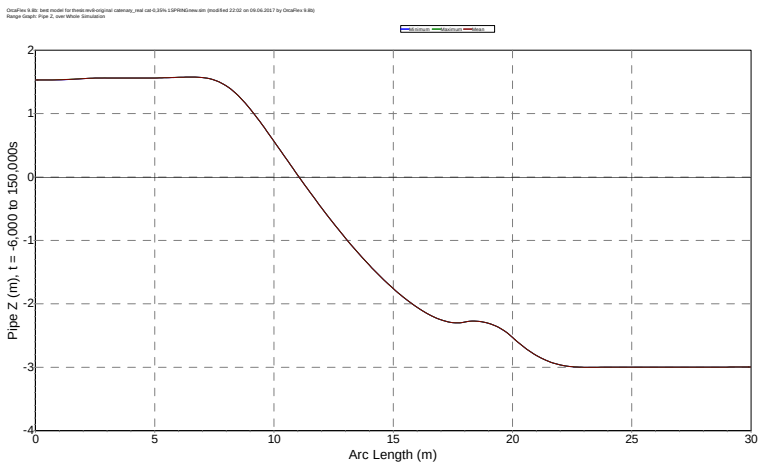

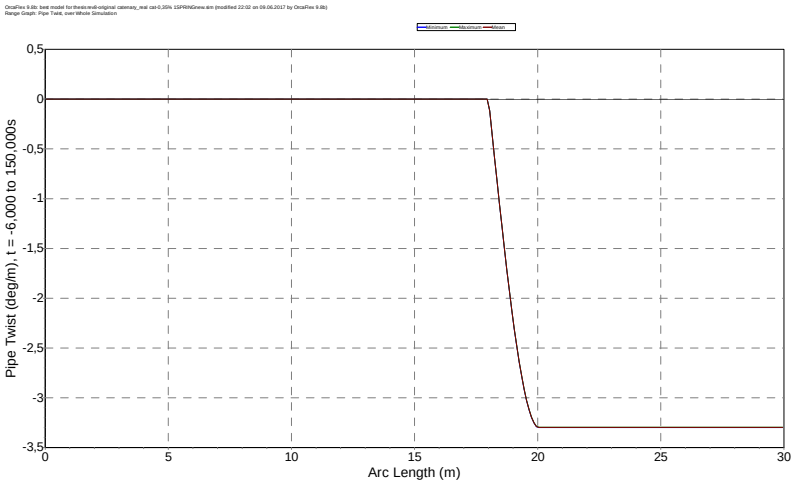

3. Fixed Boundary Condition – 0.40% Residual Strains

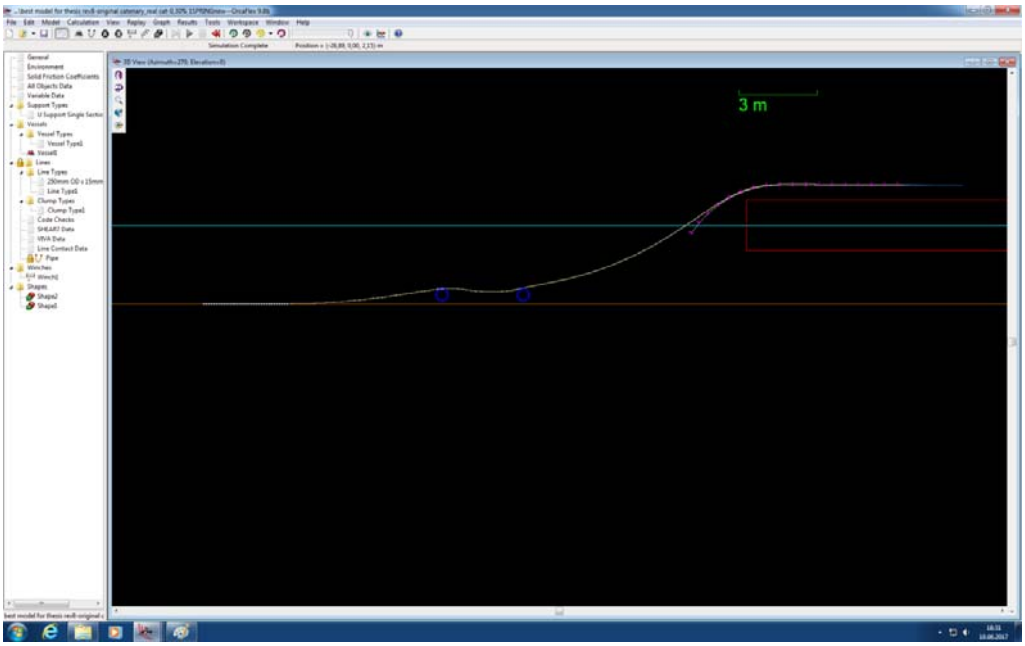

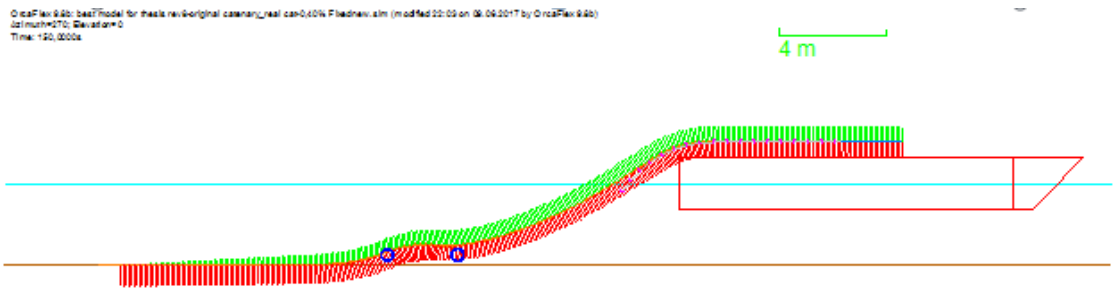
4 m

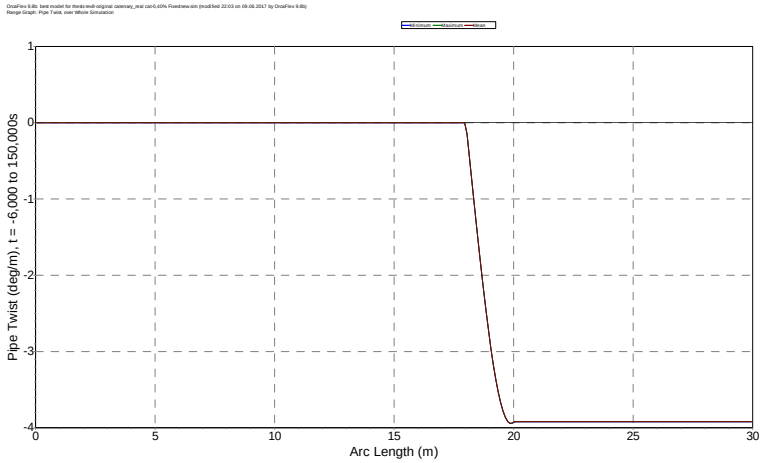
Pipe Twist (deg/m), t = -6,000 to 150,000s
Arc Length (m)
1
0
-1
-2
-3
-4
0
5
10
15
20
25
30

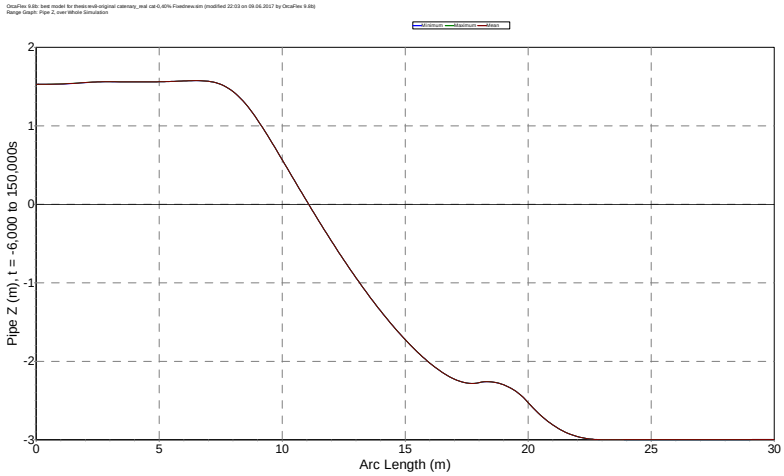
Pipe Z (m), t = -6,000 to 150,000s
Arc Length (m)
2
1
0
-1
-2
-3
0
5
10
15
20
25
30

4. 1-spring Boundary Condition – 0.30% Residual Strains

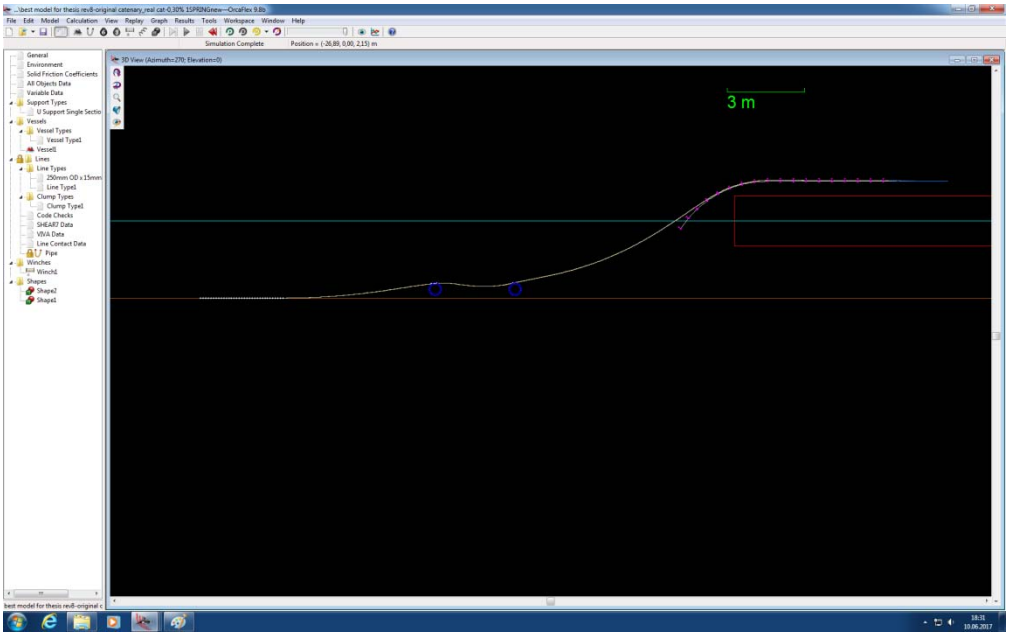

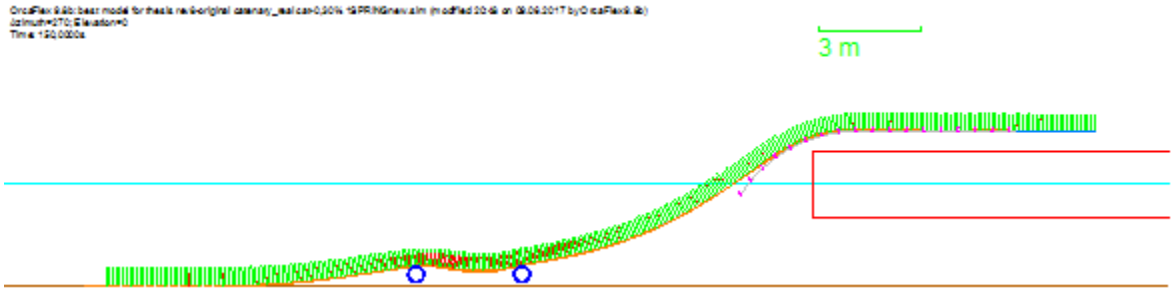

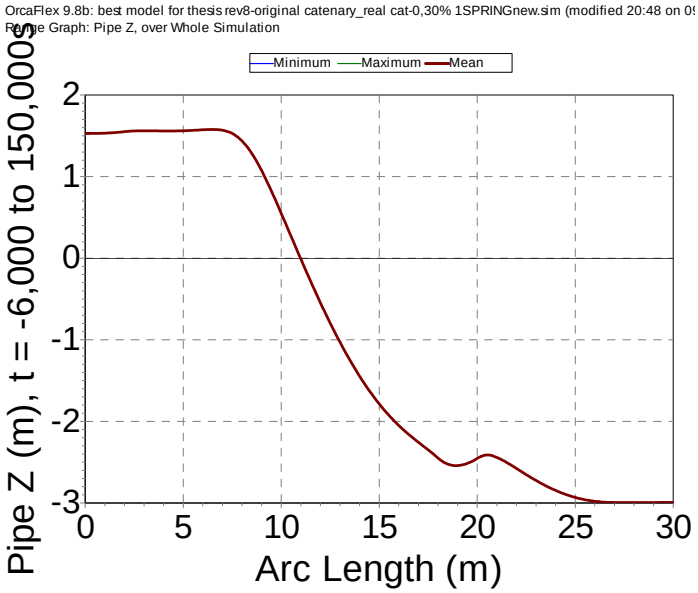

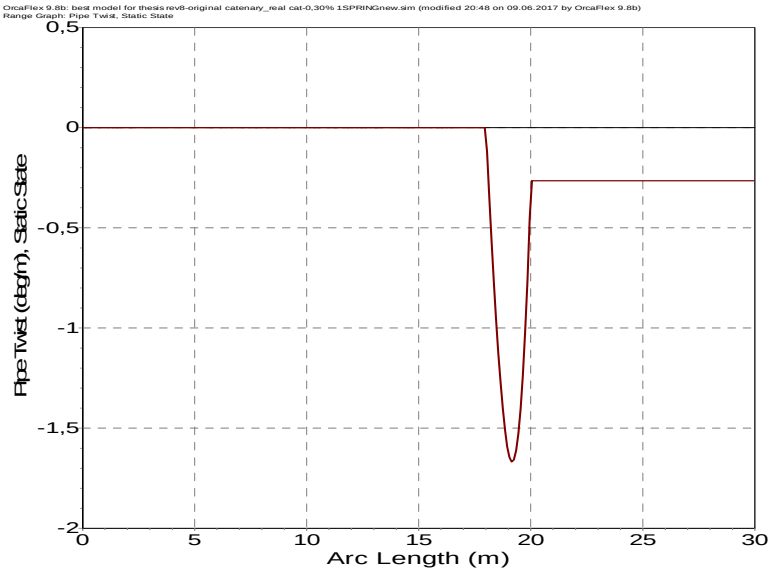

5. 1-spring Boundary Condition – 0.35% Residual Strains

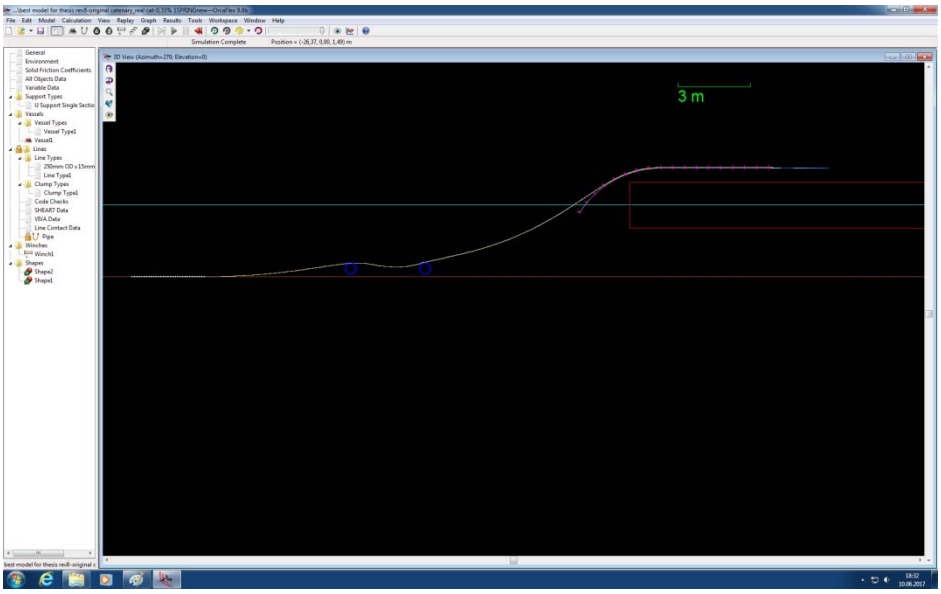

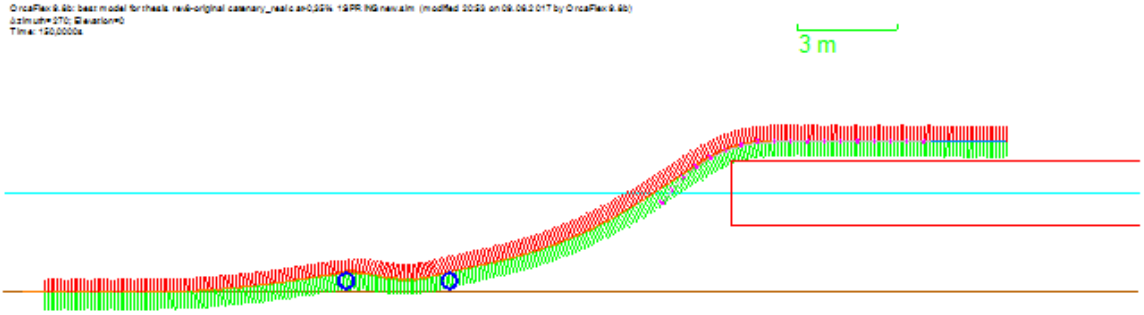

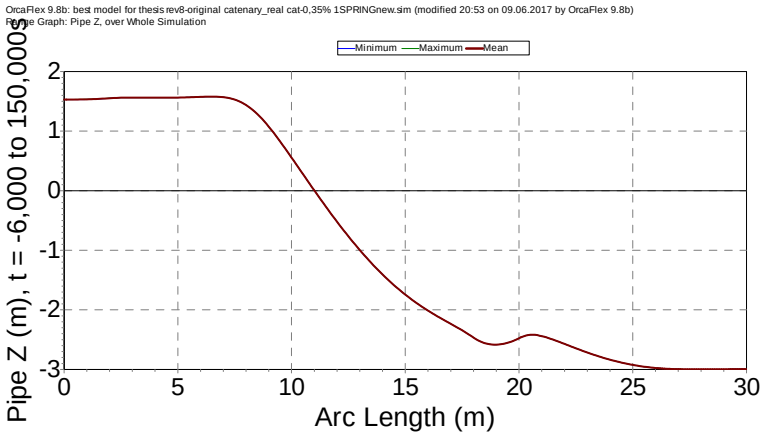

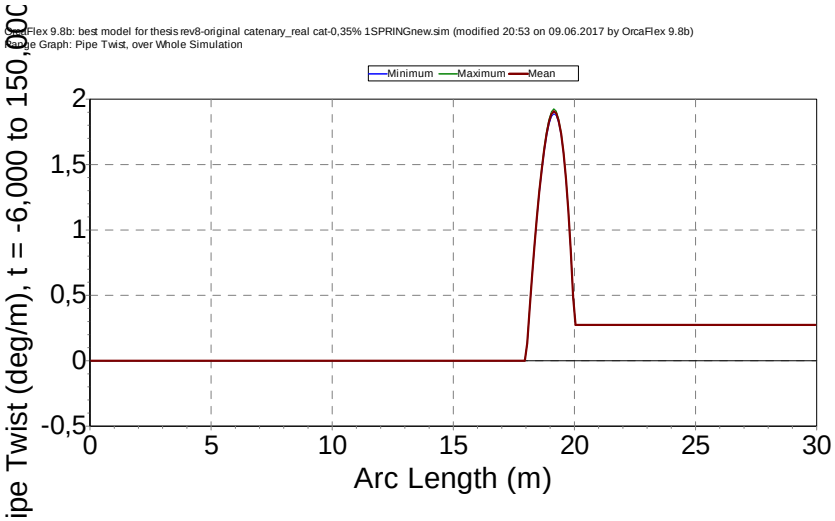

6. 1-spring Boundary Condition – 0.40% Residual Strains


4 m

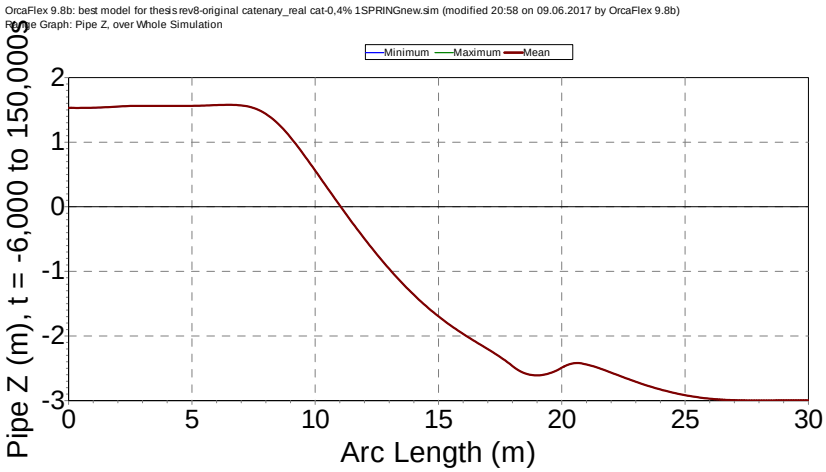
OrcaFlex 9.8b: best model for thesis rev8-original catenary_real cat-0,4% 1SPRINGnew.sim (modified 20:58 on 09.06.2017 by OrcaFlex 9.8b)
Range Graph: Pipe Z, over Whole Simulation
Minimum
Maximum
Mean
Pipe Z (m), t = -6,000 to 150,000s
2
1
0
-1
-2
-3
0
5
10
15
20
25
30
Arc Length (m)

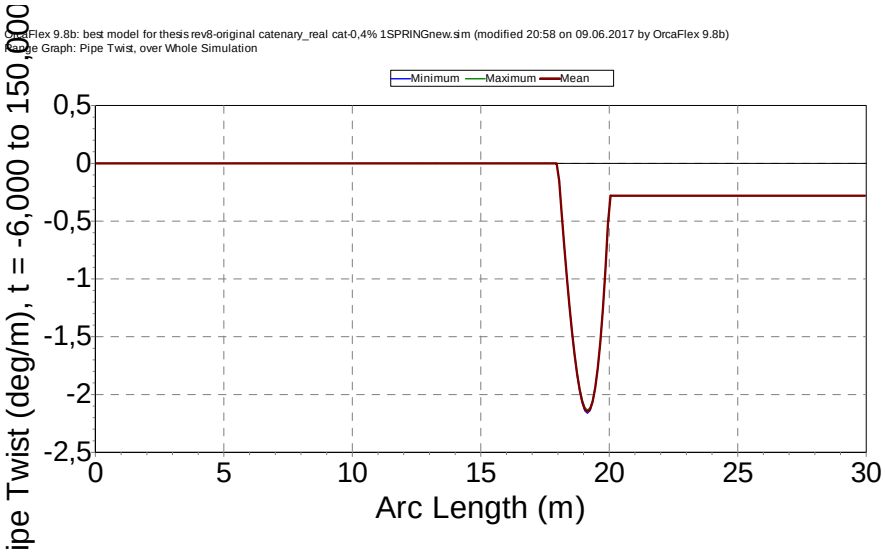
OrcaFlex 9.8b: best model for thesis rev8-original catenary_real cat-0,4% 1SPRINGnew.sim (modified 20:58 on 09.06.2017 by OrcaFlex 9.8b)
Range Graph: Pipe Twist, over Whole Simulation
Minimum
Maximum
Mean
ipe Twist (deg/m), t = -6,000 to 150,000
0,5
0
-0,5
-1
-1,5
-2
-2,5
0
5
10
15
20
25
30
Arc Length (m)

7. 2-spring Boundary Condition – 0.30% Residual Strains

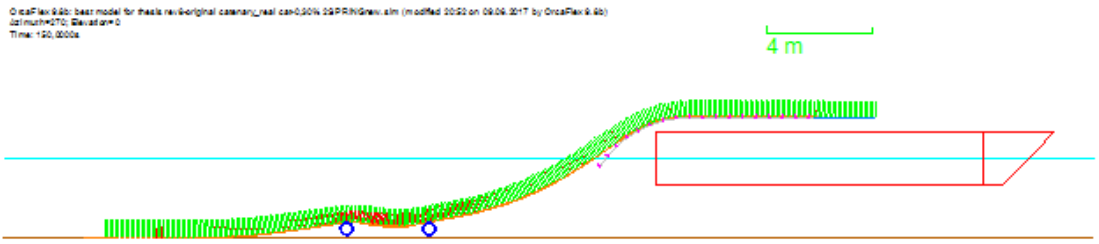

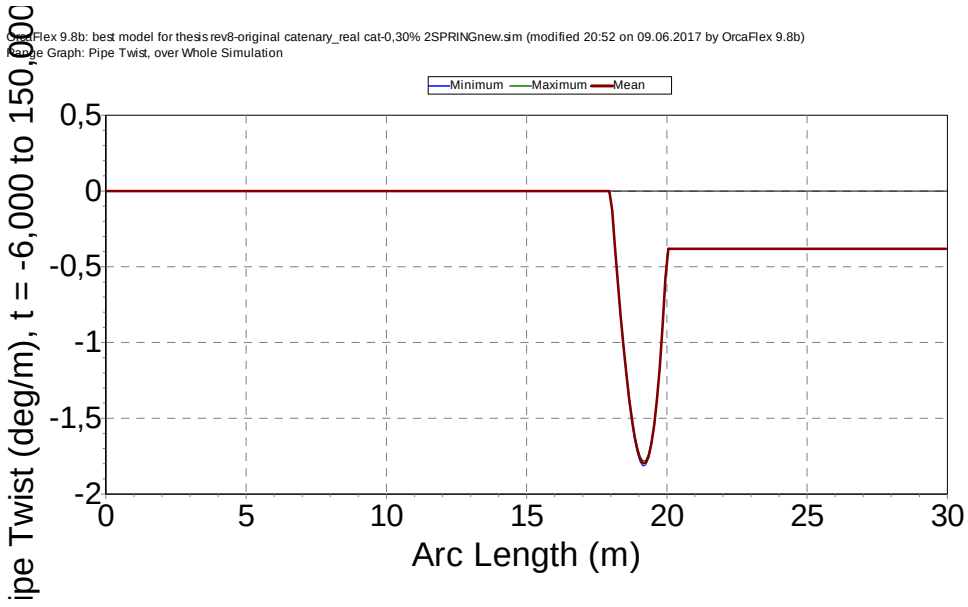

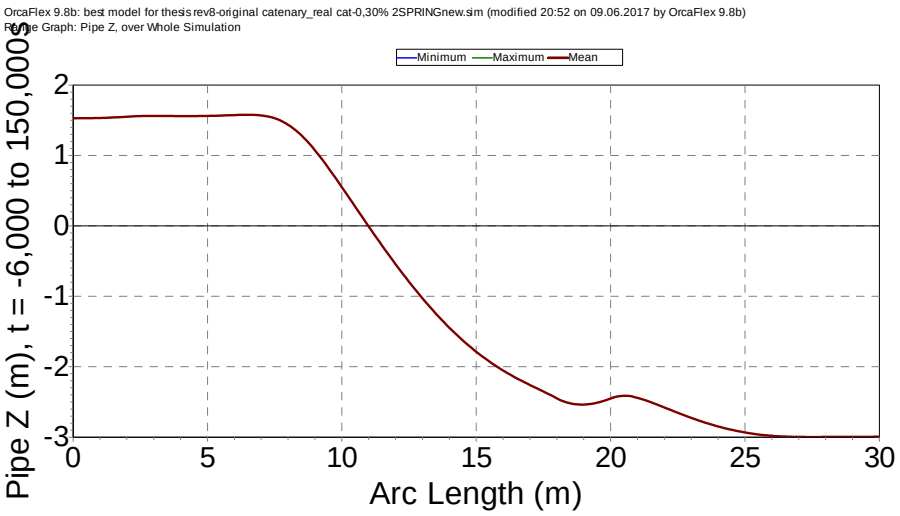

8. 2-spring Boundary Condition – 0.35% Residual Strains

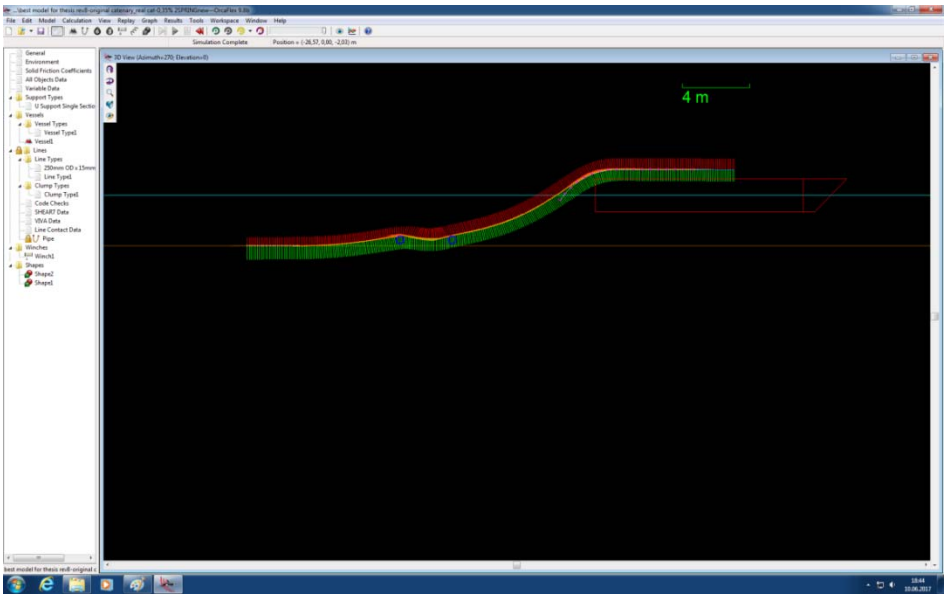

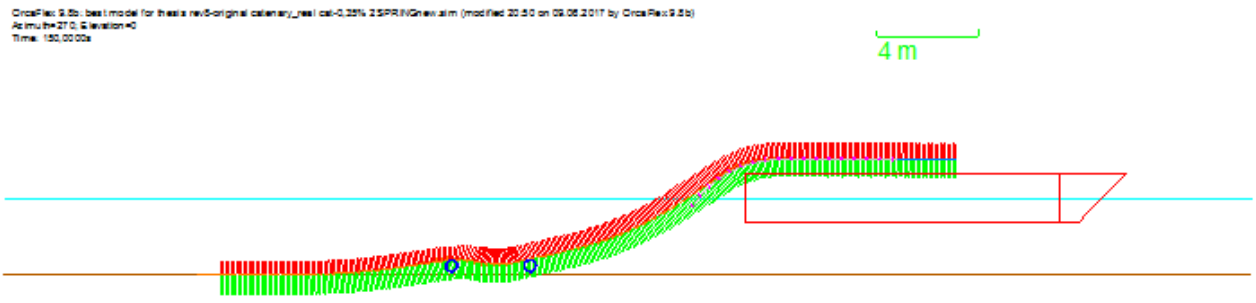

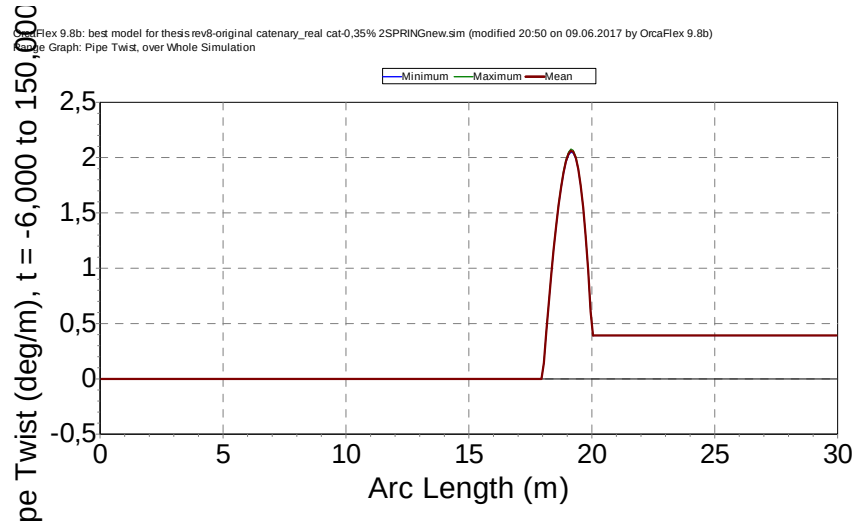

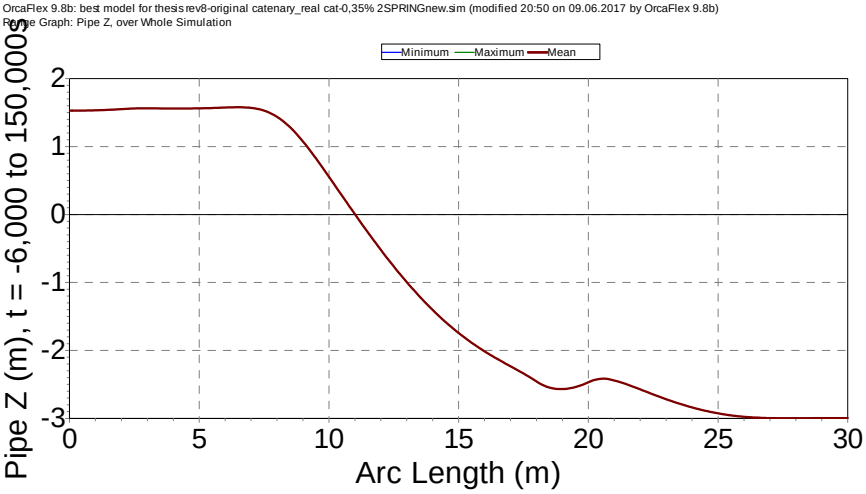

9. 2-spring Boundary Condition – 0.40% Residual Strains

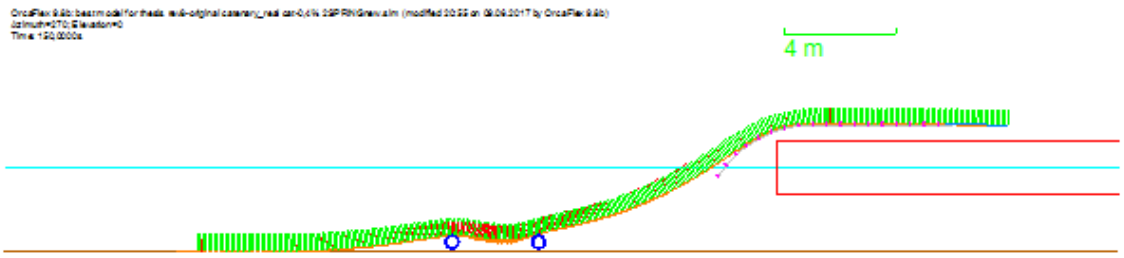
4 m

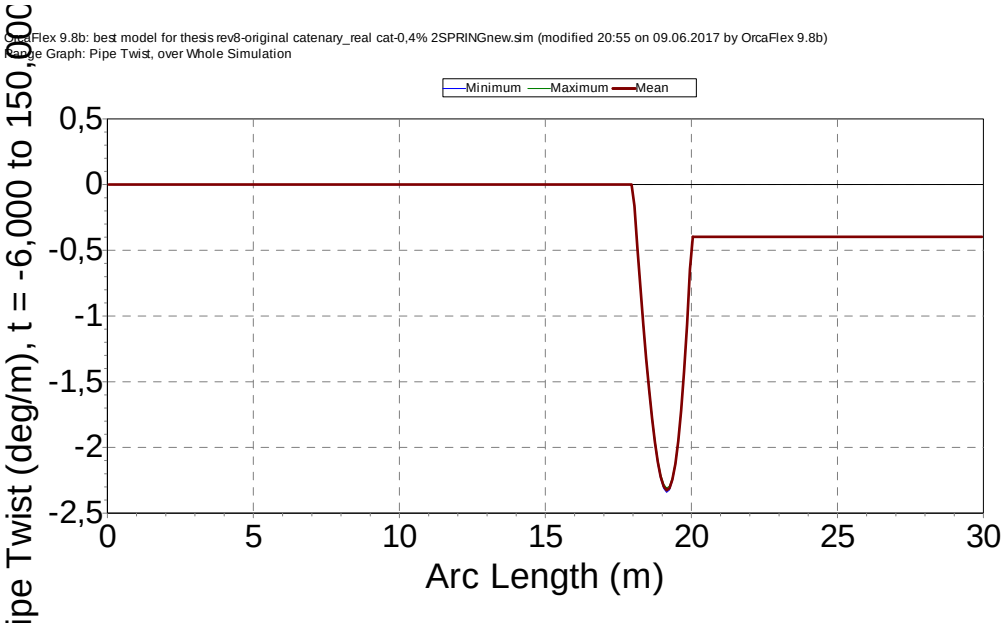
OrcaFlex 9.8b: best model for thesis rev8-original catenary_real cat-0,4% 2SPRINGnew.sim (modified 20:55 on 09.06.2017 by OrcaFlex 9.8b)
Range Graph: Pipe Twist, over Whole Simulation
Minimum
Maximum
Mean
ipe Twist (deg/m), t = -6,000 to 150,000
0,5
0
-0,5
-1
-1,5
-2
-2,5
0
5
10
15
20
25
30
Arc Length (m)

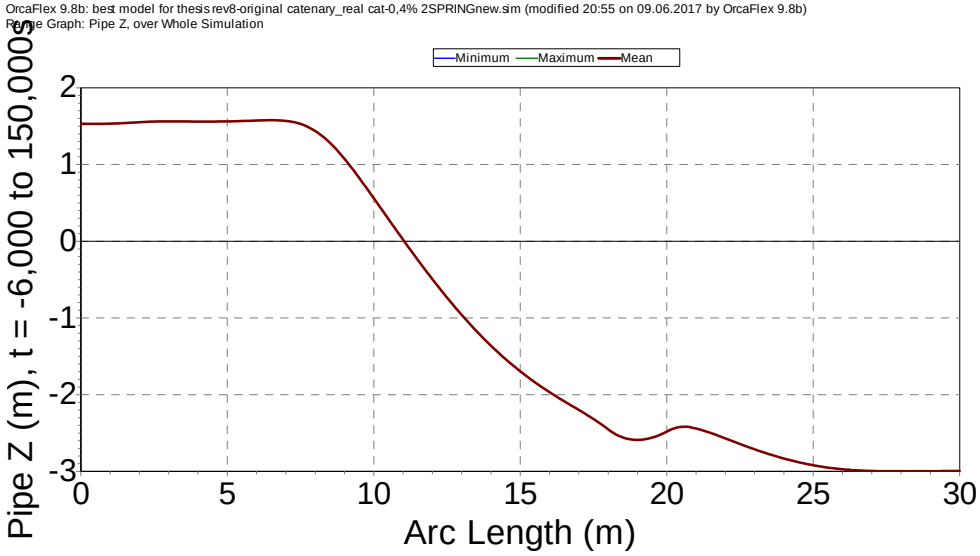
OrcaFlex 9.8b: best model for thesis rev8-original catenary_real cat-0,4% 2SPRINGnew.sim (modified 20:55 on 09.06.2017 by OrcaFlex 9.8b)
Range Graph: Pipe Z, over Whole Simulation
Minimum
Maximum
Mean
Pipe Z (m), t = -6,000 to 150,000s
2
1
0
-1
-2
-3
0
5
10
15
20
25
30
Arc Length (m)

Case 2 – 3m Residual Curvature Length

10. Fixed Boundary Condition – 0.30% Residual Strains

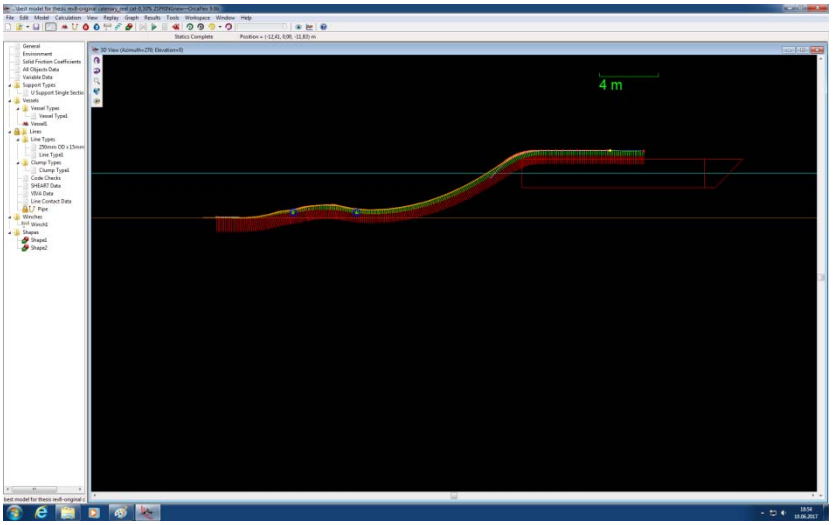

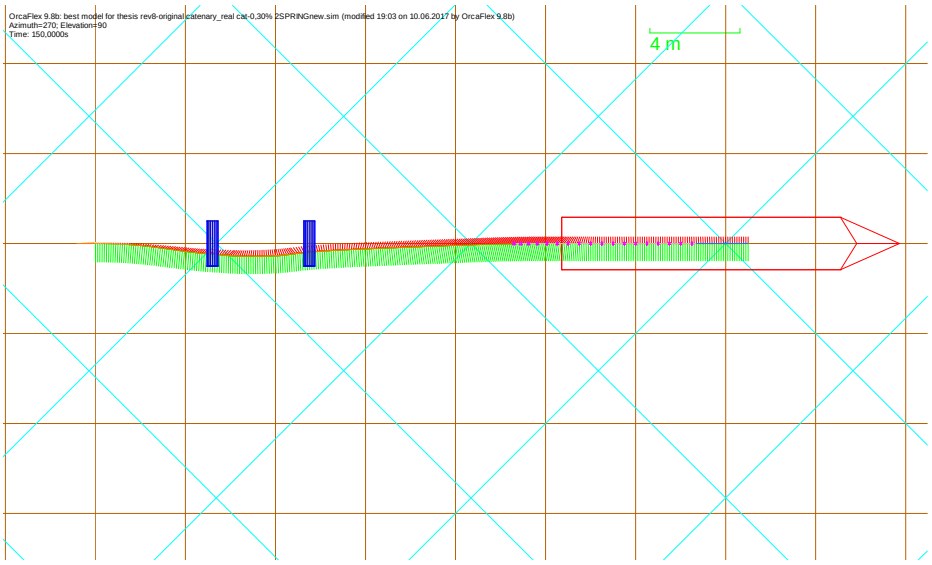

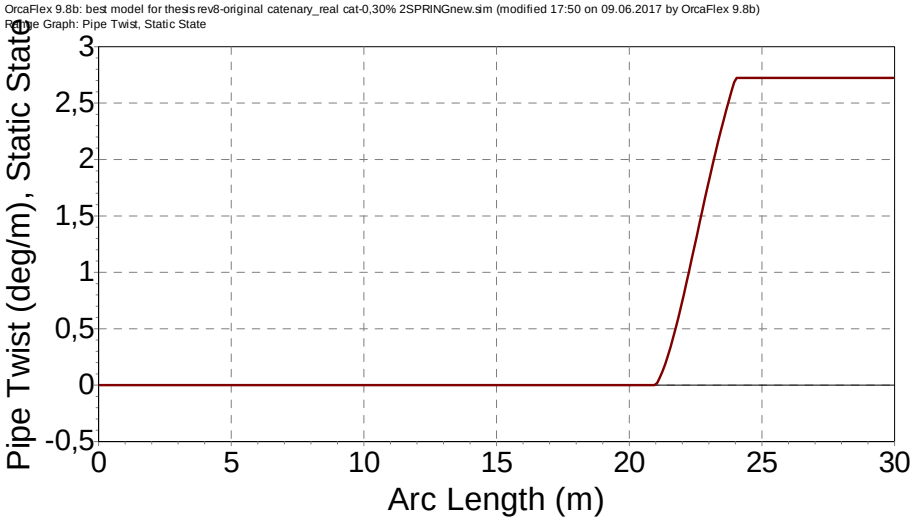

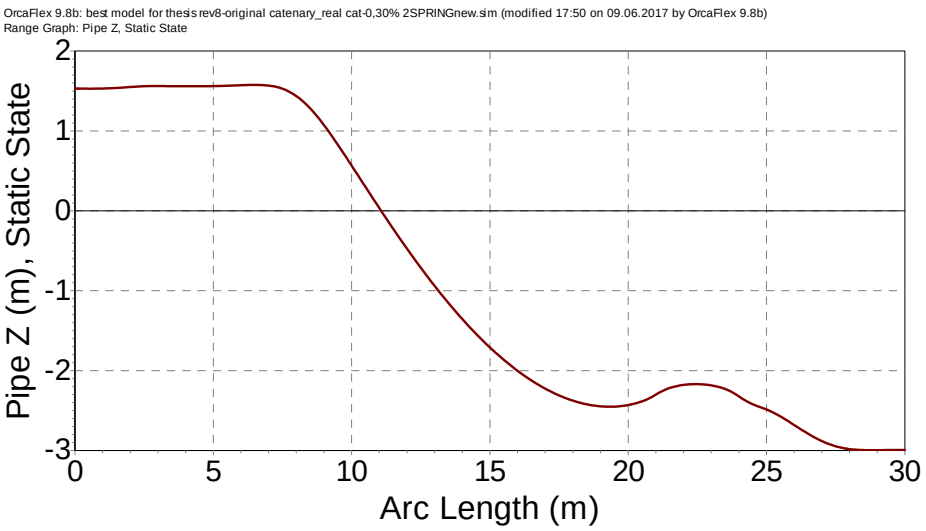

11. Fixed Boundary Condition – 0.35% Residual Strains

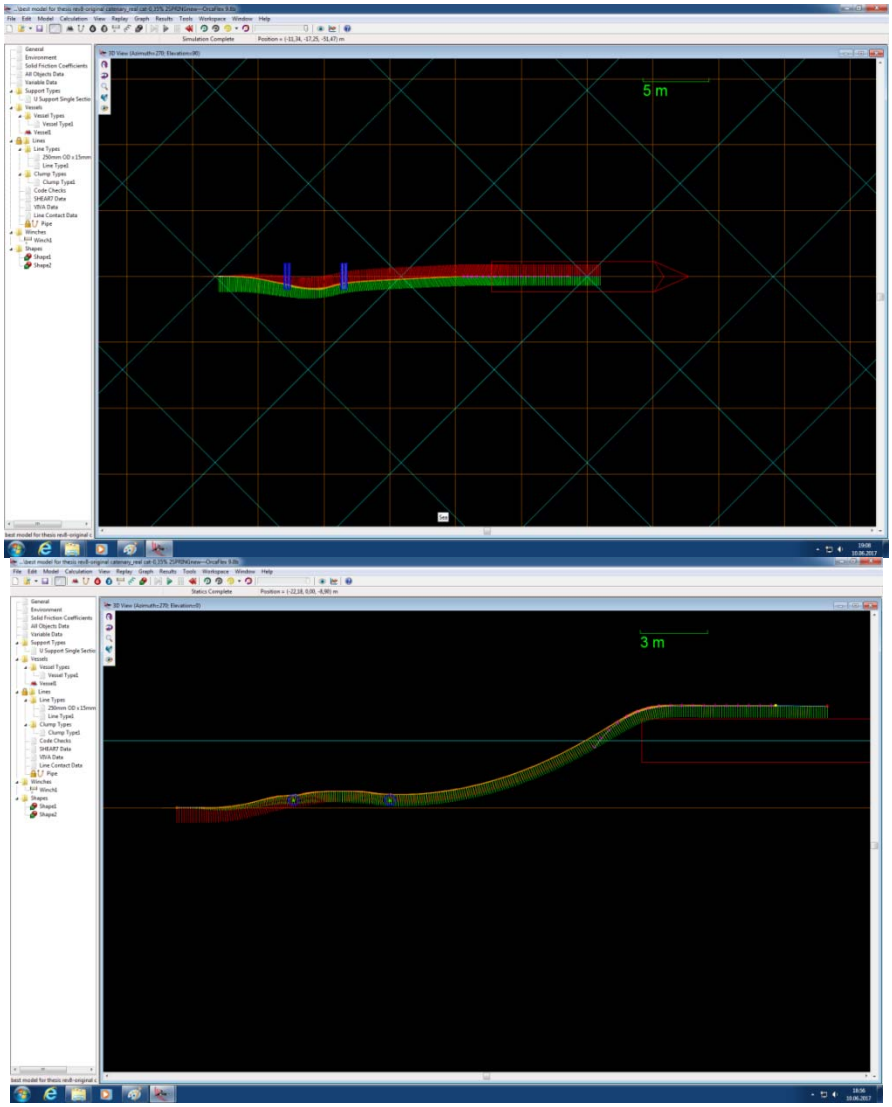

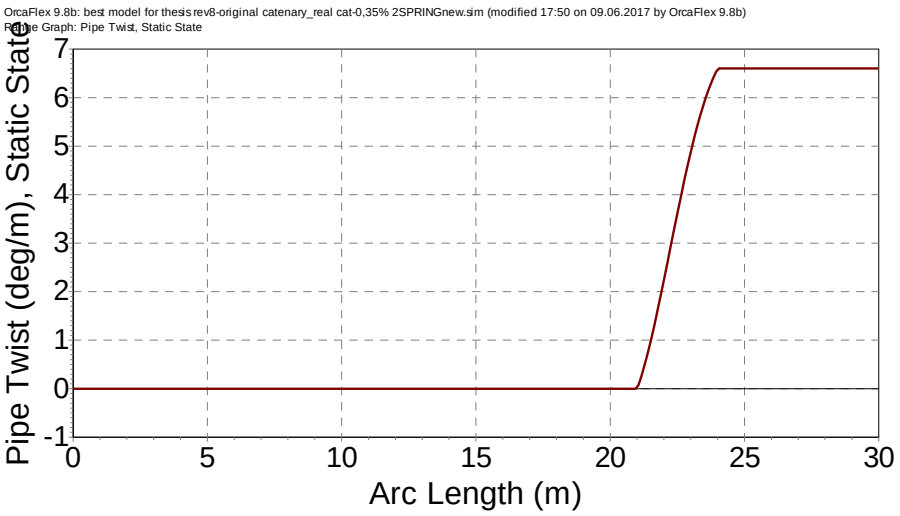

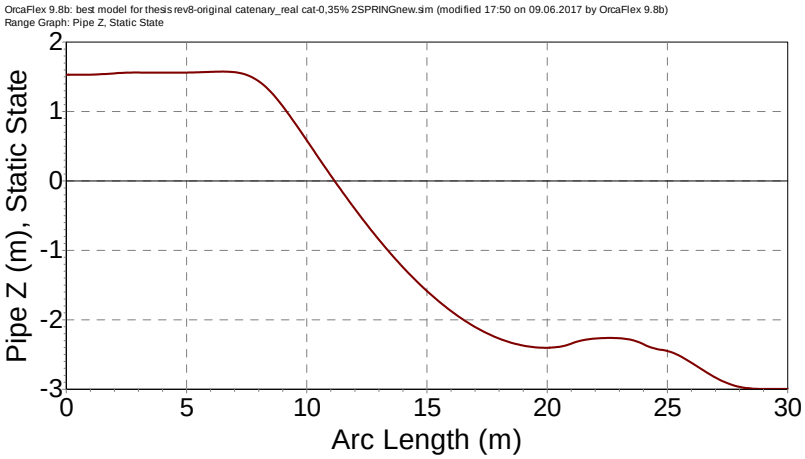

12. Fixed Boundary Condition – 0.40% Residual Strains

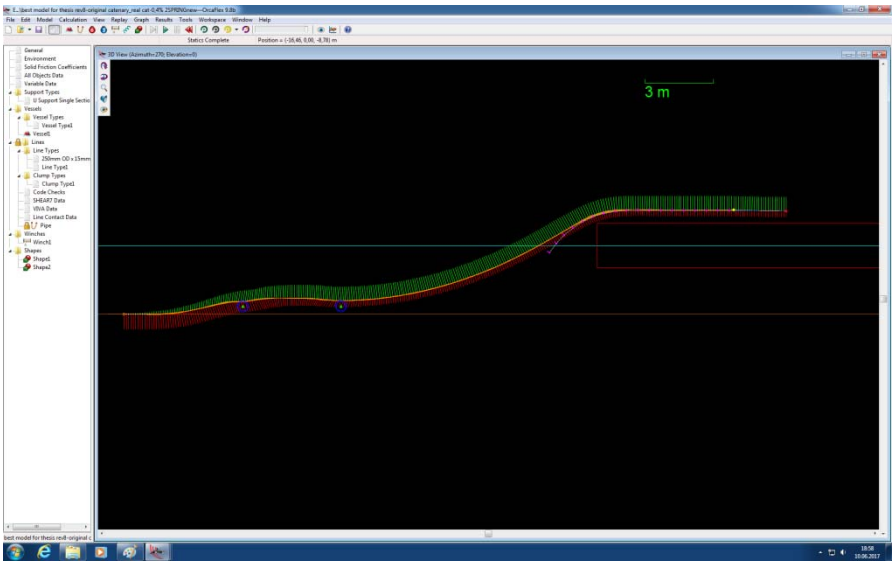

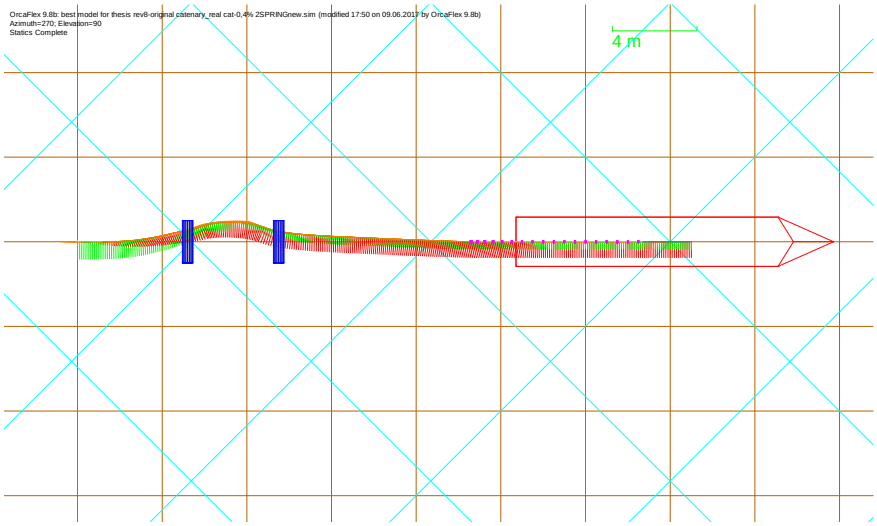
OrcaFlex 9.8b: best model for thesis rev8-original catenary_real cat-0,4% 2SPRINGnew.sim (modified 17:50 on 09.06.2017 by OrcaFlex 9.8b)
Azimuth=270; Elevation=90
Statics Complete
4 m

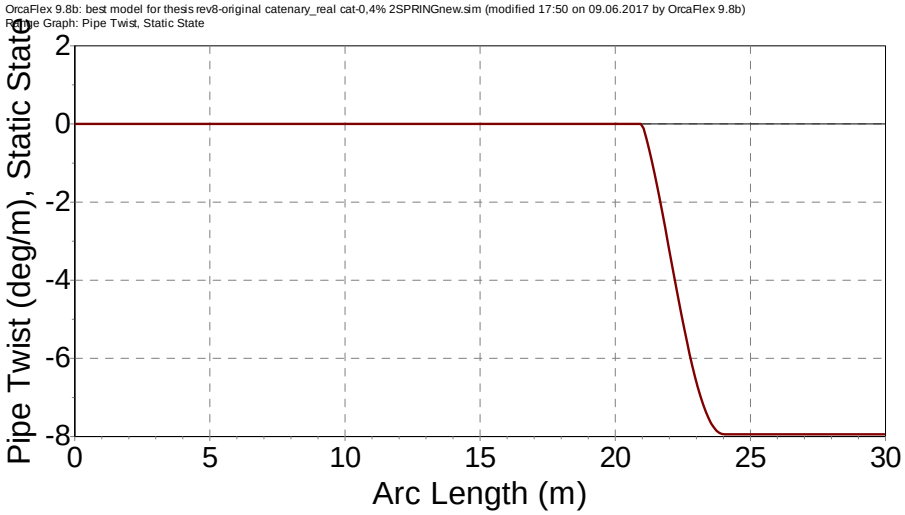
OrcaFlex 9.8b: best model for thesis rev8-original catenary_real cat-0,4% 2SPRINGnew.sim (modified 17:50 on 09.06.2017 by OrcaFlex 9.8b)
Range Graph: Pipe Twist, Static State
Pipe Twist (deg/m), Static State
2
0
-2
-4
-6
-8
0
5
10
15
20
25
30
Arc Length (m)

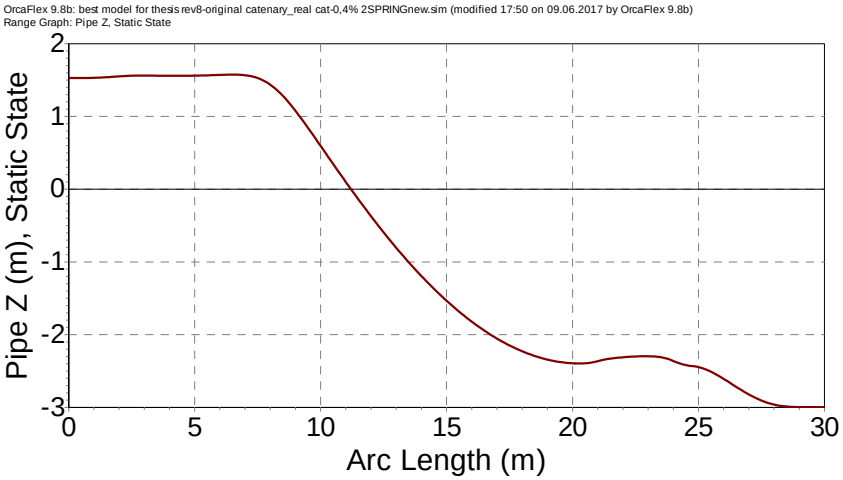
OrcaFlex 9.8b: best model for thesis rev8-original catenary_real cat-0,4% 2SPRINGnew.sim (modified 17:50 on 09.06.2017 by OrcaFlex 9.8b)
Range Graph: Pipe Z, Static State
Pipe Z (m), Static State
2
1
0
-1
-2
-3
0
5
10
15
20
25
30
Arc Length (m)

13. 1-Spring Boundary Condition – 0.30% Residual Strains

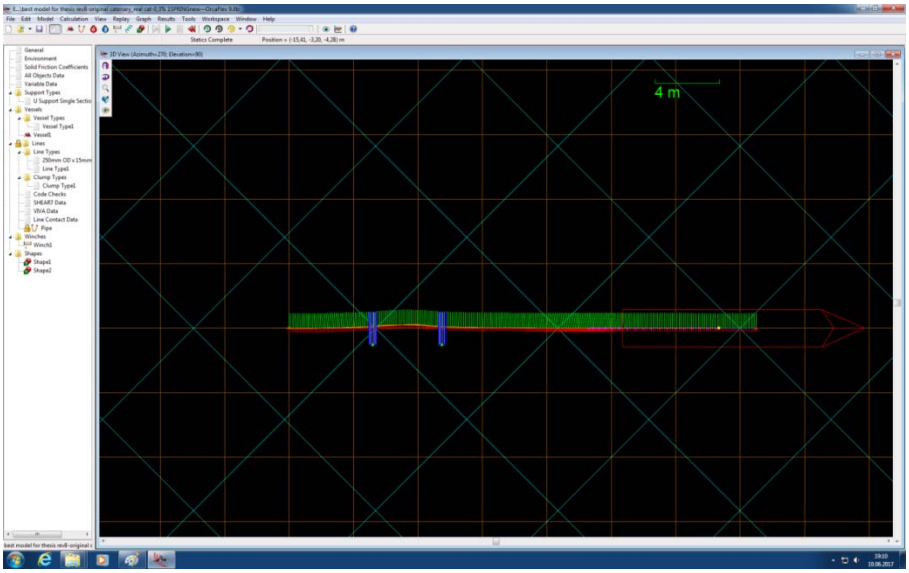

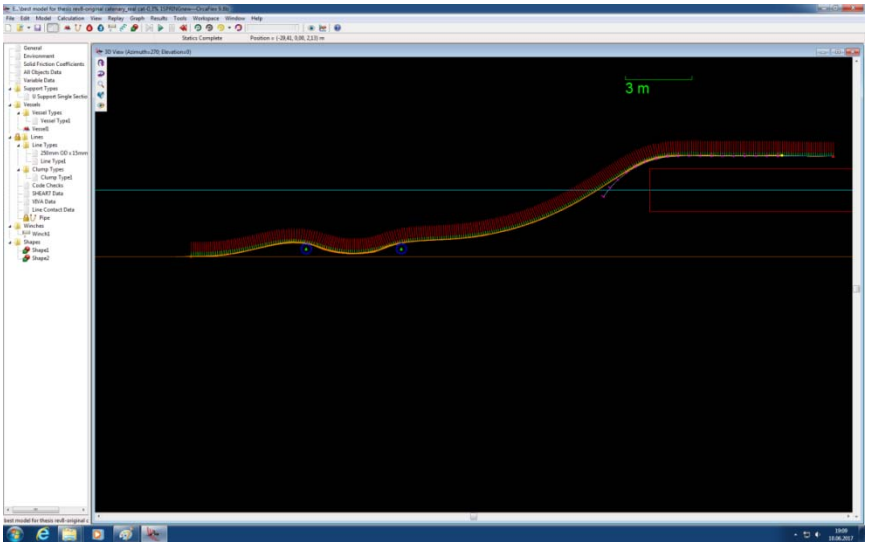

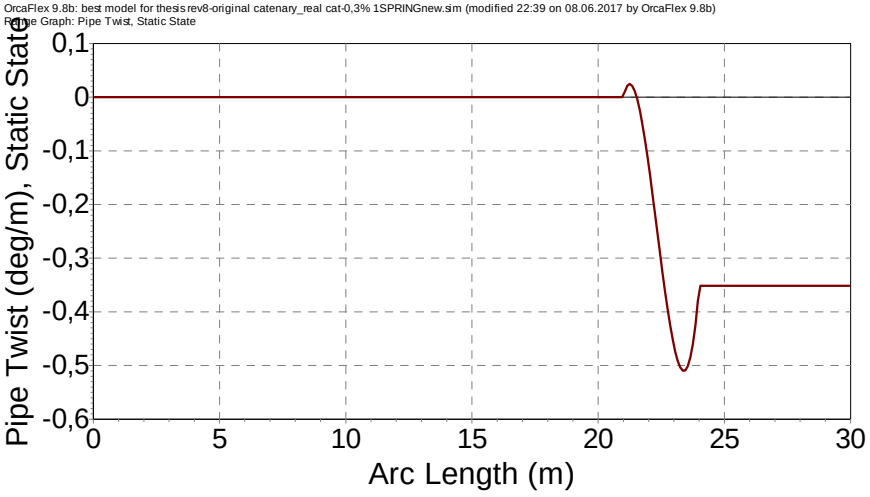

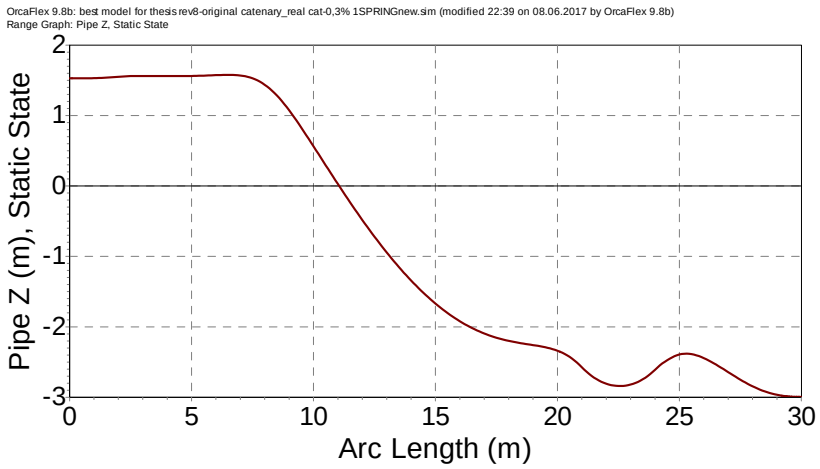

14. 1-Spring Boundary Condition – 0.35% Residual Strains

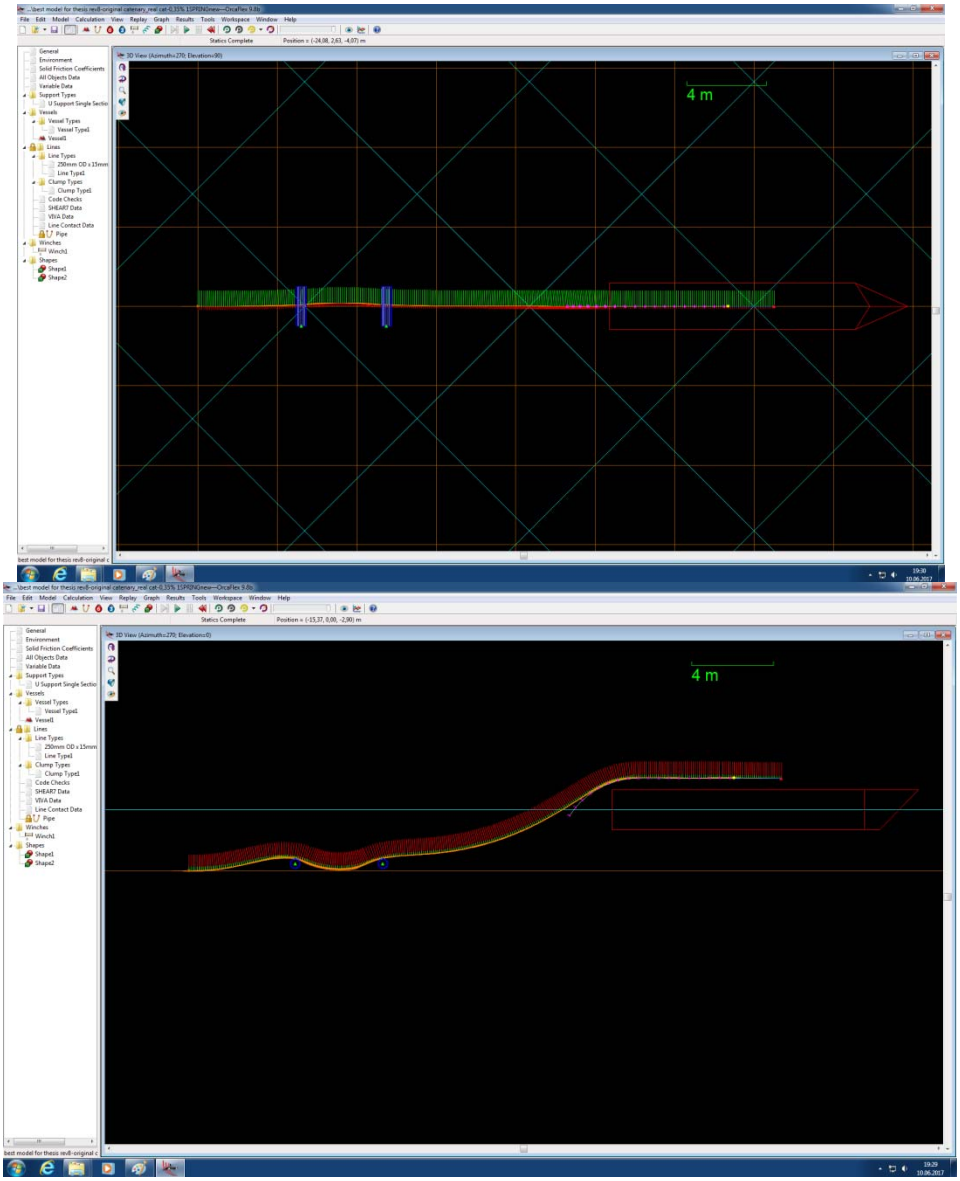

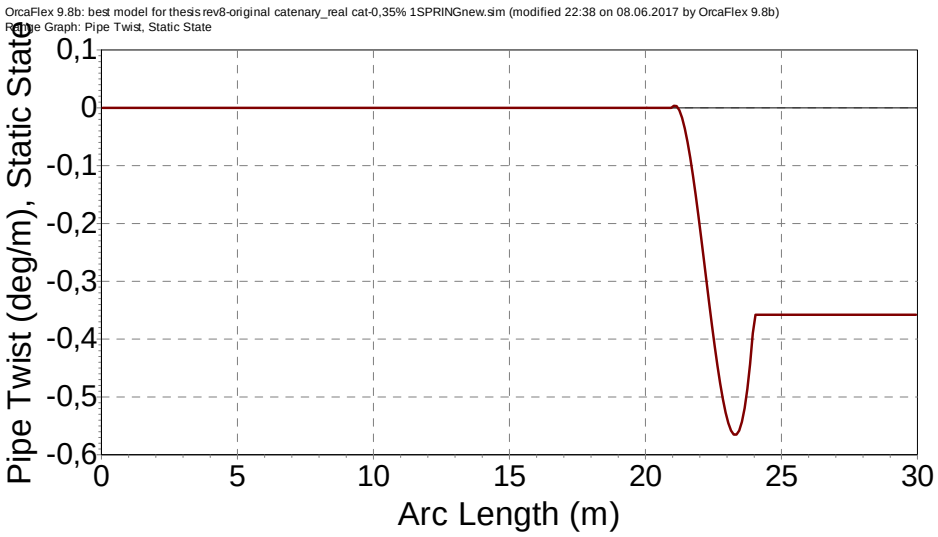

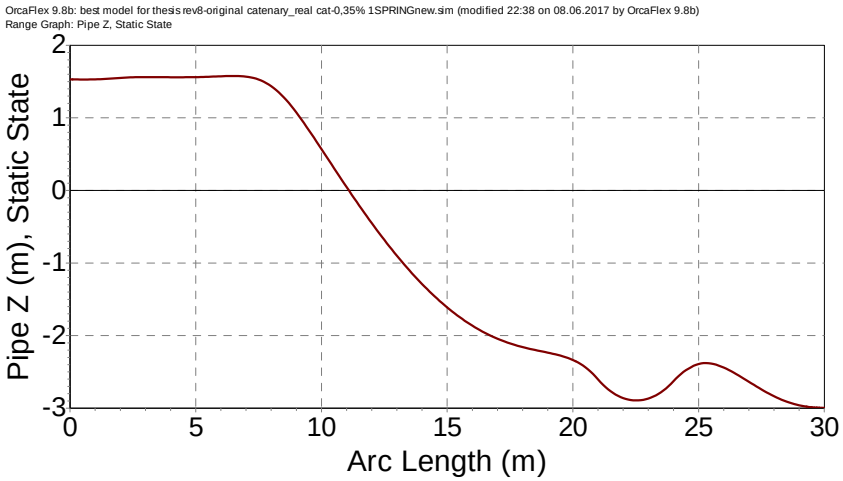

15. 1-Spring Boundary Condition – 0.40% Residual Strains

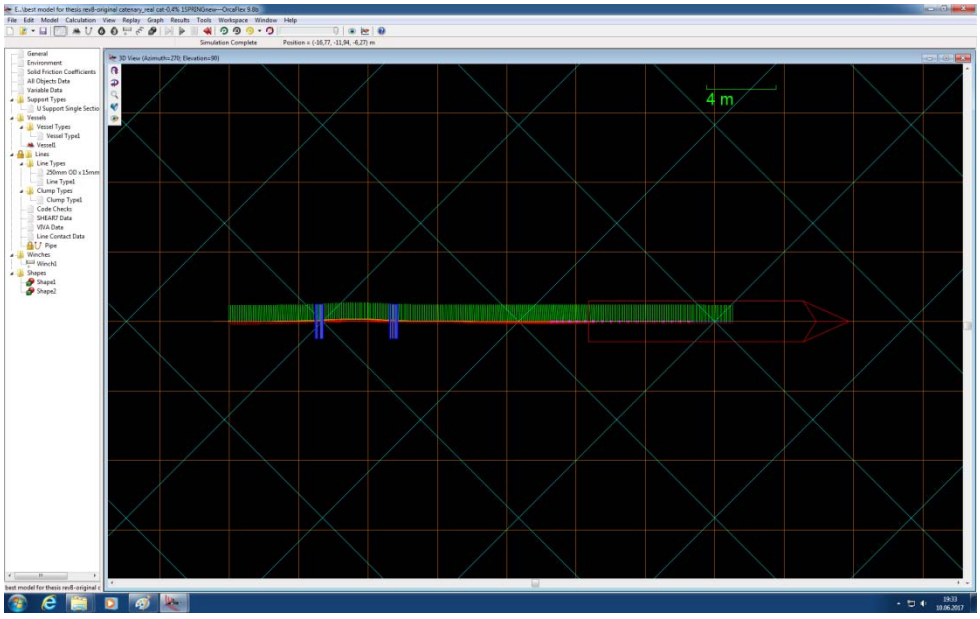

OrcaFlex 9.8b: best model for thesis rev8-original catenary_real cat-0,4% 1SPRINGnew.sim (modified 20:04 on 09.06.2017 by OrcaFlex 9.8b)
Range Graph: Pipe Twist, over Whole Simulation

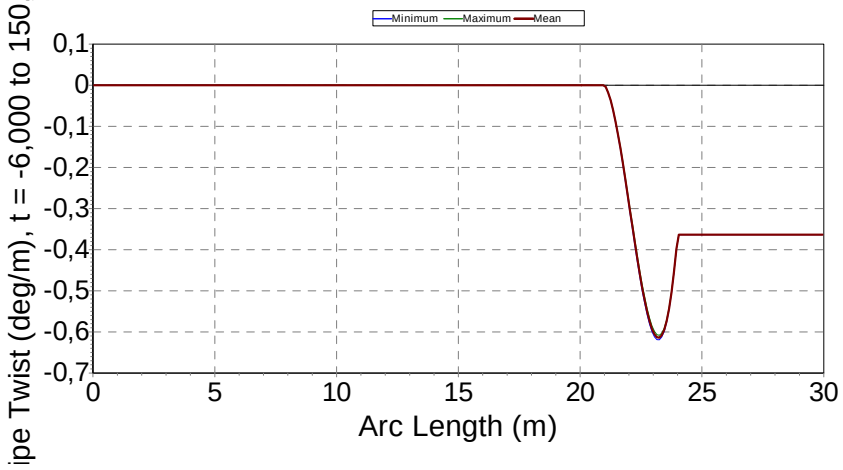

OrcaFlex 9.8b: best model for thesis rev8-original catenary_real cat-0,4% 1SPRINGnew.sim (modified 20:04 on 09.06.2017 by OrcaFlex 9.8b)
Range Graph: Pipe Z, over Whole Simulation

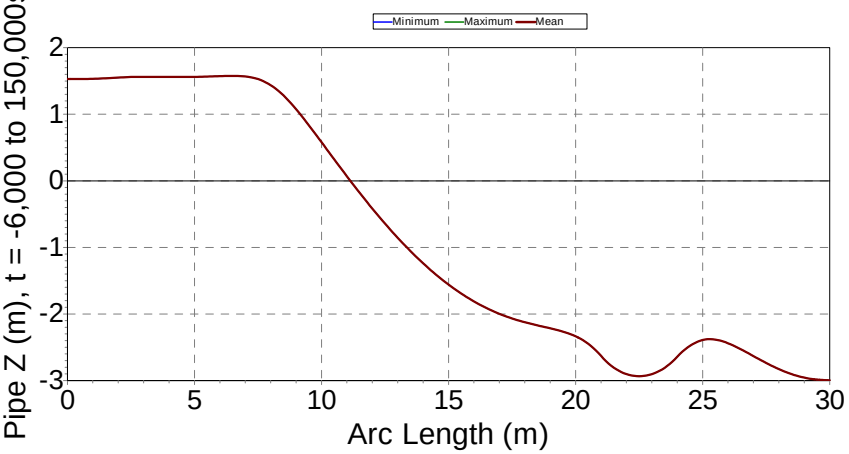

16. 2-Spring Boundary Condition – 0.30% Residual Strains

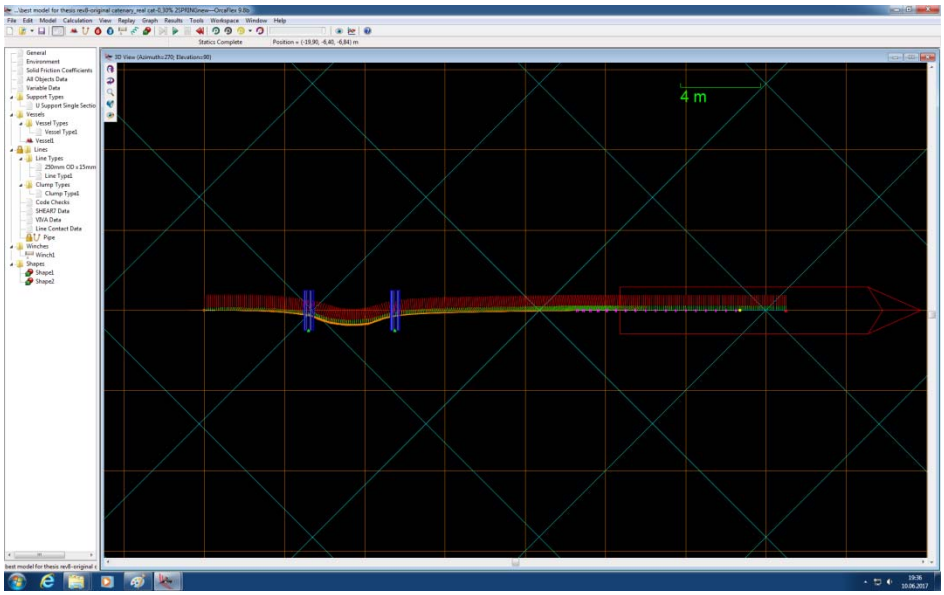

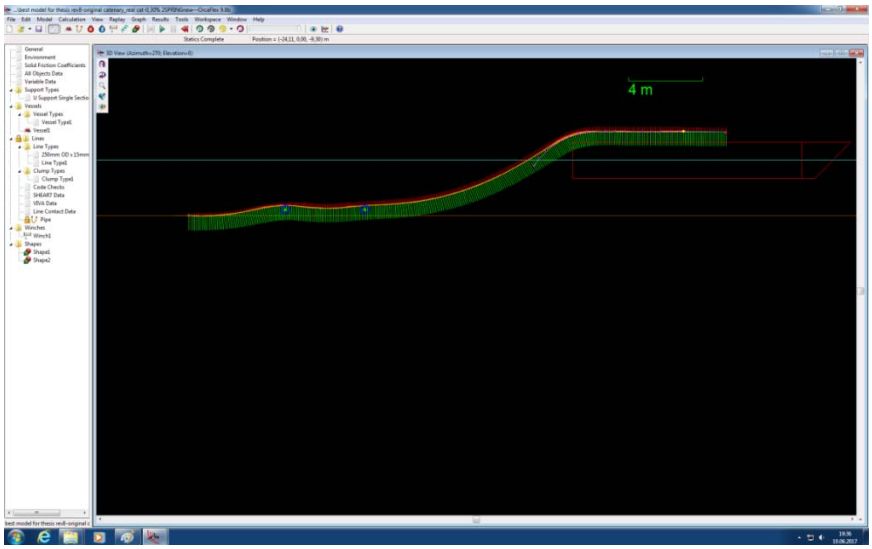

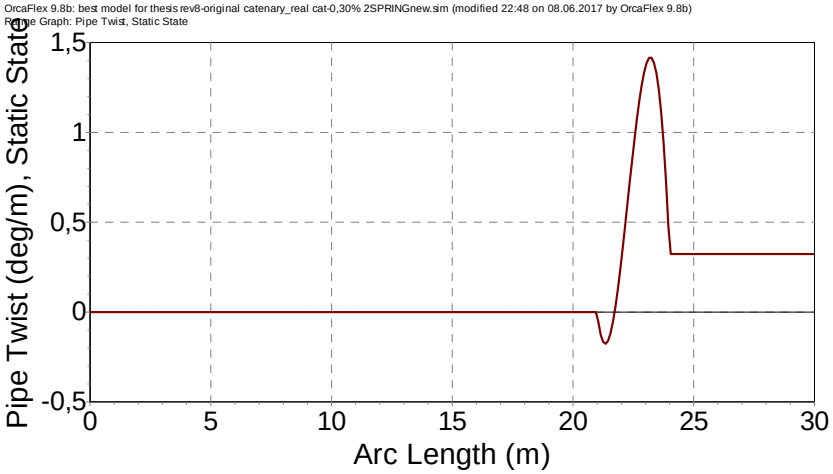

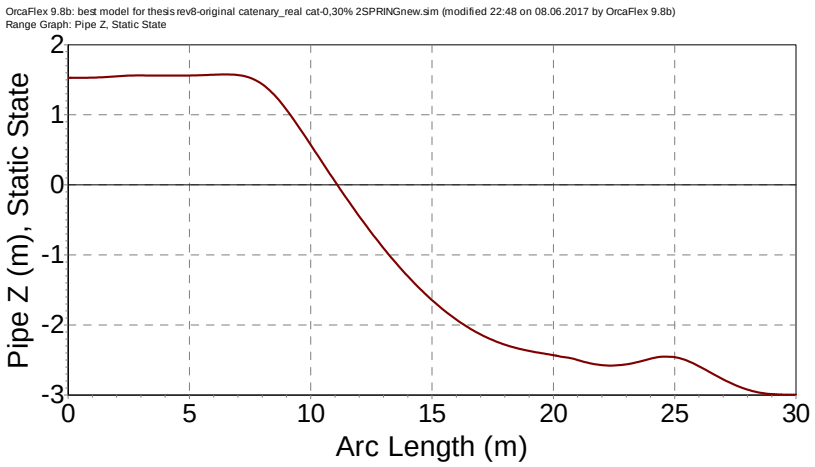

17. 2-Spring Boundary Condition – 0.35% Residual Strains

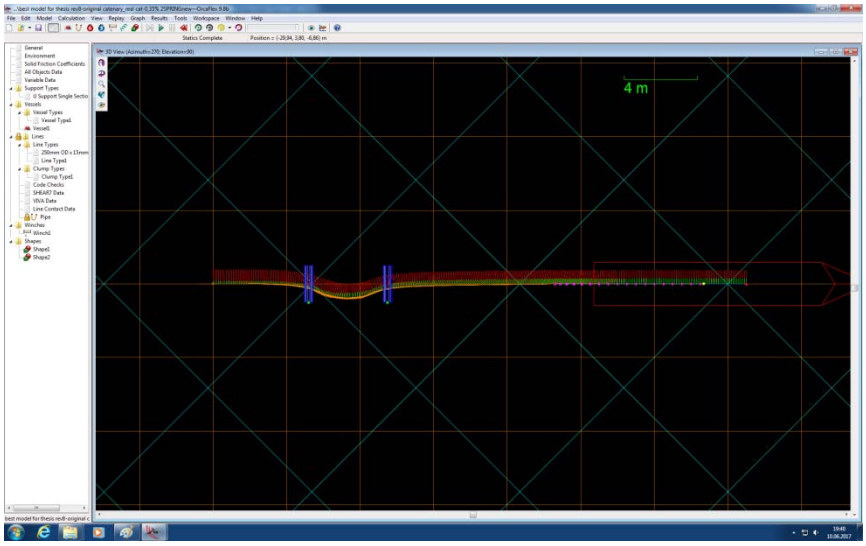

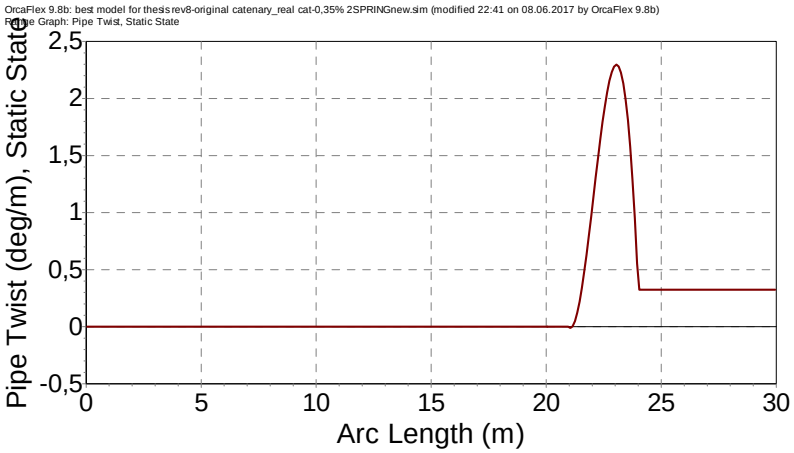

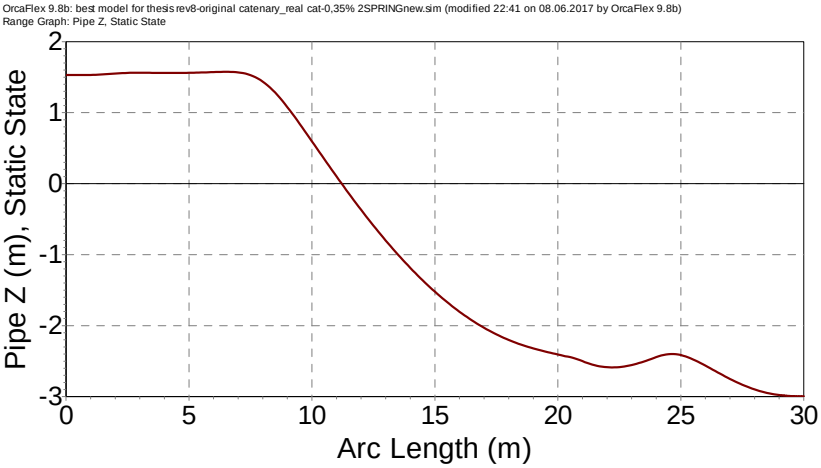

18. 2-Spring Boundary Condition – 0.40% Residual Strains

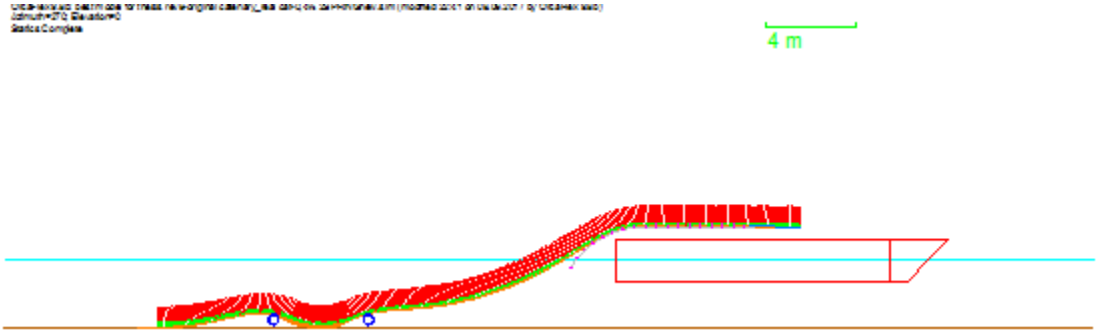

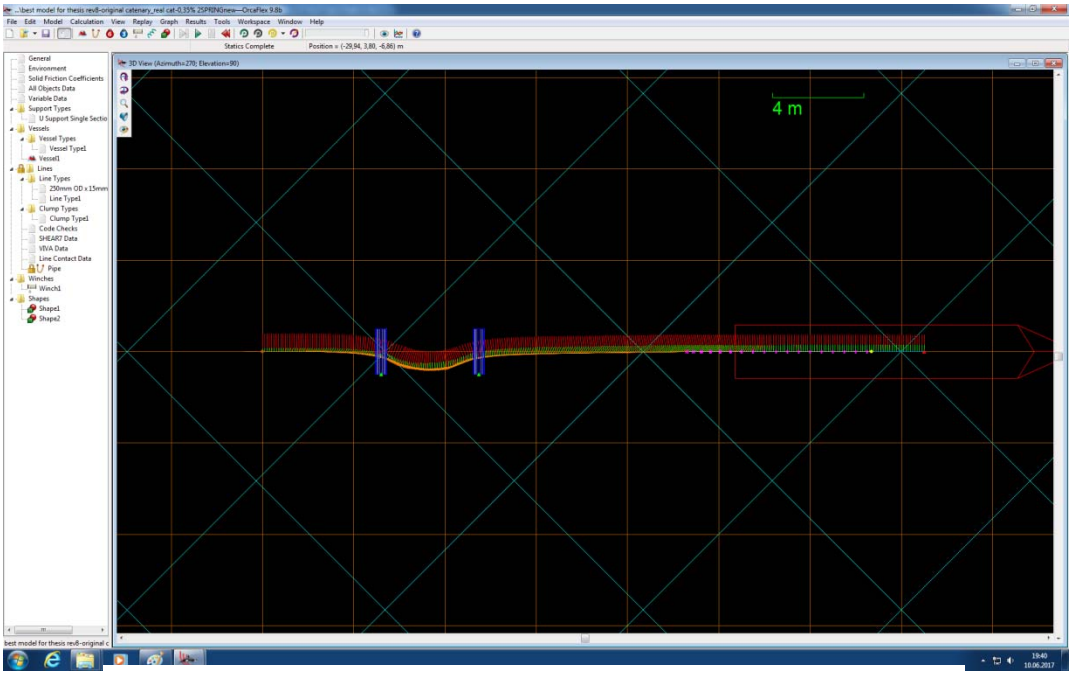
4 m

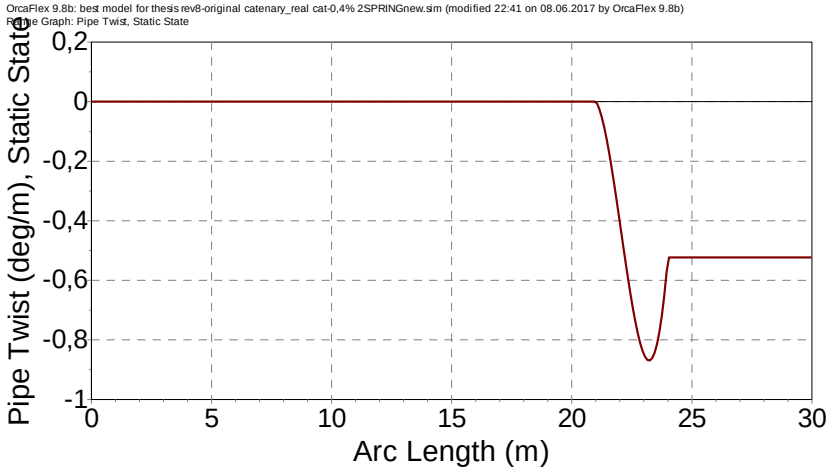
OrcaFlex 9.8b: best model for thesis rev8-original catenary_real cat-0,4% 2SPRINGnew.sim (modified 22:41 on 08.06.2017 by OrcaFlex 9.8b)
Range Graph: Pipe Twist, Static State
Pipe Twist (deg/m), Static State
0,2
0
-0,2
-0,4
-0,6
-0,8
-1
0
5
10
15
20
25
30
Arc Length (m)

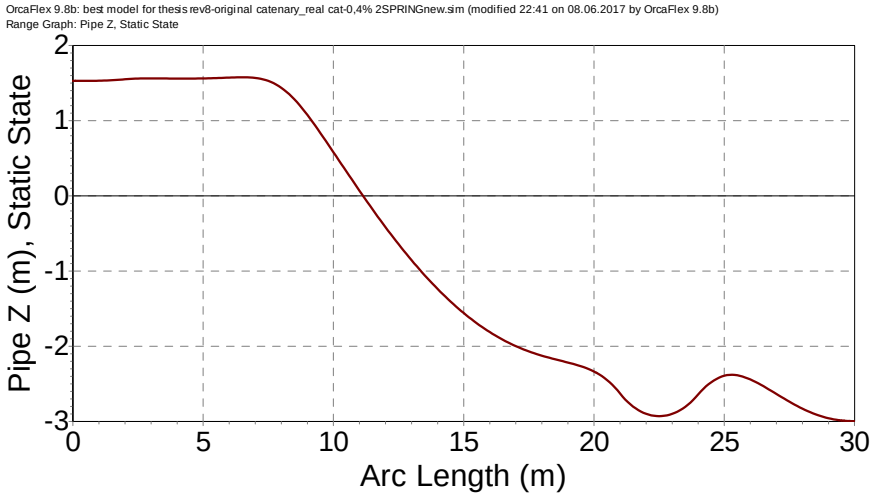
OrcaFlex 9.8b: best model for thesis rev8-original catenary_real cat-0,4% 2SPRINGnew.sim (modified 22:41 on 08.06.2017 by OrcaFlex 9.8b)
Range Graph: Pipe Z, Static State
Pipe Z (m), Static State
2
1
0
-1
-2
-3
0
5
10
15
20
25
30
Arc Length (m)

APPENDIX VI – Free-span Experiments

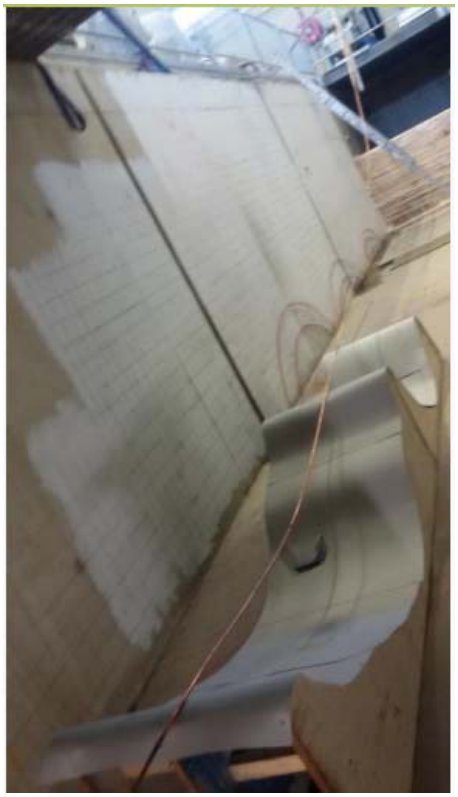

APPENDIX VII – Numerical Analysis of Rotation with both end of Pipeline Fixed

It should be noted that, the point with highest rotation angle is the TDP in both cases

- Case Study Result

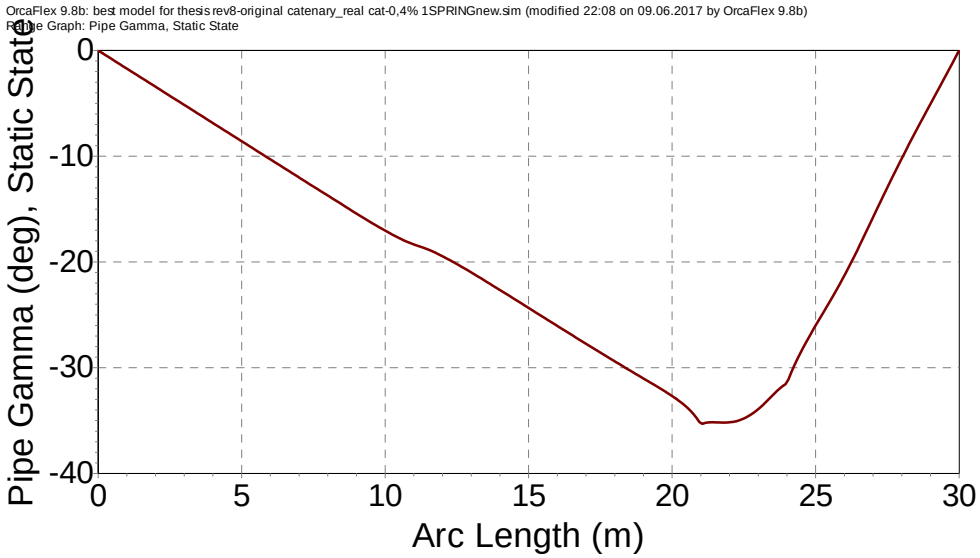

- Li Y., (2005) Study Result

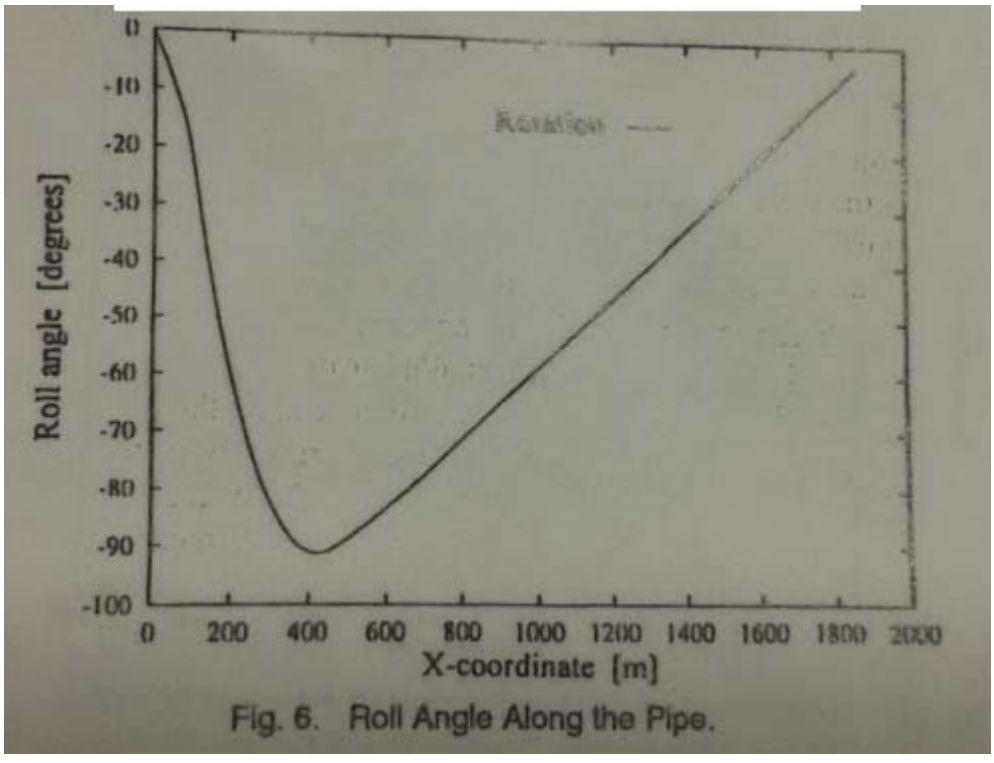

Fig. 6. Roll Angle Along the Pipe.